The role of the small GTPase, *arf-3*, in seam cell development and secretion in *C. elegans*

Aidan Walker

A thesis presented for the degree of

Doctor of Philosophy



Exeter College

University of Oxford

Trinity Term 2018

Abstract

The *Caenorhabditis elegans* seam cell lineage provides a useful model to study stem cell biology and the regulation of cellular division and differentiation. Seam cells are a population of stem-like cells that run along the length of the worm which divide both symmetrically, to expand the pool of progenitor cells, and asymmetrically to generate various differentiated cells including hypodermal and neuronal cells.

The seam cells also have a secretory function; giving rise to the cuticle and the alae. Seam cells do not retain their proliferative property through adult life, terminally differentiating at the end of development by undergoing homotypic fusion to produce the adult seam cells whose function is to secrete cuticle components. Thus the seam cells make an excellent model for studying the molecular basis of cell fate determination as well as more cell biological aspects of development, including the re-shaping of cells during differentiation, the polarity of cell fate allocation and cellular trafficking processes accompanying secretion.

In this thesis, I investigated the role of the small GTPase, *arf-3*, an ADP-ribosylation factor (ARF), in *C. elegans* seam cell development. I found that *arf-3* knockout or overexpression causes severe developmental defects including embryonic lethality and seam cell defects. Furthermore, knockdown of *arf-3* in a RNAi hypersensitive mutant causes defects in moulting and seam cell divisions. In a screen for genes interacting with *arf-3* I identified *agef-1* and *dyn-1*. I also show that their interaction with *arf-3* is linked to moulting.

arf-3 expression in the seam is driven by a 3' intronic enhancer element that also drives the expression of the "Seam Cell Marker", *scm::gfp*, a transcriptional reporter

which is used as a marker of seam cell fate. I identified two transcription factors, *elt-1* and *nhr-23* that bind the 3' enhancer to regulate *arf-3* expression in the seam cells. ARF-3::mCherry localises with the golgi, early and late endosomes in the seam cells in concert with the moulting cycle. This, and the moulting defects observed in *arf-3* knockdown suggests a role in regulating cuticle synthesis and moulting.

In summary, *arf-3* function is crucial to ensure proper development of the *C. elegans* seam cells and the regulation of moulting.

Thesis supervisor: Professor Alison Woollard

Acknowledgements

In settling into Oxford, Exeter College and the Department of Biochemistry, and even as I write, and my studies draw to a close, I have received help and kindness from many people. In acknowledging some by name, I am well aware that there are many others unnamed to whom I should also address my thanks. I can only hope that this thesis will in some way repay the debt I owe them.

For the thesis itself, the chief credit must go to my supervisor Alison Woollard. I have been inspired by her enthusiasim for scientific research and her ability to communicate science to her students and to the public. I am especially grateful for Alison's support of my personal development during my time in her lab; whatever challenges I have faced she has met them with patience and understanding. I am enormously grateful for her supervision.

I would also like to thank the members of both Alison's lab and Jonathan Hodgkin's lab, past and present, for the endless amount of advice, expertise and friendship they have shared with me throughout my D. Phil. I'd especially like to mention Abigail Guillermo, Emily Baker, Liisa Parts, and Sophie Gilbert for making me feel so welcome in the Woollard lab, I will miss talking about all things nematode over pizza.

A person rarely has the means to explore science in the way I have. I should like to thank my sponsors, the Wellcome Trust, for funding my research for the past four years. I would also like to include Exeter College and the British Society of Development Biology, the Genetics Society, and the Genetics Society of America for their contributions to the conferences I have attended. It is through their generosity

I am adding my pebble to the cairn.

I had the good fortune to begin my rowing career at Exeter College Boat Club with a group of friends who have defined my experience of Oxford University. Their company, friendship, advice, encouragement and humour over the course of my D.Phil. has made an enormous difference and meant a great deal to me. In particular, I must thank Andreas Kisling-Harris, who persuaded me to get give rowing a try and the other members of "the renaissance": Oscar North, Max Spicer, Jonathan Tan, Meng Yuan Kuok, Phil Moseley and Matt Holyoak, to name a few. I will miss rowing with you.

Finally, I would like to acknowledge the support and understanding of my Mother and Father before, during, and beyond my time at University. They instilled in me the value of education and it only through their love and encouragement that ink has met paper, in many ways theirs was the most difficult task of all.

Abbreviations

Abbreviation	Description	Abbreviation	Description
3' UTR	3' Untranslated Region	KanR	Kanamycin resistance
5' UTR	5' Untranslated Region	kb	kilobase
APC	Adenomatous polyposis coli	L	litre
ARF	ADP-ribosylation factor	let	lethal
bp	base pair	lf	loss-of-function
C. briggsae	*Caenorhabditis briggsae*	lin	lineage abnormal
C. elegans	*Caenorhabditis elegans*	LRP	lipoprotein receptor-related protein 6
C. remanei	*Caenorhabditis remanei*	M	molar
Cas9	CRISPR associated protein 9	mab	male abnormal
cDNA	complementary DNA	Mb	Megabase
ceh	*C. elegans* homeobox	MBV	Multi-vesicular body

CGC	*Caenorhabditis* Genetics Centre	miRNA	microRNA
ChIP	chromatin immunoprecipitation	MosSCI	Mos1-mediated single copy insertion
CK1	Casein kinase 1	ncRNA	non-coding RNA
cM	centimorgans	NGM	nematode growth medium
CRISPR	clustered regularly interspaced short palindromic repeat	NLS	nuclear localisation signal
DIC	differential interference contrast	ORF	open reading frame
DMSO	Dimethyl sulphoxide	pal	posterior alae
DNA	Deoxyribonucleic acid	PCR	Polymerase Chain Reaction
Drosophila	*Drosophila melanogaster*	PH	Pleckstrin Homology
DTC	distal tip cell	qPCR	quantitative PCR
E. coli	*Escherichia coli*	Rac	Ras-related C3 botulinum toxin
ECM	Extracellular Matrix	Ras	Rat sarcoma
		RFP	red fluorescent protein
eff	epithelial fusion failure	RNAi	RNA interference
egl	egg laying defective	ROCK	Rho-associated, coiled coil-containing kinase

elt	erythroid-like transcription factor family	rpm	revolutions per minute
ER	endoplasmic reticulum	Runx	Runt-related transcription factor
FITC	fluorescein	rnt	Homologue of Runt-related transcription factor
Fz	Frizzled	SC	seam cell
g	grams	Tcf	T-cell factor
gf	gain-of-function	TE	Tris and EDTA
GFP	green fluorescent protein	TF	transcription factor
GSK3β	Glycogen synthase kinase-3β	unc	uncoordinated
H2B	Histone 2B	VNC	ventral nerve cord
Hh	Hedgehog	Wnt	Wingless
WT	wild type		

Contents

1 Introduction **19**

1.1 General Introduction 19

1.1.1 Cellular and Developmental Biology 19

1.1.2 Signalling and morphogens: a common theme in developmental biology 20

1.1.3 Model organisms in developmental biology 21

1.2 An introduction to *Caenorhabditis elegans* 22

1.2.1 *C. elegans* anatomy, histology, and cellular composition 23

1.2.2 The *C. elegans* life cycle 24

1.2.3 *C. elegans* genetics and genomics 24

1.3 *C. elegans* post-embryonic development 27

1.3.1 The *C. elegans* cuticle 27

1.3.2 Moulting 30

1.3.3 Intracellular trafficking and the endocytic pathway in *C. elegans* moulting 36

1.3.4 Development of the *C. elegans* hypodermis and seam cells . . 37

1.4 Control of seam cell development 38

1.4.1 Wnt signalling controls cell fate polarity during asymmetrical seam divisions 39

1.4.2 The heterochronic pathway and transcription factors in seam cell development 42

1.5 ARF genes 44

1.5.1 ARF genes are members of the Ras Superfamily of GTPases . 44
1.5.2 ARFs role in vesicle formation 45
1.5.3 ARF genes are a eukaryotic plesiomorphy 46
1.5.4 ARF genes and health 47
1.5.5 ARFs in *C. elegans* 48
1.6 Summary 49

2 Methods **55**
2.1 Strains and maintenance of worms 56
2.2 Generation of males by heat-shock 56
2.3 Genetic crosses 56
2.4 Genotyping 57
2.4.1 *arf-3(tm1877)* genotyping 57
2.4.2 *arf-1.2(ok796)* genotyping 57
2.4.3 *blmp-1(tm548)* genotyping 57
2.4.4 *elt-1(ku491)* genotyping 57
2.4.5 *apr-1(bp298)* genotyping 58
2.4.6 *agef-1(vh4)* genotyping 58
2.4.7 Genotyping of mutants generated from genome editing by CRISPR 58
2.5 Agarose gel electrophoresis 58
2.6 RNAi by feeding 59
2.7 Single worm lysis 59
2.8 Bleach synchronization 60
2.9 Plasmid construction 60
2.9.1 Construction of seam expressed intracellular reporter markers 60
2.9.2 Construction of the *arf-3* 5' promoter expression construct . . 61
2.9.3 Construction of guide RNA expression vectors 61
2.9.4 *dyn-1* feeding RNAi clone 61
2.9.5 *F57H12.10* feeding RNAi clone 62

2.10 Fosmids . . . 62
2.11 Construction of transgenic worms . . . 62
2.12 Quantitative RT-PCR analysis . . . 63
2.13 Co-CRISPR . . . 64
2.14 Bioinformatics . . . 64
2.15 Microscopy . . . 65
2.15.1 Visualisation of *C. elegans* cuticle collagen . . . 65
2.15.2 Analysis of fluorescent vesicle dynamics . . . 66
2.16 Statistical Analysis . . . 67
2.17 Acknowledgements . . . 67

3 *arf-3* plays a role in development of the seam, embryogenesis, and cuticle integrity. 68

3.1 Overview and aims . . . 68
3.1.1 Aims and hypotheses of this chapter . . . 73
3.2 Results . . . 73
3.2.1 The *arf-3(tm1877)* mutant exhibits maternal effect embryonic lethality and seam cell defects . . . 73
3.2.2 Knockdown of *arf-3* by RNAi in a hypersensitive background phenocopies the *arf-3(tm1877)* mutant . . . 79
3.2.3 The *arf-3(tm1877)* mutant is rescued by the *arf-3* genomic locus 84
3.2.4 Overexpression of wildtype *arf-3* causes developmental and seam cell defects . . . 86
3.3 Generating CRISPR-Cas9 mediated mutations at the *arf-3* locus . . . 89
3.3.1 ARF-3::mCherry is expressed in the seam and other tissues . . 95
3.3.2 Knockdown of components of intracellular trafficking and signalling causes ARF-3::mCherry mislocalisation . . . 96
3.3.3 *agef-1* regulates *arf-3* to regulate cuticle secretion and moulting 97
3.3.4 *apr-1* interacts with *arf-3* to regulate seam cell divisions . . . 102
3.3.5 *arf-3::mCherry* partially rescues moulting defects in *dyn-1(RNAi)* 105

3.4 Discussion 108

4 ARF-3::mCherry colocalises with components of the endocytic pathway in a moulting-dependent manner 110

4.1 Overview and aims 110

4.1.1 Aims and hypotheses of this chapter 110

4.2 Results 111

4.2.1 ARF-3::mCherry puncta are concentrated on the apical cortex of the seam cells 111

4.2.2 Smaller ARF-3::mCherry vesicles move further and quicker than those larger in size 115

4.2.3 ARF-3::mCherry colocalises with RAB-6.2::GFP and RAB-7::GFP and partially with RAB-5::GFP 120

4.2.4 ARF-3::mCherry colocalisation with endocytic compartments changes in concert with the moulting cycle 122

4.2.5 Overexpression of intracellular trafficking components perturbs seam cell development 123

4.2.6 The seam cell defects observed in RAB-5::GFP, RAB-6::GFP and RAB-7::GFP animals are not rescued by knockdown of *dyn-1* or *eff-1* 124

4.3 Discussion 131

4.3.1 ARF-3::mCherry spatial dynamics are consistent with its colocalisation with RAB-5::GFP, RAB-6::GFP and RAB-7::GFP . 131

4.3.2 ARF-3::mCherry localises to endosomal compartments and may contribute to the moulting cycle of *C.elegans* 132

5 A *cis*-regulatory element of *arf-3* drives the expression of the seam cell marker *scm::gfp*. 135

5.1 Overview and aims 135

5.1.1 Aims and hypotheses of this chapter 136

5.2 Results 136
5.2.1 The 5' promoter of *arf-3* does not drive the expression of GFP::NLS as strongly, nor specifically as the intronic enhancer 136
5.2.2 Different transcription factors are predicted to bind to the 5' promoter and the intronic enhancer elements of *arf-3* 139
5.2.3 Bioinformatic analysis of the *arf-3* promotor regions reveals three highly conserved TF target sequences 142
5.2.4 BLMP-1 binds to the *arf-3* locus at 5' promoter and potentially at the 3' enhancer 145
5.2.5 Expression of *arf-3::mCherry* and *scm::gfp* is unaffected by depletion of BLMP-1 145
5.2.6 DIE-1 binds to a site 3' of the *arf-3* coding region 150
5.2.7 *die-1(RNAi)* does not affect the expression of *scm::gfp* 150
5.2.8 NHR-23 regultes the expression of *arf-3* 154
5.2.9 ELT-1 binds the 3' enhancer of *arf-3* 157
5.2.10 *scm::gfp* and *arf-3::mCherry* expression is uncoupled from seam cell fate in *elt-1(ku491)* and *elt-1(RNAi)* 157
5.3 Discussion 164

6 Discussion **167**

6.1 General Discussion 167
6.2 Key findings 167
6.3 Observations on the dissection of the *scm* enhancer 168
6.4 *arf-3* as a regulator of cuticle secretion and moulting - a link to sterol uptake? 170
6.5 Seam cell development and the integration of cellular context and signalling pathways 172

A Appendix Title **174**

A.1 Genetic Crosses 183

A.1.1 Generation of AW1792 183
A.1.2 Generation of AW1793 183
A.1.3 Generation of AW1422 183
A.1.4 Generation of AW1799 184
A.1.5 Generation of AW1800 184
A.1.6 Generation of AW1803 184

List of Figures

1.1 Anatomy of *C. elegans* 32

1.2 The *C. elegans* Lifecycle 33

1.3 The *C. elegans* Cuticle 34

1.4 The moulting cycle of *C. elegans*. 35

1.5 Intracellular Trafficking Pathways 51

1.6 Post embryonic development of the hypodermis and seam cell lineages. 52

1.7 WNT signaling in *C. elegans* 53

1.8 ARFs as regulatory switches. 54

3.1 A schematic of seam cell asymmetric divisions 70

3.2 Schematic of *scm* promoter dissection from C. Brabin, D. Phil thesis, 2011. 71

3.3 A 603bp fragment of the *arf-3* locus recapitulates the expression of *scm::gfp*. 72

3.4 Characterisation of the *arf-3(tm1877)* allele. 78

3.5 Knockdown of *arf-3* by RNAi causes defects in seam cell development and moulting. 83

3.6 Knockdown of *arf-3* in the RNAi hypersensitive strain AW718 causes cuticle defects. 85

3.7 Generating a rescue of the *arf-3(tm1877)*. 87

3.8 Overexpression of wildtype *arf-3* from its endogenous locus causes developmental defects. 88

3.9 A schematic of the Co-CRISPR strategy to generate *arf-3* deletion mutants. 92
3.10 A representative image of a transformant animal from the injections of the CRISPR-Cas9 plasmid mixture. 93
3.11 Genotyping of mutants generated from CRISPR. 94
3.12 The expression pattern of ARF-3::mCherry. 99
3.13 Mislocalisation of ARF-3::mCherry after knockdown of intracellular trafficking targets 100
3.14 Knockdown of *arf-3* in the *agef-1(vh4)* mutant background causes moulting defects. 101
3.15 *arf-3* interacts with *apr-1* to regulate seam cell divisions 104
3.16 Expression of ARF-3::mCherry rescues moulting defects observed in *dyn-1(RNAi)* animals. 107

4.1 The distribution of ARF-3::mCherry puncta within the seam cell. . . 114
4.2 Measurements of ARF-3::mCherry puncta dynamics within seam cells. 116
4.3 Strategy for the identification of ARF-3::mCherry puncta by colocalisation with fluorescent reporter markers. 119
4.4 ARF-3::mCherry colocalises with RAB-6::GFP and RAB-7::GFP and partially with RAB-5::GFP (white arrows) but not with RAB-11::GFP or SP12::GFP. 121
4.5 Colocalisation of RAB-5::GFP and ARF-3::mCherry changes over time. 125
4.6 Colocalisation of RAB-6::GFP and ARF-3::mCherry changes over time. 126
4.7 Colocalisation of RAB-7::GFP and ARF-3::mCherry changes over time. 127
4.8 Timecourse of RAB-11::GFP and ARF-3::mCherry localisation. . . . 128
4.9 Timecourse of SP12::GFP and ARF-3::mCherry localisation. 129
4.10 Overexpression of RAB-5::GFP, RAB-6::GFP and RAB-7::GFP cause seam cell defects 130
4.11 Seam cell defects caused by endocytic reporter markers are not rescued by depletion of DYN-1 or EFF-1 134

5.1 The 5' promoter sequence of *arf-3* drives the expression of GFP::NLS in the seam cells and other tissues. 138
5.2 A schematic of the *arf-3* locus 141
5.3 A schematic of the ChIP dataset analysis workflow. 144
5.4 BLMP-1::GFP binds to the *arf-3* locus in L1 larvae. 148
5.5 ARF-3::mCherry expression is unchanged in *blmp-1(tm548)*. 149
5.6 Visualisation of DIE-1::eGFP binding sites in early adult. 151
5.7 Knockdown of *die-1* causes no significant change to *arf-3* expression. 152
5.8 The predicted NHR-23 binding site is conserved in the 3' promoter region of *arf-3*. 153
5.9 Visualisation of NHR-23::eGFP ChIP binding at *arf-3* locus in L3 larvae. 155
5.10 Knockdown of *nhr-23* causes seam cell defects and perturbs ARF-3::mCherry expression. 156
5.11 The binding site of *elt-1* is conserved in the *arf-3* 3' enhancer. 160
5.12 Visualization of ELT-1::eGFP binding sites in L2 larvae. 161
5.13 Knockdown of *elt-1* causes a decrease in seam cell number and perturbs expression of *arf-3*. 162
5.14 *arf-3* expression is reduced in *elt-1(ku491)* mutant worms. 163
5.15 The *elt-1(ku491)* allele is partially rescued by knockdown of *die-1* and is exacerbated by *nhr-23 (RNAi)*. 165

List of Tables

I Wnt signalling components in *C. elegans* 42

I Solutions and Media 55

I Strains used in Chapter 3 74

II RNAi screen hits 96

I Strains used in Chapter 4 111

I Strains used in Chapter 5 137

II Conservation of transcription factor binding sites. 143

I Strains used in this study 174

IV List of targets in RNAi screen 176

II Plasmids used in this study 182

III Primers used in this study 186

Chapter 1

Introduction

1.1 General Introduction

1.1.1 Cellular and Developmental Biology

The most fascinating aspect of biology is arguably how complex it all is. A seemingly chaotic mixture of molecules are brought to order, synthesised into greater structures and compartmentalised to perform small, specific tasks that collectively produce what we call life; the most fundamental unit of which is the single cell. The complexity doesn't stop there however; single cells can cooperate and form multicellular organisms. It is this process that intrigues developmental biologists the most: how can multicellular life emerge from a single cell, the zygote? Our understanding of this question is crucial to our understanding of health and disease. Even small perturbations in the genetic code or surrounding environment can lead to catastrophic consequences in the development of an organism. However, the study of development is not limited to the period from zygote to adulthood, but goes further to address how multicellular organisms repair injured tissues and organs, or even regenerate them completely!

The zygote contains all the information required to produce the multitude of specialised cell types with distinct features and functions, despite them all sharing the same genome. These cells communicate with one another and coordinate to

make up a system of highly structured tissues and organs, all working in concert to develop a whole, multicellular organism.

Assembling a multicellular organism begins with proliferation, the zygote must divide, giving rise to daughter cells. Specialised cell types are produced from these daughters through the process of differentiation, this process abrogates their proliferative ability and leads to exit from the cell division cycle. Proliferation and differentiation are essentially opposite and organisms must carefully balance these forces during their development by the modulation of genetic programmes, in response to environmental cues. The resulting cells are able to arrange themselves into tissues through the integration of several processes: cell adhesion, communication, fusion, and migration, as well as programmed cell death.

Over time our ability to research developmental processes has improved through technological advances. Where previously we could only observe development at the anatomical level, we can now manipulate systems through forward and reverse genetics, transgenesis and use microscopic imaging to dive deeper at the level of cells, proteins and single molecules. Developmental biology has therefore become a multidisciplinary synthesis, we employ techniques and methods from a variety of fields to produce a comprehensive understanding of how complex life emerges.

The work presented in this thesis exploited the *Caenorhabditis elegans* seam cells as a model to study how a small GTPase, *arf-3*, and intracellular trafficking more generally, contribute to the stem cell mode of division and the secretory function of the seam cells.

1.1.2 Signalling and morphogens: a common theme in developmental biology

As stated above, communication between cells is critical to the formation of tissues and organs. A relatively small number of signalling pathways appear to control this process in animals. Each pathway consists of a series of biochemical events that modulate the response of a target cell to the extracellular stimuli. The stimuli can

be through cell-cell contacts or through long range morphogens, and they provide contextual information to neighbouring cells. The chemical gradient produced by these morphogens helps to establish and reinforce tissue position and identity. These pathways are used iteratively through development and it is the amalgamation of these signals that confers specificity to the cell and tissue. However, the intepretation of a signal is highly context-specific as shown through classic grafting experiments (Nüsslein-Volhard, Frohnhöfer, and Lehmann 1987; Wagner et al. 1990). These experiments established the role of certain tissues inducing cell fate changes when ectopically transplanted, but the inductive effects would vary by transplantation site because of the gene expression profile of receiving cells. We now recognise that the signals inducing these changes are secreted proteins that act on neighbouring cells and include morphogens belonging to the Wnt, Hedgehog (Hh), TGFβ, EGF, and FGF families.

1.1.3 Model organisms in developmental biology

Ethics aside, experiments on humans are impractical because of our long lifespan, small brood size and we are expensive to rear. Instead we use "model" organisms to study development since they are much more convenient and we can simplify broad, multifaceted problems down to a simpler context. The use of model organisms is further supported by the similarities with humans, for example we share 90% of our genome with mice (Waterston et al. 2002). However, each model organism presents trade-offs, some of these trade-offs are fundamental; one of the most studied organisms for understanding cell biology is baker's yeast or *Saccharomyces cerevisiae*, but yeast is not multicellular and we cannot glean much about the organisation of tissues for example. While other trade-offs are more technical, such as with the fruit fly *Drosophila melanogaster*, this species has been used as a model for over a century and many of the first genetic experiments were conducted on it, however the fly and its embryos cannot be frozen for long-term storage, meaning strains and mutants must be actively maintained or else they will be lost. Therefore before

conducting an experiment, the suitability of the organism to address the problem must be considered.

1.2 An introduction to *Caenorhabditis elegans*

While nematodes including *C. elegans* were studied from the end of the 19th, and intermittently throughout the 20th century (Nigon and Félix 2017), Sydney Brenner's first published paper on the genetics of *C. elegans* in 1974 is typically accepted as the catalyst for the current era of *C. elegans* research. Since then, this small nematode, and especially the reference strain N2, from Bristol, has become one of the best established model organisms for the study of development, genetics and genomics.

C. elegans has several key advantages: the worm's small size (adults reach a length of approximately 1mm), short generation time and transparency make it an excellent organism for studying development using microscopy. Furthermore, while *C. elegans* is naturally a soil-dwelling organism, it is easily cultured in the laboratory on Nematode Growth Medium (NGM) plates seeded with *E. coli* bacteria as substrate.

C. elegans is also genetically tractable, most natural populations are hermaphrodites (99.5%) (Brenner 1974), enabling self-fertilization and clonal expansion. Additionally males can be generated through heat shocking or crossing with High Incidence of Males *him* mutants (Hodgkin, Horvitz, and Brenner 1979), these can be used to conduct genetic crosses. Most of the work presented in this thesis was performed using hermaphrodites unless otherwise indicated. Futhermore, we are able to generate large numbers of informative alleles through mutagenesis and, crucially, these strains can be stored for an indeterminate length of time by freezing in liquid nitrogen (Brenner 1974). Recent evidence suggests nematodes can survive for millenia in such a state (Shatilovich et al. 2018).

1.2.1 *C. elegans* anatomy, histology, and cellular composition

C. elegans is especially useful for answering developmental questions because it shares many of the differentiated cell types and tissues found in higher organisms (Figure 1.1A and 1.1C). Indeed, Brenner's initial interest in *C. elegans* stemmed from its potential as a model nervous system (Ward et al. 1975) and many of the earliest papers on *C. elegans* focussed on the reconstruction of the physical nervous system using electron micrographs and mapping the synapses of neurons (Ward et al. 1975; Sulston, Dew, and Brenner 1975; White et al. 1976; White et al. 1983; Chalfie et al. 1985; White et al. 1986).

As stated above, *C. elegans* is transparent and this, coupled with a simple anatomy allows for easy phenotypic assessment. Tissues and individual cells are easily visuallised by DIC, such as the male tail sensory rays shown in Figure 1.1B. This has culminated in the complete map of the invariant cell lineage from single celled zygote to adulthood for all 959 cells (or 1032 cells in males; Sammut et al. 2015), providing a reference for phenotypic analysis at single cell resolution (Sulston and Horvitz 1977; Sulston et al. 1983). The invariant cell lineage of *C. elegans* makes it an excellent model for the study of development, as well as cell divisions and programmed cell death.

The usefulness of microscopy has also been augmented by the discovery of GFP (Shimomura, Johnson, and Saiga 1962) and the amenability to produce transgenic strains (Mello et al. 1991; Mello and Fire 1995) which has allowed for the visualisation of gene expression (Chalfie et al. 1994) as well as the examination of intracellular structures and localisation of components *in vivo* (Grant and Hirsh 1999; Haag et al. 2014). Electron microscopy is also used to study the development of *C. elegans* using cross sections of the worm or to visualise the cuticle and alae as shown in Figure 1.1C. I use strains expressing transgenes and flourescent imaging throughout this work to investigate the role of *arf-3* in the seam cells.

1.2.2 The *C. elegans* life cycle

C. elegans have a short egg-to-egg development cycle which takes approximately 3.5 days at 20 °C making them an excellent model for the study of development (Brenner 1974; Figure 1.2). Better still, manipulation of the incubation temperature can accelerate *C. elegans* development, for example *ex-utero* embryogenesis takes approximately 12 hours under standard laboratory conditions (20 °C) but can be slowed down at lower temperatures e.g. 15 °C or accelerated at higher temperatures (25 °C; Byerly, Cassada, and Russell 1976).

After hatching, and in the presence of food, *C. elegans* proceeds through the four larval stages (L1 to L4) before reaching adulthood with a fully matured germline. The end of each of the four larval stages is defined by the shedding of the old cuticle and synthesis of the new one to accommodate future growth, a process termed moulting (Singh and Sulston 1978). Under starvation conditions or high population density (and therefore intense competition), L2 larvae can enter an alternative development pathway termed the dauer. The dauer is a "quiescent" state where animals exhibit higher resistance to environmental and chemical stresses (Klass and Hirsh 1976; Cassada and Russell 1975). The dauer stage has several adaptations that aid its survival, including an altered metabolism and a modified cuticle to aid water retention, indeed they can remain viable in this form for months (Golden and Riddle 1984). Dauer larvae re-enter the life cycle at the L4 stage when food becomes available. Similarly, when starved, L1 animals will enter diapause (developmental arrest) and will remain in this state until it encounters food and can survive for 6-10 days in this state (Johnson et al. 1984). This feature can be used to synchronize worm populations for post-embryonic studies.

1.2.3 *C. elegans* genetics and genomics

As mentioned earlier, *C. elegans* predominantly exist as hermaphrodites (genotype XX) but males (genotype XO) can also spontaneously arise via loss of one X chromosome by non-disjunction in gamete production. The rarity of males means that

however heterogenous a population starts, over time it will be driven to homozygosity through the reproductive selfing of hermaphroditic mothers; the genetic diversity of isolated populations is therefore low (Hodgkin and Doniach 1997). Apart from the sex chromosomes there are five pairs of autosomes (I-V, also known as linkage groups) and the first genetic map was published in 1974 (Brenner 1974) showing that each chromosome was approximately 50cM long and underwent a single crossover event per meiosis (Meneely, Farago, and Kauffman 2002).

More recently *C. elegans* was the first multicellular organism to be sequenced (C. elegans Sequencing Consortium 1998). Since then, this resource has been made easily accessible via WormBase (http://www.wormbase.org/) alongside a multitude of other information. Notably, the genomes of several closely related nematode species have also been made available, including but not limited to: *C. briggsae* (Stein et al. 2003), *P. pacificus* (Dieterich et al. 2008) and *C. remanei* (Fierst et al. 2015).

The *C. elegans* genome is comprised of 97Mb and contains around 22,000 genes, including alternatively spliced forms, non-coding RNA genes, and relatively rare pseudogenes (Harrison, Echols, and Gerstein 2001). The genetic architecture is comparable to other eukaryotic organisms, consisting of exons, introns and *cis*-regulatory elements such as promoter sequences and enhancers. Around 15% of *C. elegans* genes are organised into operons, with associated promoter sequences driving the transcription of more than one gene as a polycistronic unit (Blumenthal et al. 2002). Expression of genes from these operons is tightly associated with mRNA processing via spliced leader *trans*-splicing (Pettitt et al. 2014).

Publication of the genomes of other nematode species has improved our understanding of the evolution of developmental processes through the use of comparative genomics. Many of the genes involved in these processes are evolutionarily ancient and by aligning the orthologous sequences of different members of the *Caenorhabditis* genus we can identify and analyse key elements of conserved genetic control, including promoter sequences and transcription factor binding sites. Indeed, this ap-

proach has been used to assess the occurrence and rate of changes in *cis*-regulatory elements, and to determine the importance of such changes for the evolution of developmental mechanisms (Barrière, Gordon, and Ruvinsky 2011). I adopt a similar approach when investigating transcription factor binding sites in Chapter 6 of this Thesis.

On top of these resources, several initiatives are continually producing genetic mutants, including the *C. elegans* Knockout Consortium (C. elegans Deletion Mutant Consortium 2012), the *C. elegans* National Bioresource Project of Japan and the Million Mutations Project, as well as individual forward genetic screens. With the advent of genome editing technologies such as MosSCI (Mos1-mediated single copy insertion; Frøkjær-Jensen et al. 2014) and CRISPR-Cas9 (Chen et al. 2014) it is easier now than ever to acquire or generate a mutant for any gene in the *C. elegans* genome.

While effective, mutations can be difficult to generate and maintain, so thankfully we are also able to selectively and efficiently target genes for knockdown by RNA interference (RNAi) by injection, feeding or soaking (Fire et al. 1998; Timmons and Fire 1998; Tabara, Grishok, and Mello 1998). Again, the community has produced and made available libraries of RNAi clones (Fraser et al. 2000; Rual et al. 2004) allowing for quick, reliable, high-throughput screening.

At least 45% of *C. elegans* genes have human orthologues (Rubin et al. 2000) and about 38% of human disease genes have conserved orthologs in *C. elegans*. Thanks to the collaborative ethos of the research community *C. elegans* is an exceptional model organism to study development and disease of higher organisms. Throughout this work I used community-sourced strains and RNAi clones to target specific genes.

More recently, two consortiums have made available data on the gene regulatory landscape of *C. elegans*, these are modENCODE consortium (Niu et al. 2011) and its successor modERN (Kudron et al. 2018). Together, these two projects have released the binding profiles of hundreds of transcription factors, as well as chromatin modifications. In Chapter 6 of this thesis I have explored some of these datasets to

find transcription factors that bind at the *arf-3* locus.

1.3 *C. elegans* post-embryonic development

In 1977, Sulston and Horvitz published the complete cell lineage from hatched larva to adulthood (Sulston and Horvitz 1977). This work, and other studies (Kimble and Hirsh 1979; Sulston, Albertson, and Thomson 1980; Sammut et al. 2015) have culminated in the cellular "family tree" mapping all the cell divisions from the 558 cells present in L1 larva to the 959 cells in the adult hermaphrodite. The mapping of these lineages relied heavily on Nomarski differential interference contrast microscopy (DIC), to directly observe and record the divisions, migrations, and deaths of individual cells in living nematodes.

The main body plan of *C. elegans* remains the same throughout post-embryonic development and once the animals have reached adulthood; the cells born post-embryonically contribute to significant developmental changes in the neuronal, muscular, hypodermal, reproductive and digestive systems (Sulston and Horvitz 1977). Once the animals have reached maturity the position and number of cells also remain unchanged but the worms continue to grow through hypertrophy of the cells; *C. elegans* is therefore a eutelic organism (Sulston and Horvitz 1977).

1.3.1 The *C. elegans* cuticle

The cuticle of *C. elegans* is the barrier which protects the worm from the environment and pathogens. Much of the experimental research on the cuticle has used microscopy including DIC, scanning/transmission electron microscopy, as well as staining with antibodies or dyes, and more recently atomic force microscopy (Akhatova et al. 2018). The cuticle is an apical extracellular matrix comprised of lipids, sugars and protein. Transmission electron microscopy of the extracellular matrix revealed it is organised into five distinct layers: the surface coat, the epicuticle; and the cortical, medial and basal zones (summarised below; Figure 1.3; Cox et al. 1981).

- The surface coat (glycocalyx) is rich in carbohydrates and mucins (Zuckerman, Kahane, and Himmelhoch 1979; Himmelhoch and Zuckerman 1978). Unlike other cuticle layers, which are produced by epidermal cells, the surface coat is likely derived from the secretions of excretory gland cells (Nelson and Riddle 1984; Bird, Bonig, and Bacic 1988). The surface coat is important for protection against pathogen invasion and the *srf* and *bus* gene families are thought to play a role in its composition. Indeed, mutants in these genes have shown resistance to infection by *Microbacterium nematophilium* and altered lectin binding (Gravato-Nobre et al. 2005).

- The epicuticle is a lipid-rich layer that is most pronounced in dauer larvae.

- The cortical layer is insoluble to treatment with reducing agents such as SDS or β-mercaptoethanol, suggesting that the layer is highly crosslinked (Cox et al. 1981). The layer is comprised of cuticlins which are important for formation of patterned structures within the cuticle such as the lateral ridges or alae. Cuticulins are expressed in a stage-dependent manner, a theme common to many proteins involved in cuticle formation, for example *cut-1* was the first cuticulin identified (Sebastiano, Lassandro, and Bazzicalupo 1991) and is important for dauer alae formation, along with *cut-6* (Muriel et al. 2003); whereas *cut-3* and *cut-4* are involved in alae formation in the L1 and adult respectively (Sapio et al. 2005).

- The medial layer is considered to be fluid filled and contains columns of filamentous material, termed struts, which connect the cortical and basal layers (Cox et al. 1981). The struts are only absent in the region of the alae, where the basal and cortical layers appear fused.

- When the *C. elegans* adult cuticle is treated with reducing agents such as β-mercaptoethanol, the basal layers and struts are solubilised. This soluble fraction was determined to be collagen through the subsequent digestion with collagenase (Cox et al. 1981). The basal layer includes two sublayers of fibres

that meet each other in fish-bone pattern (Peixoto, Kramer, and Souza 1997).

The cuticle collagens are synthesised in and secreted from either the syncytial hypodermis or in the lateral seam cells. Cuticle protein synthesis peaks during each molt, and is reduced during the inter-molt period (Cox et al. 1981). This coincides with the increased formation of Golgi bodies in the seam cells and hypodermis, likely to reduce the burden of processing and secreting the new cuticle (Singh and Sulston 1978). After each moult, the extra intracellular membranes and vesicles are rapidly cleared, though this process is not understood, although it has been suggested that autophagy plays a role (A. Batas, PhD. thesis, 2017). The collagens and cuticulins undergo post-translational modification such as extensive crosslinking by peroxidases secreted by the epidermis (Edens et al. 2001; Thein et al. 2009).

The cuticle collagen family is large with 170 members in *C. elegans*. RNAi of most collagen genes does not cause overt defects; suggesting redundant roles, however several phenotypes are linked to collagen mutants inlcuding dumpy, blistered, roller, squat, long, and male ray morphology. The gene expression pattern of cuticle collagens is a growing body of work, complicated by expression changing if worms are grown in liquid or solid culture (Çelen, Doh, and Sabanayagam 2018), however, I will summarise what is known below.

The expression pattern of some collagens is dependent on the heterochronic pathway (discussed below) and displays a cyclical pattern during all larval stages (Liu, Kirch, and Ambros 1995; Johnstone and Barry 1996), while others are expressed in specific larval stages (such as *col-19* in the L4 or adult (Thein et al. 2003); or in the dauer stage (Kramer, Cox, and Hirsh 1985; Cox and Hirsh 1985; Levy and Kramer 1993). Indeed, several L4-specific collagens rely on the most downstream effector of the heterochronic pathway, LIN-29, for their expression (Abete-Luzi and Eisenmann 2018). However, recent analysis of the RNA-seq data from modENCODE suggests most of the collagen genes do not show a cyclic pattern but instead are only expressed in one stage (Gerstein et al. 2010; Jackson et al. 2014).

Those that display a temporal pattern can be divided into early, intermediate

or late patterns of expression, depending on mRNA peak abundance. It has been suggested that the temporal expression pattern aids the assembly of different cuticle structures dependent on particular components (Johnstone and Barry 1996). This is supported by the observation that early and intermediate collagens form distinct substructures in the cuticle (McMahon et al. 2003). Overall, the synthesis of the cuticle and the network of transcription factors that regulate the expression of collagens is still not well understood, but, in addition to the heterochronic pathway, several have been implicated including: the GATA transcription factors (ELT-1 and ELT-3; Gilleard and Mcghee 2001) as well as nuclear hormone receptors (NHR-23 and NHR-25; Gissendanner et al. 2004) and BLMP-1 (Horn et al. 2014).

1.3.2 Moulting

Moulting is the process of shedding and resynthesising the cuticle at the end of each larval stage (Figure 1.4). The process of moulting can be divided into three phases (Singh and Sulston 1978):

- During lethargus the worm enters a quiescent state; decreasing its activity, including feeding, until the animal essentially stops moving altogether. It is during this phase that the worm synthesises its new cuticle. This process is thought to be regulated by the EGF family protein LIN-3 (Van Buskirk and Sternberg 2007). The Notch signalling pathway has also been implicated in promoting quiescence (Singh et al. 2011).

- Apolysis is the separation of the old cuticle from the epidermis. This process is thought to involve thioredoxin and glutathione reductases which have been proposed to decrease the number of disulfide bonds in the cuticle thus disrupting its attachment to the epidermis (Stenvall et al. 2011). Additionally, apolysis may rely on the degradation of cuticular components by proteases and peptidases, indeed, RNAi of the cathepsin-like protease *cpz-1* arrested worms between the L2 and L3 moult with the old cuticle still attached (Hashmi et

al. 2004). Further supporting a role for the degradosome are the observations from experiments involving protease inhibitors, for example overexpression of *bli-5* and knockdown of *mlt-11* also caused defects in moulting (Frand, Russel, and Ruvkun 2005; Page, McCormack, and Birnie 2006).

- Ecdysis is the final stage of moulting where the animal escapes the old cuticle. The worm attempts to escape its old cuticle by beginning to move again; it regurgitates the pharyngeal cuticle and rapidly rotates around its longitudinal axis. In doing so the worm mechanically disrupts any linkage between the old and new cuticle and emerges, leaving behind its old cuticle. Again, proteases are thought to play a role in this process, with NAS-37, an astacin metalloprotease, localising to the old cuticle at the anterior where it may digest the cuticle at the tip of the head (Davis 2004).

The timing and coordination of moulting is still not well understood, however, many studies point to steroid hormones that act on NHR-23 and NHR-25, but these have not been identified. Supporting a role for steroid hormones is the evidence for the essential role of cholestrol, where the cholestrol receptor *lrp-1* is required for epidermal uptake of cholestrol and *lrp-1* mutants are unable to shed and degrade their old cuticle (Yochem et al. 1999).

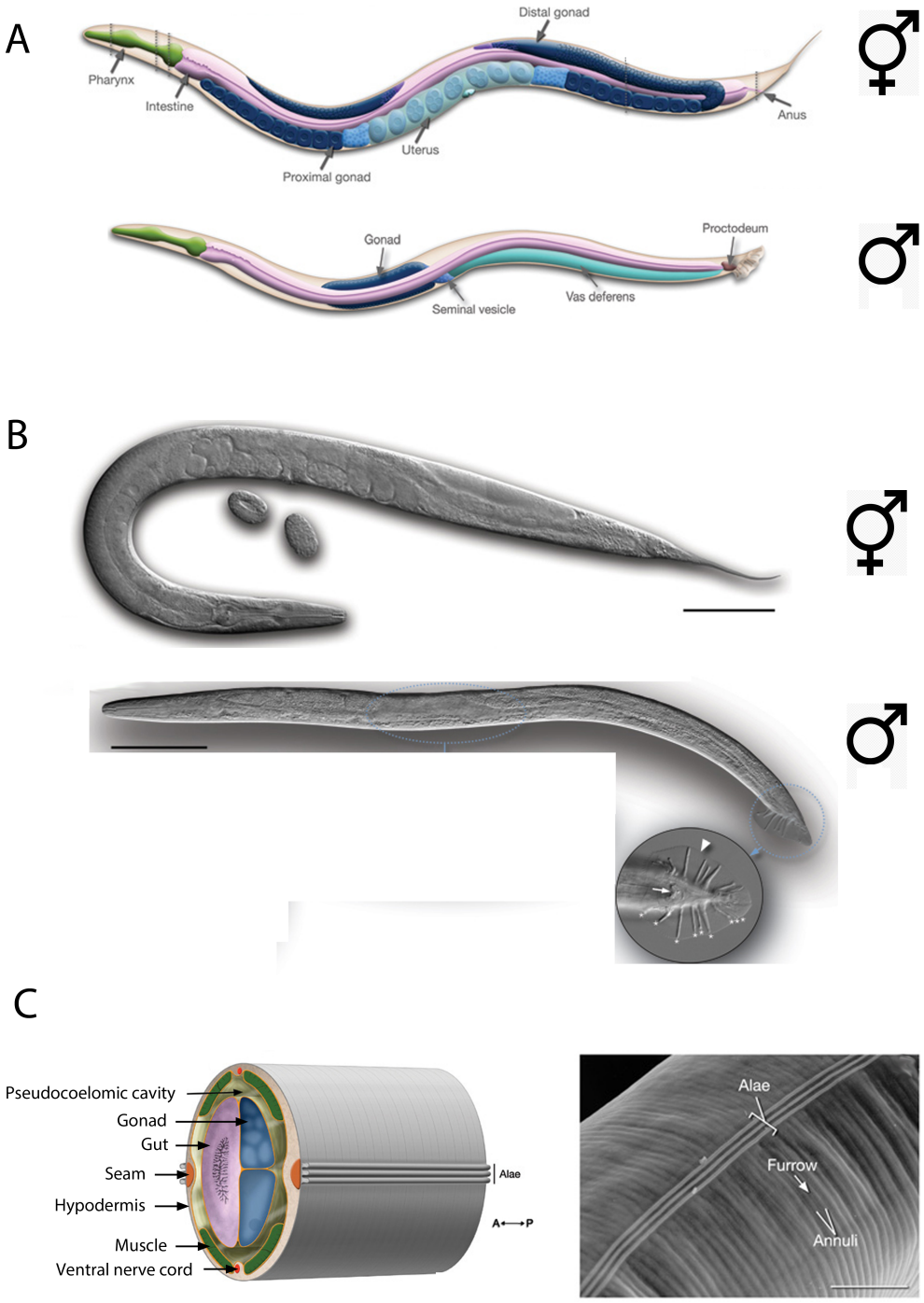


Figure 1.1: Anatomy of *C. elegans* (adapted from WormAtlas). A: Schematics of the adult hermaphrodite and male worm showing the different internal structures and tissues in each. Scale bar = 0.1nm. B: DIC images of the adult hermaphrodite and male. Males are easily distinguished by their elaborate tails which develop a fan structure to facilitate mating. C: Cross-section through an adult hermaphrodite showing the arrangement of tissues in the body cavity. The worm secretes an exoskeleton from the epidermal tissues called the cuticle which is shown in grey, visualised by electron microscopy in the right panel highlighting the alae, which are secreted by the seam cells, and the annular furrows.

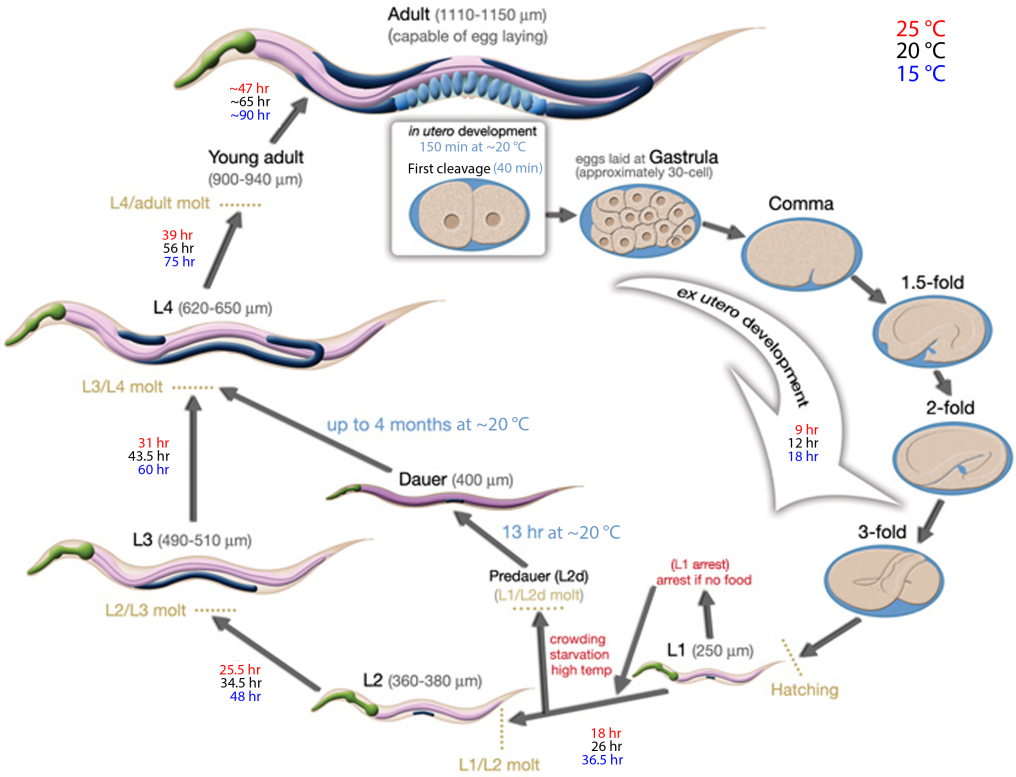


Figure 1.2: The *C. elegans* Lifecycle (adapted from WormAtlas): The time taken to reach each stage in the life cycle at 15 °C (blue), 20 °C (black) and 25 °C (red) is shown in the figure. Taking 0 minutes as the point the egg is laid, it takes roughly 60 hours at 20 °C for the worm to mature to a hermaphrodite capable of egg-laying in appropriate conditions. The worm progresses through four larval moults (L1-L4) before it reaches adulthood, each new cuticle accommodates the growth between each larval stage. The approximate size of the animal at each stage is indicated. Alternative lifecycles are also indicated such as L1 diapause where post-embryonic development is paused if there is insufficient food available, the worm may re-enter the life cycle at the same point on provision of food. Also shown is the dauer pathway which occurs due to starvation or overcrowding, the dauer larvae can survive several months without food due to morphological adaptations.

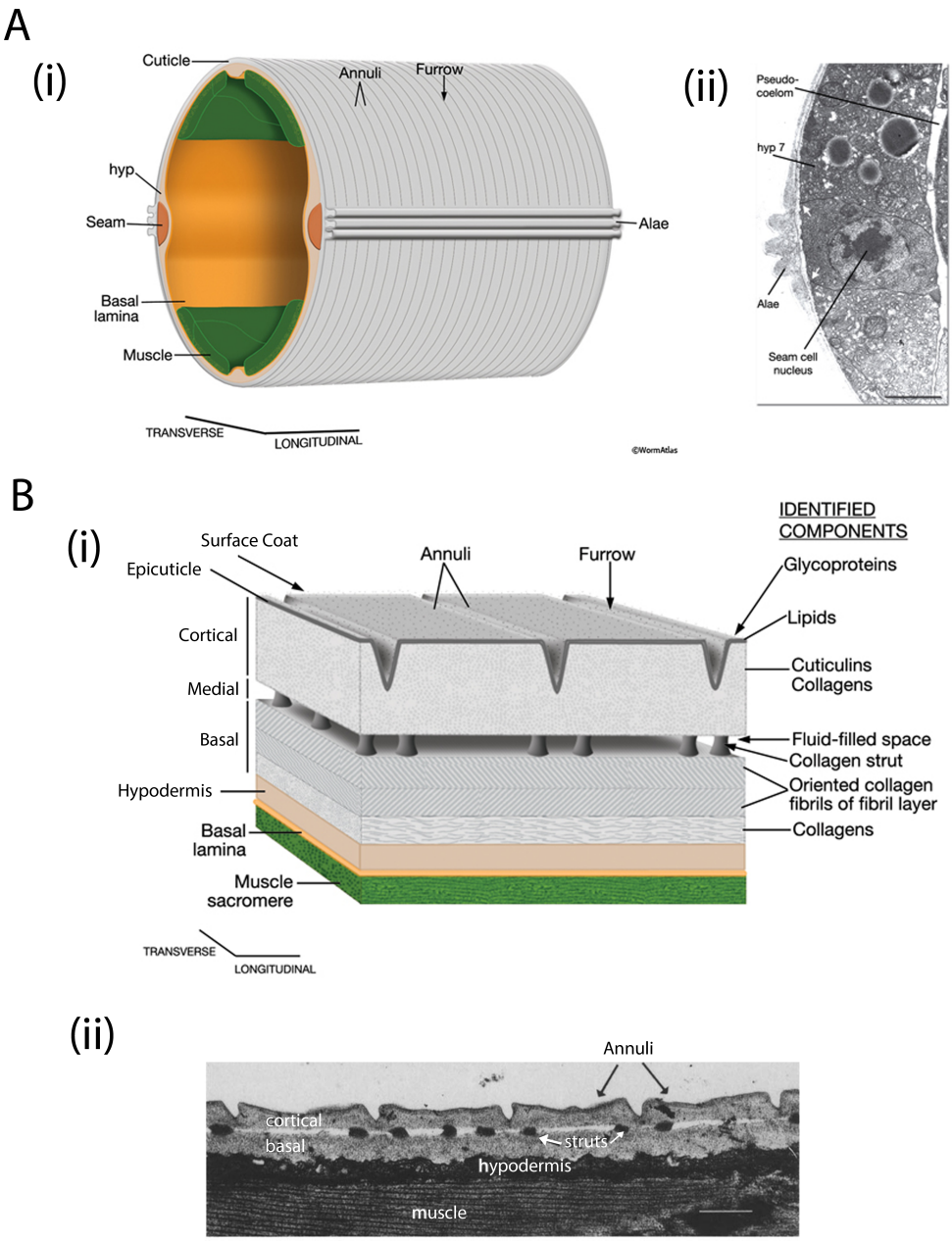


Figure 1.3: The *C. elegans* cuticle (adapted from WormAtlas). A(i): A schematic cross section of an adult hermaphrodite showing the cuticle in relation to other tissues, the second panel (ii) shows this data from a Transmission Electron Microscopy (TEM) experiment showing the cuticular alae and the underlying seam cell which is responsible for its secretion. B(i): Schematic showing the layers of the adult hermaphrodite cuticle as well as the molecular components identified in each layer. B(ii) From Cox et al. 1981, the image is a longitudinal section from a TEM experiment with the layers and structures labelled.

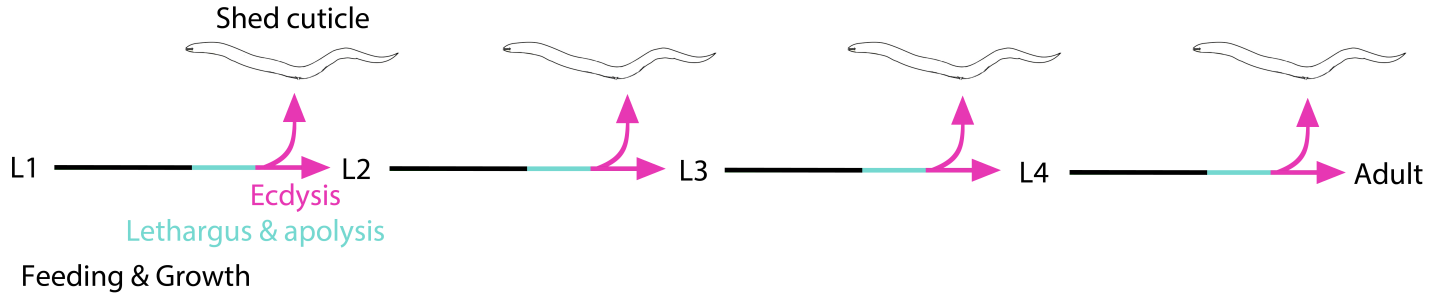


Figure 1.4: The moulting cycle of *C. elegans*. As the worm progress through its lifecycle it ends each larval stage with the shedding of it's old cuticle. The process begins with a decrease in the activity of the worm, a phase called lethargus (blue). The worm synthesises a new cuticle beneath the old one in apolysis which is followed by ecdysis where the worm begins to move again to mechanically remove itself from the old cuticle (pink). The worm then proceeds to continue its growth before the next moult, which the new cuticle can accommodate (black).

1.3.3 Intracellular trafficking and the endocytic pathway in *C. elegans* moulting

Intracellular trafficking within the seam cells and hypodermis is thought to be critical for moulting, both in the secretion and recycling of cuticule components as well as processing the signals that promote moulting through endocytosis. Trafficking of vesicles in the cell is mainly controlled by vesicular coat proteins such as the COPII complex which plays a role in the secretory pathway from the endoplasmic reticulum to the golgi; inhibition of a member of this complex, *sec-23* leads to defects in moulting (Roberts, Clucas, and Johnstone 2003).

Endocytosis is the process by which a cell internalises material from the plasma membrane, this material can include nutrients, pathogens and signalling molecules as well as membrane bound proteins. The process is shown in Figure 1.5: a target at the cell surface is trafficked into the cell by the invagination of the plasma membrane into a membrane bound vesicle. These vesicles then fuse with the early endosome (also known as the sorting endosome) where the cargo is sorted via tubulo-vesicular carriers to different organelles. Vesicles containing cargo targetted for degradation are trafficked to the lysosome. Cargoes can be recycled directly or indirectly to the plasma membrane via recycling endosomes. The characterisation of vesicles in the endocytic pathway proves a challenge as the regulation of cargo through the pathway is controlled by many overlapping proteins and and it remains unclear whether cargo is processed through a series of endosomal structures or whether endosomes "mature" through modification (Naslavsky and Caplan 2018).

In the context of moulting in *C. elegans*, the endocytic pathway is used in the uptake of sterols from the environment by LRP-1, and depletion of LRP-1 causes moulting defects at all larval stages (Kang et al. 2013).

1.3.4 Development of the *C. elegans* hypodermis and seam cells

Beneath the cuticle of the worm lies the epithelium which includes the hypodermis and specialised epithelial cells. The majority of the hypodermis is the hyp7 syncytium which is formed from the fusion of hypodermal cells in the embryo, a process regulated by *eff-1* (Podbilewicz and White 1994; Mohler et al. 2002), as well as the fusion of cells from post-embryonic cell divisions of the lateral seam cells and ventral P cells (Figure 1.6A). The hypodermis of the head (hyp3, hyp4, hyp5, and hyp6) and tail (hyp8, hyp9, hyp10, and hyp11) are not added to during post-embryonic development and are formed during embryogenesis.

The seam cells, are a group of stem-like cells that lie on the lateral sides of the worm. At hatching there are ten seam cells on each side and at adulthood there are sixteen which then cease dividing and undergo a terminal differentiation where they fuse together (Podbilewicz and White 1994). The stereotyped seam cell lineage is shown in Figure 1.6B. At each larval stage the seam cells undergo a cell divsion, these divisions can be symmetric or asymmetric. A symmetric division maintains the population of seam cells, such as at L2 stage. In an asymmetric division the posterior daughter retains the seam fate of further proliferation, while the anterior daughter cell differentiates and fuses with hyp7, there are several exceptions to this however (Sulston and Horvitz 1977).

H0 is the anterior-most seam cell and is the only seam cell that does not divide postembryonically. All the other seam cells, H1-2, V1-6 and T continue to undergo symmetric and asymmetric divisions which generate differentiated hypodermal and neuronal cells. In males, V5, V6 and T cells produce sensory rays in the male tail (Sulston, Albertson, and Thomson 1980; Sulston and Horvitz 1977). The seam cells also play a role in synthesising the cuticle and alae during L1, adulthood and dauer (Cox et al. 1981). The absence of alae at adulthood can indicate incorrect terminal differentiation or fusion defects as seen in *elt-5* and *elt-6* RNAi where the seam cells fused with the hyp7 syncytia causing alae and moulting defects (George et al. 1998;

Koh and Rothman 2001; Brooks et al. 2003; Shemer et al. 2004).

As discussed above, the seam cells, along with the hypodermal syncytia are responsible for secreting the cuticle as well as the alae. During the moult both the hypodermis and the seam cells exhibit increased biosynthetic activity as seen by an increase in the number of golgi bodies (Singh and Sulston 1978). However, the seam cells appear to play a distinct role in this process, expressing different components to the hypodermis including *bus* genes, thought to be involved in surface coat biosynthesis (Gravato-Nobre et al. 2011). Furthermore, *nas-37* the metalloprotease involved in digesting the cuticle at the tip of the head during moulting is specifically expressed in the seam cells during the final moult (Frand, Russel, and Ruvkun 2005).

1.4 Control of seam cell development

Stem cell divisions must be highly regulated because failed regulation of proliferation or differentiation can lead to disastrous consequences, for example uncontrolled cell proliferation can lead to cancer in other organisms. Additionally, if, following an asymmetrical division, both daughter cells differentiate then the population of dividing cells will be depleted.

Seam cell divisions are controlled by pathways that are conserved across metazoans including: the Wnt pathway which sets up the anterior-posterior polarity of seam cells (Gleason and Eisenmann 2010), the Hox family of transcription factors (Thompson et al. 2016) and the heterochronic pathway which govern stage-specific seam cell division patterns (Harandi and Ambros 2015), finally transcription factors such as RNT-1/BRO-1 which act to regulate seam cell fate (Kagoshima et al. 2007). Furthermore, there is much crosstalk between these pathways to provide more nuanced regulation of seam cell development (Hunter et al. 1999). Taken together this makes seam cells an excellent model for the study of stem cell divisions.

The work in this thesis originates from a previous study in the Woollard lab to dissect the "seam cell marker", *scm::gfp*. The seam cell marker is used extensively in

the study of seam cell development as a marker of seam cell fate; it is a transcriptional reporter where GFP is expressed in the nuclei of seam cells from the two-fold stage of embryonic development right through to adulthood. When seam cells undergo an symmetric division the hypodermal daughter loses the expression of *scm::gfp* (Koh and Rothman 2001). The seam cell marker was first identified by a promoter trapping screen (Hope 1991). In this screen genomic fragments were cloned upstream of a *lacZ* gene and transformed into *C. elegans* by microinjection. Lines generated were stained for β-galactosidase expression and one of these lines expressed the promoter region we now call *scm*.

This work was conducted before the genome of *C. elegans* was published and the gene controlled by this promoter was not known. Furthermore, the *scm* reporter is a large (7.8kb) construct and it was not known how much of this sequence is required for seam expression. Therefore Charles Brabin dissected the *scm::gfp* reporter further and he found that it aligned to the locus of *arf-3*, *col-115* and *mec-17* and that a minimal region of 603 bp from the final intron of *arf-3* was sufficient to drive the expression of GFP in the nuclei of seam cells. In this thesis I investigate further the role *arf-3* plays in the control of seam cell development.

1.4.1 Wnt signalling controls cell fate polarity during asymmetrical seam divisions

The Wnt signalling pathway was first identified in *Drosophila* (Sharma and Chopra 1976) and is conserved in a diverse range of metazoans including mouse, human and *xenopus* (Rijsewijk et al. 1987; McMahon and Moon 1989); Gavin, McMahon, and McMahon 1990; Yang-Snyder et al. 1996).

Wnts are lipid-modified glycoproteins that are secreted to signal to neighbouring or nearby cells where they bind Frizzled/Lrp receptor complexes (Bhanot et al. 1996; Wehrli et al. 2000; Willert et al. 2003) Wnts act as morphogens to control processes such as cell fate specification, asymmetrical division, polarity and cell migration (Eisenmann 2005; Sawa and Korswagen 2013).

The best studied Wnt signalling pathway is the "canonical" Wnt pathway (Figure 1.7A). Unlike the non-canonical pathways, this pathway acts through the effector protein β-catenin to control the transcription of target genes (Perrimon and Mahowald 1987; Noordermeer et al. 1994). In the absence of a Wnt ligand β-catenin is targeted for degradation by phosphoylation and ubiquitination by a "destruction complex" comprising of Axin, APC and two kinases CK1 and GSK3B (Peifer et al. 1993; Tamai et al. 2004). This degradation complex is inhibited by Wnt binding to Frizzled and LRP6 at the plasma membrane, this process requires the scaffolding protein Disheveled (Klingensmith, Nusse, and Perrimon 1994; Bilic et al. 2007). The stabilised β-catenin is then translocated to the nucleus where it co-activates target gene transcription with its interacting partner, a member of the Tcf family of transcription factors (Molenaar et al. 1996; Behrens et al. 1996). As stated non-canonical Wnt signalling pathways do not require β-catenin, these pathways include: the planar cell polarity (PCP) pathway and the Ror and Ryk dependent pathways (Green, Inoue, and Sternberg 2008; Angers and Moon 2009). Ror is an alternative Wnt receptor which is related to Frizzled and it can inhibit canonical Wnt signalling (Green, Inoue, and Sternberg 2008). Ryk is also an alternative Wnt receptor and is the homologue of Derailed in *Drosophila*, it is related to the Wnt inhibitor WIF (Yoshikawa et al. 2003, Lu et al. 2004). While the planar cell polarity pathway involves the asymmetric localisation of Frizzled, Dishevelled and two PCP-specific components Prickle and Van Gogh (Das 2004).

With the exception of LRP6, the Wnt signalling pathway components are conserved in *C. elegans*, this includes five Wnt genes, four Frizzled receptors, three Dishevelleds, four β-catenins and one Tcf. The non-canonical pathway is also conserved and the homologues of all these genes are summarised in Table 1.1. I will continue to describe the Wnt pathways in the context of *C. elegans* and the seam cells below.

In *C. elegans* the roles of a single β-catenin in Drosophila and two in vertebrates, have been distributed over the four β-catenin homologs: BAR-1, HMP-2, WRM-

1 and SYS-1, where BAR-1 is the only β-catenin to interact with POP-1 (Tcf) to drive the transcription of Wnt target genes (Korswagen, Herman, and Clevers 2000; Natarajan, Witwer, and Eisenmann 2001; Liu et al. 2008). Wnt signaling is responsible for most somatic divisions occurring along the anterior-posterior axis in *C. elegans* (Mizumoto and Sawa 2007) and utilizes multiple redundant WNT ligands (Yamamoto, Takeshita, and Sawa 2011). Indeed, the non-canonical Wnt/β-catenin asymmetry pathway plays a role in post-embryonic seam cell development (Figure 1.7B; Mizumoto and Sawa 2007; Gleason and Eisenmann 2010).

In a stereotypical asymmetrical seam cell division, where the anterior daughter differentiates and the posterior daughter maintains its seam fate, this pathway relies on the asymmetrical localisation of components in the dividing cell, as well as the stabilisation of the β-catenin SYS-1 (Figure 1.7B). The mother seam cell is already polarized and this polarisation is passed on to the two daughter cells with APR-1/APC, PRY-1/Axin and LIT-1/NLK localised to the anterior cortex of the cell (Takeshita and Sawa 2005). In response to a Wnt ligand binding the Frizzled and Dishevelled homologues, LIN-17 and DSH-1 respectively, localise to the posterior cortex of the dividing cell (Goldstein et al. 2006, Mizumoto and Sawa 2007). Also in the posterior cortex, the β-catenin SYS-1 is stabilised in a manner similar to the canonical pathway and is translocated to the nucleus (Huang et al. 2007; Baldwin and Phillips 2014). Once the ligand binds, the Disheveled paralog MIG-5 inhibits the posterior cortical polarisation of APR-1 (Baldwin, Clemons, and Phillips 2016). APR-1 acts to stabilise microtubules in the anterior cortex, this facilitates the nuclear export of WRM-1 to the anterior cortex of that daughter cell by kinesins (Sugioka and Sawa 2012; Baldwin and Phillips 2014). In the posterior nucleus WRM-1 activates the LIT-1 protein kinase, which phosphorylates POP-1 to facilitate its nuclear export via PAR-5/14-3-3 (Rocheleau et al. 1999; Yang et al. 2011). Thus when WRM-1 is trafficked to the anterior cortex in the anterior daughter cell this causes reciprocal POP-1 nuclear asymmetry, with more POP-1 in the anterior daughter nucleus and less in the posterior (Lo et al. 2004).

TABLE I: *Wnt signalling components in C. elegans*

Wnt Component	*C. elegans* homologue
Wnt ligand	*mom-2, lin-44, egl-20, cwn-1, cwn-2*
Frizzled	*mom-5, lin-17, mig-1, cfz-2*
Ror	*cam-1*
Ryk/Derailed	*lin-18*
CK1	*kin-19*
Dishevelled	*mig-5, dsh-1, dsh-2*
GSK3β	*gsk-3*
Axin	*pry-1, axl-1*
APC	*apr-1*
β-catenin	*bar-1, sys-1, wrm-1, hmp-2*
Tcf	*pop-1*
Van Gogh	*vang-1*
Prickle	*prkl-1*
NLK (asymmetrical pathway only)	*lit-1*

1.4.2 The heterochronic pathway and transcription factors in seam cell development

The timing of seam cell divisions is highly regulated, along with several other tissues and processes, including neurons, intestine, muscles and moulting, by the heterochronic pathway (Ambros and Horvitz 1984; Resnick, McCulloch, and Rougvie 2010). Heterochronic pathway components are conserved in other animals and plants Pasquinelli et al. 2000; Lagos-Quintana et al. 2001; Lagos-Quintana et al. 2002; Reinhart et al. 2002).

The pathway relies on the action of two main microRNAs (miRNAs), *lin-4* and *let-7*, together with a family of *let-7* miRNA genes (Ambros and Horvitz 1984; Lee, Feinbaum, and Ambros 1993 Reinhart et al. 2000). These miRNAs down-regulate target genes by binding to the 3'-UTRs of mRNAs and either induce an mRNA degradation pathway or repress translation of the mRNA, this role has been exploited experimentally by targetting specific genes for downregulation in cultured cells (Hutvágner and Zamore 2002; Zeng, Wagner, and Cullen 2002; Doench, Petersen, and Sharp 2003; Zeng, Yi, and Cullen 2003). In the heterochronic pathway *lin-4* encodes a miRNA that binds to the 3' UTR of *lin-14* mRNA blocking protein synthesis (Lee, Feinbaum, and Ambros 1993; Wightman, Ha, and Ruvkun 1993;

Olsen and Ambros 1999). This acts as a temporal developmental switch between early and late cell fates (Ambros and Horvitz 1987; Ruvkun and Giusto 1989). *let-7* targets LIN-41 in a similar fashion (Slack et al. 2000). *lin-14* gain-of-function mutants are resistant to this downregulation, leading to inappropriate accumulation of LIN-14 in the nuclei at later stages (Ruvkun and Giusto 1989). Normally the seam cells only undergo one asymmetrical division per larval moult but this accumulation of LIN-14 causes the reiteration of the L1 division, whereas *lin-14* loss of function mutants skip the division altogether and undergo the L2 symmetrical division prior to the L2 moult (Ambros and Horvitz 1984). *let-7* family members *mir-48, mir-241*, and *mir-84* are important for the L2 to L3 transitions with mutants reiterating the proliferative L2 division producing extra seam cells (Abbott et al. 2005) and *let-7* acts at the L4 to adult transition where loss-of-function mutants exhibit an extra round of seam cell division at L4 leading to an increase in the number of seam cells and a delay in the seam cell terminal differentiation and adult alae production (Reinhart et al. 2000).

The downstream effectors of Wnt signalling and the heterochronic pathway are often transcription factors, such as POP-1, LIN-14 and LIN-29, but other transcription factors also regulate seam cell development, for example: CEH-20 and UNC-62, RNT-1 and BRO-1, NHR-25, BAF-1 and CEH-16 (Chen, Eastburn, and Han 2004; Cassata et al. 2005; Silhánková, Jindra, and Asahina 2005; Kagoshima et al. 2007; Margalit et al. 2007; Huang et al. 2009; Hughes et al. 2013). As research continues this list will continue to grow, and while it is convenient to examine the roles of these pathways and transcription factors in isolation in seam cells, context is crucial to a cell's competency to respond to a given signal and therefore it is important to consider the network as a whole. The interactions between all these genes is an interesting area for future study.

1.5 ARF genes

1.5.1 ARF genes are members of the Ras Superfamily of GTPases

The ADP-ribosylation factor (ARF) genes make up a family of evolutionarily conserved small GTPases which play central roles in regulating both vesicular trafficking and signal transduction in cells. ADP ribosylation factors were first identified and purified from rabbit liver (Schleifer et al. 1982) and bovine brain (Kahn and Gilman 1986). ARF was described initially as a protein cofactor in the irreversible activation of the adenylate cyclase regulatory subunit, G_s, by covalent modification (ADP-ribosylation) catalysed by Cholera toxin (Schleifer et al. 1982). Later Kahn and Gilman discovered the GTPase activity of the ARF (Kahn and Gilman 1986). Subsequent research has demonstrated that "ADP-ribosylation factor" is a misnomer and their role associated with cholera toxin has little to do with the cellular functions of ARFs, which has much more to do with their GTPase activity (Figure 1.8A).

ARFs are members of the Ras superfamily of GTPases. The Ras GTPases were originally identified as viral genes transduced from the rodent genome and responsible for the highly oncogenic properties of RNA tumour viruses in rats (Parks and Scolnick 1977; Shih et al. 1979). Ras encodes a 21 kDa (p21) protein found to associate with guanine nucleotides GDP and GTP (Scolnick, Papageorge, and Shih 1979; Shih et al. 1980) and the plasma membrane (Willingham et al. 1980) which is dependent on the post-translational lipid modification of the N-terminus (Sefton et al. 1982). The oncogenic role of human RAS genes, first discovered in 1982 (Der, Krontiris, and Cooper 1982), drove the study of Ras structure, biochemistry and biology further. A wide variety of proteins, with diverse functions, were found to bind GTP including ras p21 protein, elongation factors such as EF-Tu and guanine nucleotide-binding proteins of adenylate cyclase (G proteins). The residues involved in guanine binding in Ras were modelled first (McCormick et al. 1985), combining

this with X-ray data of the GTP-binding domain of EF-Tu (Cour et al. 1985) and sequence comparison of other known GTP-binding proteins established a GTP-binding consensus sequence of three elements: GXXXXGKN$_{40\text{-}80 \text{ or } 130\text{-}170}$DXXGN$_{40\text{-}80}$NKXD (McCormick et al. 1985. The first two elements, GXXXXGK and DXXG interact with the phosphate portion of the GTP molecule and the last element, NKXD, is involved in nucleotide specificity (Dever, Glyniast, and Merrick 1987). Consensus spacings of either 40-80 or 130-170 amino acid residues are between the first and second elements and 40-80 amino acid residues between the second and third sequence elements (Dever, Glyniast, and Merrick 1987).

In 1988, Sewell and Kahn described the similarities between the cDNA-derived amino acid sequences of ARF to Ras and other GTP-binding proteins (Sewell and Kahn 1988). They noted that although ARF shares this consensus sequence for GTP-binding proteins, differences at the GTP-binding site and in the consensus sequence for the myristoylation of a glycine residue at the amino terminus ARFs are more similar to the heterotrimeric G protein alpha subunits than other Ras-like proteins (Sewell and Kahn 1988).

1.5.2 ARFs role in vesicle formation

Like other members of the Ras superfamily, ARFs typically cycle between active GTP-bound and inactive GDP-bound states (Randazzo et al. 1993). The binding of GTP is regulated by guanine nucleotide exchange factors (GEFs) and the hydrolysis of GTP to GDP is stimulated by GTPase-activating proteins (GAPs; Figure 1.8A). Binding of GTP or GDP induces large conformational changes, primarily in the "switch" regions (Liu, Kahn, and Prestegard 2010). These changes allow ARF GTPases to function as molecular switches; GTP binding enables interactions with effector proteins and take part in cellular processes such as vesicular transport and signalling.

Vesicle formation and fusion is mainly controlled by vesicular coat proteins (Figure 1.8B). These protein complexes are able to simultaneously select cargo and

deform the membrane. In ARFs, GTP binding causes the extrusion of the myristoylated N terminus, which enables the association with membrane phospholipids (Antonny et al. 1997). GTP-binding is also required for ARF to bind vesicle coat proteins such as coatomer (Zhao et al. 1997) and their recruitment is dependent upon ARF-GTP association with the membrane (Donaldson et al. 1992) and GTP hydrolysis triggers uncoating of Golgi- derived COP-coated vesicles (Tanigawa et al. 1993). While trafficking at the golgi is where ARFs have been best described, they can function at various intracellular compartments by interacting with different coat proteins (Nie et al. 2003; Volpicelli-Daley et al. 2005). Although monomeric in the cytosplasm ARF may oligomerize at the membrane surface and has been shown to form dimers which are essential to initiate membrane curvature to generate COPI vesicles in a GTP dependent manner (Beck et al. 2008).

1.5.3 ARF genes are a eukaryotic plesiomorphy

The ubiquity of ARFs in eukaryotes was first established through immunoreactivity assays, where ARF activity was observed in every eukaryotic tissue or cell examined, including human, yeast and *Dictyostelium* (Kahn, Goddard, and Newkirk 1988). Homologues of the ARF family were initially identified in yeast and human through the use of cross-species hybridisation of the coding region of the bovine gene (Sewell and Kahn 1988; Peng et al. 1989; Bobak et al. 1989; Kahn et al. 1991). An *in vitro* assay to determine if these putative ARF genes could also act as a cofactor in cholera toxin-dependent ADP-ribosylation of G_s was used to demonstrate the functional conservation (Kahn and Gilman 1984). The functional conservation of ARFs was later shown *in vivo* by rescuing a yeast lethal double mutant, arf1_arf2_, by expressing human ARF1 or ARF4 (Kahn et al. 1991).

A homologue in *Drosophila melanogaster* was found only after the discovery of a paralog, arl, an arf-like gene with 55% identity to ARF (Tamkun et al. 1991; Murtagh et al. 1993). Interestingly, arl could bind and hydrolyse GTP, however it was not able to act as a cofactor in cholera toxin-dependent ADP-ribosylation of G_s, whereas

extracts from homogenised whole flies were found to have ARF activity indicating the presence of a functional ARF homolog and suggesting a distinct physiological role for arl (Tamkun et al. 1991). This was the first description of the ARF-like (ARL) subfamily of GTPases. More recently the use of bioinformatics along with the publication of reference genome sequences has allowed for the identification of many more ARF and ARL family members across eukaryotes (Li et al. 2004).

1.5.4 ARF genes and health

As discussed, ARFs were first identified from their interaction with the Cholera toxin, it is perhaps unsurprising then that many other bacterial and viral pathogens also hijack ARF proteins including: Chlamydia (Balana et al. 2005), Legionella (Nagai et al. 2002), Enteroviruses (Hsu et al. 2010), Salmonella (Humphreys et al. 2013), Rickettsia (Rennoll-Bankert et al. 2015) and Hepatitis C virus (Matto et al. 2011). The ARFs can be hijacked in different ways, for example Rickettsia uses a guanine exchange factor RalF to activate and recruit Arf6 at the plasma membrane to promote the endocytosis of the bacterial pathogen (Rennoll-Bankert et al. 2015). Whereas Legionella, which uses the same guanine exchange factor, RalF, acquired through horizontal gene transfer from Rickettsia, activates and recruits Arf1 to stabilise the vacuoles where the bacteria replicate (Nagai et al. 2002; Amor et al. 2005).

ARFs and their GEFs have also been implicated in the regulation of developmental processes, particularly neuronal development. The GEF EFA6A promotes dendritic spine formation in hippocampal neurons in an Arf6-dependent manner (Choi et al. 2006), furthermore, a hyper-active mutant of Arf6 expressed in hippocampal neurons promoted the formation of dendritic spines at the expense of filopodia. In addition, evidence for of GEFs and ARFs in neuronal development is the finding that mutations in the GEF gene IQSEC2 cause nonsyndromic intellectual disability (Shoubridge et al. 2010) and mutations in ARFGEF2 which cause failure in neuronal migration leading to the cerebral cortex being severely underdeveloped

(Sheen et al. 2004).

Finally, ARFs have been shown to play a role in development in mammals through a link to the Wnt signaling pathway (Yu et al. 2014). Here, the authors showed that the mammalian homologues of *arf-3*, Arf4 and Arf5, both regulate the retrograde trafficking of Wntless (WLS) from the golgi to the endoplasmic reticulum by assisting the formation of COPI-coated vesicles. WLS is a recycling cargo receptor that moves newly palmitoleated Wnts from the ER to the Golgi and then to the plasma membrane for secretion out of the cell. Wnt signaling plays an important role in regulating asymmetrical seam cell divisions in *C. elegans*, however, to date no link to *arf-3* has been made in this context.

1.5.5 ARFs in *C. elegans*

The ARF family has diverged across eukaryotes and comprises several members that fall into three different classes based on their phylogenetic relationships. Each of these classes is represented by a single homologue in *C. elegans*; Class I - *arf-1.2* (ARF1, ARF2 & ARF3 in mammals), Class II - *arf-3* (ARF4 & ARF5 in mammals) and Class III - *arf-6* (ARF6 in mammals). To date, little is known about the role of ARFs in *C. elegans* however, they exhibit a high degree of conservation both in sequence identity and function with other eukaryotes (Li et al. 2004) thus a better understanding of their role in the nematode will provide more comprehensive understanding of ARFs in other systems. Recently some studies have been published investigating the roles of ARFs in development in *C. elegans*. *arf-1.2* has been shown to play a role in the development of the excretory system of *C. elegans* where RNAi-mediated knockdown and knockout of the *arf-1.2* gene resulted in the formation of large intracellular vacuoles at the growth sites of the excretory canals (Kage-Nakadai et al. 2018). Using fluorescent markers the authors report that a constitutively active mutant of *arf-1.2* exhibited a punctate pattern of protein localisation while a dominant negative mutant exhibited a more cytosolic distribution (Kage-Nakadai et al. 2018).

arf-1.2, *arf-3* and the homologue of human BIG1 and BIG2 GEFs, *agef-1*, have all been studied in the context of vulval development (Skorobogata et al. 2014). Here the authors showed that *agef-1*, along with *arf-1.2* and *arf-3*, inhibit the localization of LET-23 EGFR to the basolateral membrane in the vulval precursors, inhibiting vulval induction. Knockdown of *arf-1.2* or *arf-3* and the hypomorphic allele *agef-1(vh4)* suppress the vulvaless phenotype of *lin-2(e1309)* mutants.

Finally, the ARFGAP, *cnt-2* has been found to play a role in regulating the symmetry of divisions of the Q.p neuroblast (Singhvi et al. 2011). The wildtype Q.p neuroblast divides asymmetrically, producing an anterior daughter, which has the ability to divide further, yielding three neuronal cells, and a posterior daughter which undergoes programmed cell death. In *cnt-2* mutants both cells adopt the proliferative fate of the anterior daughter giving rise to extra neurons. The ARF GTPase involved in this process was not identified but *arf-3* remains the strongest candidate (Singhvi et al. 2011; Teuliere et al. 2014).

arf-3 appears to be involved in the development of several tissues in *C. elegans* including neurons, the vulva and the seam cells. In this thesis I explore its role primarily in the seam cells because of its association with *scm::gfp* as a marker of seam cell fate. The role of seam cells in the secretion of the cuticle and alae also makes it an excellent system to study the intersect between intracellular trafficking and the control of stem cell divisions.

1.6 Summary

In *C. elegans*, little is known about the function of *arf-3*, however, previous work in the Woollard lab has identified the *arf-3* locus as the promoter region driving the expression of the seam cell marker (*scm*). The seam cells are a population of stem-like cells that run along the lateral sides of the worm which divide both symmetrically, to expand the pool of progenitor cells, and asymmetrically to generate various differentiated cells including hypodermal and neuronal cells. The seam cells also have a secretory function; giving rise to the cuticle and the alae. Seam cells in

C. elegans do not retain their proliferative property through adult life, terminally differentiating at the end of development by undergoing homotypic fusion to produce the adult seam cells whose function is to secrete cuticle components. Thus the seam cells make an excellent model for studying the molecular basis of cell fate determination as well as more cell biological aspects of development, including the re-shaping of cells during differentiation, the polarity of cell fate allocation and cellular trafficking processes accompanying secretion. Given the role of ARFs in regulating intracellular trafficking, and the importance of intracellular trafficking to the integration of developmental signals and secretion (a major function of the seam cells), *arf-3* is a strong candidate for further investigation. The aims of this study are summarised below:

- To understand the role of *arf-3* in seam cell devlopment and development of the worm more generally. I will use available mutants and RNAi to perturb *arf-3* in *C. elegans*.

- To understand how ARF-3 is regulated at the level of the protein; where it is localised in the seam cells, how its distribution changes over time and how this may contribute to its role in development. I will generate transgenic strains expressing flourescent reporters, that I will image with confocal microscopy to probe this.

- To identify the transcription factors regulating the expression of *arf-3*. Specifically I will use availble ChIP datasets from modENCODE and modERN to identify factors that bind at the *arf-3* locus. I am especially interested in those that bind to the promoter region that drives *scm::gfp*.

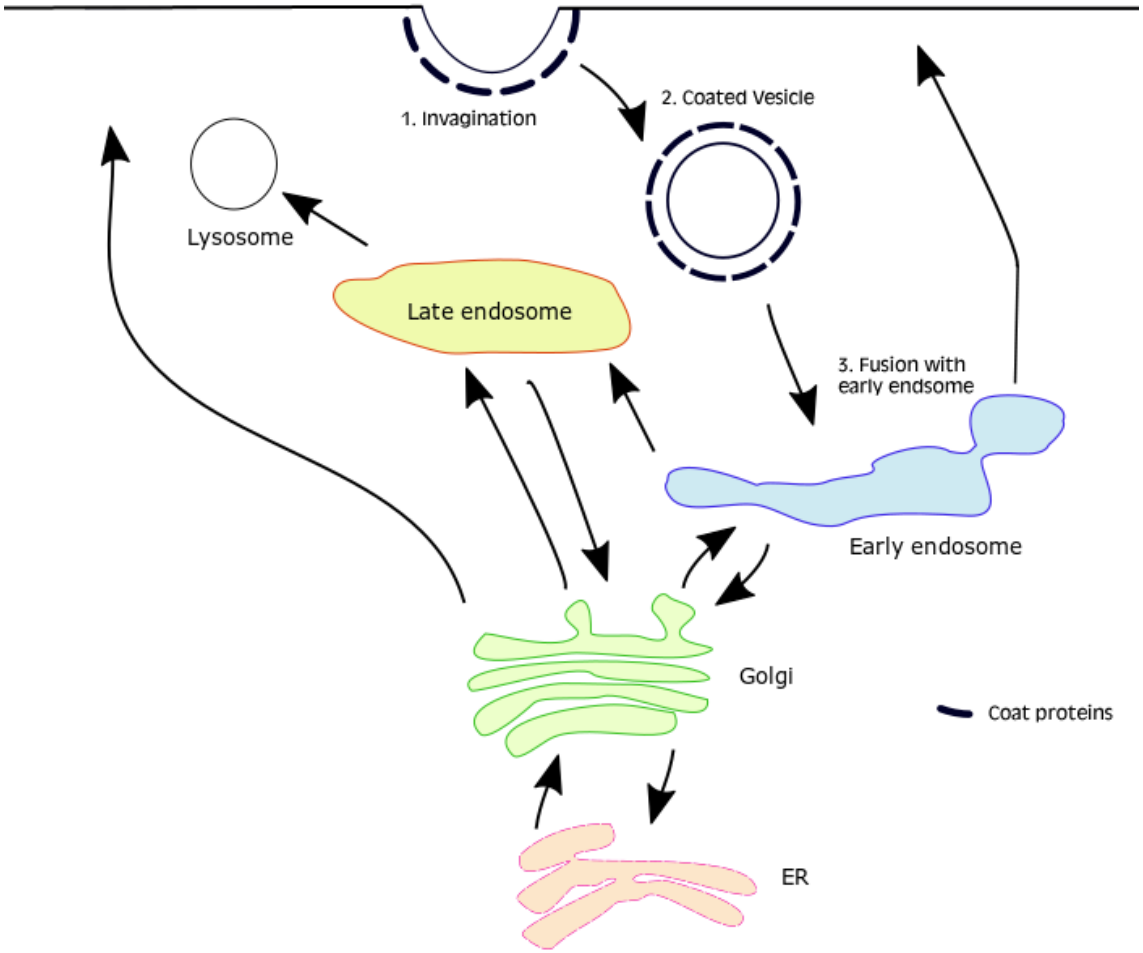


Figure 1.5: Intracellular trafficking pathways. Targets at the cell surface are internalised by invagination of the plasma membrane (1). Coat proteins are localised to the membrane surface to induce membrane curvature and formation of a vesicle (2). The coat proteins are disassembled once the vesicle is formed so that the vesicle can fuse with the early endosome (3). The early endosome trafficks the cargo to the appropriate organelle, or back to the cell surface, in a process that is not fully understood. Cargo destined for degradation is trafficked to the lysosome. Black arrowheads indicate the direction of trafficking between organelles. Coat proteins stabilise vesicles in all these pathways.

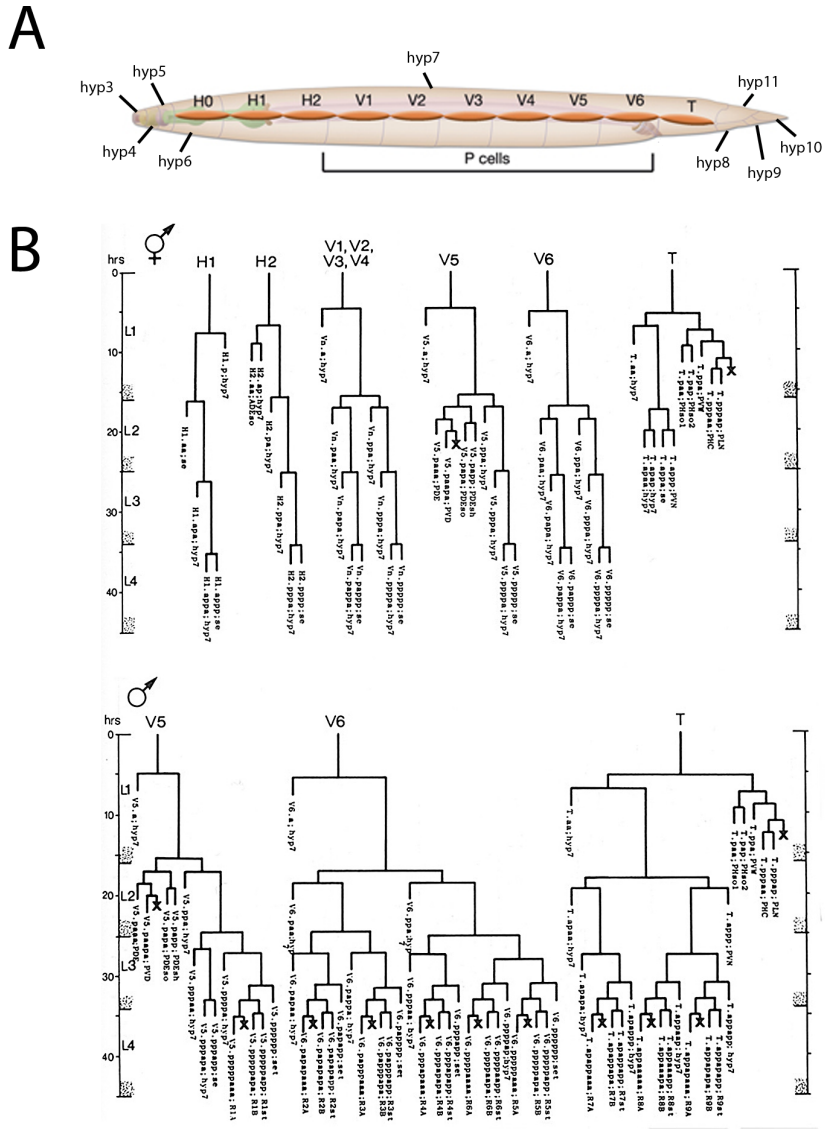


Figure 1.6: Post embryonic development of the hypodermis and seam cell lineages. A: A schematic of the hypodermal and seam tissues in the L1 animal at hatching, adapted from WormAtlas. The anterior is on the left of the image and posterior to the right. At hatching, the main ventral hypodermis is formed of P cells. During development of the L1 larva the P cells migrate to the ventral midline where they divide to contribute cells to the ventral nerve cord, hyp7, the developing vulva in hermaphrodites and the hook mating structure of the tail in males (P10 and P11). B: The post embryonic lineage of the lateral seam cells as observed in Sulston and Horvitz 1977. With the exception H0 the seam cells divide during each larval moult (hours post-hatching are shown on the left; crosses indicate programmed cell death). V1-4 and V6 display the stereotypical seam lineage in the hermaphrodite with one asymmetrical division at each larval stage until adulthood with an additional, symmetric cell division at L2. Hypodermal daughters of asymmetric seam divisions move out of the line of the seam and fuse with the hyp7 syncytium. V5 and the T cell give rise to neurons and glial cells, and proceed through a series of divisions which differ markedly from the stereotypical lineage.

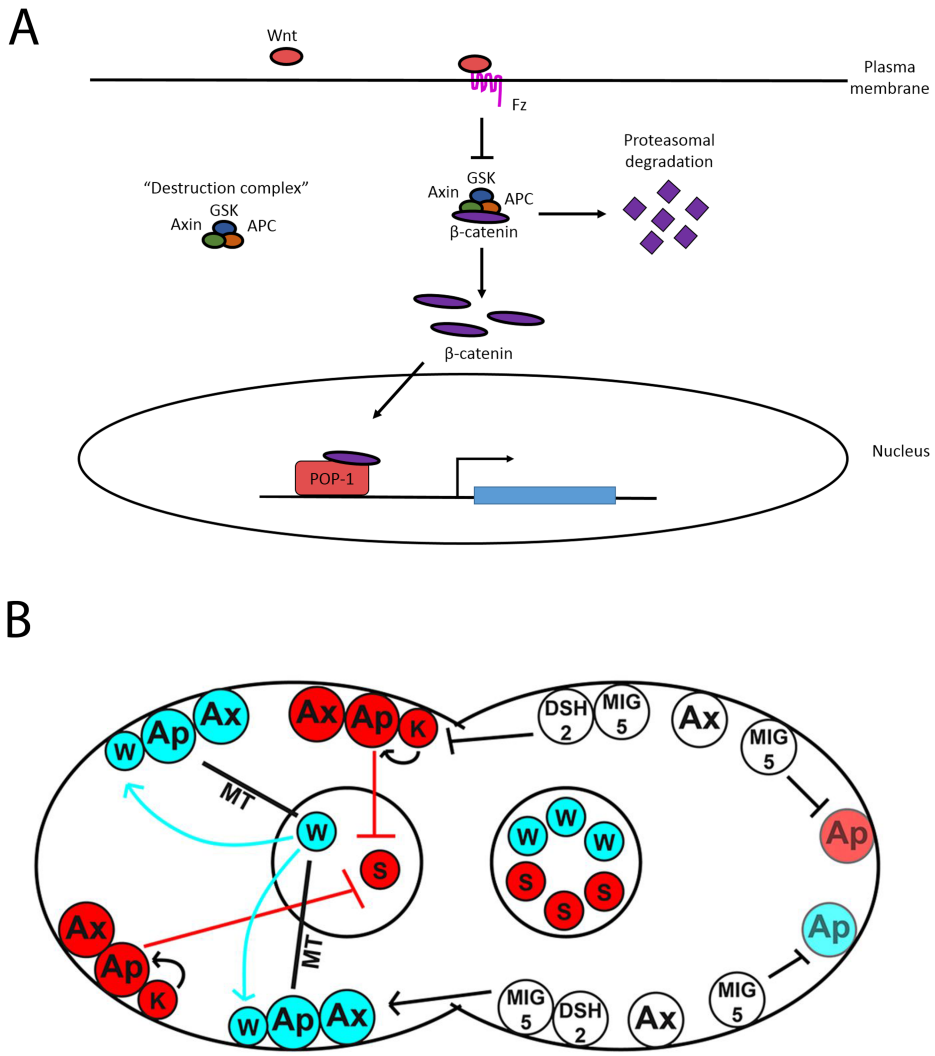


Figure 1.7: WNT signaling in *C. elegans*. A: The canonical WNT signaling pathway is shown where the degradation complex of Axin, APC and the kinase GSK3β targets β-catenin for degradation by the proteasome. When a Wnt ligand binds the receptor Frizzled (Fz) at the plasma membrane this starts a signalling cascade that inhibits the destruction complex and β-catenin is translocated into the nucleus to activate POP-1 (Tcf). B: The divergent WNT/β-catenin asymmetry pathway (from Baldwin, Clemons, and Phillips 2016 uses the asymmetrical localisation of Wnt components and the β-catenins WRM-1 and SYS-1 to generate an asymmetrical division. In the posterior cortex SYS-1 is stabilised in a manner similar to the canonical pathway and is translocated to the nucleus. MIG-5 promotes the localisation of APR-1 to the anterior cortex, where it stabilises microtubules to facilitate the localisation of WRM-1 to the anterior cortex. S = SYS-1/β-catenin (red); W = WRM-1 (blue); Ax in re = SYS-1-regulating PRY-1; Ax in blue = WRM-1-regulating PRY-1; Ap in red = SYS-1-regulating APR-1; Ap in blue = WRM-1-regulating APR-1; K in red = KIN-19; MT = microtubules.

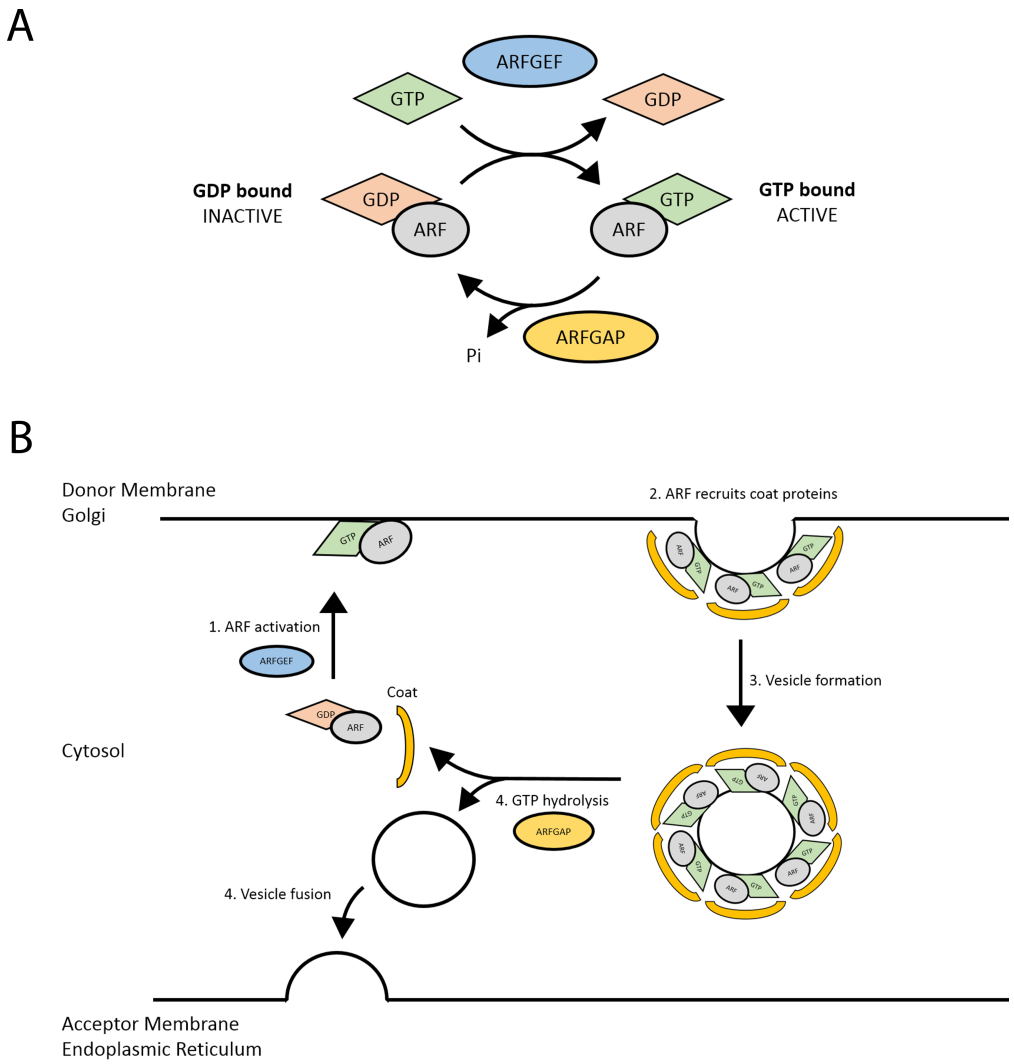


Figure 1.8: ARFs as regulatory switches. A: ARFs act as regulatory switches; in their active, GTP-bound state, they undergo a conformational change so that the ARF can associate with membranes and regulate signal transduction. GTPase activating proteins (GAPs) stimulate the GTPase activity of the ARF returning it to the inactive, GDP bound form by hydrolysis of the GTP. Guanosine exchange factors (GEFs) cause GDP to dissociate and the GTPase can bind to a new GTP. B: The canonical role of ARFs in Golgi-ER trafficking. Activation of ARF by ARFGEF allows it to localise to membranes, ARF-GTP recruit coat proteins and deform the donor membrane to form a vesicle. An ARFGAP stimulates the GTPase activity of the ARF to dissociate the ARF and coat proteins from the vesicle to allow vesicle fusion at the acceptor membrane.

Chapter 2

Methods

Table I: *Solutions and Media*

Solution or media	Recipe
BO_3 Borate buffer (40x)	618 mg H_3BO_3, 5 mL 1 M NaOH, ddH_2O to 10 mL. pH adjusted to 9.2
Bleach solution	2 ml 5% sodium hypochlorite, 1 ml 4 M NaOH, 7 ml dH_2O
C elegans freezing solution	2.93g NaCl, 3.4g KH_2PO_4, 150g Glycerol, 2.8mL 1M NaOH. Distilled water up to 500 mL and autoclaved
M9 buffer	3g KH_2PO_4, 6g Na_2HPO_4, 5g NaCl, dissolved in 1L ddH_2O. Mixed and autoclaved. Once cooled add 80 µL 1M $MgSO_4.7H_2O$.
Phosphate Buffer Saline (10x)	80g $NaCl_2$, 2g KCl, 14.4g $Na_2HPO_4.2H_2O$, 2.4g KH_2PO_4, 900 ddH_2O. Adusted pH to 7.4. Brought up to 1L with ddH_2O.
PBST	1x PBS, 0.2% Tween-20
Ruvkuv Finney Buffer (RFB; 2x)	1.6 mL 1M KCl, 80 µl 5M NaCl, 0.4 mL 0.5M EGTA, 0.6 mL 0.5 PIPES (pH 7.4), 0.1 mL spermidine, 5 mL methanol, 2.22 mL ddH_2O
TBE buffer	45 mM Tris-base, 45 mM H_3BO_3, 1 mM EDTA
Tris-Triton Buffer (TTB)	1mL 1M Tris-HCl (pH 7.4),100 µL Triton-X-100, 20 µL 0.5M EDTA, ddH_2O to 10 mL
2xTY + ampicillin plates	16g Tryptone, 10g Yeast extract, 5g NaCl, 20g Agar. Dissolve in 1L ddH_2O and autoclaved. Add Ampicillin 100mg/mL once cooled.
Worm lysis buffer	50 µmol KCl, 2.5 µmol $MgCl_2$, 10 µmol Tris-HCl pH 8.3, 0.45% NP40, 0.45% Tween 20, 0.01% gelatine and 10 mg/ml Proteinase K

2.1 Strains and maintenance of worms

All strains used were derived from the wild type N2 Bristol strain. Manipulations and maintenance of strains were performed as previously described (Brenner 1974; Wood 1988). Worms were grown on 35 mm NGM plates and fed *E. coli* strain OP50, a uracil-deficient strain that prevents bacterial lawn overgrowth. Strains were maintained by manual picking of individual animals using a flattened platinum wire or by "chunking" where a small area of agar with worms is excised and transferred onto a fresh plate. Strains were usually maintained at room temperature or at 20 °C. Strains were frozen by washing worms off a plate using M9 once they the bacterial lawn had been consumed. The worms were then suspended in a 1:1 mixture of freezing solution and M9 buffer. They were then slowly frozen in an isopropanyl freezing box at −80 °C before being moved into liquid nitrogen for long-term storage.

2.2 Generation of males by heat-shock

Males were generated from hermaphrodites for genetic crossing and outcrossing needs. 6-10 L4 hermaphrodites were picked to fresh seeded plates and heat shocked at 30 °C for 6 hours to induce chromosomal non-dysjunction. They were then transferred to room temperature to recover. Three days later male offspring were isolated and crossed back into the original stock to maintain a male population.

2.3 Genetic crosses

Genetic crosses used to generate novel strains are detailed in the Appendix. Genetic crosses were usually set up using 5 males and 2 hermaphrodites. Successful crosses between strains was deteced in several ways: by a 1:1 ratio between males and hermaphrodites in the F1 generation, by phenotyping specific traits in the F1 (for example presence of a fluorescence construct where there were none previously), or by genotyping by PCR. Homozygous F2s were picked based on either phenotype or

genotype (confirmed by genotyping PCR).

2.4 Genotyping

Where it was not possible to follow mutant alleles phenotypically, PCR was used for genotyping. In the case of deletion alleles, PCR primers were designed to anneal either side of the deletion, resulting in a single PCR product in wild type animals, a single, smaller PCR product in individuals homozygous for the deletion, and two differently-sized products in heterozygotes. Unless otherwise specified, PCR was performed using NEB Taq polymerase, using an annealing temperature of 57 °C and all other parameters as standard.

2.4.1 *arf-3(tm1877)* genotyping

The PCR reaction was cycled 30 times with an annealing temperature of 57 °C. Primers ATW49 and ATW50 were used, with an extension time of 2 minutes, 10 seconds.

2.4.2 *arf-1.2(ok796)* genotyping

The PCR reaction was cycled 30 times with an annealing temperature of 57 °C. Primers ATW55 and ATW56 were used, with an extension time of 2 minutes.

2.4.3 *blmp-1(tm548)* genotyping

The PCR reaction was cycled 30 times with an annealing temperature of 57 °C. Primers OB5 and OB6 were used, with an extension time of 1 minutes, 15 seconds.

2.4.4 *elt-1(ku491)* genotyping

The PCR reaction was cycled 30 times with an annealing temperature of 57 °C. Primers ATW51 and ATW53 were used, with an extension time of 2 minutes. The

subsequent fragment was gel purified and sequenced by Source BioScience using primers ATW65 and ATW66.

2.4.5 *apr-1(bp298)* genotyping

The PCR reaction was cycled 30 times with an annealing temperature of 57 °C. Primers ATW57 and ATW60 were used, with an extension time of 2 minutes. The subsequent fragment was gel purified and sequenced by Source BioScience using primers ATW99 and ATW100.

2.4.6 *agef-1(vh4)* genotyping

The PCR reaction was cycled 30 times with an annealing temperature of 61 °C. Primers ATW69 and ATW70 were used, with an extension time of 2 minutes. The subsequent fragment was gel purified and sequenced by Source BioScience using primers ATW67 and ATW68..

2.4.7 Genotyping of mutants generated from genome editing by CRISPR

The PCR reaction was cycled 30 times with an annealing temperature of 60 °C. Primers ATW86 and ATW87 were used, with an extension time of 4 minutes.

2.5 Agarose gel electrophoresis

DNA fragments were separated by 0.5-2% in TBE buffer. Ethidium bromide (final concentration 0.5µg/µL) was added to the gel mix cooled to 50 °C, before the gel was poured into a gel tank and allowed to set. DNA samples were mixed with loading dye buffers (10 mM Tris.HCl pH 7.4, 1 mM EDTA, 10 % glycerol, 0.1% w/v xylene cyanol or bromophenol blue). Gels were electrophoresed in 1x TBE buffer at 70 V until the desired separation of the fragments was achieved. DNA was visualised by exposure to EV transilluminator and images were collected using camera with

AlphaImager software. Molecular weight markers used: 10 kb ladder or 1kb ladder (NEB).

2.6 RNAi by feeding

RNAi was performed by feeding worms HT115 bacteria expressing double-stranded RNA corresponding to the target gene. Frozen glycerol stocks were taken from a commercially available RNAi library (Kamath et al. 2003). The desired clones were taken out of the library, sequenced, and checked for off-target effects prior to use. Custom RNAi clones were made if there was no available clone in the Ahringer library. The *pop-1* RNAi feeding clone was made by Dr Pete Appleford. Feeding bacteria were grown overnight shaking at 200 rpm at 37 °C in 2 mL of 2xTY broth containing 25 µg/mL ampicillin. 100 µl of the overnight culture was inoculated onto RNAi-optimized NGM plates (modified from regular NGM to include 10 ng/mL IPTG and 25 ng/mL carbenecillin) for a day before worms were added. RNAi experiments take place at 20 °C. Embryonic lethality resulting from *pop-1* RNAi was used as a positive control and HT115 bacteria transformed with empty L4440 vector was used as the negative control.

L4 larvae were picked onto the HT115 lawn and incubated at room temperature or 20 °C until their progeny were assessed three days later. Alternatively nematode populations were synchronised by bleaching (detailed below), and pipetted directly onto the HT115 lawn and assayed the larvae post-embryonically. For L4 RNAi, three to five L4 larvae were placed onto seeded RNAi plates and plates were incubated at room temperature or 20 °C until their progeny were ready to be examined.

2.7 Single worm lysis

Genomic *C. elegans* DNA templates for PCR, cloning into plasmids or genotyping were obtained by single worm lysis (Williams et al. 1992). A single worm was picked into a PCR tube containing 2.5 µl of worm lysis buffer and snap frozen in a thin-

walled Eppendorf tube at −80 °C for > 20mins. The tubes were then transferred to a PCR machine where they were incubated for 1 hour at 60 °C and then the Proteinase K was inactivated by 15 mins at 95 °C. The tube contents could now be used directly in a PCR reaction.

2.8 Bleach synchronization

Worms were synchronized to L1 stage by bursting gravid mothers with bleach in order to release eggs that are more resistant to bleach. Gravid worms were washed off the plates with M9 and washed three times with M9 to remove residual bacteria. Gravid adults were treated with bleaching solution (1%(v/v) alkaline hypochlorite solution) to dissolve the cuticle and obtain eggs. Wild type N2 worms dissolved after 10 minutes at room temperature. Time taken for mutant animals to dissolve varied. To remove hypochlorite eggs were pelleted by centrifugation at 560g for 1.5 min and the pellet was washed three times with M9 buffer. Eggs were left to hatch overnight at 15 °C to give rise to a population of synchronized L1 larvae.

2.9 Plasmid construction

Plasmids used in transgenic strains are listed at the start of each chapter and a complete list is in the Appendix. Where PCR products were generated from genomic DNA, N2 worms were lysed and the entire 2.5 µL lysis mix used as a template for the reaction.

2.9.1 Construction of seam expressed intracellular reporter markers

Plasmids carrying fluorescent reporters for intracellular organelles under the control of an intestinal *vha-6* promoter were provided by Barth Grant. I designed primers ATW07 and ATW08 to amplify the coding sequence but not the *vha-6* promoter.

Linearised vector backbones for each translational reporter were generated through two-step PCR amplification using primers ATW07 and ATW08.

A fragment containing the seam-specific promoter, *bro-1*-CNE, was PCR amplified using the primers ATW05 and ATW06 from pAW566. These fragments were then combined into a reaction mixture with 0.05 pmol of vector and 0.2 pmol of the fragment to be inserted along with the Gibson Assembly Master Mix (NEB). The reaction was incubated at 50 °C for 15 minutes and assembled plasmids stored at −20 °C for subsequent transformation.

2.9.2 Construction of the *arf-3* 5' promoter expression construct

pAW918, was made by amplifying the sequence 5' of *arf-3* using ATW97 and ATW98. These primers insert XbaI and SalI overhangs for restriction cloning into the minimal promoter vector pPD107.94.

2.9.3 Construction of guide RNA expression vectors

pAW919 and pAW920 were made by overlap extension PCR with primers ATW75 & ATW77 and ATW76 & ATW78 to amplify the guide RNA vector (Addgene #46169) respectively. The PCR reaction used Phusion high fidelity Taq polymerase at 53 °C with an extension time of 3 minutes, 30 seconds.

2.9.4 *dyn-1* feeding RNAi clone

dyn-1 cDNA was amplified using primers ATW93 and ATW94 with Phusion high fidelity Taq polymerase at 60 °C with an extension time of 1 minute. The resulting PCR product was cloned into pCR-XL-TOPO (Invitrogen) using T/A cloning, giving pAW921 as per the manufacturer's instructions, in which the insert lies in the forward orientation. This fragment was then cut from this plasmid with NotI and SpeI, and transferred into the L4440 RNAi feeding vector (pAW522), which had

been cut with NotI and NheI. This plasmid was named pAW922.

2.9.5 *F57H12.10* feeding RNAi clone

F57H12.10 cDNA was amplified using primers ATW01 and ATW02 with Phusion high fidelity Taq polymerase at 60 °C with an extension time of 1 minute. The resulting PCR product was cloned into pCR-XL-TOPO (Invitrogen) using T/A cloning, giving pAW923 as per the manufacturer's instructions, in which the insert lies in the forward orientation. This fragment was then cut from this plasmid with NotI and SpeI, and transferred into the L4440 RNAi feeding vector (pAW522), which had been cut with NotI and NheI. This plasmid was named pAW924.

2.10 Fosmids

I attempted to rescue *arf-3* using fosmid WRM0636aA10 which contains the *arf-3* gene as part of a 33 Kbp genomic DNA fragment in the fosmid vector pCC1FOS (Source BioScience). The fosmid was obtained from the *C. elegans* fosmid library produced by Don Moerman (see https://www.sourcebioscience.com/products/life-sciences-research/clones/genomic-clones/c-elegans-genomic-clone-collections/c-elegans-fosmid-library/).

To obtain a high copy number of fosmid DNA for injection, a single colony containing fosmid was grown overnight, with shaking at 37 °C in 5 mL 2xTY medium (with 12.5 µg chloramphenicol). The culture was inoculated into a 5 mL of 2xTY medium and grown overnight. Cells were centrifuged and DNA was purifed using the Qiagen miniprep kit according to manufacturer's instructions.

2.11 Construction of transgenic worms

I used microinjections to produce stable lines carrying transgenes as extrachromosomal arrays Injections were performed as described previously (Mello and Fire 1995) using the following transformation markers: unc-119^{+} (pDP#MM016β; (Maduro

and Pilgrim 1995)) at 10-20ng/µL; *myo-2::mCherry* (pCFJ90, Addgene #19327) at 2ng/µL (Frøkjær-Jensen et al. 2008); *unc-122::RFP* (Addgene #8938) at 10ng/µL (Miyabayashi et al. 1999).

2.12 Quantitative RT-PCR analysis

qPCR primers were designed over exon-exon boundaries to generate 150 bp amplicons (primers are listed in Table 2 in the Appendix). qPCR was performed on *elt-1(ku491)* or N2 mixed populations cultured on OP50 plates.

RNA was extracted from animals using Trizol/chloroform: animals were washed off the plates in M9, spun down for 2 minutes at 7,000 rpm, resuspended in 250 µl Trizol (Invitrogen) and snap frozen in liquid nitrogen for 30 minutes. The samples were then transferred to a 65 °C heat block and the volume of Trizol brought up to 1 mL. After 15 minutes incubation the samples were transferred to phase lock tubes and mixed vigourously with 200 µl chloroform. The samples were then centrifuged at 4 °C for 15 minutes at 14,000 rpm and the aqueous phase was transferred to a new tube. 0.5 mL of isopropanol was added to each sample and mixed gently.

The tubes were spun down for 10 minutes (4 °C, 14,000 rpm) and the supernatant was discarded. The pellet was washed twice with ice cold 70% ethanol and the spun down for five minutes (4 °C, 14,000 rpm). The pellet was dried at room temperatre for 20 minutes and then resuspended in 10 µl of RNase free water. The samples were treated with DNase I (Invitrogen) according to maufacturer's instructions and the concentration and quality of RNA was assessed using a Nanodrop-micro-spectrophotometer (Thermo Scientific).

The reverse transcriptase step was performed on 2µg of extracted RNA using the EvoScript kit (Roche) according to manufacturer's instructions. Samples of cDNA were then strored at −20 °C.

qPCR was then performed using SYBR green and Applied Biosystems kits according to manufacturer's instructions. Primers used for *arf-3* as well as controls are listed in the appendix. Relative quantification of the transcript abundance was

calculated using the $\delta\delta$Ct method (Livak and Schmittgen 2001). Each experiment was performed in three technical replicates as well as in three independent biological replicates.

2.13 Co-CRISPR

Plasmids used in transgenic strains are listed and described in the Appendix. An injection mixture of plasmids encoding gRNAs targetting *arf-3* and *dpy-10* (50ng/µL, as well as Cas9 (25ng/µL) and *myo-2::mCherry* (2ng/µL) as a selection marker. were injected into N2 animals. Transformants were selected and isolated based on expression of mCherry in the pharynx and mutations to *dpy-10*. The progeny of *dpy-10* mutants were isolated and screened for mutations at the *arf-3* locus by genotyping by PCR.

2.14 Bioinformatics

All Caenorhabditis sequences were obtained from https://wormbase.org/. BLAST searches were performed using the databases available at http://blast.ncbi.nlm.nih.gov, and in https://www.wormbase.org/tools/blast_blat. Sequences were handled and annotated using Snapgene (http://www.snapgene.com/), and alignments between *Caenorhabditis* genomic and protein sequences were performed using CLC Main Workbench 11 (https://www.qiagenbioinformatics.com/products/clc-genomics-workbench/). Transcription factor binding analysis was performed using JASPAR (Khan et al. 2018). modENCODE and modERN ChIP-seq datasets were downloaded from http://epic.gs.washington.ed ELT-1, NHR-23, BLMP-1 and DIE-1 were examined for transcription factor binding sites at the *arf-3* locus.

2.15 Microscopy

Worms were maintained using a low power Leica dissecting microscope (1-6.3x objective). This could also be used for examining obvious phenotypes such as Pvl, Unc and Dpy without the need for mounting the worms.

A low power Leica MZIII fluorescent dissecting microscope (1-10x objective) was used to visualize bright fluorescence without the need for mounting. This was primarily used for screeing the F1 generation after microinjection to identify transformants carrying fluorescent selection markers such as *myo-2::mCherry*.

Worms were picked into a 4µL drop of 25 mM Levamisole on a coverslip to immobilise them. The coverslip was then mounted on 2% agarose pads by slowly lowering the coverslip on top of the pad. Microscopy was performed on an epifluroescent Zeiss microscope fitted with with Nomarski (DIC), FITC, GFP, mCherry filters and a 63x oil immersion objective. The Zeiss microscope is fitted with an AxioCam camera and Axiovision software (Release 4.5) was used to capture fluorescent and DIC images. A Leica SP5 confocal laser scanning microscope fitted with a 488nm argon laser was used to capture all fluorescent confocal images of seam cells and the dynamics of ARF-3::mCherry puncta.

2.15.1 Visualisation of *C. elegans* cuticle collagen

Method for immunolocalisation of DPY-7 cuticle collagen was derived from the thesis of Anastasios Batas (A. Batas, PhD. thesis, 2017). *C. elegans* populations of mixed developmental age were washed off NGM agar in M9 buffer and were collected in a 1.5 mL Eppendorf tube. The animals were washed 5 times with M9 buffer and once with RFB buffer +2% formaldehyde. The worms were resuspended in 1 mL RFB buffer +2% formaldehyde. Tubes were snap frozen in a dry-ice/ethanol bath. Tubes were subsequently transferred to ice/ice water bath and samples were washed once with TTB. Samples were resuspended in TTB + 1% β-mercaptoethanol at 37 °C with gentle agitation for 1 hour. Samples were washed once with Borate buffer and incubated in Borate buffer + 0.3% (v/v) H_2O_2 at room temperature with gentle

agitation for 15 minutes. Samples were washed once again with Borate buffer and spun down to pellet the worms and resuspended in PBS-T with 0.02% sodium azide.

The samples were spun down and supernatant was discarded and the worms were resuspended in 100µL of PBS-T 1% milk and incubated overnight at 4 °C for blocking. Supernatant was removed and samples were inclubated in 100µL of PBS-T 1% milk plus the primary antibody (1:200; DPY7-5a monoclonal antibody (McMahon et al. 2003, provided by Anastasios Batas) for 4 hours at room temperature. The samples were washed three times with PBS-T, each wash was performed at room temperature for 20 minutes with gentle agitation. The samples were then incubated in 100µL of PBS-T 1% milk plus the secondary antibody (1:200; anti-mouse monoclonal Dylight 594) overnight at 4 °C. The samples were washed three times with PBS-T, each wash was performed at room temperature for 20 minutes with gentle agitation. Supernatant was removed and the samples were resuspended in 100µL of mounting solution (50% (v/v) glycerol in PBS). 30µL of each sample was placed on a polylysine coated slide and an 18mm x 18mm coverslip was gently lowered over the sample to prevent formation of air bubbles. Excess mounting solution was removed from the edge of the coverslip and the slide fixed in place with clear nail polish. Specimens were visualised using the Leica SP5 confocal microscope.

2.15.2 Analysis of fluorescent vesicle dynamics

Worms of the desired stage were mounted in 4µL drop of 25 mM Levamisole on 2% agarose pads. Two sets of images for each seam cell were taken on the Leica SP5 confocal microscope with the seam cell in focus. Z-stacks were imaged from the alae to the bottom of the seam cell. Time series were taken over the course of 300 seconds. Distance measurements and dynamics of puncta were made in Fiji using the Trackmate plugin v3.4.2 at 6 px estimated blob diameter and a threshold value of 100 (Tinevez et al. 2017). Detected spots were then filtered based on estimated size of the puncta to separate smaller vesicle dynamics from larger organelles.

2.16 Statistical Analysis

Statistical analyses were performed as indicated using GraphPad Prism (GraphPad software).

2.17 Acknowledgements

I would like to thank Charles Brabin and Sara Maxwell for the many strains and constructs created before I started this project. Furthermore I'd like to thank the *Caenorhabditis* Genetics Center (CGC), from whom some strains were obtained.

I would also like to thank Barth Grant for providing me with the organelle reporter constructs and Iain Johnstone and Anastasios Batas for sending me the DPY7-5a monoclonal antibody and the method used for immunolocalisation. Finally to Peter Appleford and Sara Maxwell for their helpful advice in producing transgenic strains via microinjection.

Chapter 3

arf-3 plays a role in development of the seam, embryogenesis, and cuticle integrity.

3.1 Overview and aims

The work in this thesis originates from a previous study in the Woollard lab to dissect the "seam cell marker", *scm::gfp*. The seam cell marker is used extensively in the study of seam cell development as a marker of seam cell fate because when seam cells undergo an symmetric division the hypodermal-fated daughter loses the expression of *scm::gfp* (Figure 3.1; Koh and Rothman 2001). The reporter is a transcriptional reporter where nuclear localised GFP is expressed in seam cells from the two-fold stage of embryonic development to adulthood.

The seam cell marker was first identified by a promoter trapping screen (Hope 1991) where genomic fragments were cloned upstream of a *lacZ* gene and transformed into *C. elegans* by microinjection. The promoter region we now call *scm* was found to drive the expression of β-galactosidase expression specifically in the seam cells. Previous work in the Woollard lab demonstrated that the 7.8 Kbp *scm* promoter region aligned to chromosome IV at the sequence containing *arf-3*, *mec-17*

and *col-115* (Figure 3.2A). We dissected the *scm::gfp* reporter further by cloning smaller fragments from *scm* into the pPD107.94 vector to identify the specific region that would drive the expression GFP-NLS in seam cells (Figure 3.2B). The 603bp region overlapping the final exon and intron of *arf-3* was found to recapitulate the seam cell expression of *scm::gfp* (Figure 3.3).

arf-3 encodes a member of the ADP-ribosylation factor (ARF) family of GTPases (Li et al. 2004). ARFs are known to regulate intracellular trafficking by acting as regulatory switches whereby activation by a guanine exchange factor (GEF) allows the ARF to associate with a plasma membrane and recruit coat proteins for the formation of a vesicle. Why a regulator of intracellular trafficking would have such specific expression in seam cells is a mystery. However, the intepretation of extracellular signals, such as Wnts, is crucial to the regulation of seam divisions. Indeed the divergent asymmetrical Wnt signalling pathway regulates asymmetrical seam cell divisons by the asymmetrical localisation of Wnt signalling components (Baldwin, Clemons, and Phillips 2016). Another role of the seam cells is the secretion of cuticle collagens and the alae (Singh and Sulston 1978), a process which relies heavily on intracellular trafficking to process proteins through the endocytic pathway.

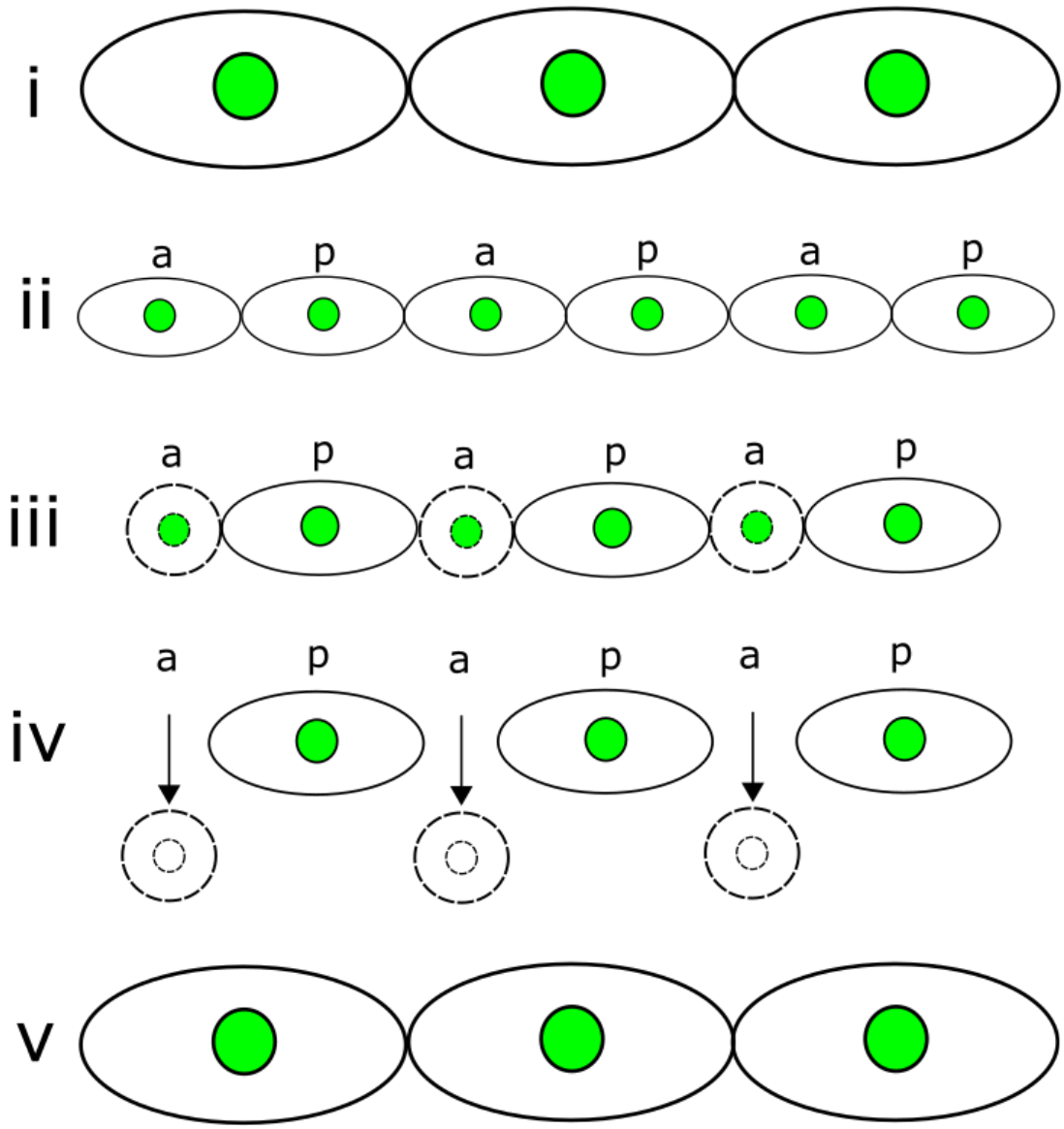


Figure 3.1: A schematic drawing of three seam cells undergoing an asymmetric divisions. a is the anterior daughter, p is the posterior daughter. GFP::NLS is expressed in the seam cell nuclei (i). The seam cells divide (ii). The anterior daughter rounds off (iii) and moves out the line of the seam (iv) and the expression of GFP is lost. Figure is not drawn to scale.

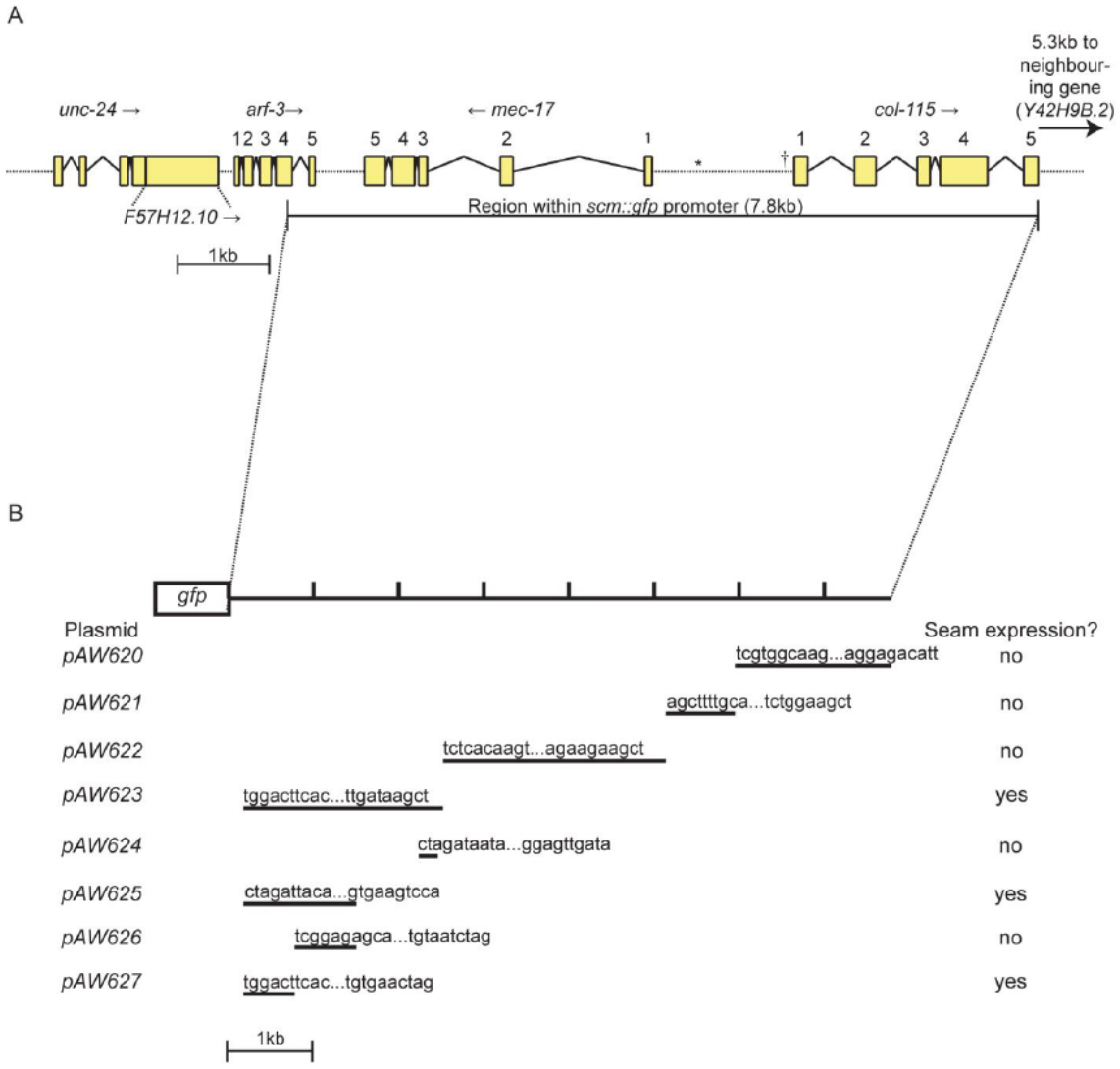


Figure 3.2: Schematic of *scm* promoter dissection from C. Brabin, D. Phil thesis, 2011. A: The *scm::gfp* promoter aligns with a region on chromosome IV. The 7.8kb region spans three genes: *arf-3* (left) and *col-115* (right), with which it overlaps partially, and *mec-17*, which it covers completely. The asterisk and dagger show the position of two genes encoding 21 nucleotide small RNAs (*F57H12.8* and *Y42H9B.4* respectively). B: Dissection of the *scm::gfp* promoter was performed by cloning the fragments shown into the minimal promoter vector *pPD107.94*, giving the plasmids listed on the left-hand side. This approach allowed the region required for seam expression to be narrowed down to the 603 bp fragment *pAW627*.

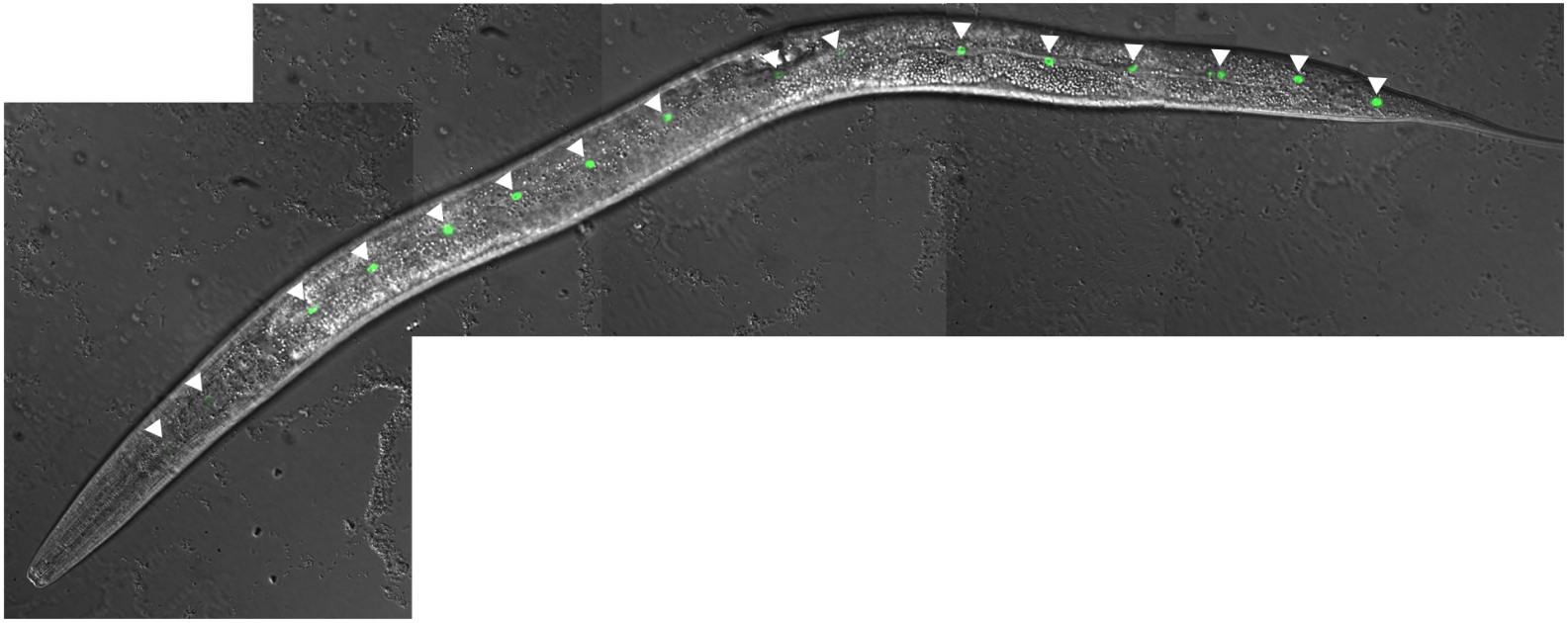


Figure 3.3: A worm expressing GFP::NLS driven by the 603 bp *scm* fragment that was cloned into pAW627. The white arrowheads indicate GFP::NLS expression in the seam cells.

3.1.1 Aims and hypotheses of this chapter

The aims of the work presented in this chapter were:

- To dissect the role of *arf-3* in *C. elegans* development through the use of available mutants and RNAi.
- To generate a rescue of the *arf-3(tm1877)* allele.
- To perform a forward genetic screen to discover potential genetic interactors of *arf-3*.

I hypothesized that:

- Knockout or knockdown of *arf-3* would cause defects in seam cell development.
- Any developmental defects observed in the seam cells in arf-3 mutants could be rescued by expression of wildtype ARF-3.
- ARF-3 in seam cells is regulated by the orthologue of human ARFGEF1

3.2 Results

3.2.1 The *arf-3(tm1877)* mutant exhibits maternal effect embryonic lethality and seam cell defects

To investigate the role of *arf-3* in seam cell development we acquired *arf-3(tm1877)* mutants from the Mitani lab. The *tm1877* allele encodes a 631bp deletion from the upstream ncRNA, *F57H12.10*, to the third exon of *arf-3* (Figure 3.4A). The *tm1877* allele was balanced with *dpy-20(e1282); unc-24(e138)* to give strain AW715 and the *scm::gfp* marker was crossed in by Charles Brabin to generate AW716. In these strains *tm1877* homozygotes exhibit 80% embyronic lethality; the embryos typically die between the comma and 2-fold embryonic stages (Figure 3.4B), this may suggest

TABLE I: *Strains used in Chapter 3*

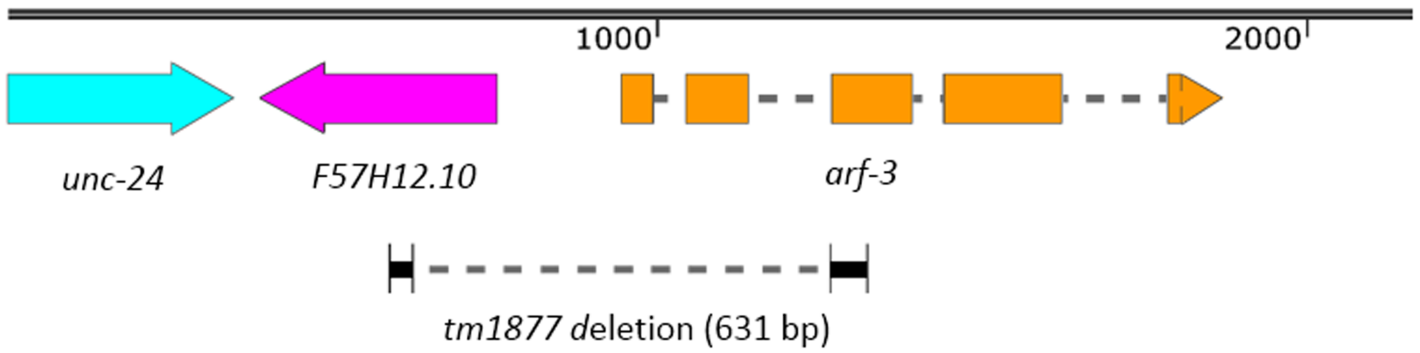
Strain	Genotype	Plasmids in extrachromosomal arrays
AW60	*him-5 (e1490); wIs51[scm::gfp + pAW135]V*	pAW135 = unc-119 rescue plasmid
AW715	*arf-3(tm1877)IV / dpy-20(e1282)IV; unc-24(e138)IV*	
AW716	*arf-3(tm1877)IV / dpy-20(e1282)IV; unc-24(e138)IV; wIs51[scm::gfp + pAW135]V*	pAW135 = unc-119 rescue plasmid
AW718	*rrf-3(pk1426)II; wIs51[scm::gfp + pAW135]V*	pAW135 = unc-119 rescue plasmid
AW740	*dpy-20(e1282)IV; unc-24(e138)IV; wIs51[scm::gfp + pAW135]V*	pAW135 = unc-119 rescue plasmid
AW860	*unc-119(ed3)III; ouEx721[pAW740 + pAW135]*	pAW740 = arf-3::mCherry; pAW135 = unc-119 rescue plasmid
AW1791	*arf-3(tm1877)IV / dpy-20(e1282)IV; unc-24(e138)IV; wIs51[scm::gfp + pAW135]V; ouEx1197[pAW558 + pAW378 + pCFJ90]*	pAW558 = arf-3 locus including F57H12.10 pAW378 = unc-122p::rfp pCFJ90 = myo-2::mCherry
AW1792	*dpy-20(e1282)IV; unc-24(e138)IV; wIs51[scm::gfp + pAW135]V; ouEx1197[pAW558 + pAW378 + pCFJ90]*	pAW558 = arf-3 locus including F57H12.10 pAW378 = unc-122p::rfp pCFJ90 = myo-2::mCherry; pAW135 = unc-119 rescue plasmid
AW1793	*arf-3(tm1877)IV; wIs51[scm::gfp + pAW135]V; ouEx1197[pAW558 + pAW378 + pCFJ90]*	pAW558 = arf-3 locus including F57H12.10; pAW378 = unc-122p::rfp; pCFJ90 = myo-2::mCherry; pAW135 = unc-119 rescue plasmid
AW1801	*pAW627 + pAW135*	pAW627= scm::gfp fragment; pAW135 = unc-119 rescue plasmid
HZ194	*apr-1(bp298)I; wIs51[scm::gfp + pAW135]V*	pAW135 = unc-119 rescue plasmid
QR180	*agef-1(vh4)I*	

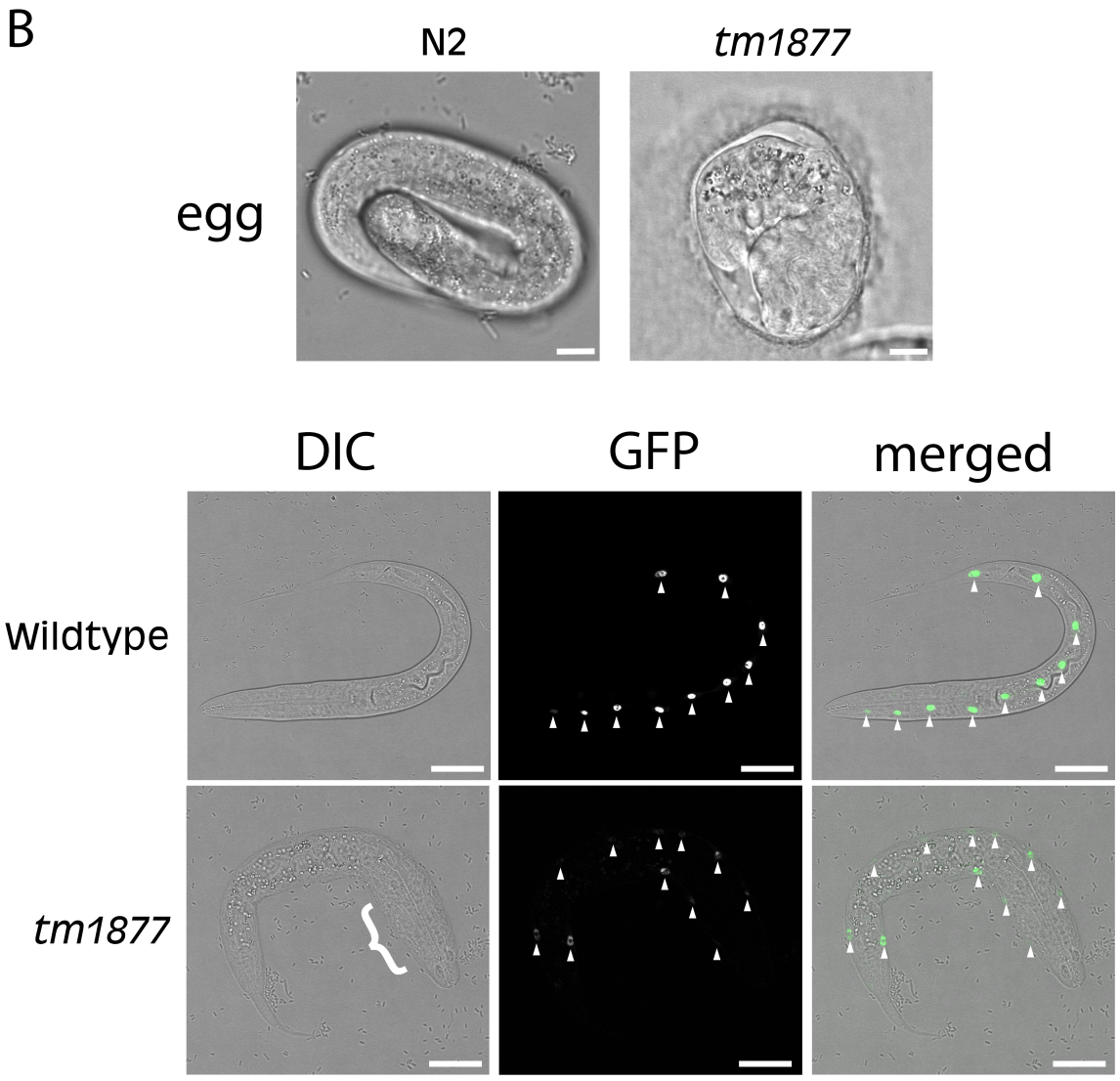
a role for *arf-3* during elongation which is known to involve the seam and epithelial cells.

Animals that survive to L1 exhibit a "lumpy dumpy" phenotype likely due to the partial rescuing effect of maternally contributed *arf-3* RNA or protein, they also exhibit seam cell defects including gaps in the seam and aberrant divisions (Figure 3.4B).

To test if any *tm1877* homozygotes survive to adulthood I isolated superficially wildtype (non-dumpy; non-unc) L4 worms from AW715 and let them develop to adulthood and reproduce for 24 hours. I then genotyped these animals by PCR to see if any *tm1877* homozygotes reached adulthood. Typically, the frequency of genotypes expected to reach adulthood from a balanced heterozygote selfing would be: 25% homozygotes for the wildtype allele; 50% heterozygotes carrying the wildtype allele and the mutant allele; and 25% of the population carrying only the mutant allele. A totally embryonic lethal allele would change these expected proportions to: 33% homozygotes for the wildtype allele, and 66% heterozygotes; with no homozygotes for the mutant reaching adulthood. I selected only superficially wildtype L4 worms; this meant I expected all of the animals to be heterozygotes. Instead, I observed 1-4% (1-4/100 in three biological replicates) of isolated animals were *tm1877* homozygotes (Figure 3.4C). Those that were *tm1877* homozygotes as determined by PCR were sterile and produced no progeny. This suggests enough maternally derived *arf-3* RNA or protein was present to survive embryonic development, and for the animals to present as wildtype at L4. However, given these animals were sterile and produced no progeny this may mean *arf-3* is also playing a role in post embryonic development.

A




B
N2
tm1877
egg
DIC
GFP
merged
Wildtype
tm1877

C

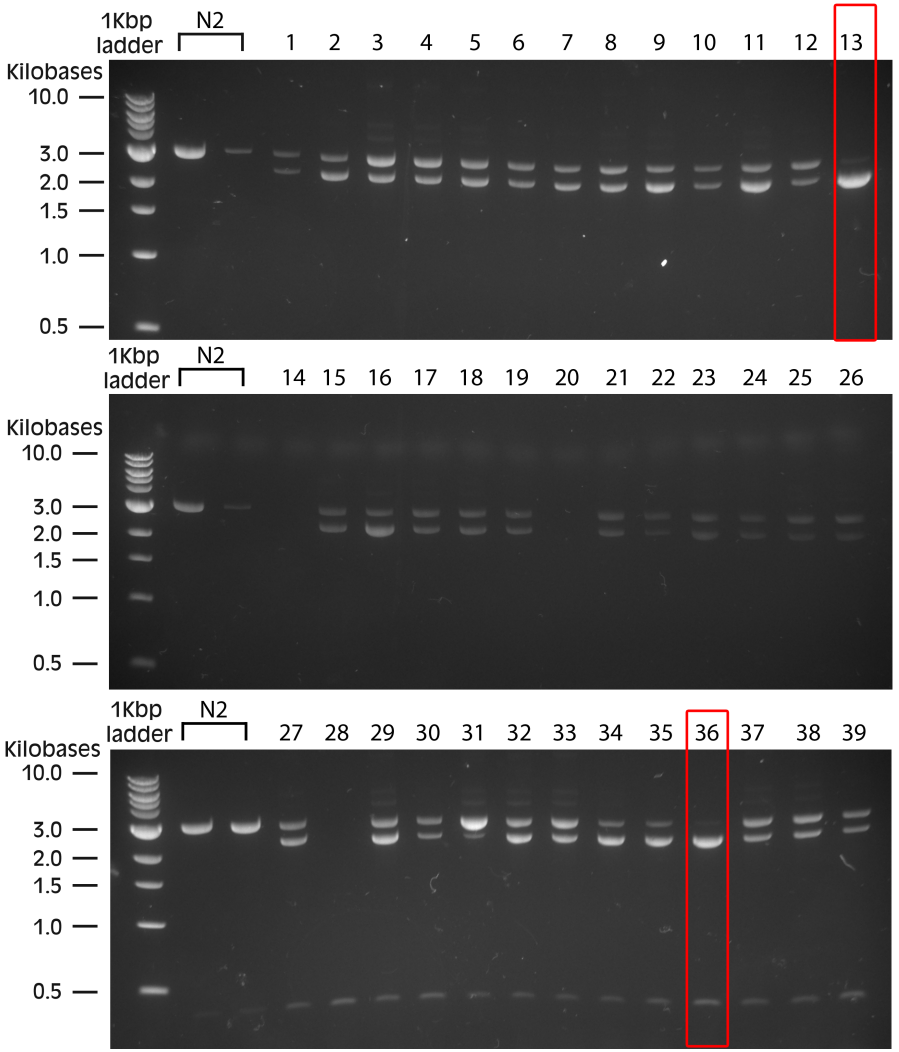


Figure 3.4: Characterisation of the *arf-3(tm1877)* allele. A shows a schematic of the *arf-3* locus including the 631bp deletion carried by *arf-3(tm1877)* mutant animals. The deletion spans from an upstream non-coding RNA to the third exon of *arf-3*. B shows representative images of *tm1877* mutant animals in the embryo and L1. Wildtype L1 larvae expressing *scm::gfp* have 10 seam cells per side whereas homozygotes for *tm1877* exhibit fewer seam cells at L1 (*scm*-positive nuclei indicate by white arrowheads). The animals exhibit a lumpy dumpy phenotype as well as seam cell defects (white bracket). C shows a representative gel from genotyping by PCR 40 AW715 adult worms. Homozygote *tm1877* adults are identified by presence of only the lower band in wells 36 and 13 (lane outlined in red).

3.2.2 Knockdown of *arf-3* by RNAi in a hypersensitive background phenocopies the *arf-3(tm1877)* mutant

Use of the *tm1877* allele is complicated because the 631bp deletion also effects and upstream ncRNA, *F57H12.10*, therefore I cannot determine if the embryonic and larval lethality I observed is because of the mutation of *arf-3* or this ncRNA. Therefore to further investigate its role in seam cell development I targetted *arf-3* specifically by RNAi in the AW60 strain, which carries *wIs51[scm::gfp]* (Figure 3.5Ai). In these animals I saw an increase in the variability of seam cell number as identified by GFP-positive nuclei, however the average seam cell number remains unchanged and the result is not statstically significant. As stated above, the *tm1877* deletion also affects an uncharacterised ncRNA, *F57H12.10*, and observed phenotypes may be wholly or patially caused by the loss of *F57H12.10* function. I used RNAi to also target this ncRNA to see if I could observe any seam cell defects and I did not (Figure 3.5Aii), supporting the role for *arf-3* in seam cell development. However, targetting such small gene products by RNAi is difficult and *F57H12.10* expression may not have been affected.

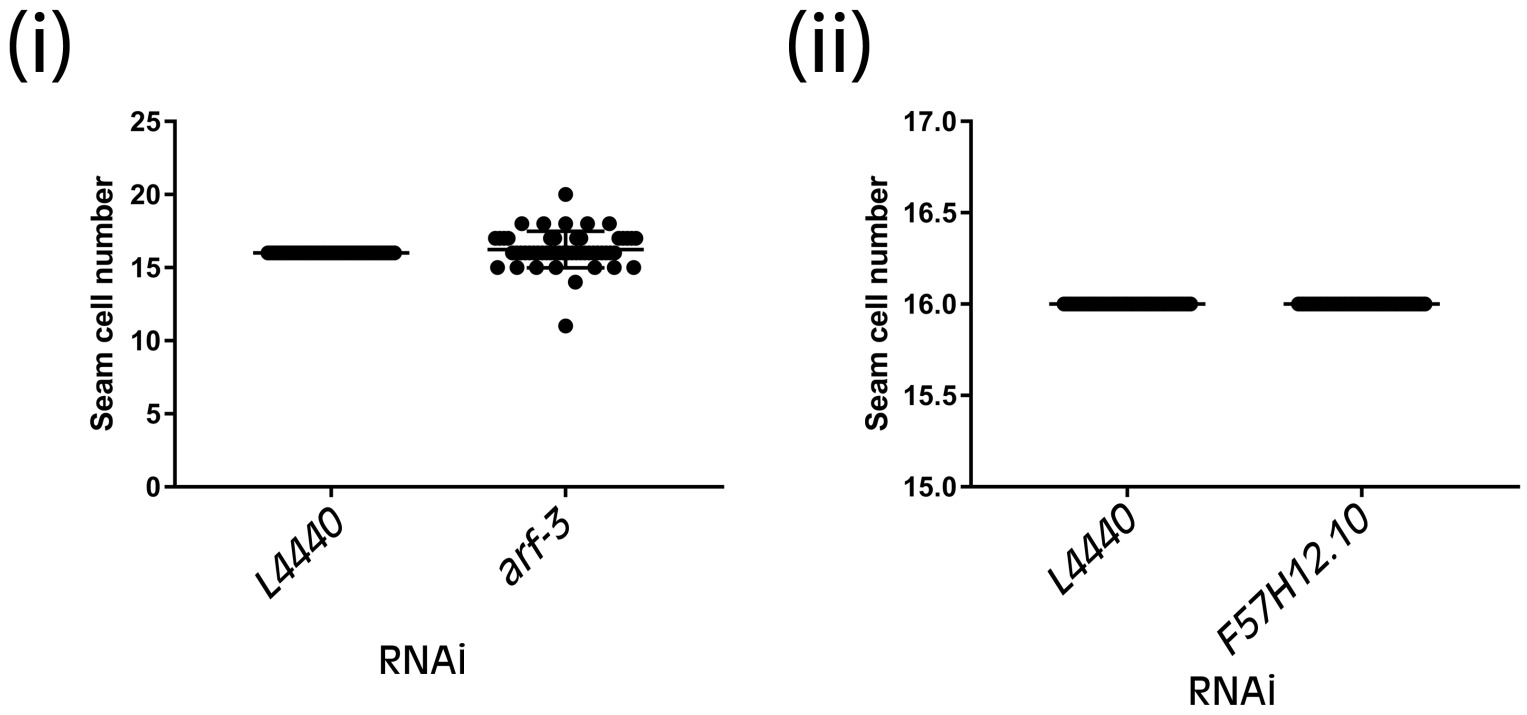
Knowing that the knockdown of genes by RNAi can vary by cell type, tissue and individual genes. I decided to use the same approach except in an RNAi-hypersensitive background using our AW718 strain which carries the integrated *wIs51[scm::gfp]* as well as *rrf-3(pk1426)*. AW718 animals treated with *arf-3(RNAi)* recapitulated the phenotypes oberseved in *tm1877*, although with a lower penetrance. I observed seam cell defects including gaps in the seam at L1 (Figure 3.5B) as well as a significant increase in the average and variability of seam cell number at the adult stage (Figure 3.25).

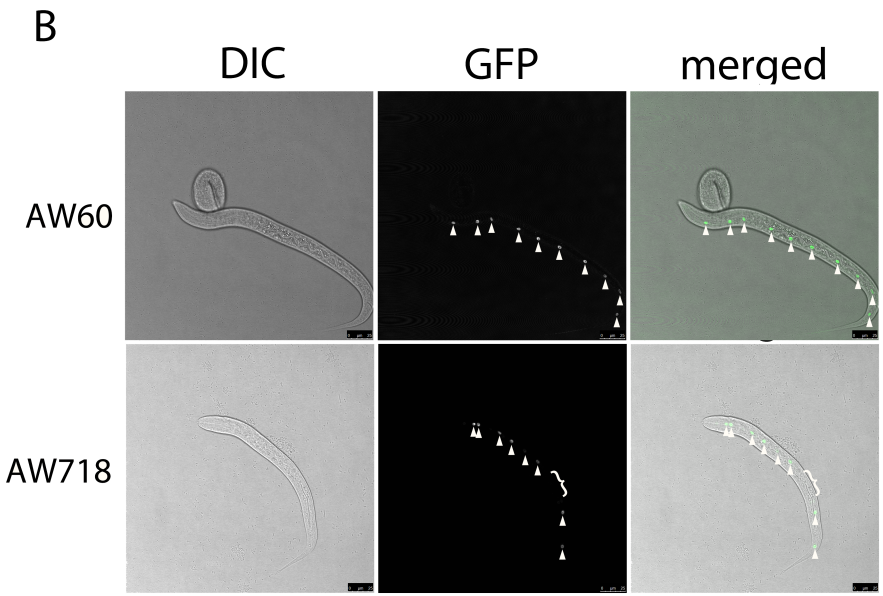
In addition to seam cell defects I also observed defects in moulting when RNAi sensitive worms were treated with *arf-3(RNAi)* (Figure 3.5D). Given the role of the hypodermis and seam in secreting the cuticle and alae I asked whether the treated animals are more sensitive to bleach. I observed a significant decrease in the time taken to the first cuticle break when treated animals were subjected to a bleaching

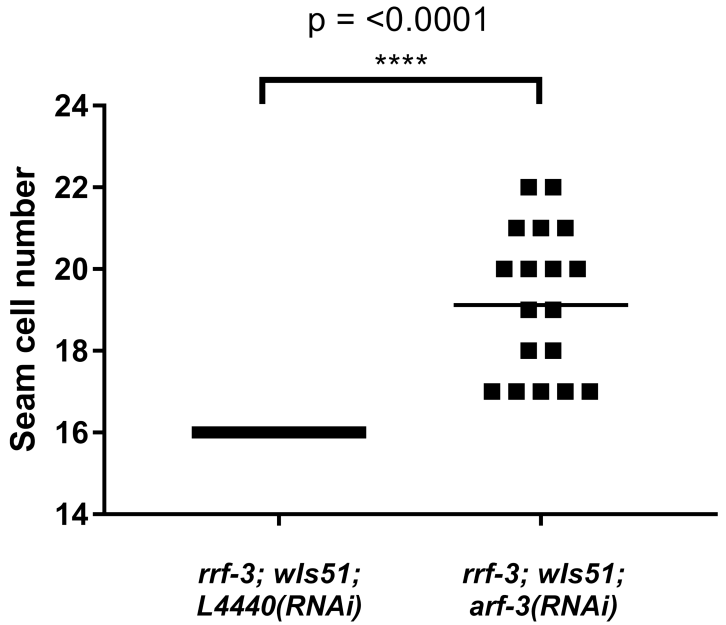
assay (Figure 3.5E) further supporting the role of *arf-3* in moulting and formation of the cuticle.

To investigate the cuticle integrity defects further I used immunolocalisation of DPY-7 collagen using an antibody provided by Anastasios Batas to visualise the annular furrows in control animals and in animals subjected to *arf-3)* RNAi. In *arf-3(RNAi)* the animals display an irregular annular furrow pattern compared to control animals (Figure 3.6). *arf-3* may be playing a role in the correct secretion and deposition of cuticle collagens. However, animals that are hypsersensitive to reducing agents are known to exhibit an irregular annular furrow pattern when exposed to *beta*-mercaptoethanol. I therefore cannot conclude that this defect is caused by perturbing secretion.

A


(i)
Seam cell number
25
20
15
10
5
0
L4440
arf-3
RNAi
(ii)
Seam cell number
17.0
16.5
16.0
15.5
15.0
L4440
F57H12.10
RNAi


B
DIC
GFP
merged
AW60
AW718


C
p = <0.0001
****
Seam cell number
24
22
20
18
16
14
rrf-3; wIs51;
L4440(RNAi)
rrf-3; wIs51;
arf-3(RNAi)

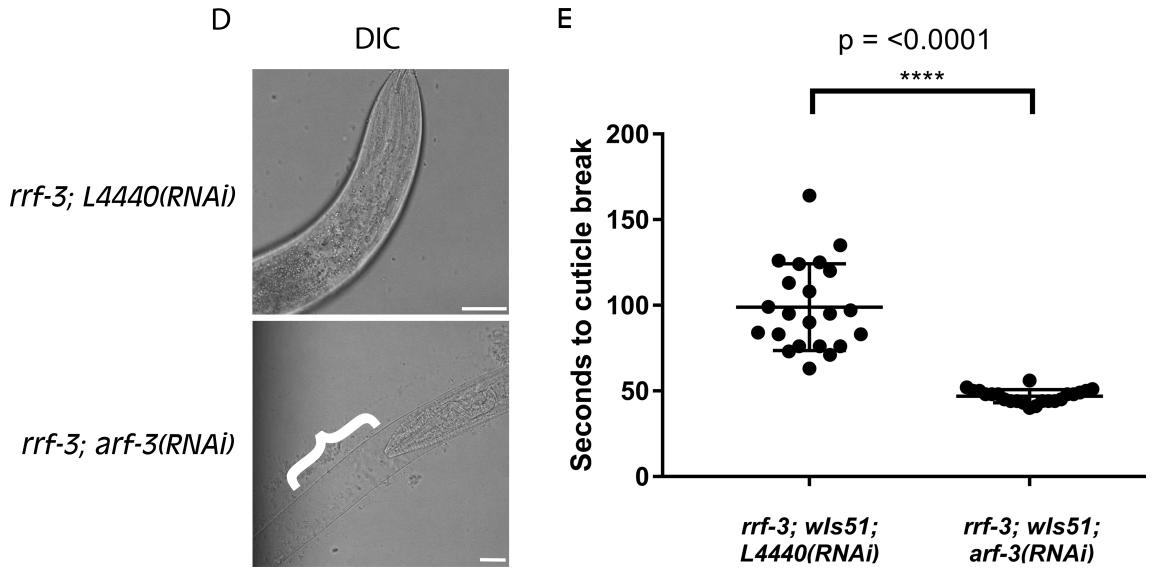


Figure 3.5: Knockdown of *arf-3* by RNAi causes defects in seam cell development and moulting. Ai shows the result of *arf-3(RNAi)* versus control *L4440(RNAi)* in *wIs51[scm::gfp]* animals. There is no significant change in average seam cell number but the variability in the population increases (N = 50). Aii shows the result of *F57H12.10(RNAi)* versus control *L4440(RNAi)* in *wIs51[scm::gfp]* animals, there is no change in seam cell number. B shows an L1 animal exhibiting a gap in the seam cells at L1 after treatment with *arf-3(RNAi)* in the RNAi hypersensitive strain AW718 (white bracket). C shows the quantification of seam cell defects in AW718 after the final L4 division a signicant increase in the average seam cell number is observed (N = 18). D shows a representative image of an AW718 *arf-3(RNAi)* worm exhibiting a moulting defect when treated with *arf-3(RNAi)* (white bracket). Moulting defects were observed in a minority of animals (12%; N = 50). E shows the result of a bleaching assay in AW718 *arf-3(RNAi)* versus control. Cuticle integrity is significantly decreased upon knockdown of *arf-3* (N > 20).

3.2.3 The *arf-3(tm1877)* mutant is rescued by the *arf-3* genomic locus

To show that the deletion of *arf-3* is responsible for the phenotypes observed in *tm1877* homozygotes I attempted to rescue these worms by expressing wildype *arf-3* from the genomic locus as a multicopy transgenic array. I was unable to generate a strain expressing an extrachromosomal array carrying the fosmid WRM0636aA10. This may be because the worms are sensitive to increasing the copy number of some or all the genes present in the fosmid. I therefore chose to express as little of the *arf-3* genomic locus as possible; not knowing where the 5' promoter was exactly I amplified the region from *unc-24* to downstream of the stop codon, including the ncRNA *F57H12.10*, with the oligos ATW49 and ATW50 and cloned the resulting fragment into TOPO-XL (Figure 3.7A).

I injected AW716 worms with this plasmid as well as *myo-2p::mCherry* and *punc-122::RFP* as selection markers. I isolated one line, AW1791 carrying the new extrachromosomal array: ouEx1197. This line was homozygous for the balancer *dpy-20(e1282); unc-24(e138)*. I generated balanced heterozygotes for *arf-3(tm1877)* which also carry the array by crossing AW1791 with AW716 males and selected non-dumpy, non-unc, *mCherry*-positive animals (AW1792). Finally to determine if the array could rescue the lethality of the *tm1877* allele I isolated wildtype adults expressing the array and genotyped mothers whose progeny were 100% mCherry-positive. I genotyped by PCR using primers ATW85 and ATW86; these primers straddle the *arf-3* genomic locus beyond the region present in the array, thus producing a band from the *arf-3* genomic locus at chromosome IV and not the array. As shown in Figure 3.7B 5/6 mothers were homozygotes for *tm1877*. Figure 3.7C shows a representative worm from the progeny of one of these *tm1877* mothers expressing the array, the selection markers are easily visible: mCherry in the pharynx and RFP in the coelomocytes. This data shows that the exogenous expression of wildtype *arf-3* can rescue the *tm1877* allele to generate viable progeny which can reproduce.

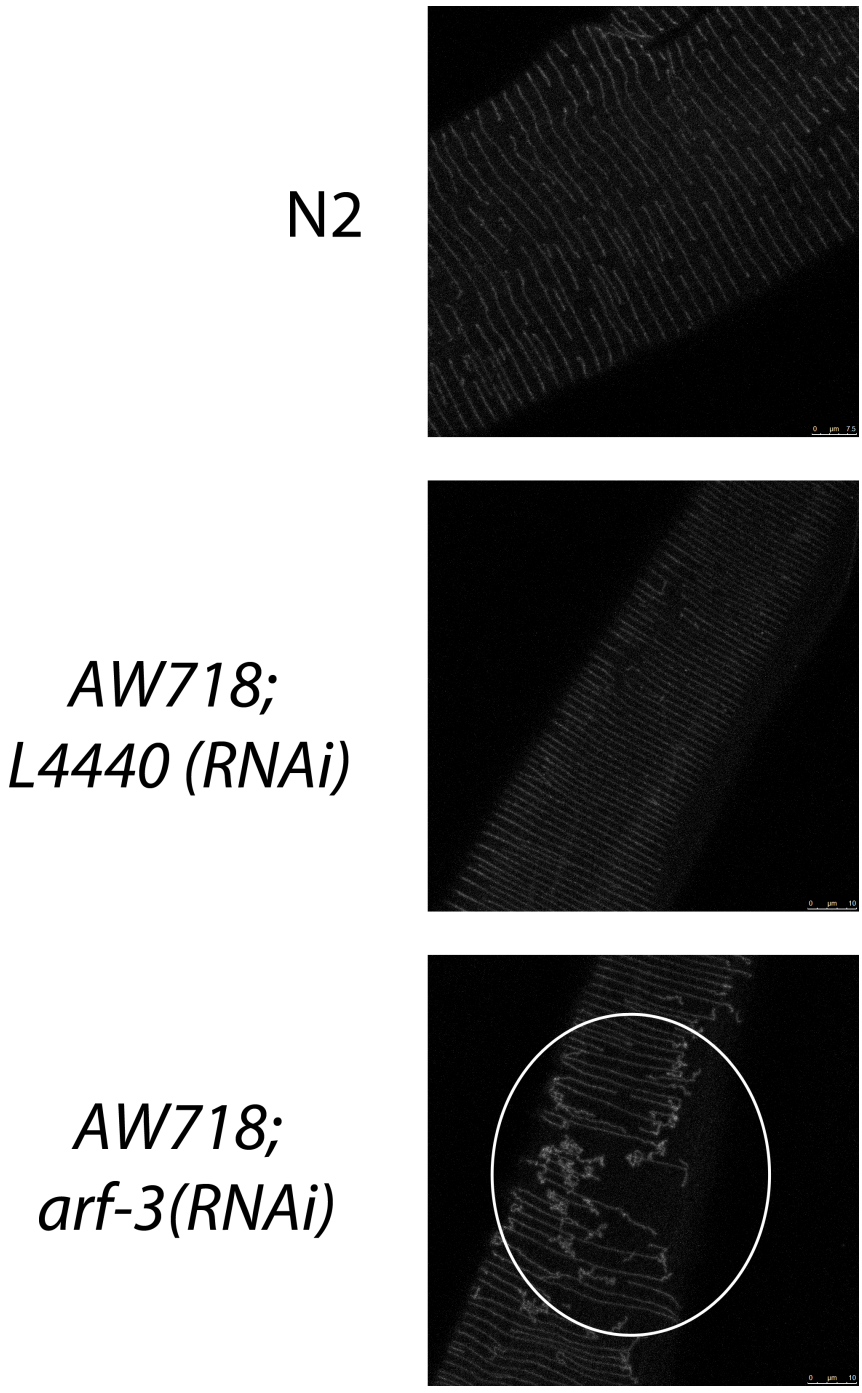


Figure 3.6: Knockdown of *arf-3* in the RNAi hypersensitive strain AW718 causes cuticle defects compared to control RNAi (L4440) and N2 controls. After treatment with RNAi the worms were stained with anti-DPY-7 primary antibody (1:200) followed by anti-mouse monoclonal IgG conjugated to Dylight 594 (1:200). N2 and AW718 exhibit a regular furrow pattern whereas in *arf-3(RNAi)* the furrows are broken and irregular (white circle). Scale bars = 10 µm.

3.2.4 Overexpression of wildtype *arf-3* causes developmental and seam cell defects

Unfortunately, there is a major caveat with this rescue: while the sterility of *arf-3(tm1877)* adults was rescued by our array there is a significant proportion of progeny that are embryonic and larval lethal. Many adults are also egg laying defective and have a tendency to bag. To determine if these phenotypes were caused by an interaction with the *tm1877* allele or by the array alone I examined animals from AW1791; homozygotes for the balancer strain carrying the array. In these worms I also saw embryonic and larval lethality (Figure 3.8A) as well as seam cell defects (Figure 3.8B). The presence of these phenotypes in animals not carrying *tm1877* shows that it is the array, *ouEx1197*, that is causing developmental phenotypes, complicating the rescue experiment. I cannot be certain if these defects are the result of overexpression of *arf-3* and *F57H12.10* or either one individually. I originally intended to follow this rescue with the generation of another extrachromosomal array which did not include the ncRNA *F57H12.10*. Instead, the introduction of a single copy of *arf-3* through MoSCI or CRISPR would be more suitable.

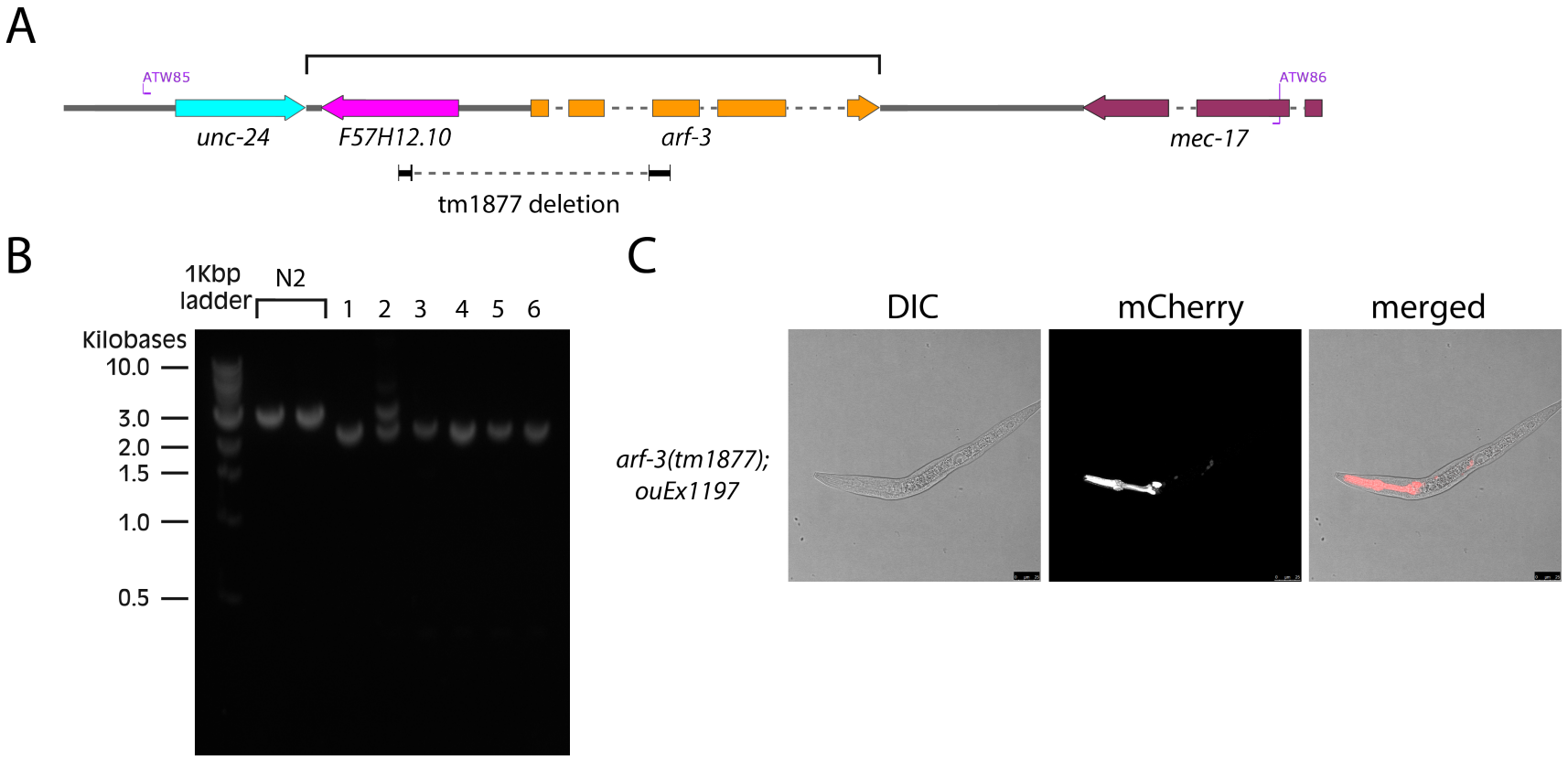


Figure 3.7: A shows a schematic of the *arf-3* locus. The black bracket indicates the fragment cloned into TOPO-XL to rescue the *tm1877* allele. The primers used to genotype worms for the *tm1877* allele are shown: ATW85 and ATW86 will only amplify a fragment from the genomic *arf-3* locus and not from the rescuing construct. B shows the genotyping of hermaphrodites carrying the rescuing array. N2 shows the wildtype *arf-3* band at 3kbp. Worms carrying the *tm1877* allele display a band that runs at 2kbp. Lanes 1, 3, 4, 5, and 6 are homozygotes for the *tm1877* allele. C shows a worm carrying the extrachromosomal array. *myo-2::mCherry* and *unc-122::RFP* were used as selection markers.

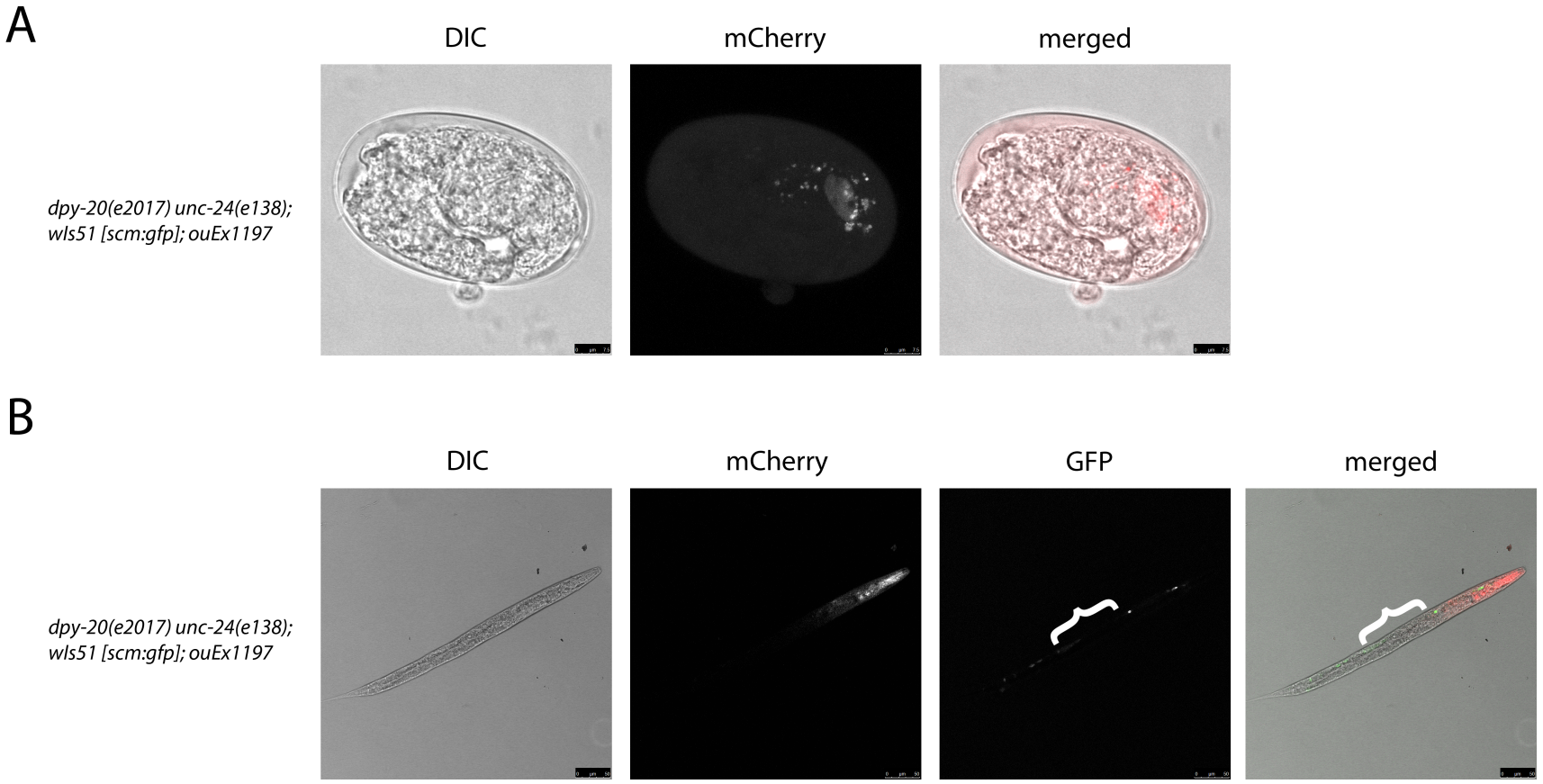


Figure 3.8: Overexpression of wildtype *arf-3* from its endogenous locus causes developmental defects. The extrachromosomal array carrying wildtype *arf-3* causes defects in embryonic development as shown in A. Defects are also observed in animals that hatch, in B the animal is dying there are gaps in the seam (white bracket).

3.3 Generating CRISPR-Cas9 mediated mutations at the *arf-3* locus

As discussed above, use of strains carrying the *tm877* allele is complicated by the unknown impact of the deletion of the upstream ncRNA *F57H12.10*. While I suspect that this ncRNA is playing no role in the context of seam cell development as I have observed no difference in *F57H12.10(RNAi)* animals, a clean deletion of just the *arf-3* coding region would be a more useful mutant for future experimentation. Therefore I aimed to develop a protocol for the use CRISPR-Cas9 in *C. elegans* in the Woollard Lab. I attempted to generate a clean deletion mutant of *arf-3* as a proof-of-principle.

I used some of the techniques already discussed in this chapter in combination with CRISPR to generate mutants in *C. elegans*. The nuclease Cas9, and guide RNAs (gRNAs) that target a specific locus, are expressed from plasmids that are injected into the gonad of early adult animals. The gRNAs target Cas9 to a specific sequence within the genome. I selected targets at the *arf-3* locus that contained the optimal PAM sequence GGNGG (Figure 3.9; Farboud and Meyer 2015). Transformants from these injections are selected and isolated based on the expression of mCherry in the pharynx. The progeny of these mothers are screened for mutations generated by Cas9. The presence of an extra chromosomal array does not necessarily mean that Cas9 is expressed and active in the germline, therefore I used co-CRISPR as an additional selection tool. Co-CRIPSR involves an additional guide RNA targetting Cas9 to the *dpy-10* locus along with a repair template containing the the dominant *rol* mutation *cn64*. The *dpy-10* locus is especially amenable to genome editing mediated by Cas9 and mutations result in phenotypes that are easy to spot. Furthermore, the phenotype varies depending if the animal is homozygous for the *cn64* mutation or heterozygous for a wildtype allele or *dpy-10* mutant. These phenotypes are summarised below:

$$\frac{dpy-10(o)}{dpy-10(o)} = dumpy(dpy) \tag{3.1}$$

$$\frac{dpy-10(cn64)}{+} = roller(rol) \tag{3.2}$$

$$\frac{dpy-10(cn64)}{dpy-10(o)} = dumpyroller(DpyRol) \tag{3.3}$$

Animals that displayed one of these phenotypes were isolated and allowed to reproduce through selfing and then genotyped for mutations at the *arf-3* by PCR using primers ATW86 and ATW87. I injected animals with the plasmid mixture shown in 3.9. I was able to reliably and reproducibly generate mutations at the *dpy-10* locus; Figure 3.10 shows a *dpy-10* mutant worm carrying the extrachromosomal array ouEx1203.

I was specifically looking for mutants that were heterozygotes for a deletion at the *arf-3* locus because we know homozygotes for the *tm1877* allele exhibit embryonic and larval lethality. Unfortunately I never observed a clean deletion allele generated through my screening. This may be because either one, or both of the gRNAs targetting Cas9 were not working. Indeed, the efficiency of gRNAs is extremely variable and few reliably generate mutations at the target site (Friedland et al. 2013). Therefore I chose to genotype by sequence at each of the target sites to see if any mutations were generated. I never observed any mutants at the 3' target site, however, promisingly, I did identify mutants at the 5' target site. Indeed one of these mutants was a predicted null allele (Figure 3.11). Unfortunately the worm carrying this null allele must have been a homozygote because it produced no viable progeny. The 5' target site is in very close proximity to the start site of *arf-3*, therefore in future generating a null mutation here will be the priority. Using a repair template that encode a null mutation will hopefully increase the chances of future success.

Overall I have developed a reliable co-CRISPR protocol for the Woollard lab

which can generate mutants at the *dpy-10* locus. Further efforts need to be made to generate a null at the *arf-3* locus.

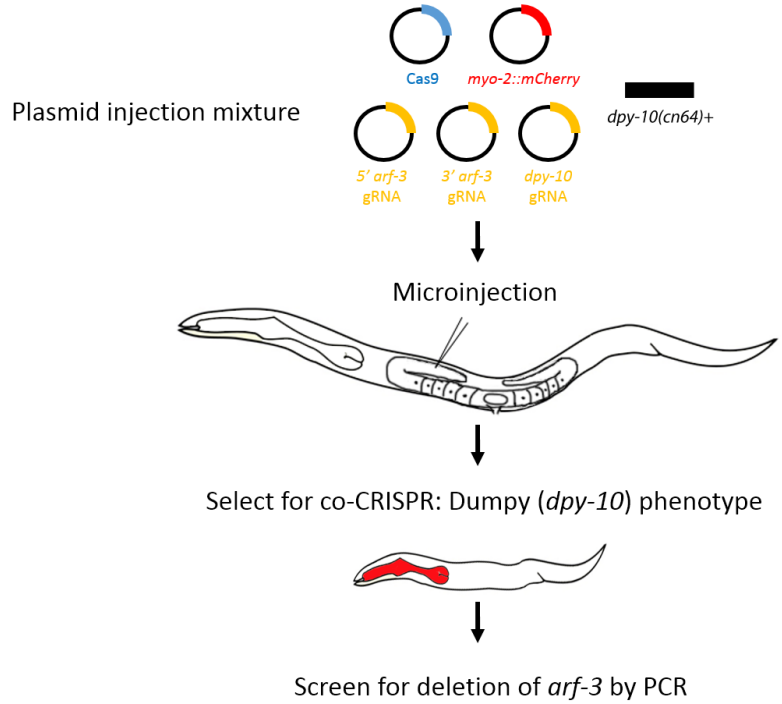


Figure 3.9: A schematic of the Co-CRISPR strategy to generate *arf-3* deletion mutants. *myo-2::mCherry* was used as a selection marker for transformants. A plasmid expressing a guide RNA for *dpy-10* and a repair template for *dpy-10(cn64)* were included to aid selection of animals expressing functional Cas9 within the germline. Transformants that carried the extrachromosomal array which expressed a functional Cas9 would display a *dpy-10* phenotype as well as a red pharynx. The offspring of these worms could then be screened for generation of an *arf-3* deletion allele.

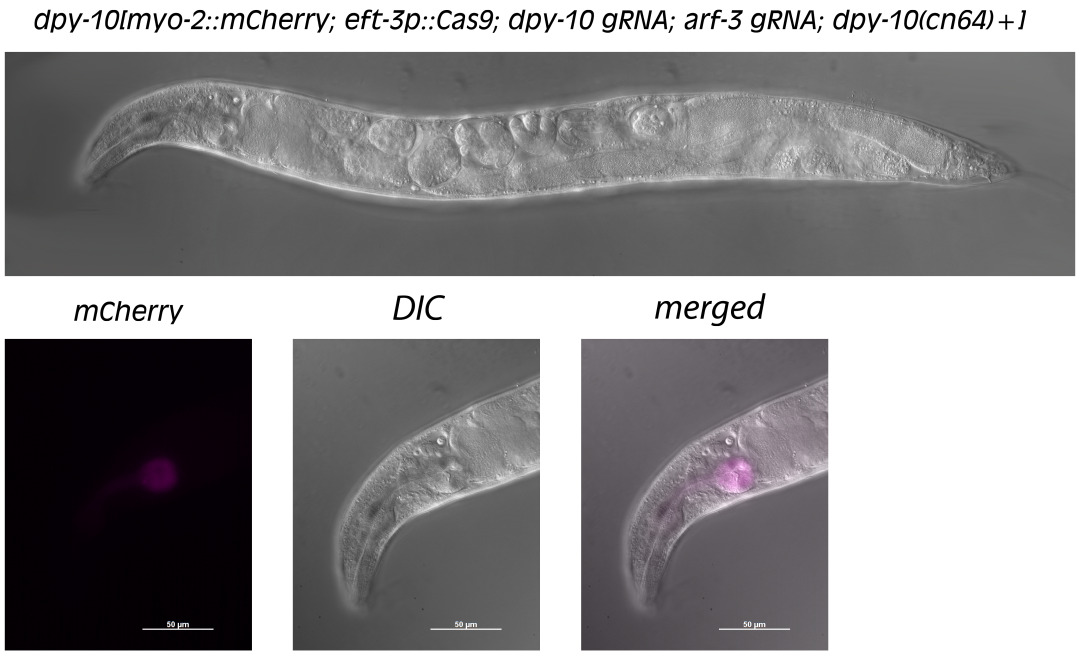


Figure 3.10: A transformant from the inection mixture shown in Figure 3.9. The worm is expressing *myo-2::mCherry* in the pharynx and the worm exhibits a *dpy* phenotype showing that Cas9 is functional.



Figure 3.11: Genotyping mutants generated from CRISPR. The wildtype *arf-3* sequence is shown at the top of the image. The first exon is indicated in the schematic in orange, the amino acid translation is also shown. Beneath this is the alignment of ten mutants genotyped for mutants at the *arf-3* locus. Most of the animals genotyped are wildtype (black brackets on the left hand side). A synonymous mutation was identified (9) as well as two missense mutants (5 and 10), these animals all exhibit wildtype phenotype. Mutant 8 encodes a mutant with an insertion at the start codon generating a presumed null, this mother produced no viable progeny.

3.3.1 ARF-3::mCherry is expressed in the seam and other tissues

The phenotypes observed for the deletion mutant suggest that *arf-3* has roles in other tissues as well as the seam. To test this we produced a translational reporter to examine the expression pattern of *arf-3* from its endogenous locus, the reporter is a C-terminal mCherry fusion of the full-length *arf-3* locus from *unc-24* to the intergenic region between *arf-3* and *mec-17*, including the endogenous promoter sequences. We chose to fuse mCherry to the C-terminus of ARF-3 because the N-terminus is essential for N-myristoylation, which is crucial for the function of ARFs. This reporter was injected into *unc-119(ed3)* animals with an *unc-119* rescue plasmid as a selection marker to produce the strain AW860. *arf-3::mCherry* expression is observed from the >200 cell embryo and continues through to adulthood (Figure 3.12). Tissues expressing ARF-3::mCherry include hypodermis, seam cells, vulva cells, body wall muscle, pharyngeal muscle and head neurons. This data suggests that while the 3' enhancer sequence drives expression of *arf-3* in the seam cells specifically, the 5' promoter drives the expression in other tissues.

Expression of this translational reporter does not rescue the *tm1877* allele but nor do animals expressing this array exhibit the developmental defects observed when wildtype *arf-3* is overexpressed, this suggests that ARF-3::mCherry may not be fully functional. However, ARF-3::mCherry does appear to behave as an ARF is expected, localising to distinct membranous puncta in the cytoplasm similar to the distribution of ARF-1.2::GFP in the excretory cell observed in Kage-Nakadai et al. 2018. Other studies have found that modification of either terminus affects the function of ARFs significantly (Jian et al. 2010), however that is not to say that the data obtained from the use of these experiments is biologically irrelevant, we can still learn much from the distribution, localisation and interacting partners of epitope tagged ARFs.

TABLE II: *RNAi screen hits*

Component	Family/Pathway	Cosmid	Gene name	Mislocalisation
Adaptor protein	Molting	*M110.5*	*dab-1*	+
Adaptor protein	Endocytosis	*Y71H2B.10*	*apb-1*	+
Adaptor protein	Vesicular trafficking	*K11D2.3*	*unc-101*	+
APC	Wnt signaling	*K04G2.8*	*apr-1*	+
ARF	Small GTPase	*Y57G11C.13*	*arl-8*	+
ARF GEF	Golgi Transport	*Y6B3A.1*	*agef-1*	+
ARF-GAP	Golgi Transport	*Y17G7B.15*	*cnt-1*	+
ARF-GAP	Golgi Transport	*Y39A1A.15*	*cnt-2*	+
Intracellular phospholipase	Lipid metabolism	*M03A1.6*	*ipla-1*	+
Other SNAREs	Vesicle fusion	*Y57G11C.4*	*vti-1*	+
RAB	Small GTPase	*T25G12.4*	*rab-6.2*	+
Rho GTPase	Small GTPase	*R07G3.1*	*cdc-42*	+
Rho GTPase	Small GTPase	*Y32F6B.3*	*crp-1*	+
Rho Kinase	Rho Kinase	*C10H11.9*	*let-502*	+

3.3.2 Knockdown of components of intracellular trafficking and signalling causes ARF-3::mCherry mislocalisation

To explain how *arf-3* contributed to the phenotypes discussed above I wanted to identify potential physical or genetic interactions. I selected a candidate list of *C. elegans* genes known to be involved in intracellular trafficking, including homologues of genes identified as interactors of ARFs in other organisms, as well as signalling pathways involved in regulating seam cell divisions. I was particularly interested in identifying the guanine exchange factor(s) and GTPase activating protein(s) that may be activating and deactivating *arf-3* respectively in the seam cells. I used RNAi to knockdown the candidate genes in our translational reporter strain, AW860, to look for changes to ARF-3::mCherry localisation. This is a heuristic approach: any change to ARF-3::mCherry distribution does not necessarily imply a direct

interaction with the knocked down gene, but it does provide sufficient evidence to investigate the genes and the pathways they are involved in further.

The list of genes targetted by RNAi is shown in Table 4 of the appendix. Table 2 in this chapter shows the targetted genes where a change to ARF-3::mCherry localisation was observed. Changes to localisation include size, shape and distribution of ARF-3::mCherry puncta. The most striking of these changes to ARF-3::mCherry localisation was the change shown in Figure 3.13, where ARF-3::mCherry puncta, which are normally distributed in distinct puncta throughout the cytoplasm, was instead distributed to a hyperconnected tubular structure upon knockdown of *agef-1, apr-1, let-502 and rab-6.2*. Of particular interest is *agef-1* the orthologue of ARFGEF1 in *C.elegans* as well as *rab-6.2* as this resides at the *trans*-golgi, where ARFs are known to function. Given the effects of knockdown and overexpression of *arf-3* and the *tm1877* allele on seam cell divisions the link to Wnt signalling through *apr-1* is especially interesting: asymmetric seam cell divisions are controlled by asymmetrically distributing Wnt components within the nucleus and cortex of seam cells in response to signalling. It is still unclear how the Wnt signal is transduced to the inactivation of the β-catenin destruction complex, *arf-3* may play a role here or in the trafficking of wnt components to the correct cortex.

3.3.3 *agef-1* regulates *arf-3* to regulate cuticle secretion and moulting

To investigate the possible interaction between *agef-1* and *arf-3* further, I acquired a viable hypomorphic allele from the Roucheleau lab *agef-1(vh4)*. *agef-1(vh4)* encodes a missense mutation (c.3082G>A; p.Glu1048Lys) in the coding region of *agef-1*. I tested whether this allele exhibited any seam cell defects by crossing in our seam cell marker *wIs51[scm::gfp]*, but I saw no significant difference.

Knockdown of *arf-3* in the *agef-1(vh4)* mutant animals causes moulting defects in approximately 40% of worms, moulting defects are typically only observed in *arf-3* knockdown in the RNAi hypersensitive strain and not in N2 or the *agef-1(vh4)*

control (Figure 3.14A and B).Given *agef-1* is the orthologue of ARFGEF1, and is therefore likely to be a regulator of ARF it is interesting to observe an additive moulting defect with *arf-3(RNAi)*. This observation supports a genuine interaction between *agef-1* and *arf-3*. *agef-1* may be activating *arf-3* through the exchange of GDP for GTP and therefore promoting moulting.

Given this link to moulting and the effect of *arf-3* knockdown on cuticle integrity in RNAi hypersensitive animals I also examined this effect in *agef-1(vh4)*. Homozygous animals for *vh4* have decreased cuticle integrity compared to N2 and are hypersensitive to bleach. Cuticle integrity was also slightly, but significantly, decreased when also treated with *arf-3(RNAi)* (Figure 3.14C).

I attempted to cross our *arf-3::mCherry* construct into the *agef-1(vh4)* background, however, heterozygotes from the cross died in the embryo or early larval stages. It is possible that *agef-1* is haploinsufficient in the presence of the overexpression of ARF-3::mCherry. The mutant allele is hypomorphic, so there is not enough wildtype *agef-1* available to perform its typical activity on ARFs.

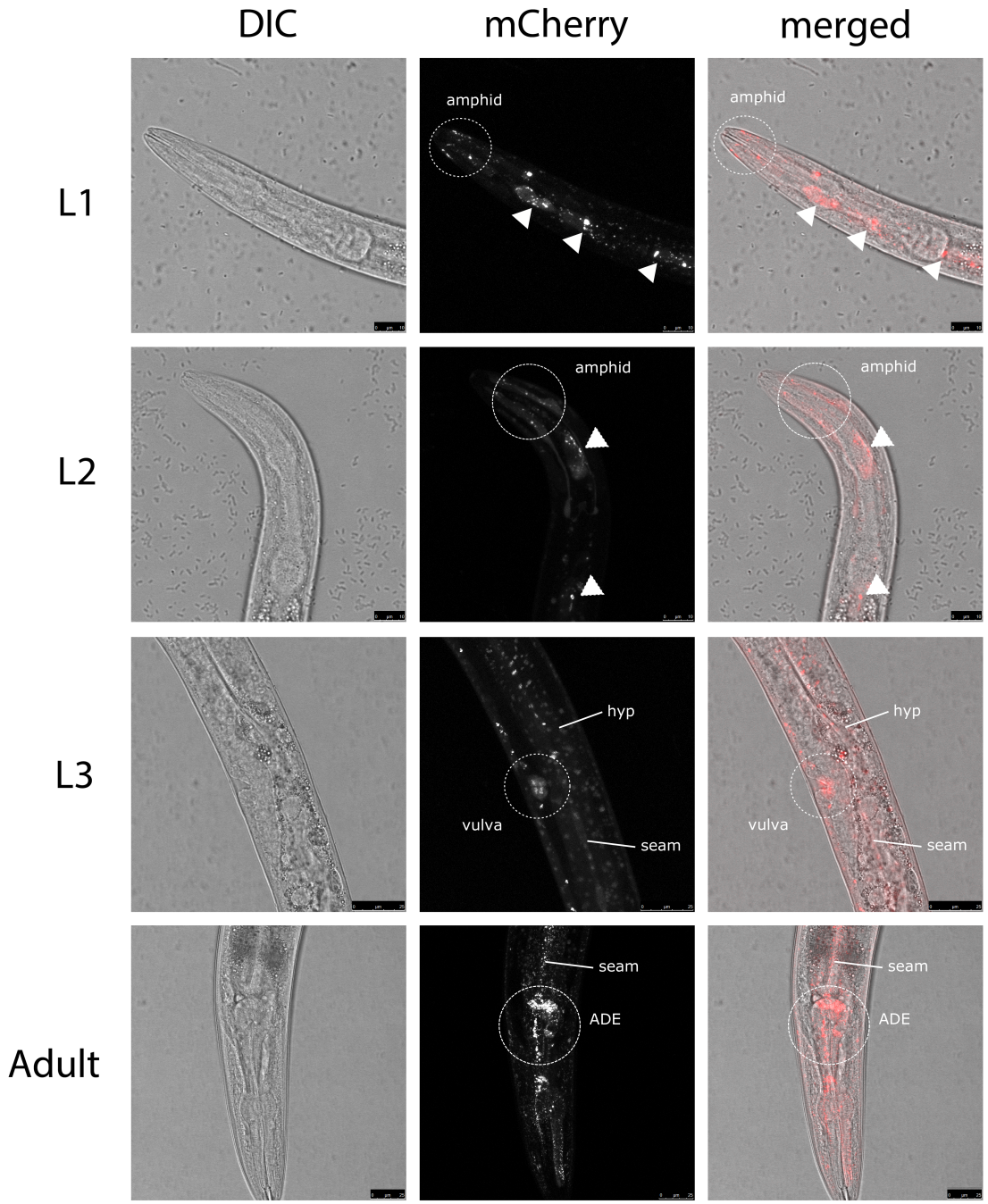


Figure 3.12: Expression of *arf-3::mCherry* at different larval stages. At L1 expression is observed in the seam cells (arrowheads) as well as sensillary neurons (circled), espeically at the nose. At L2 expression is observed in the seam cells (arrowheads) and again in sensillary neurons thought to be amphids (circled). The localisation of ARF-3::mCherry is less punctate in the tissue at this stage. At L3 *arf-3::mCherry* is observed in the vulva (circled), seam and hypodermis. At L4 and adult expression of ARF-3::mCherry continues in the seam cells, hypodermis and head neurons (circled). Scale bars are indiciated in the bottom right of each image (L1 & L2 = 10 µm; L3 & Adult = 25 µm)

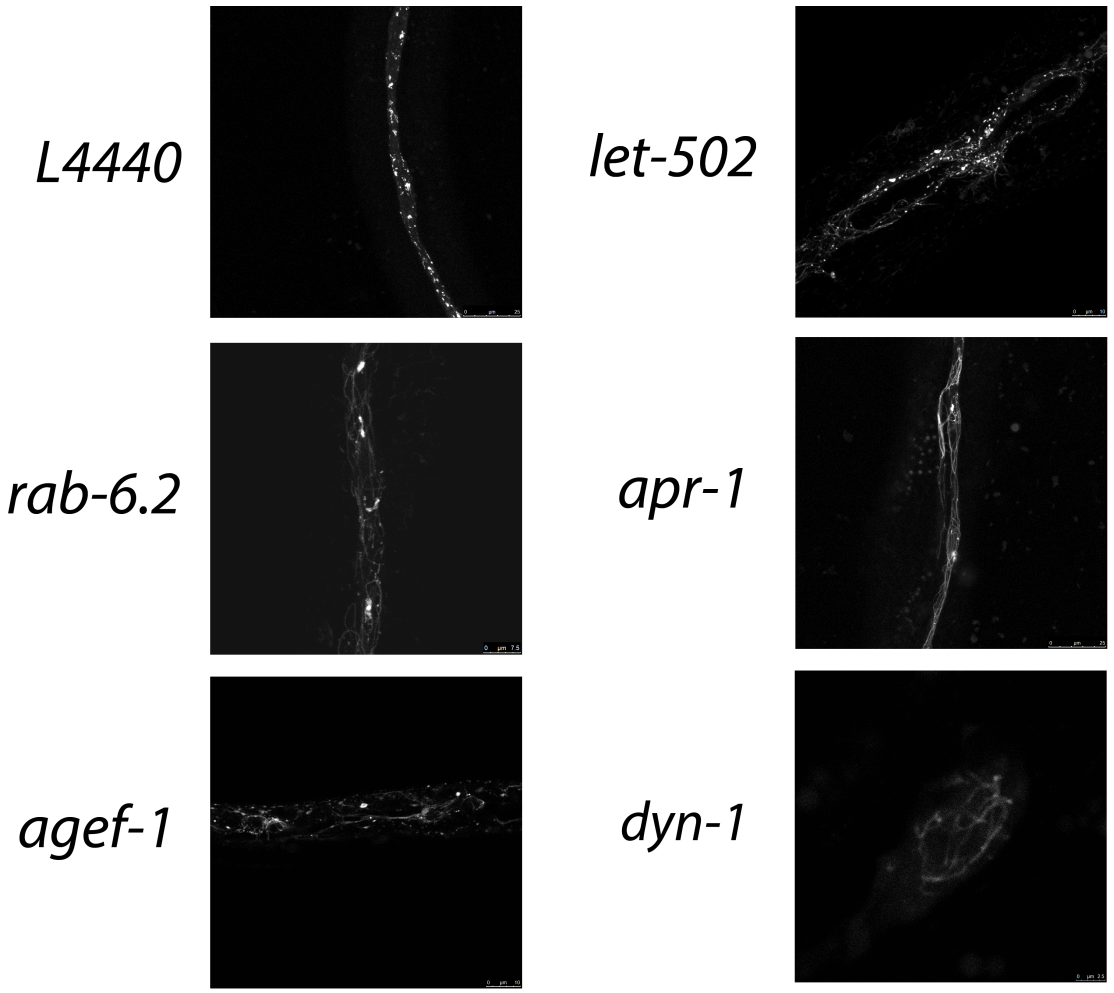


Figure 3.13: Expression of *arf-3::mCherry* at the L4 after knockdown of genes involved in intracellular trafficking and signalling. Control RNAi (L4440) is shown exhibiting the normal punctate expression of ARF-3::mCherry in the cytoplasm. The localisation of ARF-3::mCherry is less punctate upon knockdown of *agef-1, apr-1, rab-6, let-502* and *dyn-1*, instead of puncta ARF-3::mCherry localises to tubular-like structures.

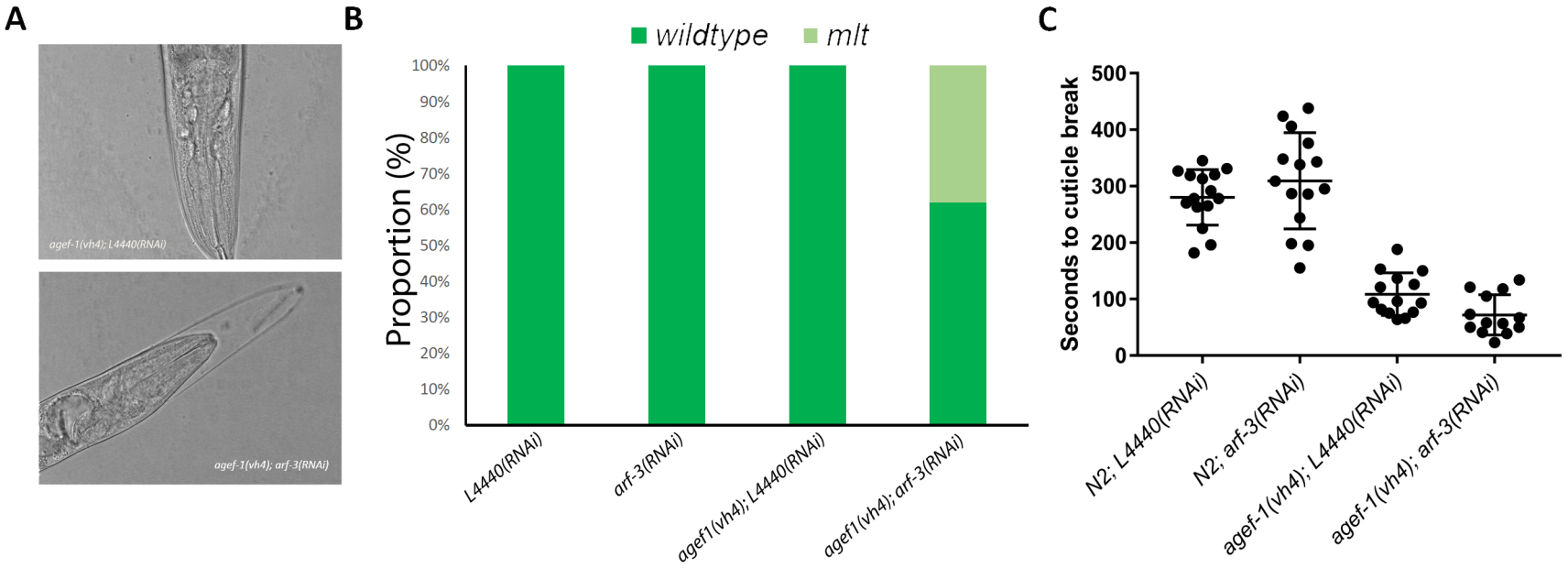


Figure 3.14: Knockdown of *arf-3* in the *agef-1(vh4)* mutant background leads to moulting defects compared to control. A = Representative images of *agef-1(vh4)* worms subjected to *arf-3(RNAi)* or control. B = Graph showing the proportion of *agef-1(vh4)* animals exhibiting moulting defects upon *arf-3(RNAi)*. No moulting defects were observed in the N2 background when *arf-3* was knocked down or either N2 or*agef-1(vh4)* controls (N = >20). C = Cuticle integrity assay performed on wildtype animals treated with *arf-3(RNAi)* or L4440 negative control and in the *agef-1(vh4)* mutant. There is no significant change to cuticle integrity in *arf-3(RNAi)* in N2. *agef-1(vh4)* mutant animals have decreased cuticle integrity and *arf-3(RNAi)* leads to an additional small but significant decrease (N = >15). A significant difference among the group overall was determined by one-way ANOVA ($P < 0.0001$). Planned pairwise comparisons made with Sidak's multiple comparison test identified significant differences between the N2 and *agef-1(vh4)* genotype populations ($P < 0.0001$). However no significant difference was observed within the genotype populations treated with control or *arf-3* RNAi respectively.

3.3.4 *apr-1* interacts with *arf-3* to regulate seam cell divisions

The striking change to ARF-3::mCherry localisation in *apr-1(RNAi)* was particularly interesting given the seam cell defects we have observed in *arf-3(RNAi)* and *arf-3(tm1877)* mutants. Seam cell divisions are known to be controlled by Wnt signalling in a divergent non-canonical pathway. During an asymmetrical division the Wnt components in seam cells are distributed asymmetrically between the anterior and posterior cortex. The asymmetric localisation of these components is heavily dependent on the funtion of *apr-1* (Baldwin and Phillips 2014). I therefore wanted to investigate any interactions between *arf-3* and *apr-1* further. I used combinatorial RNAi by feeding to knockdown both genes at the same time: a single colony of HT115 cells carrying *apr-1*, *arf-3* or the empty vector control (L4440) was used to innoculate overnight cultures. The bacterial cells were pelleted then resuspended in 400µL of fresh 2xTY, 20µL of each culture was mixed pairwise and seeded on RNAi plates (NGM + IPTG to induce dsRNA expression). Three to five L4 animals were picked onto each plate and the progeny screened for defects in seam cell development. Knockdown of *arf-3* and *apr-1* led to a significant increase in the mean seam cell number compared to controls (Figure 3.15A). Simultaneously targetting *arf-3* and *apr-1* by feeding animals with two different dsRNA-expressing bacteria, appears to reduce the strength of the phenotype produced by either gene individually. This is especially true for *apr-1*: depletion of *apr-1* ordinarily induces severe seam cell hyperplasia (Figure 3.15B) but when mixed with L4440 this was not observed (mean seam cell number = 16.08).

As a regulator of intracellular trafficking *arf-3* could be playing a role at several points in the divergent Wnt signalling pathway in seam cells; such as in transducing the Wnt signal from the plasma membrane. Alternatively *arf-3* could be involved in trafficking of Wnt components to the correct cortex during asymmetric divisions, a process known to be coordinated by *apr-1* (Baldwin and Phillips 2014). To examine this more I acquired the *apr-1(bp298)* mutant from the *Caenorhabditis* Genetics

Center. The *bp298* allele encodes a point mutation in the fourth of seven armadillo repeats of *apr-1* (c.1309$G > A$; p.Gly338Glu). Homozygotes for this mutant exhibit seam cell hyperplasia similar to the phenotype observed in *apr-1(RNAi)* (Figure 3.15B). There is no significant change to seam cell number when *arf-3* is knocked down in *apr-1(bp298)* animals; the *bp298* allele appears to mask the depletion of *arf-3* suggesting that *apr-1* is epistatic.

Wnt signalling also has a well established role in vulval development (Eisenmann and Kim 2000; Tian et al. 2008) where mutants for Wnt signalling components cause a protruding vulva (Pvl) and *apr-1(bp298)* homozygotes also exhibit a protruding vulva phenotype that can range from mild to severe. When I crossed the *arf-3::mCherry* extrachromosomal array, ouEx721, into this mutant background the animals no longer exhibited any protruding vulva (Figure 3.15C).

Wnt signalling promotes the adoption and maintenance of vulva precursor cell fate (VPCs) through the activation of LIN-39 (Eisenmann et al. 1998). LET-23 also activates LIN-39 to promote proliferation and vulval induction (Maloof and Kenyon 1998). *arf-3* has previously been shown to antagonize LET-23 (Skorobogata et al. 2014). Overexpression of ARF-3::mCherry may counteract the hyperactivation of Wnt signalling by *apr-1(bp298)* by inhibiting this parallel pathway. This would be consistent with the observation that *bar-1* mutant phenotypes are enhanced by reduced activation of the *let-23* RTK/*let-60* Ras/ *mpk-1* signalling pathway (Maloof and Kenyon 1998; Eisenmann et al. 1998).

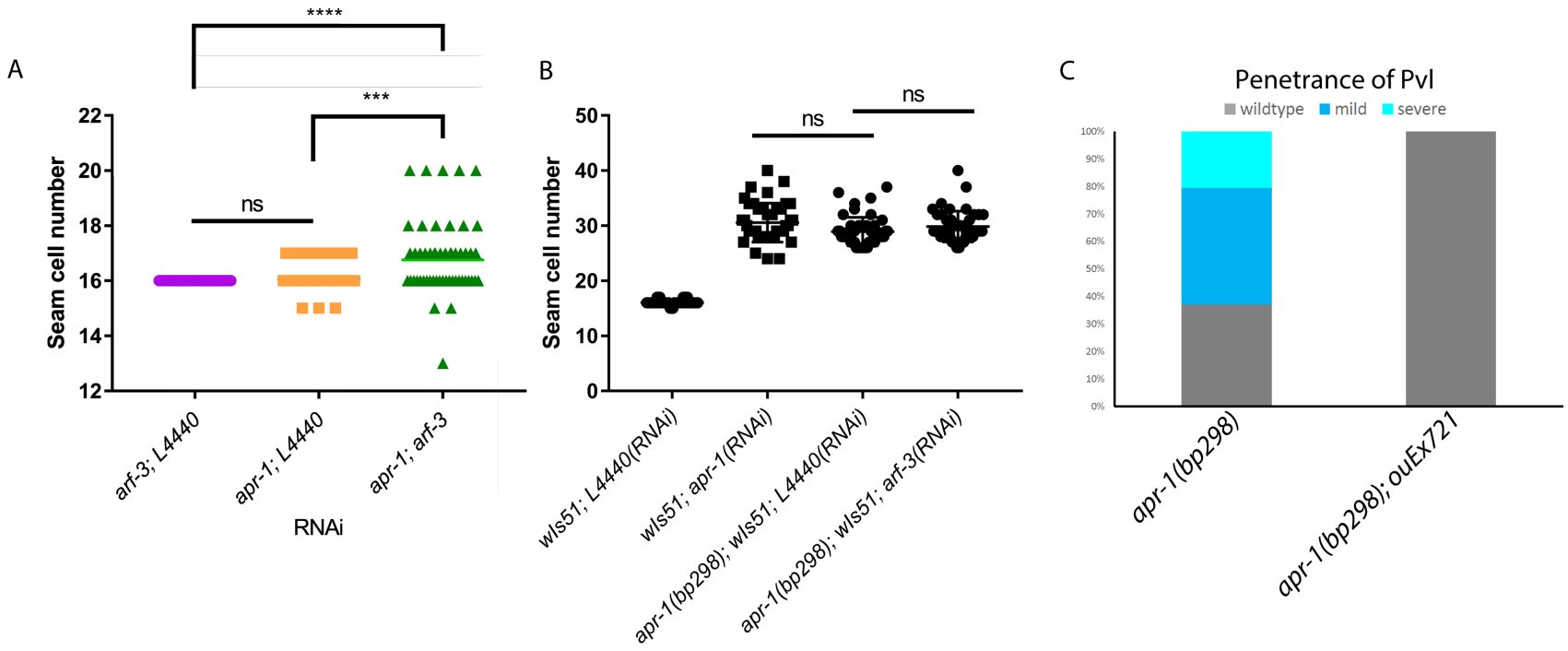


Figure 3.15: *arf-3* interacts with *apr-1*. A shows the combinatorial knockdown of *arf-3* and *apr-1* versus combinatorial negative controls (*arf-3, L4440*; & *apr-1, L4440*). Student's T-test was used to determine significance *** = $p < 0.0005$; **** = $p < 0.0001$. B shows the effect on average seam cell number when *apr-1* activity is depleted by RNAi or the hypomorphic allele *bp298*. This causes severe hyperplasia and an increase in the average seam cell number. Knockdown of *arf-3* by RNAi in the *bp298* mutant background caused no signifcant difference in average seam cell number compared to the mutant N = > 50. Student's T-test was used to determine significance (ns = P>0.1) C shows the penetrance of the protruding vulva phenotype in *apr-1(bp298)*. The phenotype ranges from mild to severe and affects 63% of animals. The protruding vulva phenotype is completely rescued by expression of *arf-3::mCherry* N = 210.

.

3.3.5 *arf-3::mCherry* partially rescues moulting defects in *dyn-1(RNAi)*

ARF-3::mCherry localisation was also altered by post-embryonic knockdown of *dyn-1*. Post-embryonic depletion of *dyn-1* by RNAi also caused moulting defects in 50.4% of *unc-119(ed3)* animals as shown in Figure 3.15A (white bracket). However, moulting defects were partially rescued by the presence of the extrachromosomal array ouEx721 (*arf-3::mcherry; unc-119+*) as shown in Figure 3.15B where only 11.9% of animals expressing the extrachromosomal array exhibited moulting defects. Moulting defects were not observed in animals fed the empty vector control L4440. The interpretation of this experiment is limited by the presence of the *unc-119* rescuing construct pAW135: I cannot rule out the possibility that the overexpression of *unc-119* rescues the observed moulting defect. However, the use of *unc-119* rescue as a selection marker is widespread and does not interfere with the vast majority of applications (Maduro 2015) leaving ARF-3::mCherry as the likely candidate.

Nematodes cannot synthesise sterols *de novo* and so require dietary sterol supplementation (Hieb and Rothstein 1968). Moulting in *C. elegans* requires cholesterol in order to synthesise steroid hormones which regulate the moulting cycle including *nhr-23* and *nhr-25* (Kostrouchova et al. 2001; Gissendanner and Sluder 2000). Indeed, sterol starvation causes moulting defects (Bottjer, Weinstein, and Thompson 1985; Coggins, Schaefer, and Weinstein 1985). The uptake of sterols in the epidermis is thought to be driven by the low-density lipoprotein (LDL) receptor-like protein LRP-1 (Yochem et al. 1999). LRP-1 binds lipoproteins at the plasma membrane and they are internalised via endocytosis. DYN-1 has been observed to play a role in this process: knockdown of *dyn-1* by RNAi leads to an accumulation of LRP-1::GFP at the plasma membrane of the hyp7 cells (Kang et al. 2013). Overexpression of *arf-3::mCherry* may compensate for the depletion of *dyn-1* by promoting the activity of the endocytic pathway to internalise LRP-1 and promote moulting.

A role for ARFs in the regulation of sterol uptake is further supported by the observation that knockdown of *arf-1.2* by RNAi leads to the increased nuclear levels

of GFP::SBP-1 (Smulan et al. 2016). SBP-1 is the homologue of the transcription factor SREBP-1 (Sterol regulatory element binding protein). When intramembrane levels of cholesterol are low SREBP-1 is activated to regulate genes required for fatty acid, triglyceride, phosphatidylcholine and cholesterol synthesis (Goldstein et al. 2006).

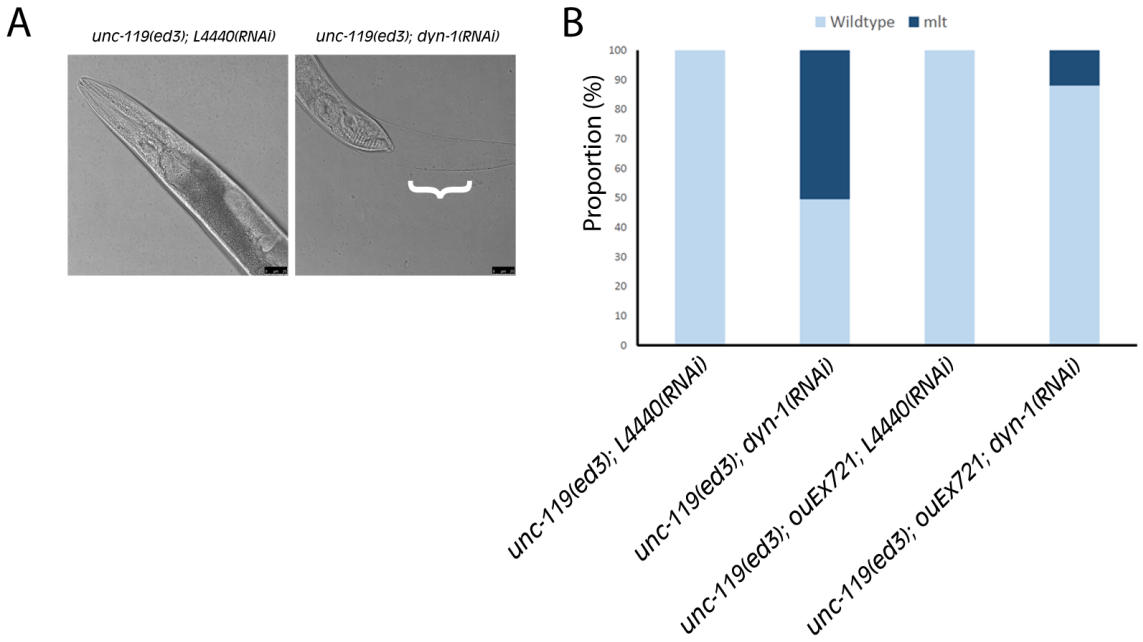


Figure 3.16: *dyn-1(RNAi)* causes moulting defects. A shows representative images of *unc-119(ed3)* worms treated with *dyn-1(RNAi)*, or the empty vector control (*L4440*). White bracket indicates unshed cuticle in animal treated with *dyn-1(RNAi)*. B shows the quantification of moulting defects. Moulting defects are observed in 49.5% of *unc-119(ed)* animals treated with *dyn-1(RNAi)* and this is reduced to 11.9% in animals carrying the *arf-3::mCherry* extrachromosomal array ouEx721 (N = >100).

3.4 Discussion

In this chapter, I have explored the effects of perturbing *arf-3* by knockout or depletion by RNAi on the development of *C. elegans*. I explored knockout of *arf-3* through the deletion allele *tm1877* and found animals displayed embryonic and larval lethality, animals that survived to adulthood were sterile and produced no viable progeny. Animals that survive the embryonic and early larval lethality are likely able to do so because of the presence of maternal RNA or protein. There may also be some redundancy between ARFs, for example *arf-3* and *arf-1.2* have both been found to antagonise LET-23 localisation in vulval induction (Skorobogata et al. 2014).

Knockdown of *arf-3* in a RNAi-hypersensistive background phenocopied the defects of the *arf-3(tm1877)* allele, including gaps seam cell defects such as gaps in the seam and a significant increase in seam cell number at adulthood. Notably, these animals also exhibited weakened cuticle interity, as measured by sensitivity to bleach and deformed annular furrows as well as moulting defects.

I was able to rescue the sterility of *tm1877* homozygotes by expressing wildtype *arf-3* in a transgenic multicopy array. However, the rescue was complicated by the array causing severe developmental defects, thus overexpression of *arf-3* appears to be deleterious to the survival of *C. elegans*. Nevertheless, these results clearly establish *arf-3* as an important player in the development of *C. elegans*.

The *tm1877* allele and overexpression of *arf-3* both cause defects in development, therefore I wanted to establish a protocol for genome editing using the CRISPR-Cas9 system. I successfully generated mutations at the *dpy-10* and *arf-3* loci. Although I was able to identify several mutations at the 5' guide RNA target site of *arf-3*, unfortunatly, I was not able to maintain a viable line.

Generating a mutant using CRISPR-Cas9 is not as straightforward as one would like. A familiar hurdle when generating transgenic strains is the presence of dedicated cosuppression mechanisms which limit the expression of heterologous genes in the germline (Kelly and Fire 1998). The main issue I encountered when targetting

arf-3, was in the design of guide RNAs. Only two "optimal" guides with the PAM sequence GGNGG are present at the *arf-3* locus. Luckily, the guide RNA that successfully generated mutations targets the 5' end of *arf-3* so in future I may have more success generating a null allele.

In a screen for genetic interactors of *arf-3* I identified several genes involved in intracellular trafficking and signalling that led to the mislocalisation of ARF-3::mCherry whe depleted including: *agef-1, dyn-1* and *apr-1*. Knockdown of these genes caused ARF-3::mCherry to be distributed to tubular structures of unknown identity.

Evaluation of the interaction between *agef-1* and *dyn-1* further supports a role for *arf-3* in regulation of moulting and cuticle synthesis, possibly through the regulation of the endocytic pathway and the internalisation of sterols. The potential interaction with *apr-1* and the Wnt signalling pathway is interesting in the context of regulating seam cell asymmetric divisions which rely on the asymmetric localisation of Wnt signalling components. Combinatorial RNAi of *arf-3* and *apr-1* led to a significant increase in seam cell number and variability, however, it would be pertinent to examine the localisation of APC and other Wnt components in response to *arf-3* depletion in order to establish a direct interaction.

Chapter 4

ARF-3::mCherry colocalises with components of the endocytic pathway in a moulting-dependent manner

4.1 Overview and aims

As discussed in the previous chapter, ARF-3::mCherry is expressed in several tissues. ARF-3::mCherry is expressed from the two-fold embryonic stage and in all juvenile stages of the worm post-hatching through to adulthood. Within the seam cells ARF-3::mCherry localises to distinct puncta of unknown identity but they are likely to be vesicular in nature given the role of *arf-3* as a GTPase. Given that *arf-3* appears to play a role in the moulting cycle and may also regulate seam cell development we wanted to characterise these puncta and their function.

4.1.1 Aims and hypotheses of this chapter

The aims of the work presented in this chapter were:

- To investigate the dynamics of the ARF-3::mCherry puncta within seam cells.

TABLE I: *Strains used in Chapter 4*

Strain	Genotype	Plasmids in extrachromosomal arrays
AW860	*unc-119(ed3); ouEx721[pAW740 + pAW135]V*	pAW740 = arf-3::mCherry; pAW135 = unc-119 rescue plasmid
AW1794	*unc-119(ed3)III; ouEx1198[pAW740 + pAW913 + pAW135]*	pAW740 = arf-3::mCherry; pAW913 = rab-5::gfp; pAW135 = unc-119 rescue plasmid
AW1795	*unc-119(ed3)III; ouEx1199[pAW740 + pAW914 + pAW135]*	pAW740 = arf-3::mCherry; pAW914 = rab-6::gfp; pAW135 = unc-119 rescue plasmid
AW1796	*unc-119(ed3)III; ouEx1200[pAW740 + pAW915 + pAW135]*	pAW740 = arf-3::mCherry; pAW915 = rab-7::gfp; pAW135 = unc-119 rescue plasmid
AW1797	*unc-119(ed3)III; ouEx1201[pAW740 + pAW916 + pAW135]*	pAW740 = arf-3::mCherry; pAW916 = rab-11::gfp; pAW135 = unc-119 rescue plasmid
AW1798	*unc-119(ed3)III; ouEx1202[pAW740 + pAW917 + pAW135]*	pAW740 = arf-3::mCherry; pAW917 = SP12::gfp; pAW135 = unc-119 rescue plasmid

- To uncover the precise spatial and temporal localisation of ARF-3::mCherry during development.
- To understand the role intracellular trafficking contributes to the development of seam cells.

I hypothesized that:

- ARF-3 follows the canonical role of ARFs and localises to the golgi and ER.
- ARF-3 plays a role in retrograde trafficking between the golgi and ER.

4.2 Results

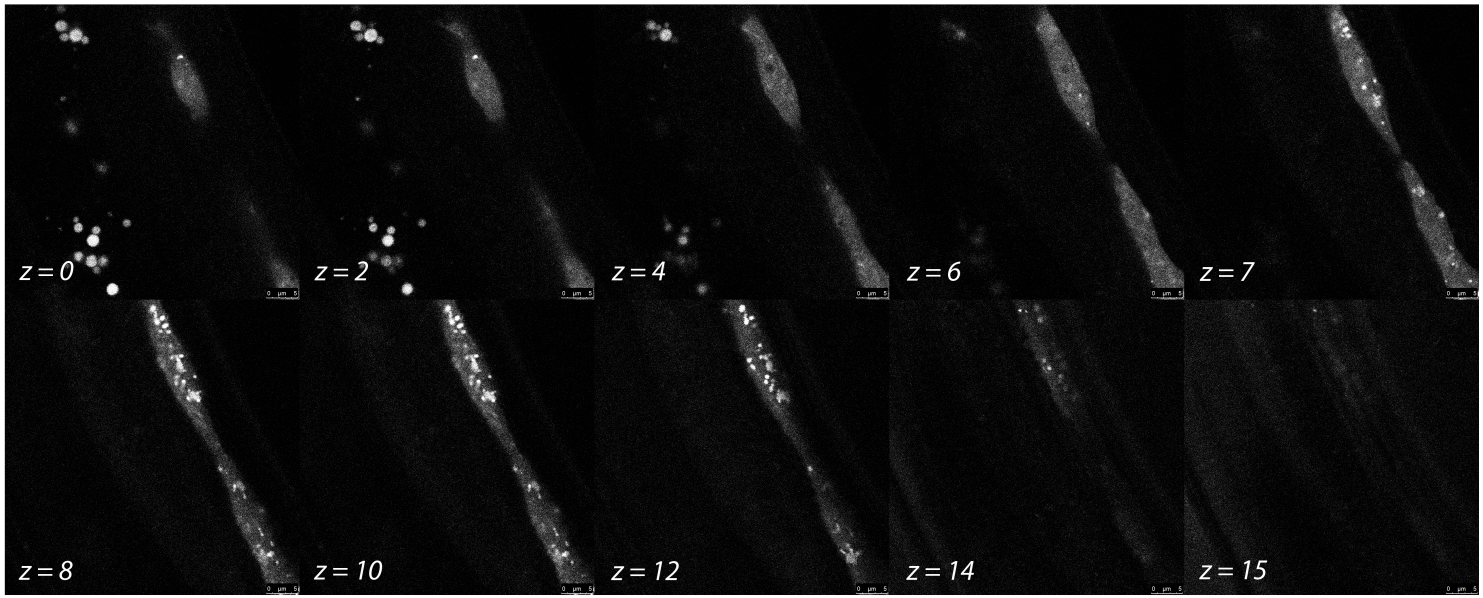
4.2.1 ARF-3::mCherry puncta are concentrated on the apical cortex of the seam cells

I began my study of the functional role of *arf-3* by dissecting the spatial and dynamic regulation of ARF-3::mCherry because I would be using this reporter in downstream colocalisation experiments.

Firstly I examined the distribution of ARF-3::mCherry puncta within a seam cell at the L4 stage using confocal microscopy. Figure 4.1A shows the z-stack of an individual seam cell where the distribution of ARF-3::mCherry is predominantly located at the apical membrane surface. The nucleus of the seam cell can be observed at slice $z = 4$ with the majority of puncta coming into focus in the subsequent slices. At slice $z = 15$ the image captured is above the cuticle of the seam cell and the shadow of the alae is seen. Figure 4.1B shows a schematic of a seam cell viewed along the perpendicular based on the z-stack in Figure 4.1A, where the majority of ARF-3::mCherry puncta are distributed above the nucleus and beneath the apical membrane underlying the cuticle and alae.

A

arf-3::mCherry



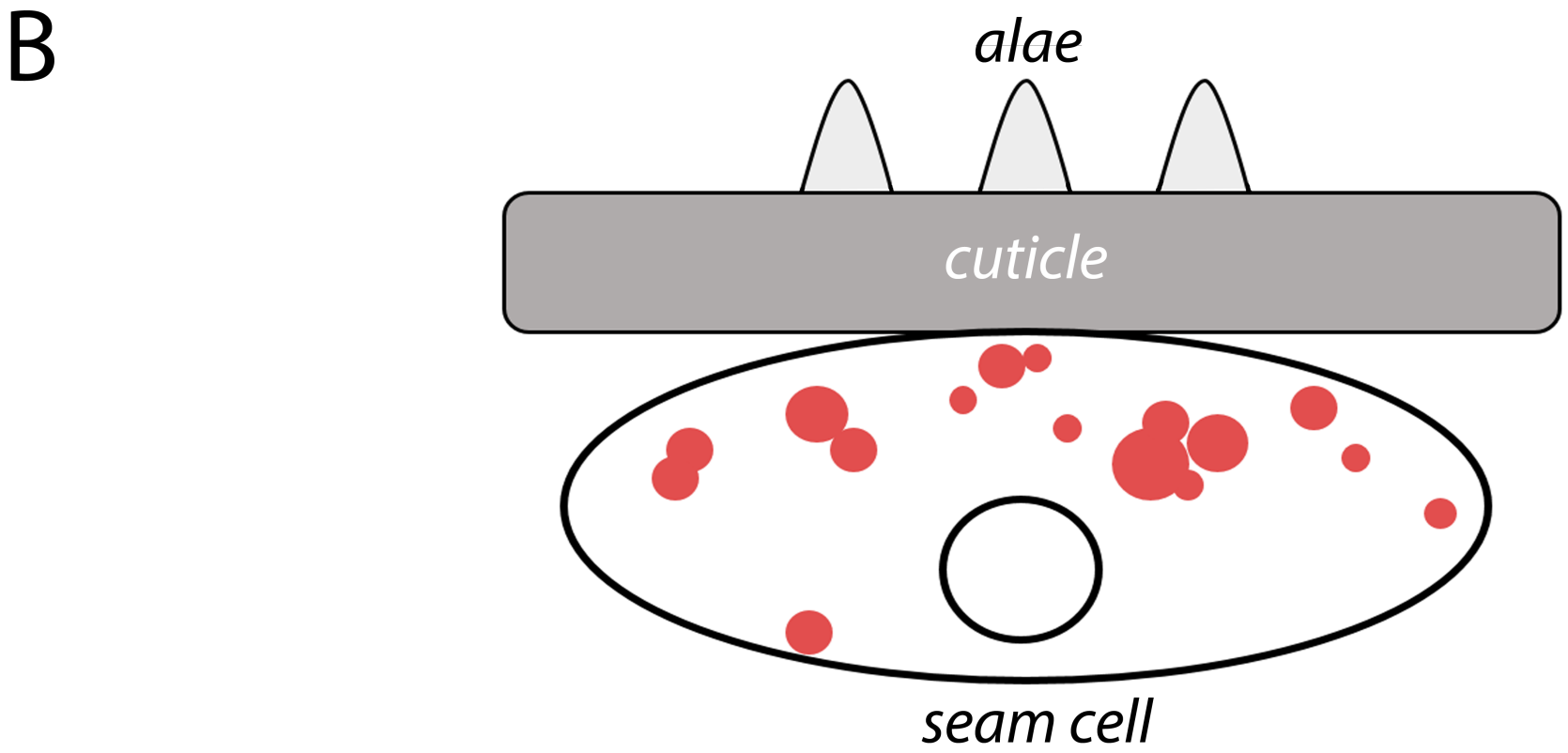


Figure 4.1: Distribution of ARF-3::mCherry puncta within the seam cell. A = z-stack of slices of seam cell expressing ARF-3::mCherry. B = Representative schematic of the puncta distribution in an indivdual seam cell. ARF-3::mCherry puncta are shown in red.

4.2.2 Smaller ARF-3::mCherry vesicles move further and quicker than those larger in size

Through viewing individual seam cells on the microscope I had observed ARF-3::mCherry puncta of varying size and shape moving through the cytoplasm. Therefore I was interested in quantifying the differences in size and the dynamics of ARF-3::mCherry puncta. Again I used confocal microscopy to image the AW860 strain expressing ARF-3::mCherry. I recorded the movement of puncta over 300 seconds and quantified the dynamics using the Trackmate plugin on Fiji (Tinevez et al. 2017).

I filtered puncta based on size and quality so that trackmate could identify spots which corresponded to larger intracellular structures (between 300 and 700 nm; Figure 4.2A-C), or those more likely to be smaller vesicles (less than 300 nm; Figure 4.2D-F). The blue lines overlaying the image in 4.2A and 4.2D show the tracks called by Trackmate for individual spots over the entire period. Figures 4.2B and E show a histogram of track displacement for the larger and smaller puncta respectively. While the track displacement is similar between the two groups the mean track velocity is greater for smaller vesicles (Figure 4.2C and F).

Figure 4.2G shows a timelapse of the posterior region of a seam cell. Here I observed the assembly of vesicles into a longer chain, or tubule at 216s. Once assembled the structure was trafficked to the posterior of the cell to merge with a superstructure at 296s. We do not know what cargo is being transported in these vesicles but sorting of cargo in tubule structures is commonly associated with endosomeal trafficking. The distribution of ARF-3::mCherry puncta is uniform throughout the cells without any asymmetrical distribution to either cortex. The only aggregation observed is to larger puncta within the seam cell, which are possibly the golgi.

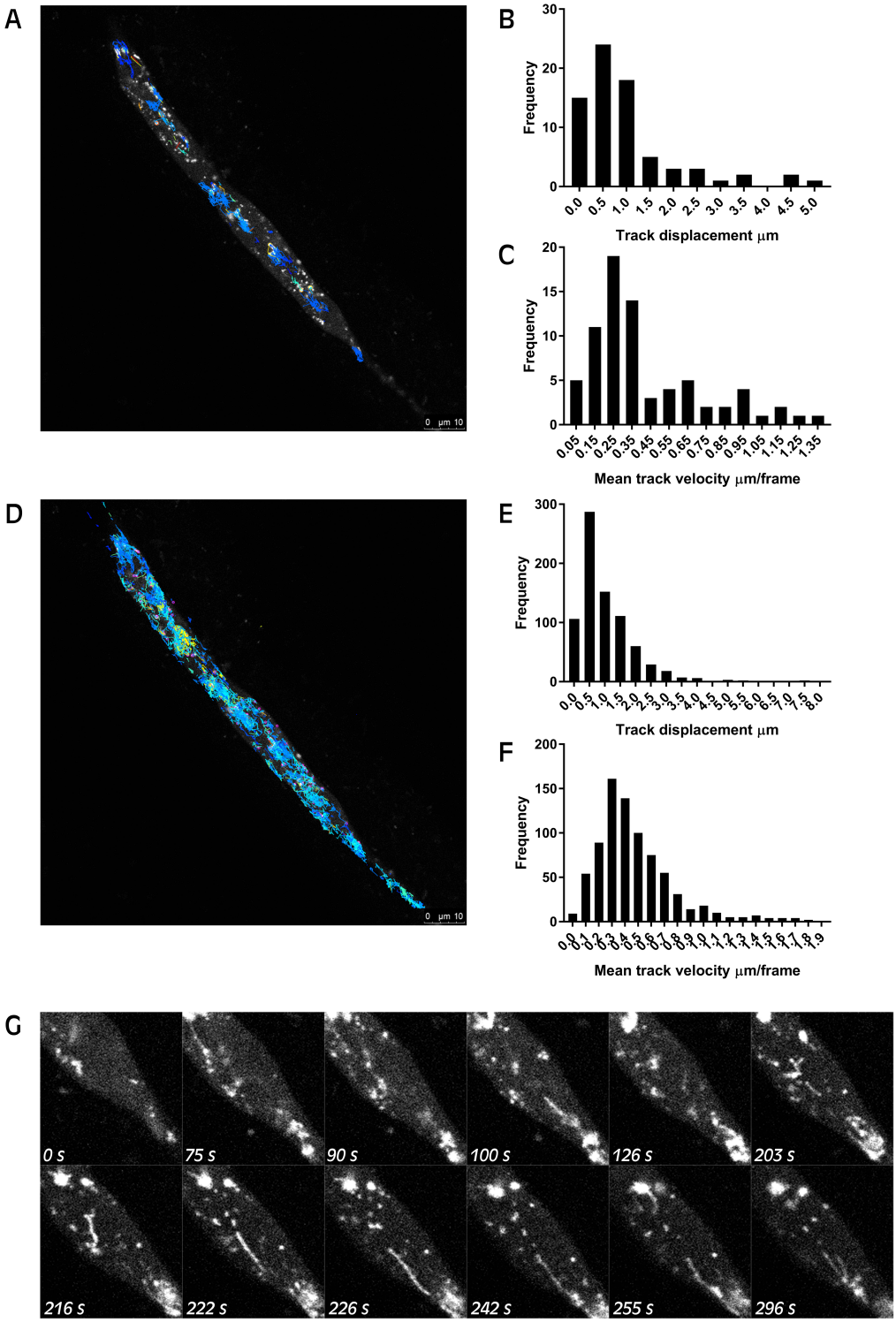
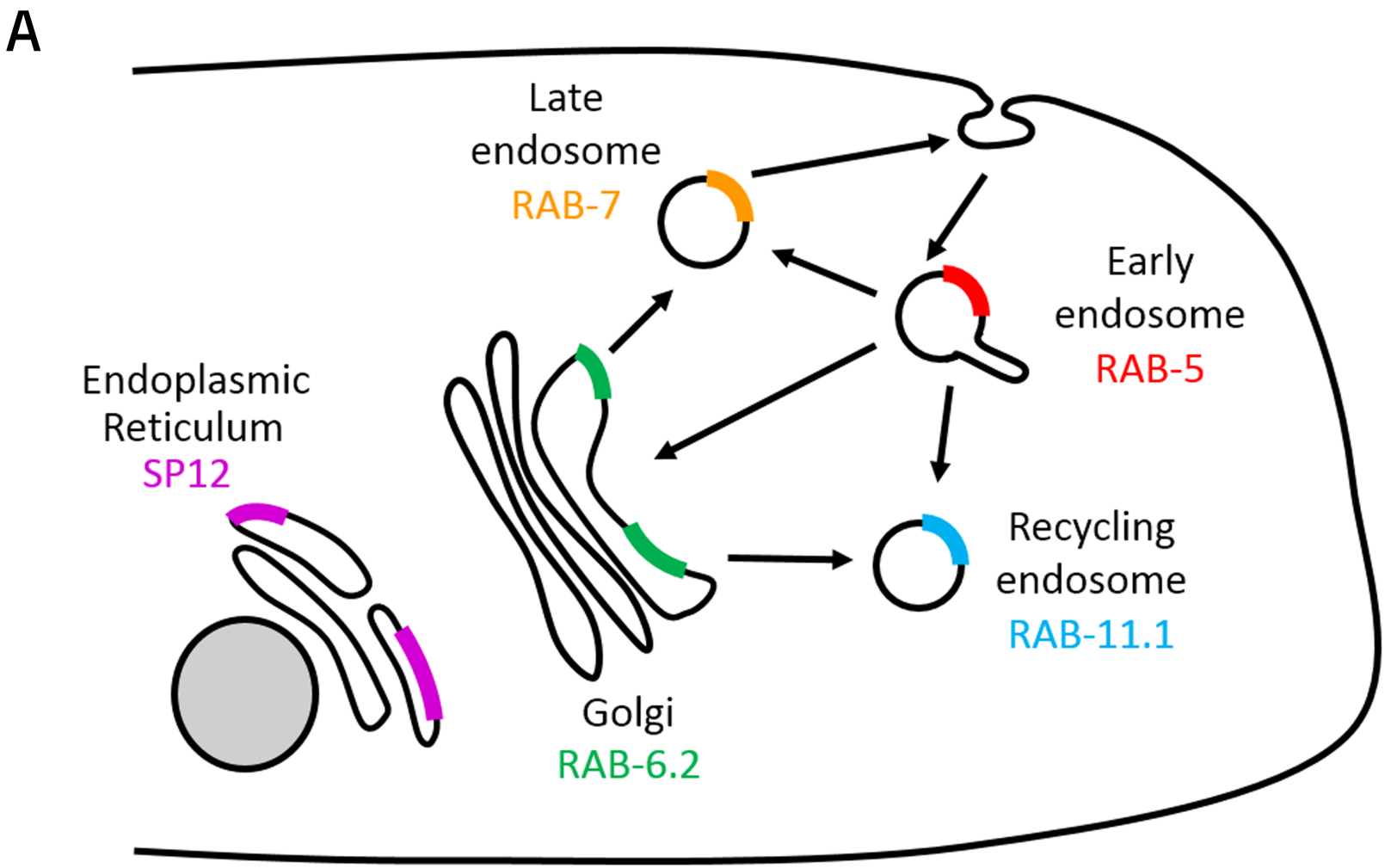
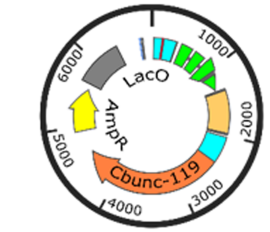


Figure 4.2: Measurements of ARF-3::mCherry puncta dynamics within seam cells. A = Tracks of ARF-3::mCherry puncta filtered for those 300-700 nm in seam cells in early adult worms; B = Distribution of the track displacement for each puncta 300-700 nm, i.e. distance travelled. C = Distribution of the mean track velocity of each puncta 300-700 nm. D = Tracks of ARF-3::mCherry puncta filtered for those less than 300 nm in seam cells in early adult worms; E = Distribution of the track displacement for each puncta less than 300 nm, i.e. distance travelled. F = Distribution of the mean track velocity of each puncta less than 300 nm. G = Time lapse of ARF-3::mCherry puncta close to posterior cell boundary


A
Late
endosome
RAB-7
Early
endosome
RAB-5
Endoplasmic
Reticulum
SP12
Recycling
endosome
RAB-11.1
Golgi
RAB-6.2

B

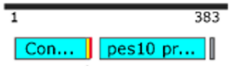


seamp::gfp::rab-6.2
6966 bp

GIBSON ASSEMBLY

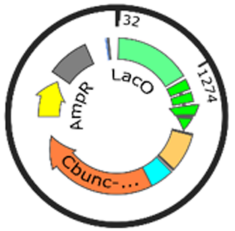


Linearised vector



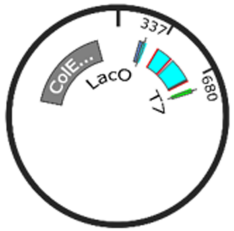
bro-1 CNE fragment

PCR



vha-6p::gfp::rab-6.2
7786 bp

PCR



pAW566 TOPO XL plusbro-1 CNE
3865 bp

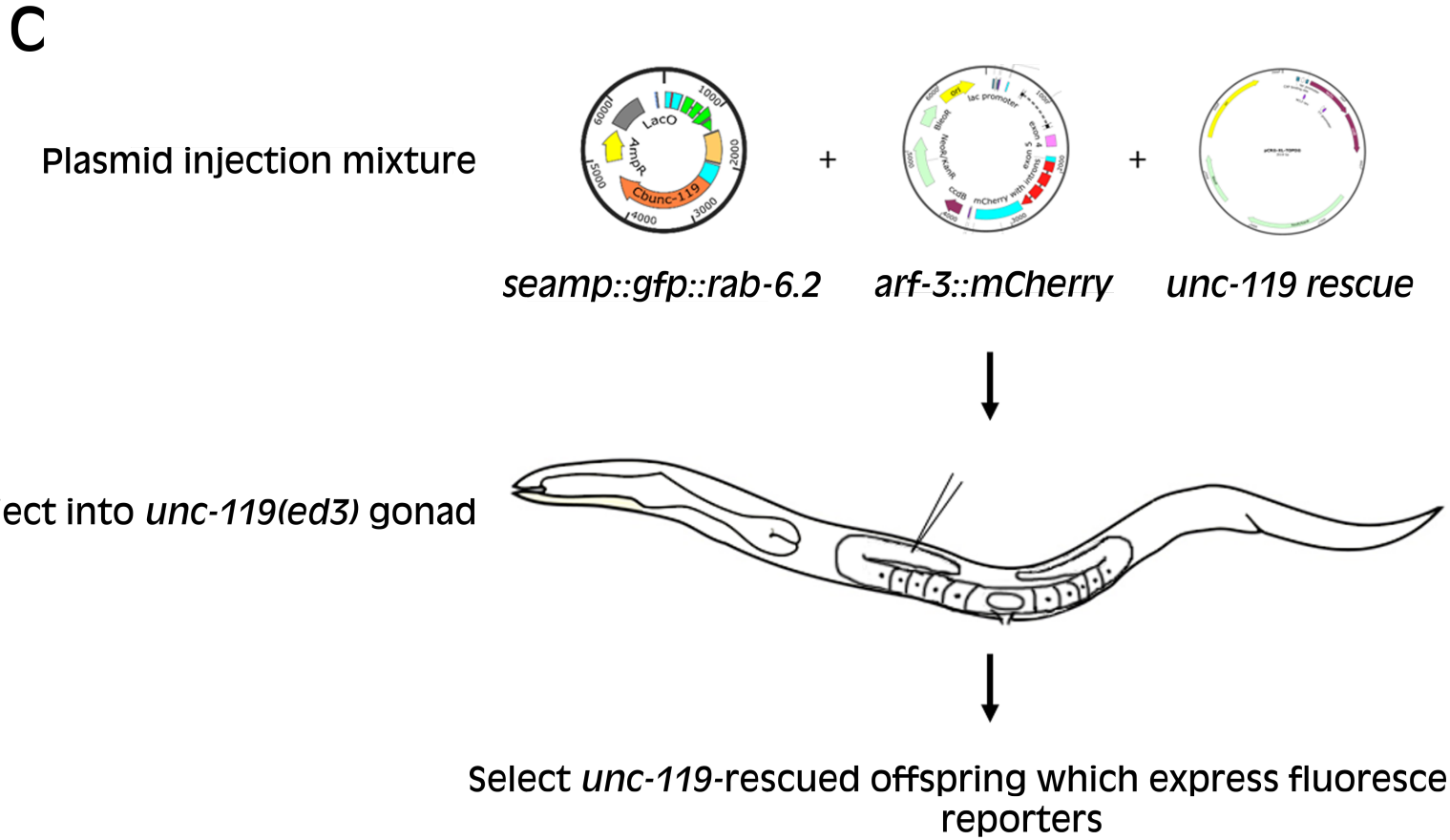


Figure 4.3: Identification of ARF-3::mCherry puncta by colocalisation with fluorescent reporter markers. A = schematic of ARF-3 colocalisation strategy. The organelles are labelled with the respective reporter markers for each also shown. Plasmids for the reporter markers fused to GFP were provided by Barth Grant. B = Cloning strategy for generating seam-specific expression vectors of the reporter markers using gibson assembly and the *bro-1* CNE. C = Example plasmid mixture used to generate transgenic lines expressing seam-specific organelle reporter markers along with *arf-3::mCherry*. *unc-119* rescue was used to identify transformants.

4.2.3 ARF-3::mCherry colocalises with RAB-6.2::GFP and RAB-7::GFP and partially with RAB-5::GFP

ARF-3::mCherry localises to puncta of varying sizes and different dynamics. Knowing the ARFs exhibit GTPase activity it is likely these puncta are membranous in nature. Therefore I wanted to determine which organelles ARF-3::mCherry is associated with in seam cells. I used a colocalisation strategy. We have obtained plasmids expressing GFP-tagged markers of membrane identity for the golgi, ER, early, late and recycling endosomes from Barth Grant (Figure 4.3A). The Woollard lab has previously produced a seam specific promoter known as the *bro-1* conserved non-coding element (CNE). I used Gibson assembly to insert this seam specific promoter in front of these reporter markers (Figure 4.3B). We generated strains coexpressing each of these markers with our ARF-3::mCherry construct through microinjection using *unc-119* rescue as a selection marker (Figure 4.3C).

Figure 4.4 shows the coexpression of these markers in seam cells at the L4 stage. ARF-3::mCherry colocalises with RAB-6::GFP and RAB-7::GFP fully and RAB-5::GFP partially, these are the markers for the golgi, late endosomes and early endosomes respectively. I could now attribute some meaning to the quantification of ARF-3::mCherry puncta in Figure 4.2. It is likely that the large spots associated with ARF-3::mCherry are the golgi and the smaller, faster moving puncta are endosomal in nature. The dynamic accumulation and trafficking of vesicles along tubules is aso supported by an interaction with the endosomal pathway.

ARF-3::mCherry does not colocalise with RAB-11::GFP or SP12::GFP. The generation of a strain carrying ARF-3::mCherry and RAB-11::GFP proved more troublesome than the other markers as these worms were very sick and exhibit some embryonic lethality it was only through dropping the concentration of RAB-11::GFP to 1 ng/µL in the injection mixture that we were able to generate a strain.

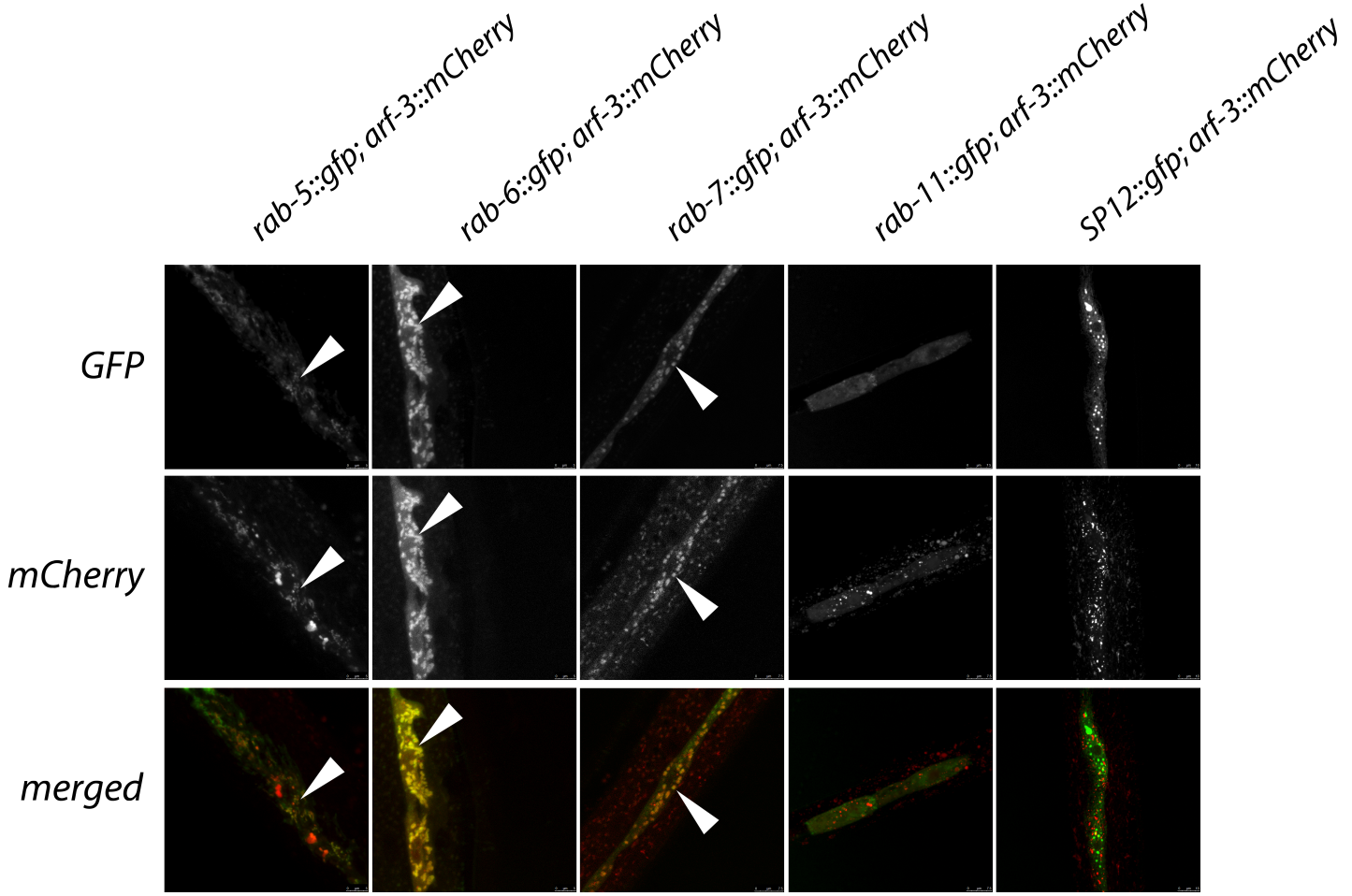


Figure 4.4: Colocalisation of ARF-3::mCherry with reporter markers for organelles. ARF-3::mCherry colocalises with RAB-6::GFP and RAB-7::GFP and partially with RAB-5::GFP (white arrows) but not with RAB-11::GFP or SP12::GFP.

4.2.4 ARF-3::mCherry colocalisation with endocytic compartments changes in concert with the moulting cycle

I noticed that the pattern of colocalisation was not uniform throughout the lifecycle of the worm. Intrigued, I questioned which event was contributing to the change in ARF-3::mCherry localisation. I consulted the literature of the cell biology of seam cells: in 1978, Singh and Sulston described the cyclic nature of the "granularity" of the seam cells where during cuticle deposition, large Golgi bodies are seen in the seam cells, and following ecdysis this granularity is lost. I wanted to use my reporter strains to ask whether I could also observe this cycle.

I performed a time course for each of my reporter markers (Figures 4.5-4.9). The number and size of RAB-6::GFP and ARF-3::mCherry puncta increases prior to ecdysis (Figure 4.6, 35-41 hours) and this is lost in the adult seam at 48 hours. This data recapitulates the observation Singh and Sulston made in 1978. I found no correlation with the change in puncta size and distribution with seam cell divisions (symmetric or asymmetric). Interestingly I also observed this trend with RAB-5::GFP and RAB-7::GFP, but not RAB-11::GFP nor SP12::GFP. Singh and Sulston also described vesicles containing darkly staining material budding off from the Golgi bodies and moving to the surface of the cell, possibly depositing the new cuticle. This may explain why RAB-5::GFP, RAB-6::GFP and RAB-7::GFP appear to have the similar changes in cellular distribution; these vesicles might be part of the endocytic pathway and are therefore likely to be in close proximity at these stages.

The localisation of SP12::GFP does change in association with the cell cycle (Figure 4.9) alternating between a dispersed reticulate state (interphase) and a highly organized sheet state. Similar changes to ER distribution have been observed in cultured cells, fly and *C. elegans* previously (Bobinnec et al. 2003; Poteryaev et al. 2005; Puhka et al. 2007). As the seam cells undergo their final cell division the endoplasmic reticulum exhibits a sheet like structure. Once divided this structure is gradually reduced (39-41 hours). At 48 hours the adult seam cells have fused and the endoplasmic reticulum is observed in a more reticulate state commonly associated

with interphase.

4.2.5 Overexpression of intracellular trafficking components perturbs seam cell development

The data presented here are, to an extent, confounded by the presence of seam cell defects in the strains carrying our extrachromosomal arrays. These defects are never observed when ARF-3::mCherry is expressed on its own in AW740. While the RAB-11::GFP and SP12::GFP strain exhibit a wildtype seam cell lineage, animals carrying RAB-5::GFP, RAB-6::GFP and RAB-7::GFP exhibit seam defects, especially at adulthood (Figure 4.10). The seam cells at this stage exhibit fusion defects, including the development of processes, gaps in the seam, migration defects and abberrant divisions. The most extreme defects are observed in RAB-5::GFP, as shown in figure 4.10 where several cells expression RAB-5::GFP and ARF-3::mCherry can be seen out of the lateral line of the seam and presenting with processes.

These defects are highly penetrant; the proportion of animals presenting at least one seam cell exhibiting these defects is 100% in RAB-5::GFP, or 88% for RAB-6::GFP and RAB-7::GFP respectively (N = 25). Seam cells exhibiting the long processes and aberrant migration of seam cells (70-87%) occur with higher frequency than gaps in the seam (52-65%) for each of these reporter markers.

It is unclear why overexpression of endocytic pathway components in seam cells would cause these defects. However, *arf-3* interacts with *dyn-1* as shown in Chapter 3. *dyn-1* negatively regulates the fusion of cells by internalising EFF-1 from the plasma membrane (Smurova and Podbilewicz 2016). I hypothesised that overexpression of the endocytic pathway components caused EFF-1 to be sequestered inside the seam cells, leading to defects in cell fusion of the seam cells.

4.2.6 The seam cell defects observed in RAB-5::GFP, RAB-6::GFP and RAB-7::GFP animals are not rescued by knockdown of *dyn-1* or *eff-1*

The fusion of seam cells has been linked to the activity of the fusogen EFF-1 (Mohler et al. 2002). EFF-1 localises to the plasma membrane of cells at the boundary where they will fuse. This process is inhibited by endocytosis of EFF-1 from the plasma membrane by RAB-5 and DYN-1 (Smurova and Podbilewicz 2016). I therefore chose to knockdown *dyn-1* and *eff-1* post-embryonically by RNAi in my reporter strains to determine whether I could rescue, suppress, or exacerbate the observed seam cell defects.

Neither knockdown of *dyn-1* nor *eff-1* rescued the seam cell defects observed in the reporter marker strains (Figure 4.11). The frequency of seam cell defects per animal, including morphological defects and gaps in the seam was unchanged. It is therefore unlikely that excessive internalization of EFF-1 is leading to a failure in seam cell fusion.

There is a significant increase in the frequency of seam cell defects per worm in the RAB-5::GFP strain fed with the empty vector control compared to RAB-6::GFP and RAB-7::GFP fed with the empty vector control respectively. This indicates that the overexpression of RAB-5::GFP perturbs the endocytic pathway in the seam cells to a greater extent than the other components.

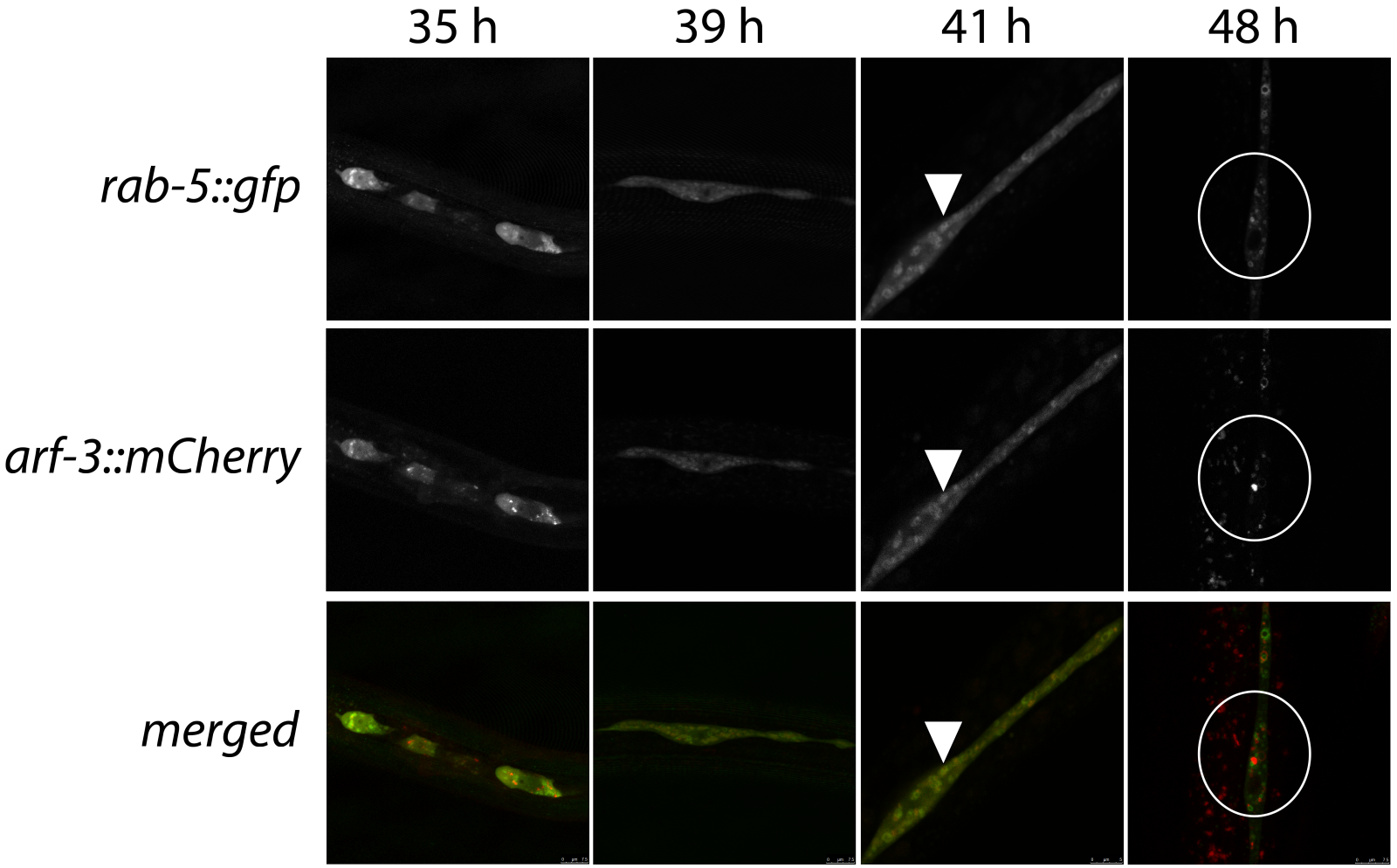


Figure 4.5: Localisation of RAB-5::GFP and ARF-3::mCherry over time. Time when the image was taken is at the top of each image beginning at 35 hours and ending after the final moult is completed at 48 hours. White arrowheads indicate colocalisation of RAB-5::GFP and ARF-3::mCherry at 39 and 41 hours. The colocalisation is lost after the final moult (white circle).

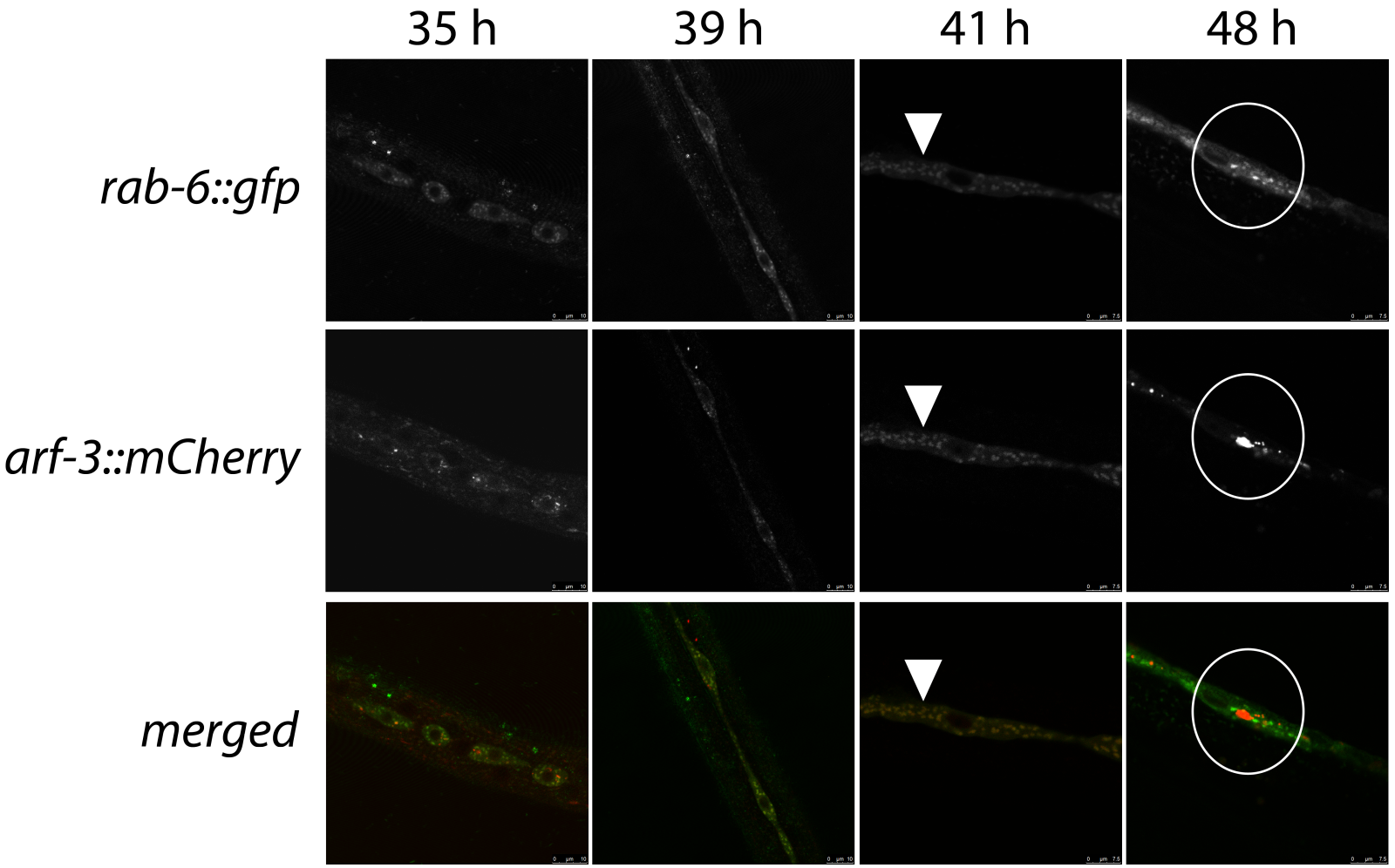


Figure 4.6: Localisation of RAB-6::GFP and ARF-3::mCherry over time. Time when the image was taken is at the top of each image beginning at 35 hours and ending after the final moult is completed at 48 hours. White arrowheads indicate colocalisation of RAB-6::GFP and ARF-3::mCherry at 39 and 41 hours. The colocalisation is lost after the final moult (white circle).

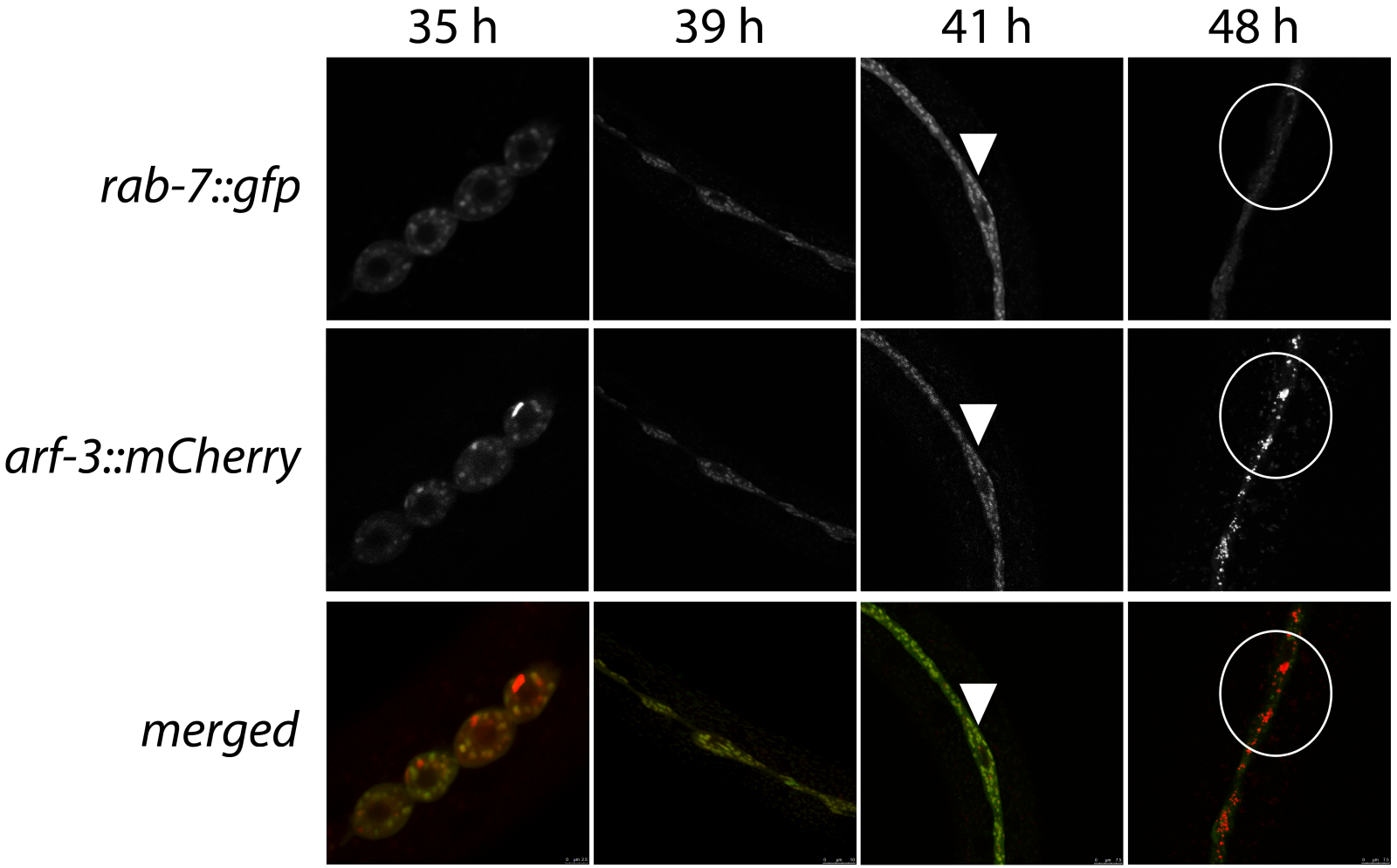


Figure 4.7: Localisation of RAB-7::GFP and ARF-3::mCherry over time. Time when the image was taken is at the top of each image beginning at 35 hours and ending after the final moult is completed at 48 hours. White arrowheads indicate colocalisation of RAB-7::GFP and ARF-3::mCherry at 39 and 41 hours. The colocalisation is lost after the final moult (white circle).

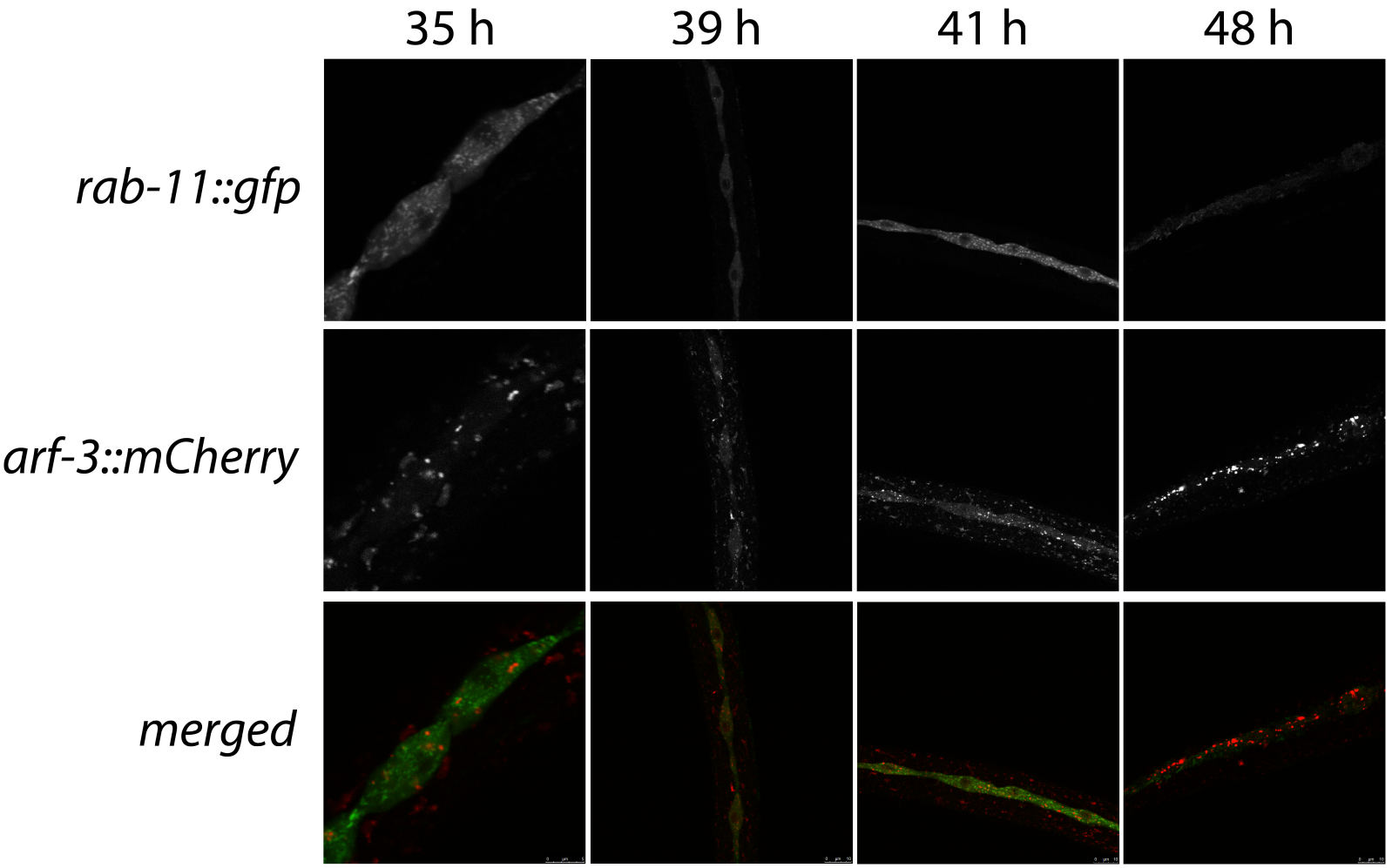


Figure 4.8: Localisation of RAB-11::GFP and ARF-3::mCherry over time. Time when the image was taken is at the top of each image beginning at 35 hours and ending after the final moult is completed at 48 hours. ARF-3::mCherry and RAB-11::GFP never colocalise. ARF-3::mCherry distribution is more to distinct puncta while RAB-11::GFP is more diffuse.

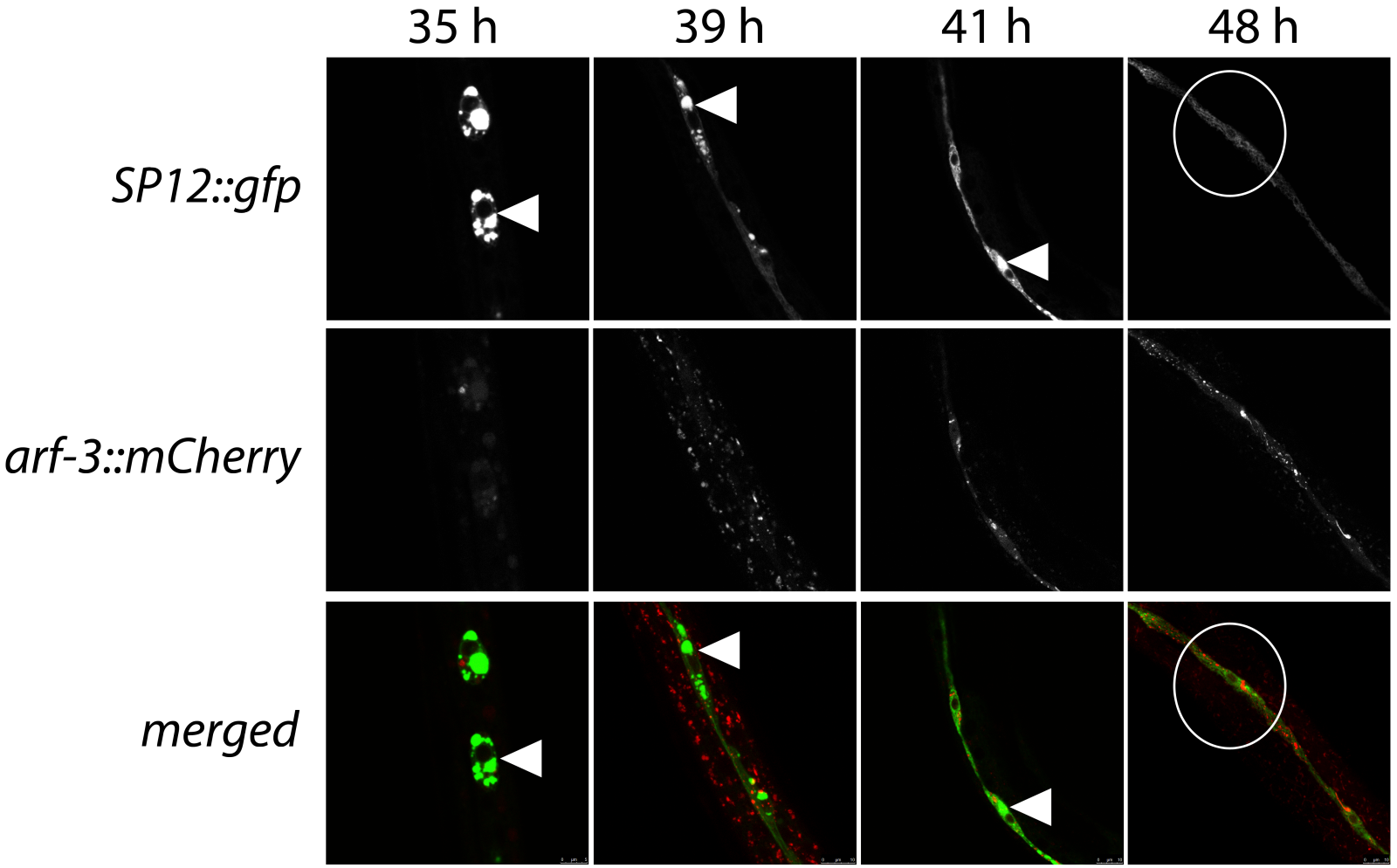


Figure 4.9: Localisation of SP12::GFP and ARF-3::mCherry over time. Time when the image was taken is at the top of each image beginning at 35 hours and ending after the final moult is completed at 48 hours. White arrowheads indicate the localisation of SP12::GFP to bright sheet structures of the endoplasmic reticulum. White circle indicates the more dispersed structure of the endoplasmic reticulum once seam cells stop dividing and enter prolonged interphase.

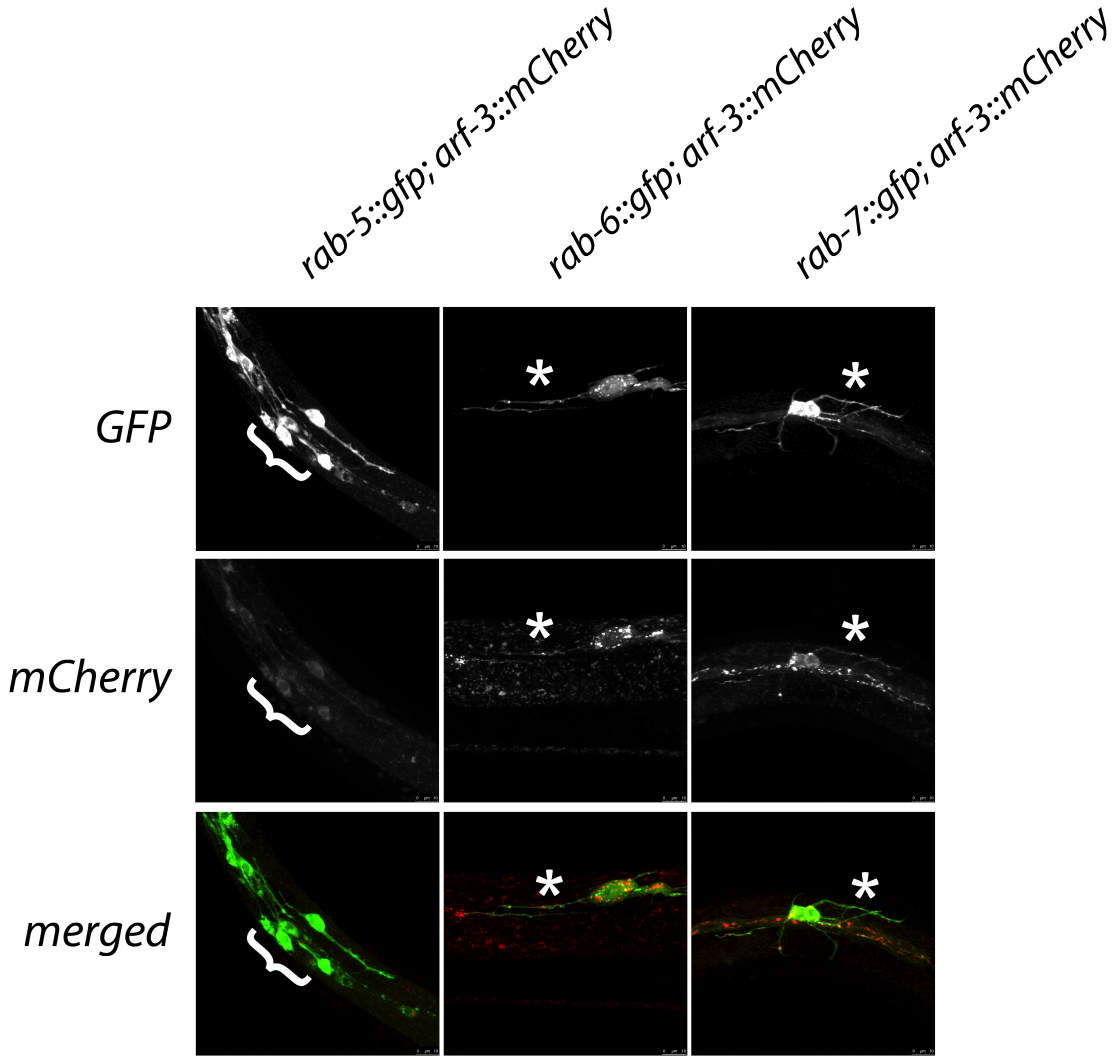


Figure 4.10: Overexpression of RAB-5::GFP, RAB-6::GFP and RAB-7::GFP cause seam cell defects including putative severe fusion defects (white bracket). Seam cell morphology also changes (white asterisk) with cells displaying processes.

4.3 Discussion

4.3.1 ARF-3::mCherry spatial dynamics are consistent with its colocalisation with RAB-5::GFP, RAB-6::GFP and RAB-7::GFP

In this chapter I have shown that ARF-3::mCherry puncta in seam cells consist of different sizes and dynamics, including larger, slower moving puncta ¿700 nm or smaller, faster moving puncta 300 nm. These larger puncta are likely to be golgi given ARF-3::mCherry colocalises with RAB-6.2::GFP while the smaller puncta are more likely endosomal given the colocalisation with our early and late endosomal markers, RAB-5::GFP and RAB-7::GFP respectively.

The canonical role of Class I and Class II ARF GTPases is in ER-Golgi trafficking and the mammalian homologues of *arf-3*, Arf4 and Arf5 have both been described in this context. However, ARFs have been implicated in a wider range of roles including organelle movement on microtubules (Yadav, Puthenveedu, and Linstedt 2012) and clathrin-independent endocytosis through the CLIC/GEEC pathway, which has recently been shown to play a role in wing patterning in drosophila through endocytosis of the morphogen Wingless (Hemalatha, Prabhakara, and Mayor 2016). Indeed, in *C. elegans* the study of the ARFGEF GBF-1 in oocytes and intestinal epithelial cells has revealed a potential link to the regulation of early/late endosomes (Ackema et al. 2014). Ackema *et al.* describe the response of RAB-5::GFP and RAB-7::GFP to *gbf-1(RNAi)* in intestinal cells where accumlation of RAB-5::GFP at the apical membrane was reduced and RAB-7::GFP increased to form large aggregates. Whether GBF-1 plays a role in regulating the dynamics of early and late endosomes in seam cells, and whether this occurs through *arf-3* remains unclear.

While RAB-6.2::GFP is a golgi marker, crucially, *rab-6.2* is known to play a role in retrograde transport from endosomes to the *trans*-golgi (Zhang et al. 2012). Interestingly *rab-6.2* has been described in the retrograde recycling of MIG-14, the *C. elegans* Wntless homologue (Zhang et al. 2016). Taken together, these findings

support a role for *arf-3* in the regulation of endosomal trafficking, although what cargo *arf-3* is sorting remains unknown.

The overexpression of our reporters in the seam cells causes highly penetrant seam cell defects, especially in RAB-5::GFP. I suspected these defects may have arisen from the dysregulation of the fusogen EFF-1. EFF-1 has a well documented role in cell fusion in epithelial cells and other tissues, including the seam, in *C. elegans* (Mohler et al. 2002, Shemer et al. 2004, Cassata et al. 2005). It is also known to be regulated through endocytosis (Smurova and Podbilewicz 2016); EFF-1 localises to the cell boundary of fusing cells, however dynamin (*dyn-1*) and *rab-5* suppress this by endocytosis of EFF-1 from the plasma membrane, preventing excessive fusion. I therefore targetted EFF-1 and DYN-1 for knockdown by RNAi but I was not able to rescue the observed defects. It is possible that the overexpression of these reporters is so great that knockdown of *dyn-1* by RNAi is not sufficient to perturb the internalisation of EFF-1. A forward genetic screen for suppressors of these seam cell defects would help our understanding of how they arise and to identify what role the endocytic pathway is playing in regulating seam cell fate and morphology.

Given our ARF-3::mCherry reporter strain, AW860, does not exhibit these defects in the absence of the other reporter markers, *arf-3* may not be playing a role in this process however the colocalisation with these molecules does point to a role in endosomal trafficking.

4.3.2 ARF-3::mCherry localises to endosomal compartments and may contribute to the moulting cycle of *C.elegans*

A major success of this study has been to recapitulate the results of Singh and Sulston (Singh and Sulston 1978). In their study, Singh and Sulston described the cyclic nature of the "granularity" of the seam cells as observed by normarski microscopy. Closer analysis using electron micrographs revealed large Golgi bodies expanding in the seam cells over during lethargus and following ecdysis this granularity was lost.

Using our fluorescent reporter markers I have observed the same increase in num-

ber and size of golgi bodies prior to ecdysis as marked by RAB-6.2::GFP. In addition I have also observed an increase in the number and size of the early and late endosomal compartments as marked by RAB-5::GFP and RAB-7::GFP respectively. This is probably because the golgi resides at the intersection of the secretory, lysosomal, and endocytic pathways and the processing and secretion of new cuticle, as well as the alae, increases the load on these pathways. Notably, ARF-3::mCherry also followed this pattern: ARF-3::mCherry puncta increased in size and number prior to ecdysis, colocalising with the other endocytic pathway reporter markers. This suggests *arf-3* is playing a role in the endocytic pathway, in a moulting dependent manner. This builds on top of the data shown in the previous chapter, where *arf-3* was shown to interact with *dyn-1* and *agef-1* to regulate moulting and secretion of the cuticle. We can now consider these defects in the context of the endocytic pathway. It is still unclear exactly what is being trafficked but it is likely to be cuticle collagens being secreted during the deposition of the cuticle and potentially the internalisation of sterols or other unidentified signalling molecules. It is also unclear how this links to regulation of seam cell development however, intracellular trafficking is evidently playing a role as shown by the seam defects observed in animals overexpressing the endocytic pathway reporter markers.

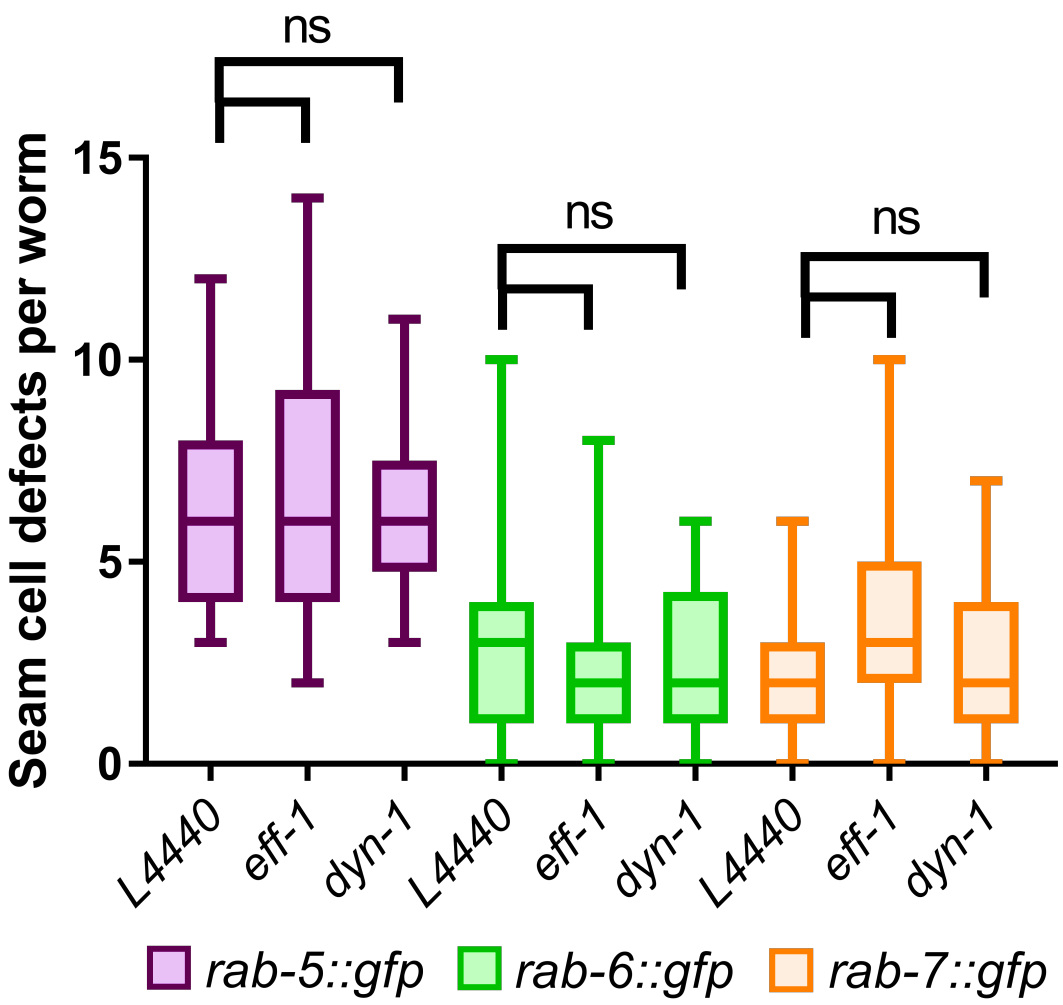


Figure 4.11: Depletion of DYN-1 and EFF-1 cause no signicant difference to the number of seam cell defects per animal observed in RAB-5::GFP (purple), RAB-6::GFP (green) and RAB-7::GFP (orange) reporter strains (N = 23). A significant difference among the groups overall was determined by one-way ANOVA ($P < 0.0001$). Planned pairwise comparisons made with Sidak's multiple comparison test identified significant differences between the number of seam cell defects observed in RAB-5::GFP treated with the empty vector control versus RAB-6::GFP and RAB-7::GFP treated with the empty vector control respectively ($P < 0.0001$). However no significant difference was observed within each genotype treated with control or *eff-1* or *dyn-1* RNAi. (ns: $P>0.2$). Finally no significant difference was observed between RAB-6::GFP and RAB-7::GFP treated with control or *eff-1* or *dyn-1* RNAi. (ns: $P>0.2$).

Chapter 5

A *cis*-regulatory element of *arf-3* drives the expression of the seam cell marker *scm::gfp*.

5.1 Overview and aims

As discussed in Chapter 3, we have identified an enhancer sequence at the 3' end of the *arf-3* coding region that drives expression in the seam cells specifically. This same region drives the expression of the seam cell marker, *scm::gfp*, which is commonly used by researchers as a marker of seam cell fate. However, expression of ARF-3 is not exclusive to the seam cells and is expressed in other tissues including neurons, body wall muscle and the vulva (Chapter 3, Figure 3.5).

Dissecting the transcriptional regulation of *arf-3* and the *scm* promoter is of value for several reasons. The expression of *scm* is tightly associated with seam cell fate; the expression of *scm::gfp* fades relatively rapidly in cells which leave the seam and differentiate, thus *scm*-positive is taken to mean seam fated. The 3' enhancer element appears to reside in the final intron of *arf-3*. Intronic enhancers are not unique to *C. elegans*, indeed, in higher eukaryotes many regulatory elements have been discovered residing in the first intron of a gene (Park, Hannenhalli, and

Choi 2014). We have observed intronic enhancers in several genes which play major roles in regulating seam cell development (Sophie Gilbert thesis) and this particular enhancer is interesting because it lies in the final intron. Our understanding of gene regulation via *cis*-regulatory enhancer elements is far from complete, but it is a conserved mechanism found across metazoan evolution.

5.1.1 Aims and hypotheses of this chapter

The aims of the work presented in this chapter were:

- To investigate how the sequence 5' of *arf-3* contributes to its expression and to visualize any spatial and temporal differences with the 3' intronic enhancer.
- To identify potential regulators of *arf-3* gene expression.
- To dissect the role of these regulators in controlling seam cell fate and secretion of the cuticle

I hypothesized that:

- *arf-3* is regulated by a network of transcription factors.
- The dysregulation of *arf-3* gene expression would cause seam and cuticle defects similar to those observed in our *arf-3(tm1877)* allele and by knockdown of *arf-3* by RNAi.
- The intronic enhancer element would not drive the expression of GFP::NLS as strongly as the 5' promoter region.

5.2 Results

5.2.1 The 5' promoter of *arf-3* does not drive the expression of GFP::NLS as strongly, nor specifically as the intronic enhancer

The promoter region that drives the expression of *scm::gfp* aligns with a region of chromosome IV which includes three genes: *arf-3*, a member of the Arf family of GTPases (Li et al. 2004), *mec-17*, which is required for the function of touch

TABLE I: *Strains used in Chapter 5*

Strain	Genotype	Plasmids in extrachromosomal arrays
AW60	*him-5 (e1490); wIs51[scm::gfp + pAW135]V*	
AW860	*unc-119(ed3)III; ouEx721[pAW740 + pAW135]*	pAW740 = arf-3::mCherry; pAW135 = unc-119 rescue plasmid
AW1421	*blmp-1(tm548)I*	
AW1422	*blmp-1(tm548)I; wIs51[scm::gfp + pAW135]V*	pAW135 = unc-119 rescue plasmid
AW1799	*heIs63[wrt-2p::GFP::PH + wrt-2p::GFP::H2B + lin-48p::mCherry]V; ouEx721[pAW740 + pAW135]*	pAW135 = unc-119 rescue plasmid; pAW740 = arf-3::mCherry
AW1800	*elt-1(ku491)IV; wIs51[scm::gfp + pAW135]V*	pAW135 = unc-119 rescue plasmid
MH4799	*elt-1(ku491)IV*	
AW1802	*pAW918 + pAW135*	pAW135 = unc-119 rescue plasmid; pAW918 = arf-3 5' promoter::gfp
SV1009	*heIs63 [wrt-2p::GFP::PH + wrt-2p::GFP::H2B + lin-48p::mCherry]V*	

receptors in the worm (Chalfie and Au 1989; Zhang et al. 2002), and the collagen gene *col-115*.

Given that promoter elements are generally considered to lie in sequence 5' of the ATG of the relevant gene, I cloned the region spanning the sequence from unc-24 to the ATG of *arf-3* into pPD107.94 and assayed for ability to drive seam expression. GFP is expressed weakly in the seam cells from this promoter but only in H0, H1 and H2 (Figure 5.1B). The intronic enhancer element drives expression in the seam cells specifically, whereas the 5' promoter drives expression in other cells and tissues (Figure 5.1C).

These data suggest that while the two promoter elements share the ability to drive expression in the seam, their specificity is different, leading to a different expression pattern.

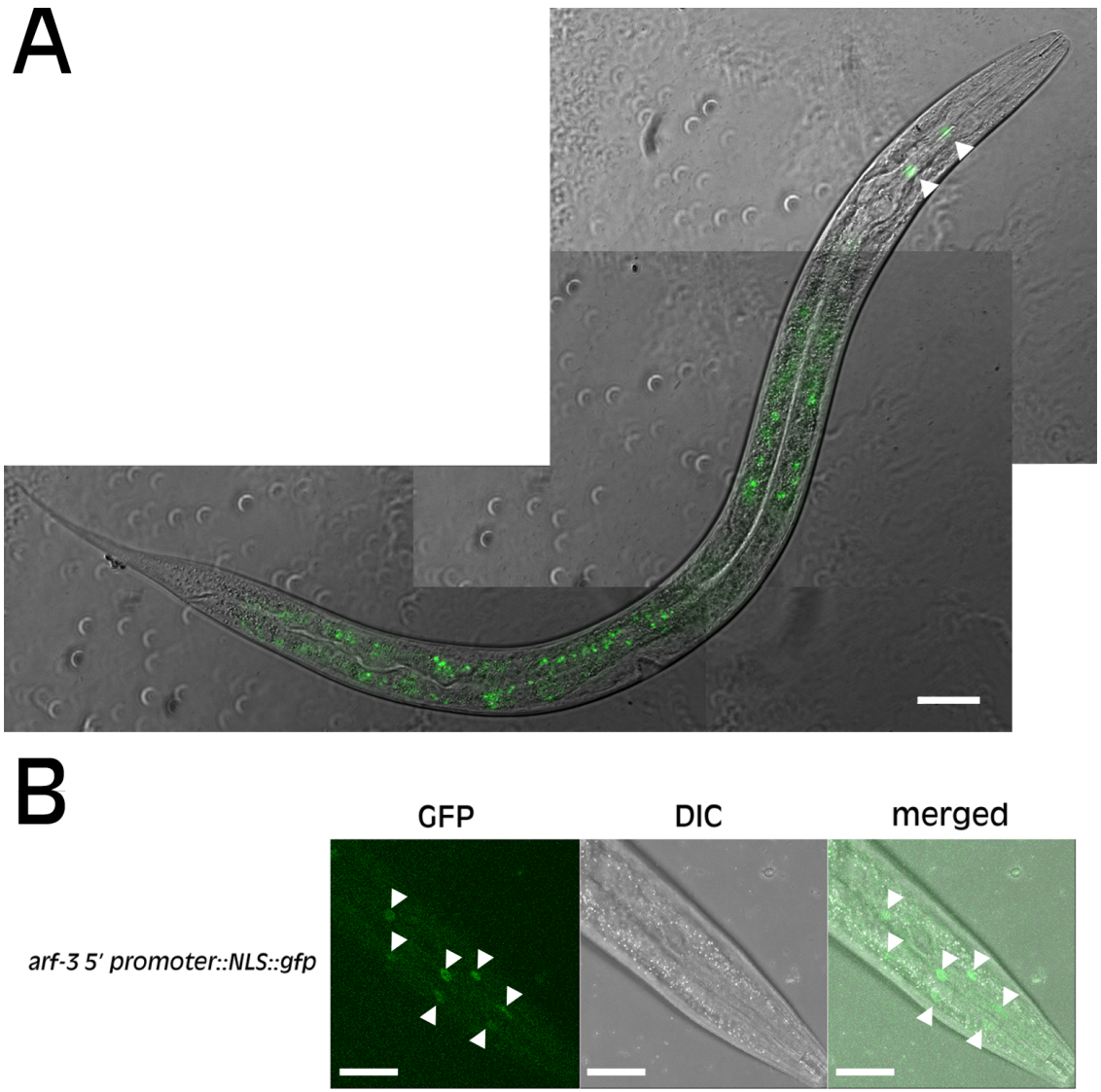


Figure 5.1: The 5' promoter sequence of *arf-3* drives the expression of GFP::NLS in the seam cells and other tissues. A = Worm expressing the GFP::NLS driven by the 5' sequence of the *arf-3* coding region. GFP-positive seam cell nuclei are observed in the head. B = Magnified head of a worm expressing the same extrachromosomal array. Weak GFP::NLS expression is observed in other cells, potentialy neurons. White arrows indicate nuclei expressing GFP. Scale bars = 25 µm

5.2.2 Different transcription factors are predicted to bind to the 5' promoter and the intronic enhancer elements of *arf-3*

The 3' and 5' regions of *arf-3* both drive seam cell expression, however, the difference in specificity and magnitude of expression suggest different patterns of regulation. To identify the transcription factors regulating *arf-3* gene expression, I submitted the two promoter elements into the transcription factor (TF) binding site prediction software JASPAR (Mathelier, Zhao et al. 2014). I probed the JASPAR nematode and vertebrate database with sequences of the *arf-3* locus. The vertebrate database was recommended in addition to the nematode database because it is larger and more accurate for predicting sites of real interaction (S. Gilbert, pers. comm.). JASPAR scans sequences for transcription factor motifs to identify potential interactors. I used a 90% relative profile score threshold when probing both databases, and the top hits (scores >10.0) are shown in Figure 5.3A (nematode database) and 5.3B (vertebrate database).

Binding sites were spatially conserved between the hits from both databases. In the 3' region sites localised within the final intron of *arf-3* as well as downstream from the coding region. At the 5' region binding sites localised between the ncRNA and the start site. Interestingly, the two regions each bind a distinct complement of transcription factors. Only *blmp-1* and *ces-2* from the nematode database are predicted to bind both the 5' promoter and 3' intronic enhancer. From the vertebrate database only SOX5, the *egl-13* homologue, is predicted to bind both the 5' promoter and 3' intronic enhancer. I also included the predicted binding sites of *lin-29*, *sox-2* and *rnt-1* from the vertebrate database which, although they scored slightly lower, have previously been shown to play a role in regulating seam cell development by our lab and others.

These data support the idea that different expression patterns in our transcriptional reporters arise from different transcription factors binding to the promoter

elements.

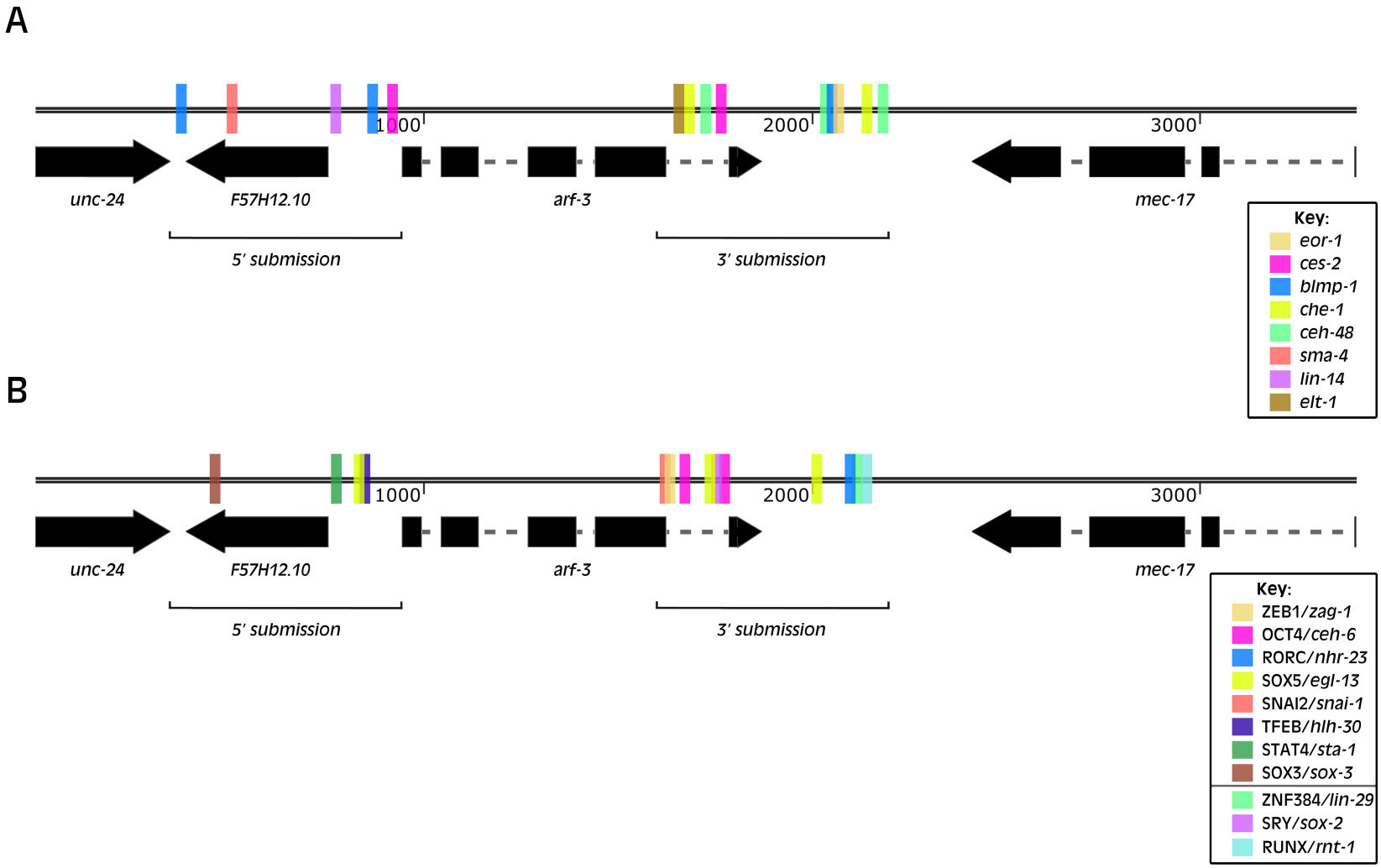


Figure 5.2: A schematic of the *arf-3* locus. Black brackets indicate the sequences submitted to JASPAR for identification of candidate transcription factors. The top hits (scores >10.0) from JASPAR are shown in the key and highlighted in their respective colour on the map. Hits from the vertebrate database that scored slightly less are also included if they have known expression in the seam (lower part of box inlcuding *lin-29, sox-2* and *rnt-1*).

5.2.3 Bioinformatic analysis of the *arf-3* promotor regions reveals three highly conserved TF target sequences

It is unlikely that all the candidate binding sites identifed by JASPAR are real, for example *egl-13* is not known to be expressed in seam cells. Thus, to filter the hits from the JASPAR database and select transcription factors for further analysis I asked whether the candidate transciption factor binding sites are conserved across nematodes.

We have previously used comparative genomics in the lab to identify conserved promoter regions of enhancer elements between *C. elegans*, *C. Briggsae* and *C. Remanei* (Brabin, Appleford, and Woollard 2011). I used this strategy to align the genomic sequence of *arf-3* and probed the individual hits from JASPAR (Table 1). Interestingtly the predicted binding sites for transcription factors *elt-1* and *rnt-1*, known to play a role in seam cells, are highly conserved. Several of the highest scoring hits from JASPAR are not well conserved including the sites of *eor-1* and *ces-2*. If a gene had multiple, distinct, predicted binding sites I looked for conservation at both sites (e.g. *blmp-1* and che-1), in the instance of *blmp-1* only one of these sites, at the 5' promoter region, was well conserved.

Recently, ChIP-seq datasets for many transcription factors have been published through modENCODE (Model Organism ENCyclopedia Of DNA Elements; Niu et al. 2011) and it's successor modERN (model organism Encyclopedia of Regulatory Networks; Kudron et al. 2018). Candidates which had conserved binding sites as well as seam cell expression were selected for further analysis if a ChIP-seq dataset was also available (Figure 5.4), these were *blmp-1, nhr-23, elt-1, rnt-1* and *die-1*. While *die-1* was not identified through Jaspar, a yeast-one hybrid screen has been previously performed in the lab using the 5' region of *arf-3* and *die-1* was the only candidate identified as a positive clone. Since then, a chromatin immunoprecipitation sequencing (ChIP-seq) dataset for DIE-1::eGFP has been made available on the modERN website (http://epic.gs.washington.edu/modERN/) so I decided to follow up on this work. The modERN consortium, along with its predecessor

modENCODE, has published the binding profiles of chromatin immunoprecipitation (ChIP) sequencing data of several hundread transcription factors (Kudron et al. 2018).

TABLE II: *Conservation of transcription factor binding sites.*

Gene	Homologue	Binding site conservation	Seam cell expression	ChIP dataset
blmp-1	BLIMP1	-(3'site)	Yes	Yes
blmp-1	BLIMP1	++ (5' site)	Yes	Yes
che-1 (i)	gl (fly)	– (3'site A)	No	Yes
che-1 (ii)	gl (fly)	+++ (3' site B)	No	Yes
ceh-48	HNF6	+++	No	Yes
ceh-6	OCT4	+	No	Yes
ces-2	N/A	—		No
egl-13	Sox5	+++	No	Yes
elt-1	GATA	+++	Yes	Yes
eor-1	PLZF	—	Yes	Yes
hlh-30	TFEB	++	Yes	Yes
lin-14	N/A	++	Yes	No
lin-29	ZNF384	+	Yes	No
nhr-23	RORC	++	Yes	Yes
rnt-1	RUNX	+++	Yes	Yes
sma-4	DPC4	—	No	No
snai-1	SNAI2	+++	No	No
sox-2	SRY	—	Yes	No
sox-3	SOX3	—	No	No
sta-1	STAT4	++	Yes (ubiquitous)	No
zag-1	ZEB1	+++	No	Yes

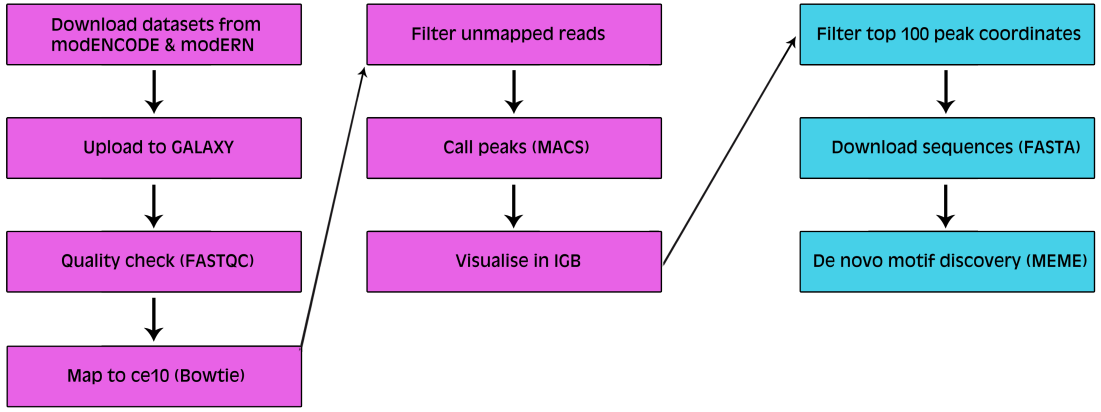


Figure 5.3: A schematic of the ChIP dataset analysis workflow. The pink boxes indicate the steps taken for all the candidate genes. The blue boxes indicate additional steps taken for candidates where no motif has previously been identifed such as *die-1*

5.2.4 BLMP-1 binds to the *arf-3* locus at 5' promoter and potentially at the 3' enhancer

The predicted binding site of BLMP-1 at the 5' promoter sequence is well conserved (purple bar, Figure 5.4A), whereas there is no conserved site in the 3' region suggesting the predicted site called by JASPAR is not real (Figure 5.4B).

I therefore probed the available BLMP-1::eGFP ChIP dataset from modENCODE to determine if any binding can be observed at the *arf-3* locus (Figure 5.4C). Figure 5.3 shows the workflow of ChIP-seq analysis: the reads of two biological replicates and the corresponding controls were aligned with the *C. elegans* genome (WS220) and subjected to peak calling using MACS (Model-based Analysis of ChIP-Seq data; Zhang et al. 2008).

MACS called a peak at the 5' site which was in both replicates, providing further evidence that this binding site contributes to the transcriptional regulation of *arf-3*. MACS also called a broader peak potentially overlapping with the 3' promoter region 1, indicating their may be some binding, however this was only identified in one replicate and the binding site is not conserved. There is a relatively well conserved potential binding site that lies just upstream of the 3' enhancer (purple bar Figure 5.4B), however this conservation is more likely due to its location within exon 4.

Taken together this suggests *blmp-1* may be playing a role in driving expression of *arf-3* but since it is predominantly binding at the 5' promoter sequence it may not be driving expression in the seam cells specifically.

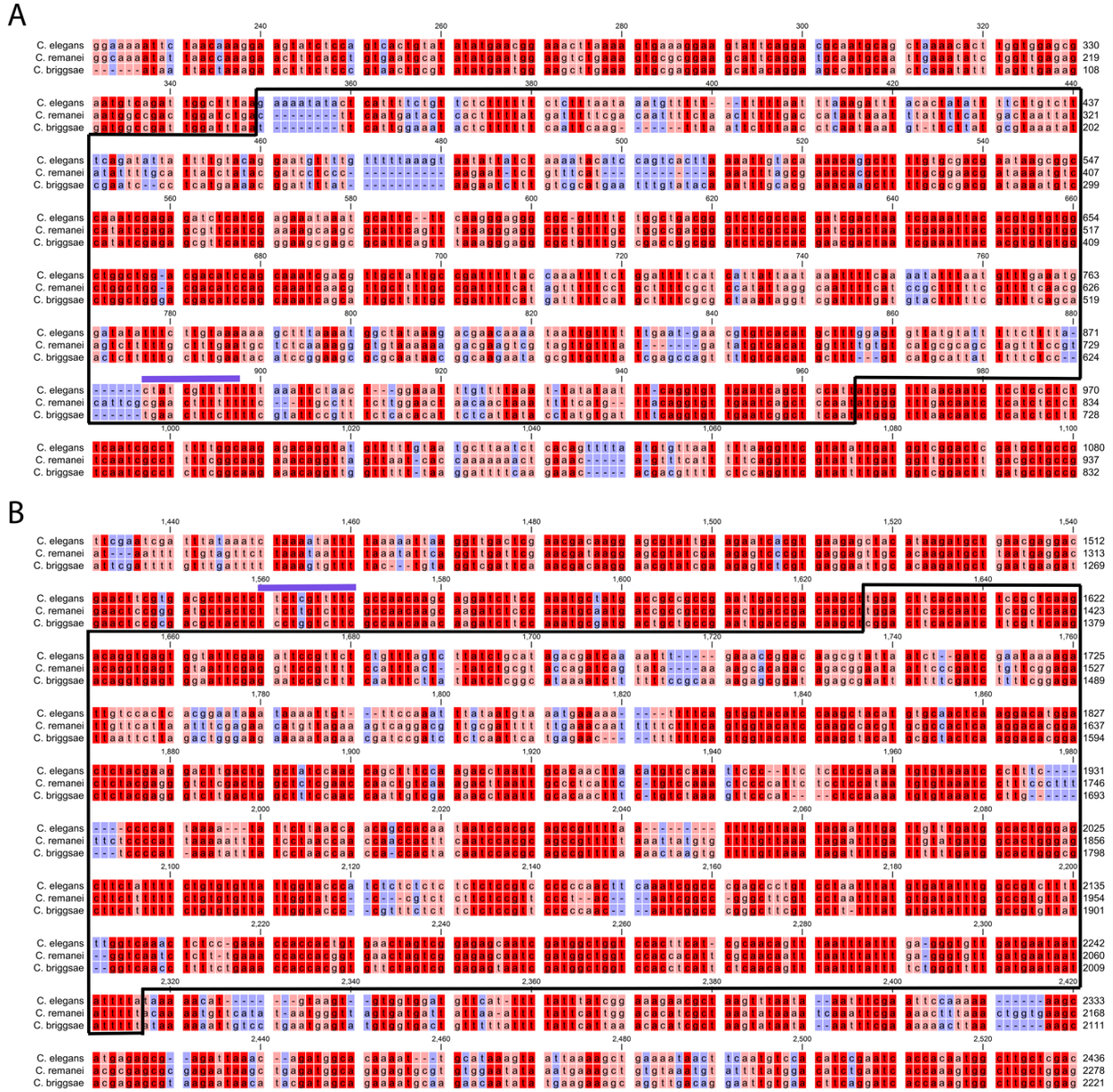
5.2.5 Expression of *arf-3::mCherry* and *scm::gfp* is unaffected by depletion of BLMP-1

Once I had established BLMP-1 binds to *arf-3* through ChIP I used RNAi and an available deletion allele, *tm548* to probe the role of *blmp-1* in regulation of *arf-3* and seam cell development. *blmp-1(tm548)* carries an 810 bp deletion removing part of

exon 3 and part of intron 3, this results in a frameshift, suggesting it is a null allele.

blmp-1(tm548) animals exhibit no change in terminal seam cell number as measured by counting *scm*-positive nuclei corroborating the findings of previous studies (Horn et al. 2014). To further investigate any role BLMP-1 may be playing in regulating *arf-3* expression I crossed our translational reporter, ARF-3::mCherry, with *blmp-1(tm548)* to generate AW1803. The expression pattern of ARF-3::mCherry was unchanged at all larval stages, with ARF-3::mCherry expressed in the seam, hypodermis, bodywall muscle and head neurons as in AW860 (Figure 5.5).

Horn and colleagues did not report *arf-3* among the list of genes that were differentially expressed in *blmp-1(tm548)* as determined by RNA-seq (Horn et al. 2014). However, Horn *et al.* harvested the animals for RNA-seq at the mid-L3 stage but the ChIP-seq data suggests it binds *arf-3* at L1. Taken together, while BLMP-1 appears to bind at the *arf-3* locus, we cannot determine whether it is acting to upregulate or downregulate *arf-3* expression.


A
B
C. elegans
C. remanei
C. briggsae

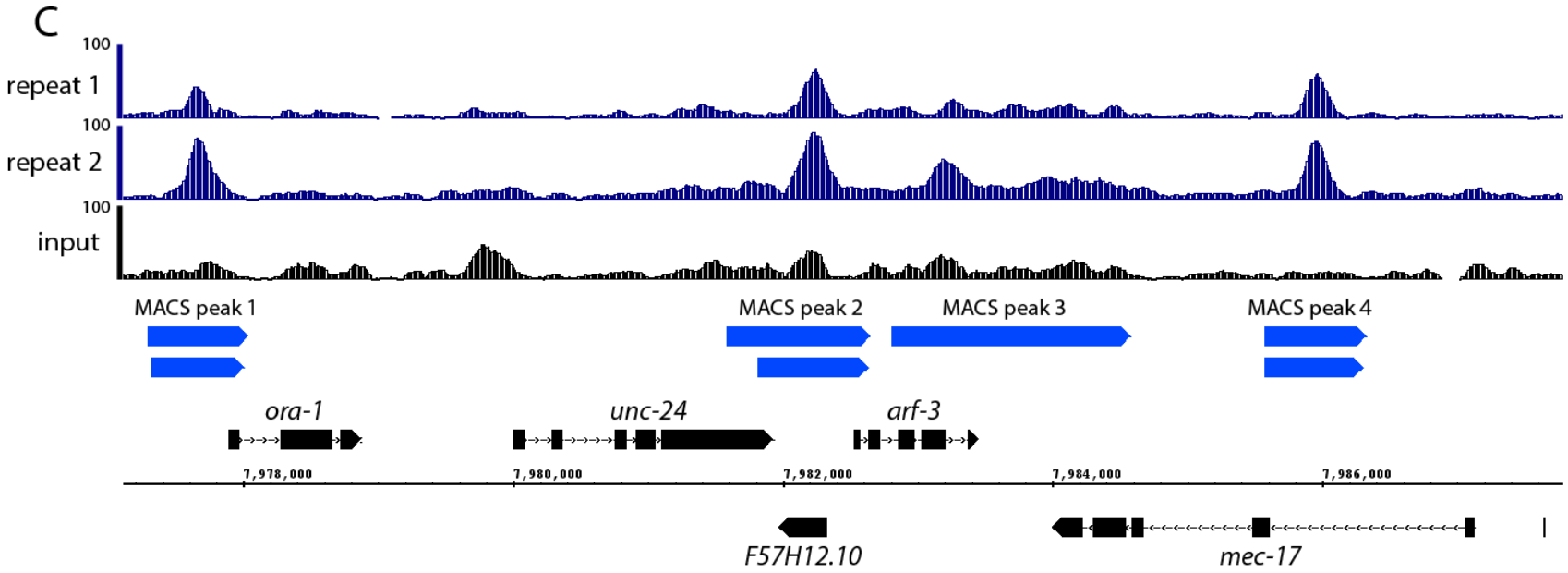


Figure 5.4: A = Sequence alignment of the 5' promoter region of *arf-3* locus between *C. elegans, C. briggsae and C. remanei.* Black outlined region indicates the sequence submitted to Jaspar. Purple solid line indiciates the conserved *blmp-1* binding site. B = Sequence alignment of the 3' enhancer region of the *arf-3* locus between *C. elegans, C. briggsae and C. remanei.* The purple solid line shows a potential conserved binding site outside the region submitted to JASPAR. Regions of high conservation are indicated in red; low conservation is shown in blue. C = Visualisation of BLMP-1::eGFP ChIP binding at *arf-3* locus in L1 larvae. In dark blue are the biological repeats of BLMP-1::eGFP ChIP and in black is the input control. Below the tracks is a schematic of the *arf-3* locus with the peaks called by MACS shown above.

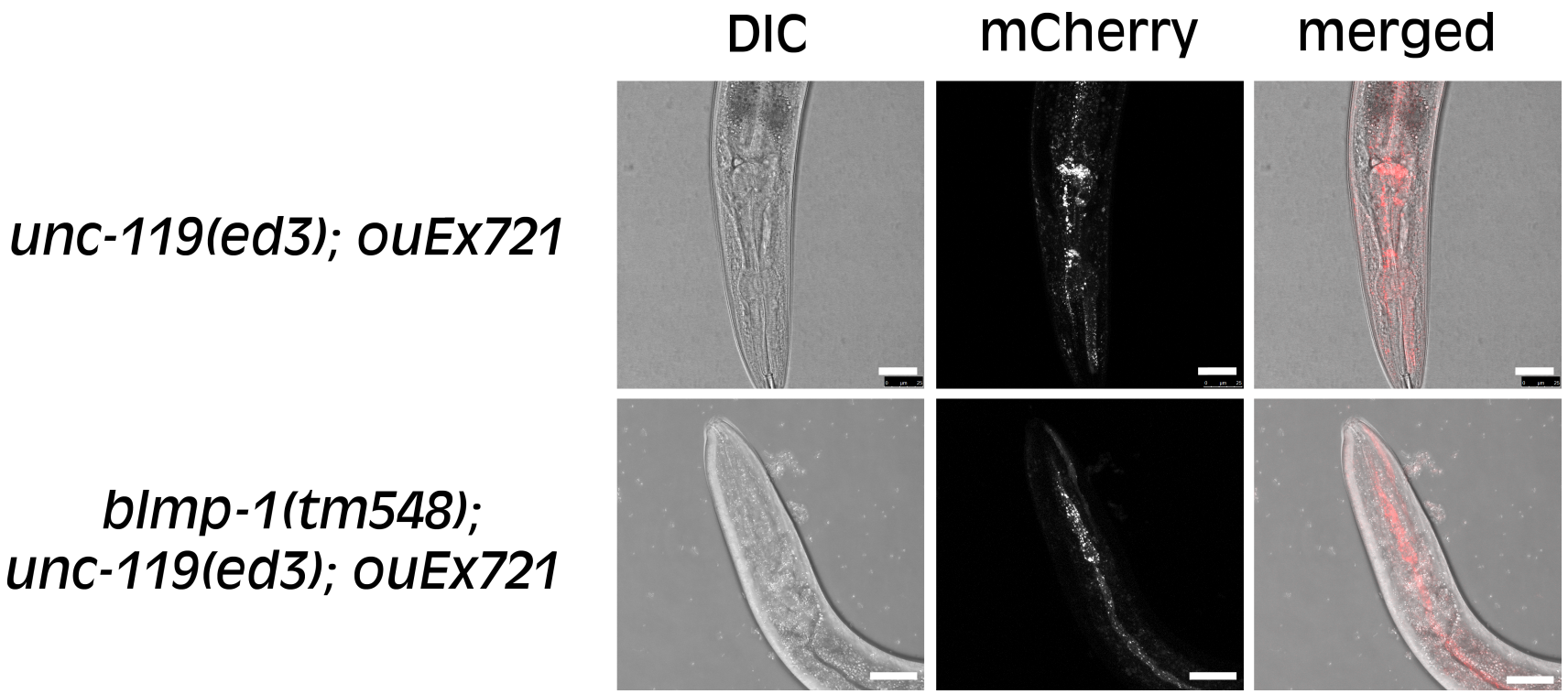


Figure 5.5: A representative image of the expression pattern of ouEx721[*arf-3::mCherry; unc-119+*] in *blmp-1(tm548)* animals. ARF-3::mCherry expression is indistinguishable from AW860 animals.

5.2.6 DIE-1 binds to a site 3' of the *arf-3* coding region

We have previously attempted to use a yeast one-hybrid screen to discover transcription factors that bind to the *arf-3* locus. Unfortunately, only yeast carrying the 5' promoter region were viable and when screened *die-1* was identified as a positive hit. Therefore I wanted to probe the available ChIP dataset from modERN to see if this result was supported *in vivo* in *C. elegans*. The ChIP binding profile at the *arf-3* locus is shown in Figure 5.6A. MACS called a peak in one replicate, downstream of *arf-3* lying in the intergenic region *arf-3* and *mec-17*. Curiously, MACS did not call a peak at the 5' promoter region, which our own data would suggest could be a binding site for *die-1*. I used the top 100 peaks identified through MACS in both replicates to attempt *de novo* motif discovery with MEME (Figure 5.6B). Probing the region at the *arf-3* locus using this motif does not identify any potential binding sites. This data suggests *die-1* may be binding at the *arf-3* locus, although not at the promoter regions I targetted.

5.2.7 *die-1(RNAi)* does not affect the expression of *scm::gfp*

Given our evidence that DIE-1 binds at the *arf-3* locus we were interested in discovering any potential role in seam cells or *arf-3* in *C. elegans*. I used RNAi to knockdown *die-1* expression post embryonically in the ARF-3::mCherry and *rrf-3(pk1426); wIs51[scm::gfp]* strains respecitvely (Figure 5.7A & B respectively). This would allow us to determine any potential role in regulating seam cell divisions, or expression of the *scm::gfp* construct (by counting *scm*-positive nuclei at L4) as well as any changes to *arf-3::mCherry* expression since this is driven by the endogenous promoter. The expression pattern of ARF-3::mCherry was unchanged and I observed no significant change to seam cell number compared to control.

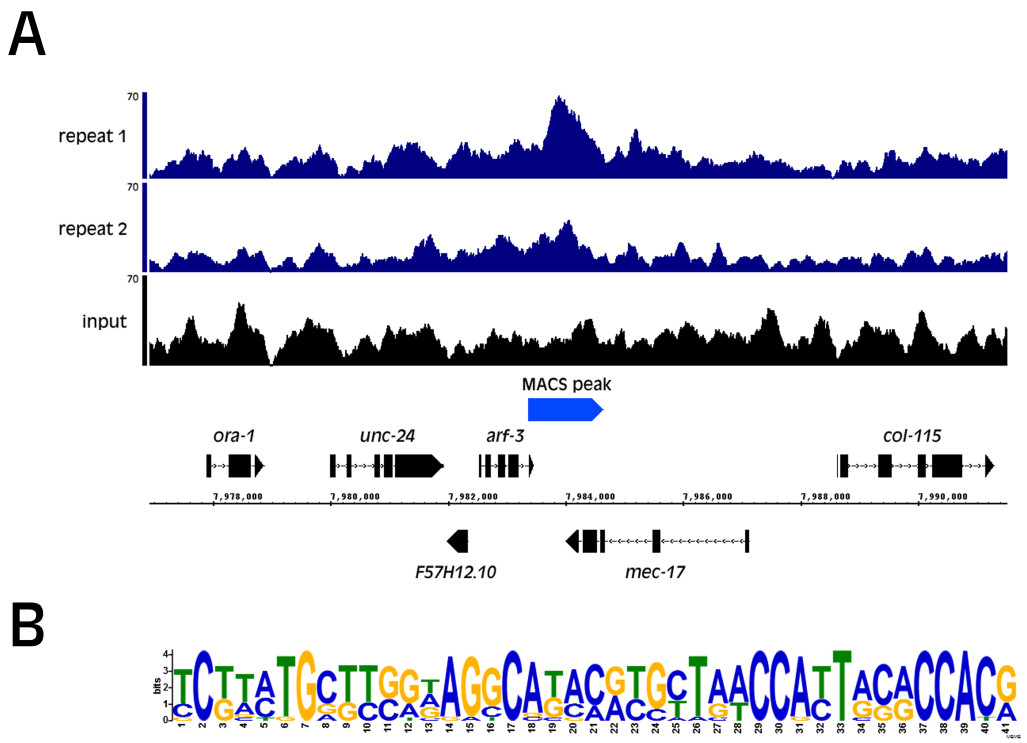


Figure 5.6: Visualisation of DIE-1::eGFP binding sites in early adult. A = DIE-1 peaks from two biological replicates were predicted using MACS and visualized using IGB. Representative DIE-1 binding sites in 10kb region on chromosome IV that spans the arf-3 locus. B = motif called by MEME from top ChIP peaks. In dark blue are the biological repeats of DIE-1::eGFP ChIP and in black is the input control. Below the tracks is a schematic of the *arf-3* locus with the peaks called by MACS shown above

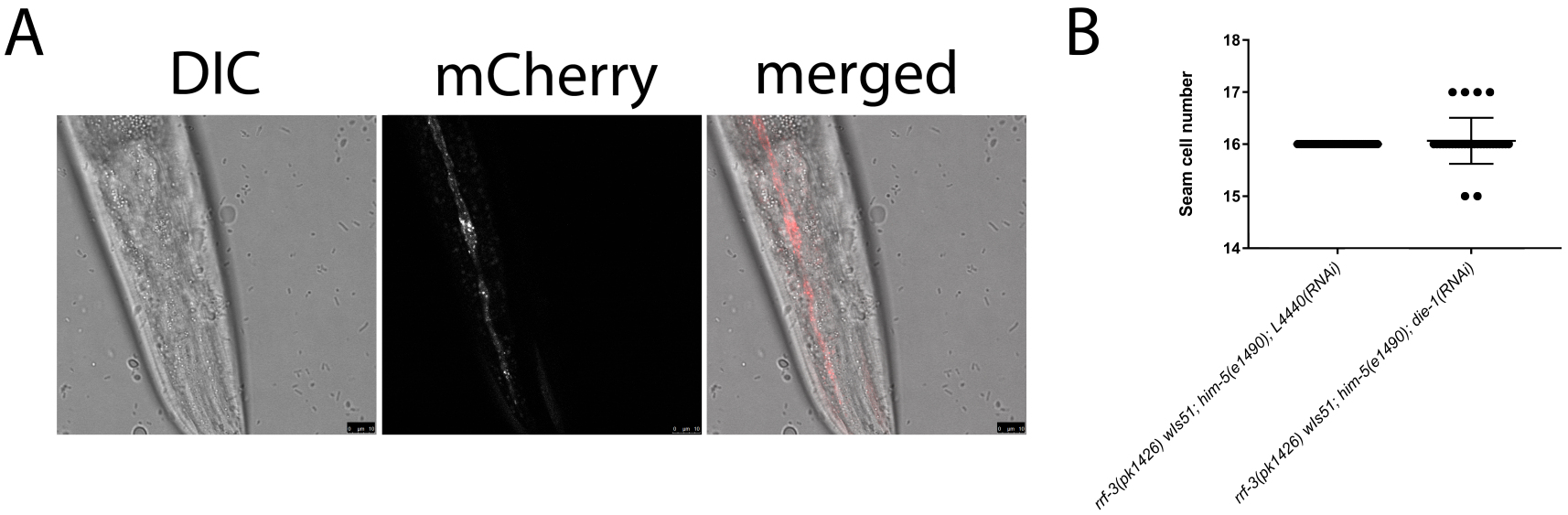


Figure 5.7: Knockdown of *die-1* causes no significant change to *arf-3* expression. A = The expression pattern of *arf-3::mCherry* in AW860 (ouEx721*arf-3::mCherry; unc-119+*) treated with *die-1(RNAi)* is unchanged. B = Seam cell counts after post-embryonic treatment with *die-1(RNAi)* or empty vector control in a RNAi hypersensitive mutant background (*rrf-3(pk1426); wIs51[scm::gfp) (N = 49). Student's T-test was used to determine significance (ns:P>0.5)*

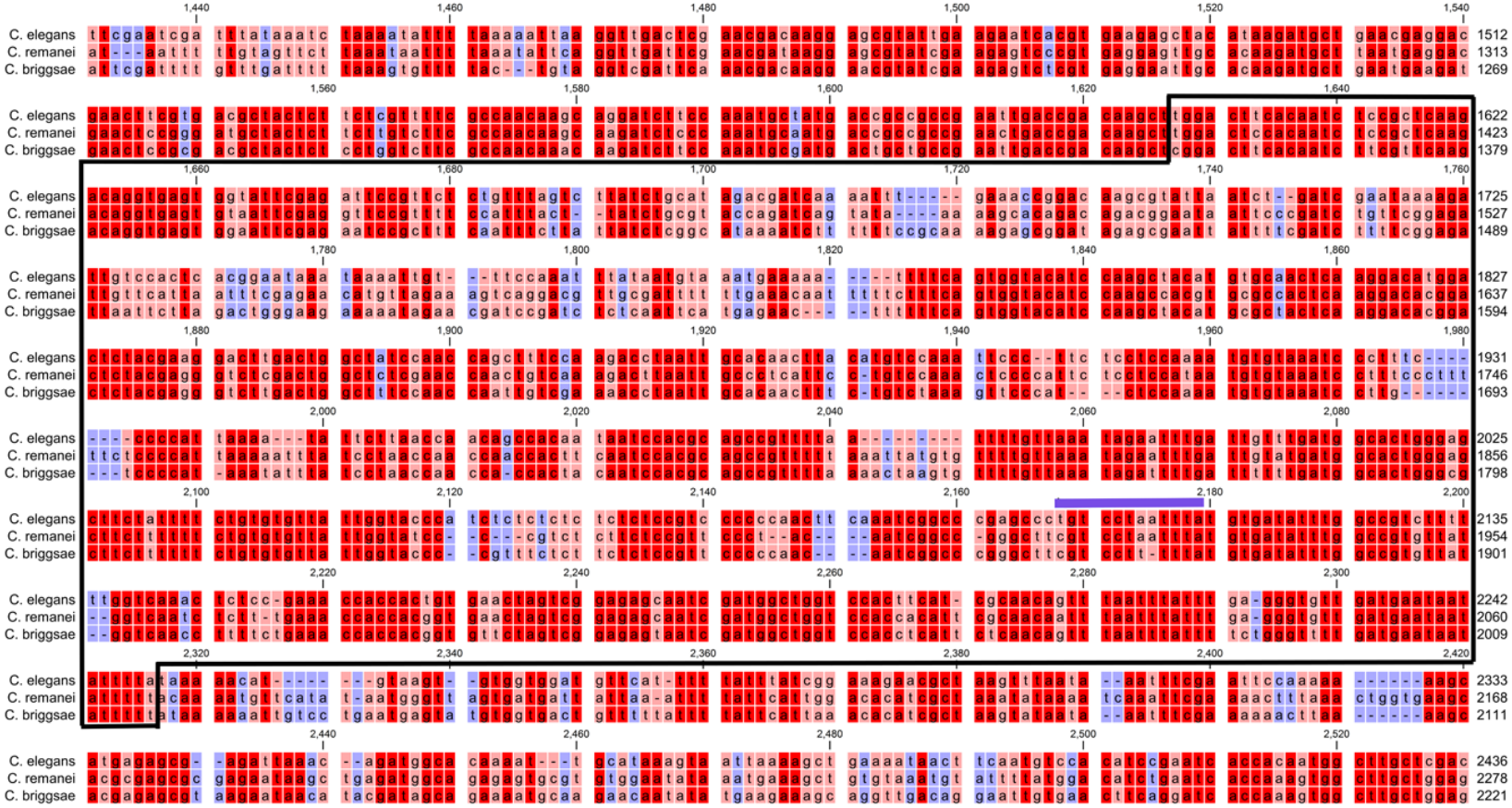


Figure 5.8: Figure shows a sequence alignment of the 3' enhancer region of *arf-3* between *C. elegans, C. briggsae and C. remanei*. Black outlined region indicates the enhancer sequence submitted to Jaspar. Purple solid line indiciates the conserved *nhr-23* binding site. Regions of high conservation are indicated in red; low conservation is shown in blue.

5.2.8 NHR-23 regultes the expression of *arf-3*

The predicted binding site of NHR-23 at the 3' enhancer sequence is well conserved Figure 5.8. I therefore probed the available NHR-23::eGFP ChIP dataset from modENCODE to determine binding at the *arf-3* locus (Figure 5.9). Surprsingly, MACS called several peaks across the *arf-3* locus. These peaks coincided with both promoter elements and were reproducible between the ChIP replicates providing strong evidence that NHR-23 regulates *arf-3*.

Knockdown of *nhr-23* expression by post embryonic RNAi in *rrf-3(pk1426); wIs51[scm::gfp]* caused a signicant reduction of *scm::gfp* expression in the seam and moulting defects (Figure 5.10A and B). Knockdown of *nhr-23* had a dramatic effect on the expression of ARF-3::mCherry including aberrant expression in hypodermal fated cells which failed to fuse with the hyp7 syncytium. In order to visualise these defects better I crossed this construct into a line carrying the integrated reporter *heIs63[wrt-2p::gfp::PH; wrt-2::gfp::H2B]* which marks the nuclei and cell boundaries of seam cells with GFP. Figure 5.10C shows the expression of ARF-3::mCherry in the seam cells as well as abberrant expression not in the seam (white arrowhead). The ARF-3::mCherry is also mislocalised, displaying a more tubular distribution in the cytoplasm.

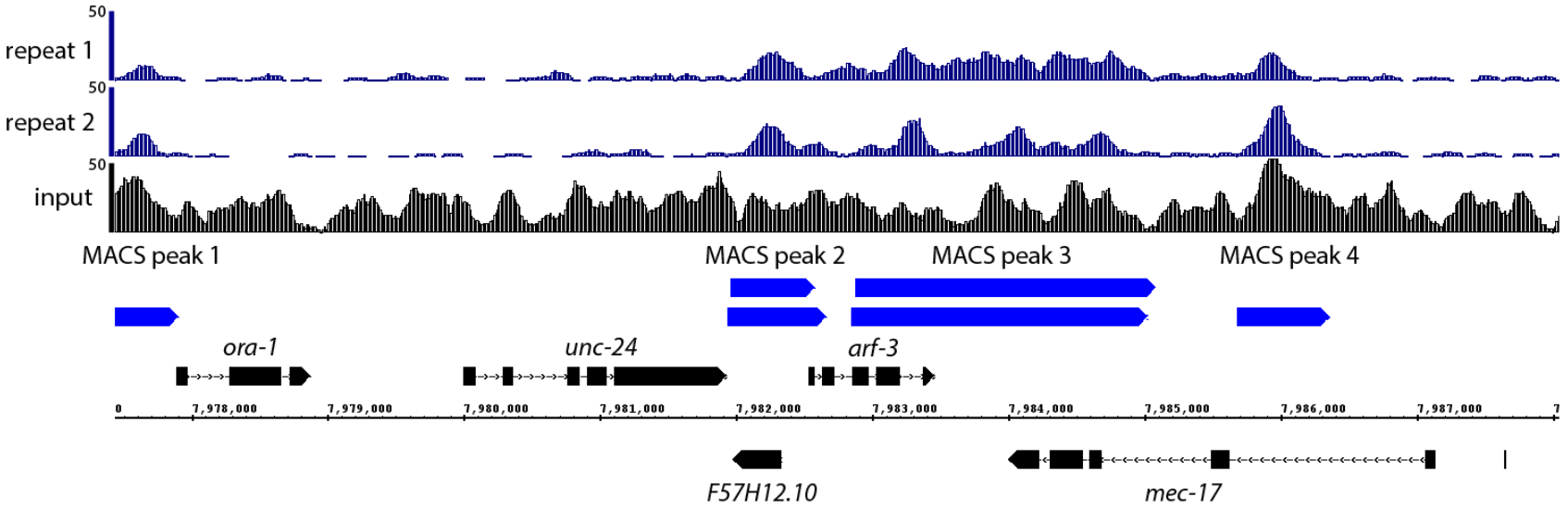


Figure 5.9: Visualisation of NHR-23::eGFP ChIP binding at *arf-3* locus in L3 larvae. In dark blue are the biological repeats of NHR-23::eGFP ChIP and in black is the input control. Below the tracks is a schematic of the *arf-3* locus with the peaks called by MACS shown above.

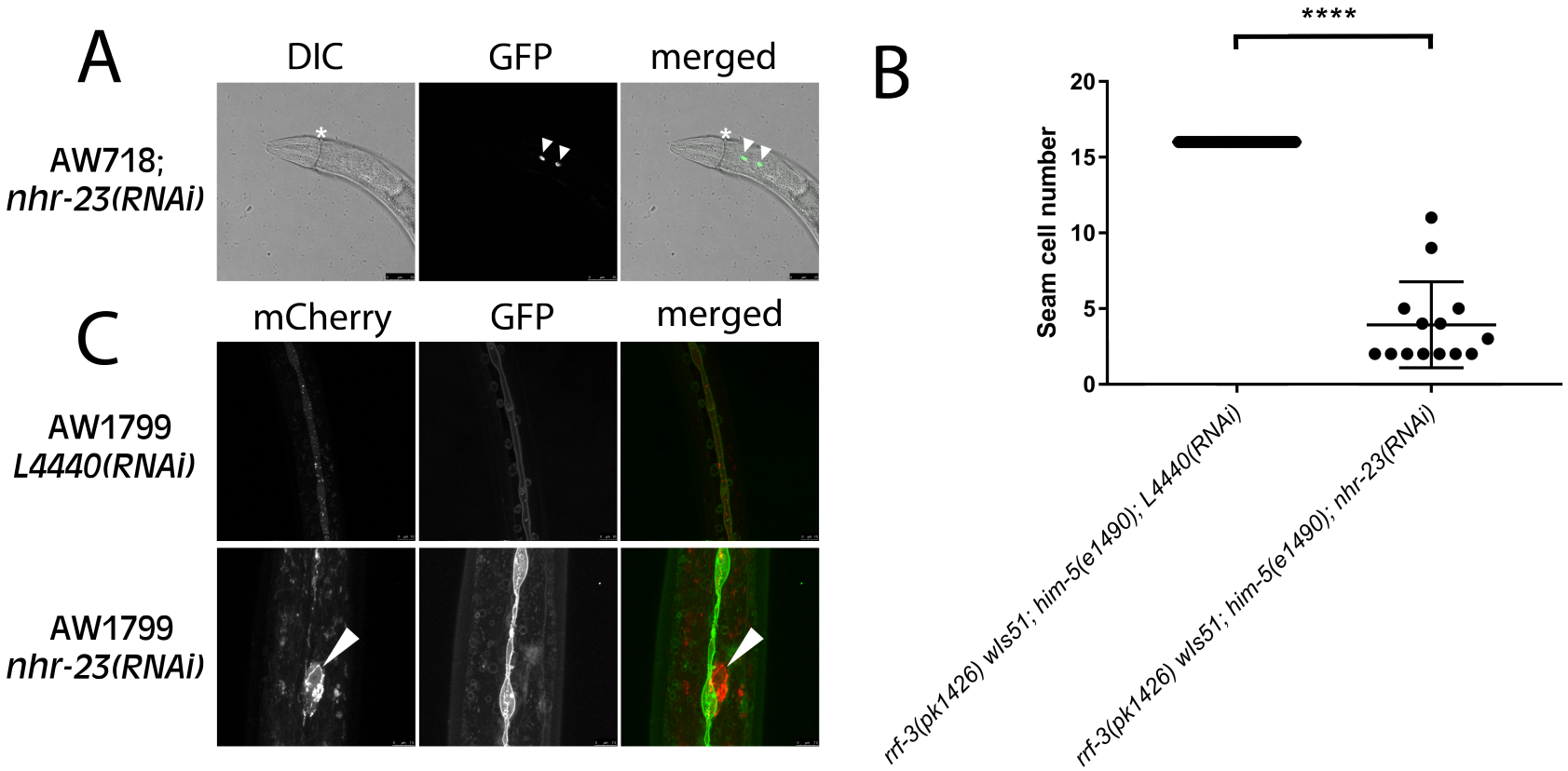


Figure 5.10: Knockdown of *nhr-23* causes seam cell defects and perturbs ARF-3::mCherry expression. A = *nhr-23(RNAi)* in *rrf-3(pk1426); wIs51[scm::gfp]* signifcantly reduces seam cell number and induces moulting defects. White asterisk indicates constricted cuticle around head. B = Count of *scm*-positive nuclei after post-embryonic knockdown of *nhr-23(RNAi)* in *rrf-3(pk1426); wIs51[scm::gfp]* (N = 14). Student's T-test was used to determine significance (P<0.0001). C = Expression pattern of *arf-3::mCherry* after knockdown of *nhr-23* in AW1799 *heIs63[wrt-2p::gfp::PH; wrt-2::gfp::H2B]; ExAW721[arf-3::mCherry; unc-119+]*. White arrowhead indicates cell aberrantly expressing *arf-3::mCherry*.

5.2.9 ELT-1 binds the 3' enhancer of *arf-3*

The Woollard lab has previously studied the GATA transcription factor *elt-1* in the context of seam cell development (Brabin, Appleford, and Woollard 2011). In this study it was found that *elt-1* directly regulates *bro-1* to maintain stem-like fate of seam cells. We also observed loss of *scm::gfp* expression in seam cells upon *elt-1* knockdown by RNAi, even though the seam cell was still present and expressing *ajm-1::gfp*, this was intepreted as a loss of seam cell fate.

Previously we described knockdown of *elt-1* causing the progressive loss of seam cells (Brabin, Appleford, and Woollard 2011). We also showed that *elt-1(RNAi)* in animals expressing the transgene *ajm-1::gfp* (AJM-1::GFP marks the apical junctions between seam cells and the surrounding hyp7 syncytium but is not expressed in hyp7) led to some seam cells losing the expression of *scm::gfp* but retaining their AJM-1::GFP boundary, they were not observed to fuse with hyp7. There is a well conserved putative GATA binding site in the 3' promoter region of the *arf-3* locus (Figure 5.11). Therefore I added this gene to my list of candidates for further analysis using the available ChIP datasets.

The ELT-1::eGFP ChIP binding profile at the *arf-3* locus is shown in Figure 5.12. MACS called a peak in one replicate, overlapping with the 3' enhancer element of *arf-3*. Although the peak was only called in one replicate, this may be unrepresentative since the 3' enhancer element appears to only drive expression in the seam cells - only 32 cells in the entire worm. Therefore any signal may be "crowded out".

5.2.10 *scm::gfp* and *arf-3::mCherry* expression is uncoupled from seam cell fate in *elt-1(ku491)* and *elt-1(RNAi)*

To investigate the role *elt-1* plays in regulating seam cell development and *arf-3* expression further I used a viable hypomorphic allele (elt-1(ku491)) and RNAi to investigate changes to the expression of *scm::gfp* and our ARF-3::mCherry construct.

First I used RNAi to recapitulate the data previously observed in our lab (Brabin, Appleford, and Woollard 2011); Figure 5.13B shows the significant severe reduction in *scm::gfp* expression when *rrf-3(pk1426); wIs51[scm::gfp]* animals are treated with *elt-1(RNAi)*. Figure 5.13A shows this also with our ARF-3::mCherry construct, loss of seam cell expression is observed especially in the V1-4 seam cell lineages. Expression of *scm::gfp* and ARF-3::mCherry is more robust at the head and tail of the worm with the H0 and T seam cells very rarely losing expression.

Previously we described knockdown of *elt-1* causing the progressive loss of seam cells (Brabin, Appleford, and Woollard 2011). We also showed that *elt-1(RNAi)* in animals expressing the transgene *ajm-1::gfp* (AJM-1::GFP marks the apical junctions between seam cells and the surrounding hyp7 syncytium but is not expressed in hyp7) led to some seam cells losing the expression of *scm::gfp* but retaining their AJM-1::GFP boundary, they were not observed to fuse with hyp7.

I used the transgene *heIs63[wrt-2p::GFP::PH; wrt-2::GFP::H2B]* to mark the seam cell boundaries and our ARF-3::mCherry reporter to recapitulate this observation (Figure 5.13C). Expression of *arf-3::mCherry* was lost in *elt-1(RNAi)* but some seam cells were still present as marked by PH::GFP.

The high copy number of the ARF-3::mCherry in the extrachromosomal array means it is greatly overexpressed, it therefore makes it difficult to quantify changes in expression. While I have seen the abrogation of its expression in *elt-1(RNAi)* a more definitive demonstration of the role of *elt-1* in regulating *arf-3* would be by qPCR. I purified the RNA of *elt-1(ku491)* animals and N2 as a control. Figure 5.14A shows the messenger RNA of the *arf-3* and the primer pairs I used to quantify its expression. Figure 5.14B shows the PCR fragment generated from N2 cDNA to test the primer pairs labelled in Figure 5.13A. I checked that I had indeed purified RNA from 3 biological replicates of N2 and *elt-1(ku491)* worms by gel electrophoresis (Figure 5.14C) 28S and 18S rRNA bands can be seen. I performed qPCR on the cDNA I generated from these samples (Figure 5.14D), the expression of *arf-3* is significantly reduced in *elt-1(ku491)* animals.

Finally, I used RNAi of the other transcription factors examined, *blmp-1, die-1* and *nhr-23* in *elt-1(ku491; scm::gfp)* to assess any interaction between them (Figure 5.15). *elt-1(ku491)* display a reduction in *scm*-positive nuclei (mean = 12.46) corroborating the data of (Cohen et al. 2015). Knockdown of *die-1* by RNAi partially rescued this phenotype (mean = 15.09). Whereas knockdown of *nhr-23* significantly exacerbated the loss of seam cells in the mutant background compared to wildtype. *blmp-1(RNAi)* caused no significant difference in seam cell number as identified by expression of *scm*.

Taken together, these data suggest *elt-1* and *nhr-23* act as positive regulators of *arf-3* and *scm::gfp*. The roles of *die-1* and *blmp-1* in the seam remain unclear but *die-1* may be acting to repress the expression of *arf-3*.

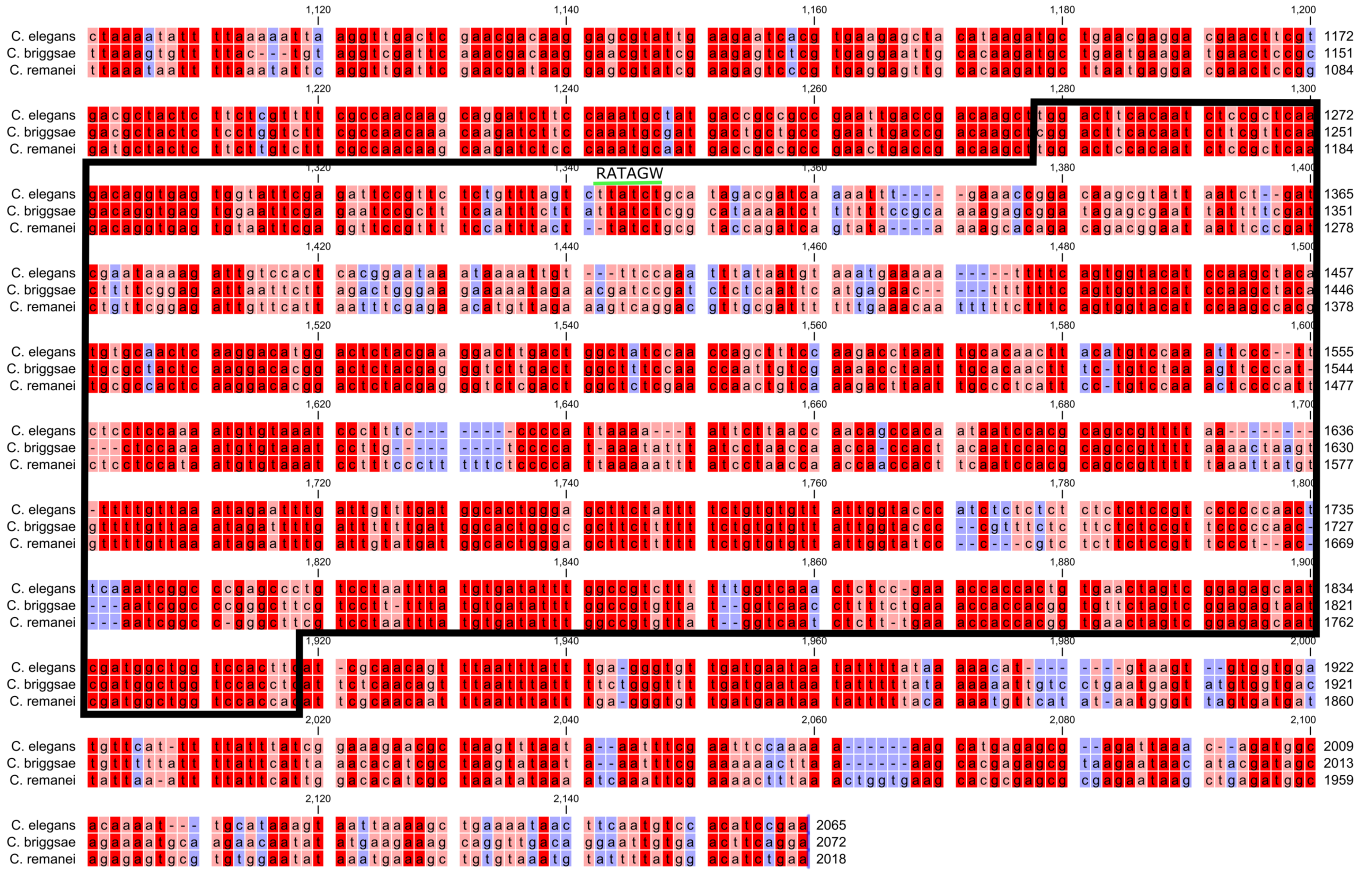


Figure 5.11: Sequence alignment of the *arf-3* genomic locus between *C. elegans, C. briggsae* and *C. remenai.* Regions of high conservation are indicated in red; low conservation is shown in blue. The black boxed area indicates the 603bp region shown to drive the expression of *scm::gfp* The green line highlights the highly conserved putative ELT-1 binding site with the canonical GATA binding sequence WGATAR.

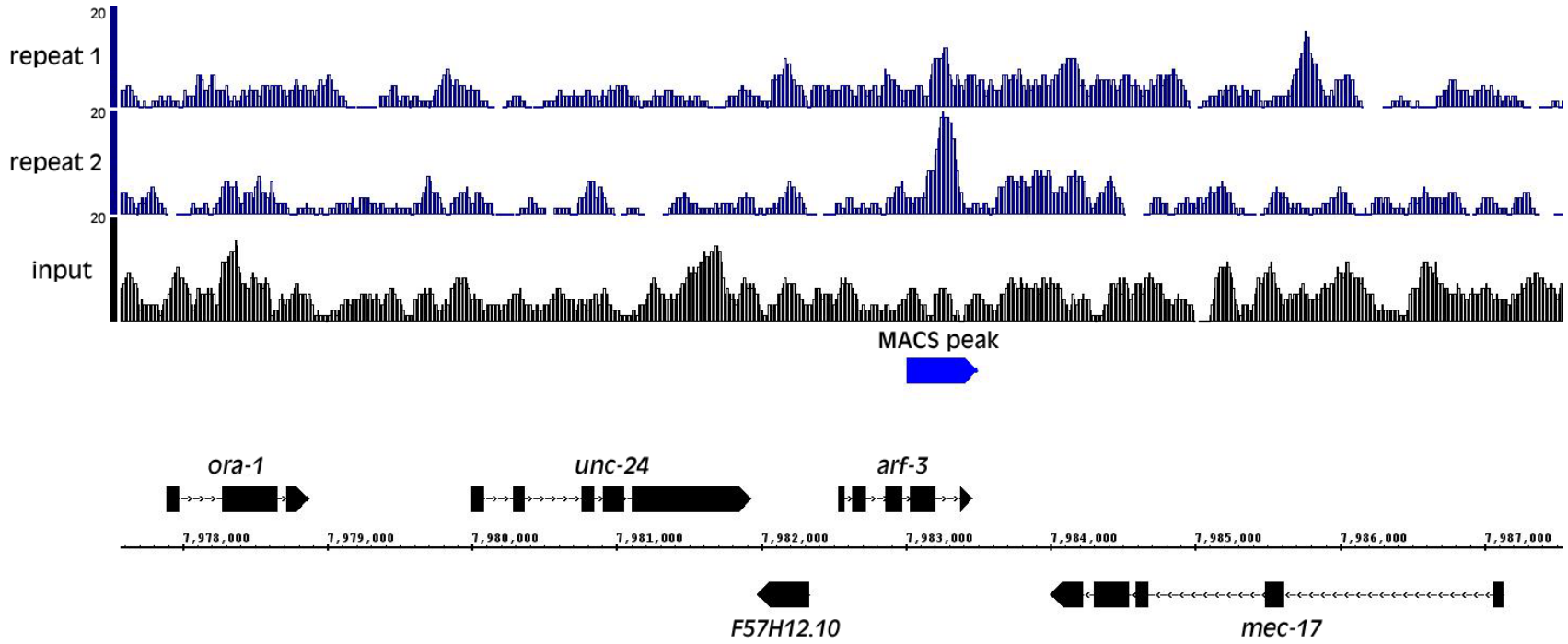


Figure 5.12: Visualization of ELT-1::eGFP binding sites in L2 larvae. ELT-1 peaks from two biological replicates were predicted using MACS and visualized using IGB. Representative ELT-1 binding sites in 10kb region on chromosome IV that spans the arf-3 locus.

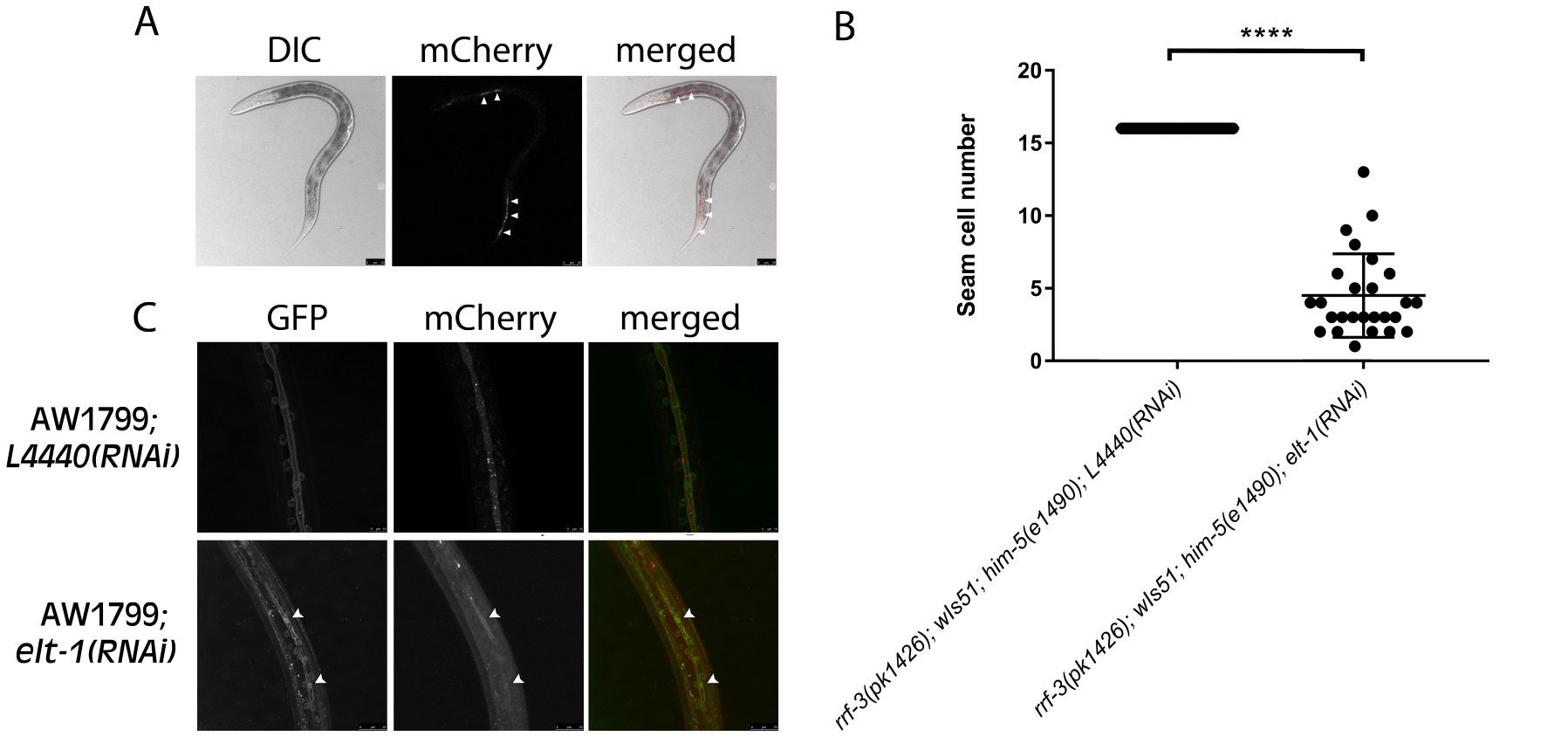


Figure 5.13: Knockdown of *elt-1* causes a significant decrease in seam cell number, gaps in the seam and loss of *scm* expression. A = Representative image of an animal after knockdown of *elt-1* by RNAi in AW860 (*arf-3::mCherry*). White arrowheads indicate seam cells expressing *arf-3::mCherry*. The loss of *arf-3::mCherry* expression is more frequent in cells from the V1-4 lineage than in the head or tail. B = Count of *scm*-positive nuclei after post-embryonic knockdown of *elt-1(RNAi)* in *rrf-3(pk1426); wIs51[scm::gfp]* (N = 26). Student's T-test was used to determine significance (P<0.0001). C = Expression pattern of *arf-3::mCherry* after knockdown of *elt-1* in AW1799 *heIs63[wrt-2p::gfp::PH; wrt-2::gfp::H2B]; ExAW721[arf-3::mCherry; unc-119+]*. White arrowheads indicate outlined seam cells cell which do not express *arf-3::mCherry*.

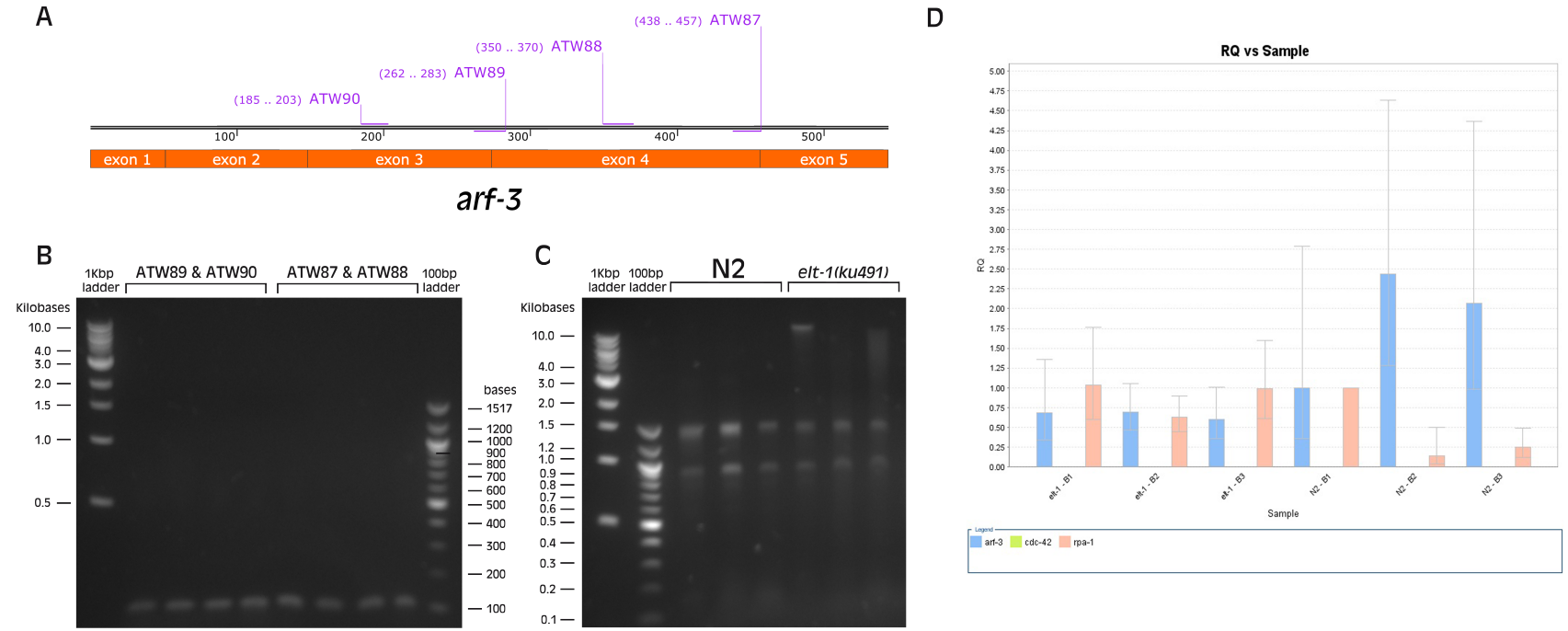


Figure 5.14: qPCR strategy for the measurement of *arf-3* expression in *elt-1(ku491)* mutant worms versus N2. A = Schematic of *arf-3* messenger RNA showing the primers used to for qPCR. B = Image of gel demonstrating PCR amplification of cDNA from N2 using the primers described in A. C = Image of gel showing purified RNA from N2 and *elt-1(ku491)*. The 28S and 18S rRNA bands are separated by gel electrophoresis at approximately 1500 and 900bp respectively. D = qPCR analysis of *arf-3* expression using primers ATW89 and ATW90. *ama-1, rpa-1* and *cdc-42* were used as internal controls. Expression of *arf-3* is significantly reduced in *ku491* compared to N2.

5.3 Discussion

In this Chapter we have identfied two regions of the *arf-3* locus that are capable of driving seam cell expression. One of these regions is a *cis*-regulatory element that lies within the final intron of *arf-3* that drives expression in the seam specifically.

The two promoter elements have distinct expression patterns, a feature that is supported by the different binding profiles of transcription factors at this locus. We have identified *elt-1* and *die-1* as factors that bind to the 3' end of *arf-3*, while *blmp-1* binds to the 5' promoter. *nhr-23* appears to bind to both promoter elements.

These findings go some way to explaining the different expression pattern between our translational reporter *arf-3::mCherry* and *scm::gfp*. It is likely because *scm::gfp* only partially represents *arf-3* expression, as it includes only the enhancer within the last intron of this gene and not the protein coding region nor the upstream sequence. It is remarkably serendipitous that in the enhancer trap that originally identified *scm::gfp* (Hope 1991) the fragment only included the latter portion of *arf-3*.

Knockdown of *nhr-23* and *elt-1* by RNAi leads to the uncoupling of *arf-3::mCherry* expression and seam cell fate. Specifically, knockdown of *nhr-23* led to *arf-3::mCherry* expression in non-seam cells (as determined by not expressing the trangene *heIs63*). Knockdown of *elt-1* led to loss of *arf-3::mCherry* expression in the seam cells. We now know that *elt-1* binds to the 3' enhancer element of *arf-3* that drives expression of *scm* to directly regulate *scm::gfp* expression.

As mentioned, the 5' promoter appears to drive *arf-3* expression in several different tissues while the 3' enhancer drives a specific seam cell expression. It remains unclear what the role of *arf-3* is in other tissues, however it has been shown to play a role in the regulation of vulval induction for example (Skorobogata et al. 2014). In this study I have focussed on expression of *arf-3* in the seam and so I have not identified transcription factors that drive the expression of *arf-3* in other tissues. Those transcription factors presumably bind at the 5' promoter and not the 3' enhancer. Whether the 5' promoter is the sole driver of *arf-3* expression in other tissues is

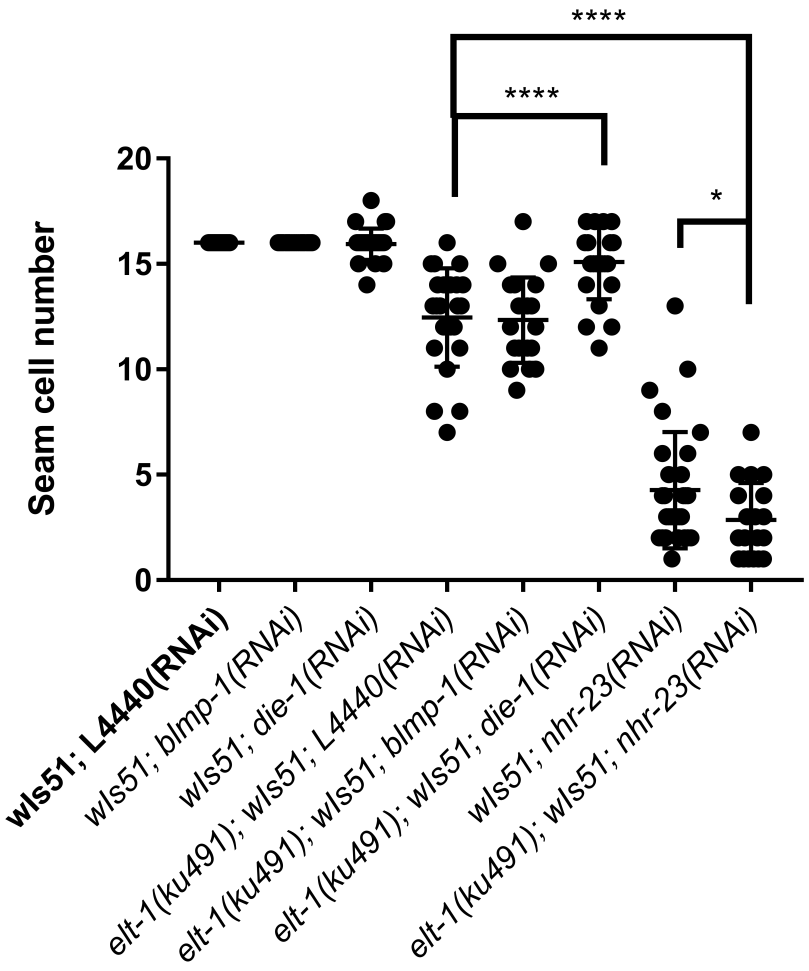


Figure 5.15: The *elt-1(ku491)* allele is partially rescued by knockdown of *die-1* and is exacerbated by *nhr-23 (RNAi)*. Post embryonic RNAi of *blmp-1, die-1* and *nhr-23* in *elt-1(ku491); wIs51[scm::gfp]* and wildtype *wIs51[scm::gfp]* background. N = > 20; * = p ¡0.05; **** = p = < 0.0001.

unknown, there may well be additional unidentified enhancers that drive expression of *arf-3*.

Chapter 6

Discussion

6.1 General Discussion

6.2 Key findings

This thesis focuses on *arf-3*, which is regulated by an enhancer in its final intron that drives the expression of the widely used *scm::gfp* seam cell marker. We have firmly established *arf-3* as being important in regulating development in *C. elegans*, with a strong link to the moulting cycle in the seam cells. *arf-3* also appears to play a role in other developmental processes including neuronal asymmetric divisions and vulval induction.

In Chapter 3 I explore the function of *arf-3* using RNAi and an available mutant allele, *tm1877*. I found that perturbing *arf-3* leads to seam cell defects as well as decreased cuticle integrity. While I was able to partially rescue *arf-3(tm1877)* through overexpression of wildtype *arf-3* on a multicopy transgenic array, this array also caused defects in embryonic and post-embryonic development. I also describe my efforts to identify physical interactors with ARF-3 in a forward genetic screen using our ARF-3::mCherry reporter. Several genes when knocked down by RNAi caused striking changes to ARF-3::mCherry distribution including *agef-1* and *dyn-1* which both appear to function, along with *arf-3*, in regulating moulting.

It is unclear exactly how *arf-3* promotes moulting but ARF-3::mCherry in the

seam cells colocalises with members of the endocytic pathway, RAB-5::GFP, RAB-6::GFP and RAB-7::GFP in a moulting-dependent manner. In Chapter 4 I also explore the seam cell defects that arose from overexpression of these reporter markers in seam cells. I initially thought I was observing defects in the terminal seam cell fusion event at L4 however, I was unable to alter or rescue these defects by knocking down EFF-1 or DYN-1 which have been shown to play a role in cell fusion events. Further investigation is needed to understand how intracellular trafficking contributes to seam cell fate.

Finally In Chapter 5 I describe my search for transcription factors that bind the *arf-3* locus. In particular I was interested in those that bind to the 3' enhancer that resides in the final intron of *arf-3*. I identified *elt-1* and *nhr-23* as factors that bind to the *arf-3* locus. When knocked down, they cause a decrease in the number of seam cell nuclei as determined by *scm*-positive cells. In some instances elt-1 (RNAi) causes loss of *scm* expression even when the seam cell is present as marked by the marker of the cell membrane, indicating that it is regulating the expression of the *scm* reporter and therefore, *arf-3*.

6.3 Observations on the dissection of the *scm* enhancer

The power of combining several experimental approaches towards a specific objective should not be understated. In my hunt for genes that bind to and regulate *arf-3/scm* at the level of transcription I began my search using JASPAR to generate a list of candidate genes that may be binding at the *arf-3* locus. I then used comparative genomics and gene expression profiles to filter this selection down further. Next I analysed freely available ChIP-seq datasets from the modENCODE and modERN projects to identify positive hits. Finally, I explored how the expression of *arf-3* and *scm::gfp* changed when I targetted these genes used RNAi and available mutants.

That being said, this work also demonstrates the shortfalls of some of these

approaches. Predictions of binding sites are limited by the scope of the prediction software. Binding site consensus sequences are not available for all transcription factors and the list of candidate regulators is limited from the outset. A greater obstacle in this study was the number of false-positives identified; most transcription factor motifs that are scanned are small in size and a chance occurrence of any given binding site within a region of interest is relatively high thus the need for filtering steps. I primarily filtered based on how well a binding site was "conserved" and therefore indicative of a "real" hit. While it is easy to designate a sequence that is 100% identical across species, it is much harder to determine what threshold one should use to exclude candidates.

A major drawback is that even if a binding site is present and conserved this information is without context. We do not know if a given factor is expressed in the right tissue or at the right time which is why I turned to the available expression data for each factor. I chose to focus on those expressed in the seam because I was particularly interested in those that bound to the 3' enhancer of *arf-3*, but *arf-3* is expressed in other tissues and I may have excluded real hits in this process. A similar critique applies to ChIP-seq datasets: we limited to a small number of ChIP-seq datasets that are publically available and we do not know what tissues the transcription factor is active in nor if a gene is upregulated or downregulated by the interaction. On the other hand most ChIP-seq experiments are conducted on synchronised populations so we can at least know what life stage a given transcription factor may be binding. Combining this information with gene expression profiles can aid our understanding of what role a transcription factor may be playing.

A significant gap in our knowledge of the expression of *arf-3* is the surrounding chromatin architecture. We have identifed an intronic enhancer in the final intron of *arf-3* but we do not know the histone modifications that support its regulation. Although ChIP-seq datasets are available, it is hard to justify their use in exploring the specific expression within the seam cells given the ChIP is performed on whole worm lysates and the complex expression pattern of *arf-3*.

Why the *scm* enhancer is located within an intron remains a mystery. However, considering overexpression of *arf-3* causes severe developmental defects it makes some sense to have a relatively weak 5' promoter to drive the expression of *arf-3* and a much stronger enhancer to only drive expression in a tissue where its activity is needed. The 3' *scm* enhancer drives the expression of *arf-3* in a tissue which periodically has an increased burden on the secretory pathway as many cuticular components need to be secreted. This may be an example of suboptimal transcription factor binding affinity in the 5' promoter, which is compensated by optimal syntax of the enhancer element within the final intron to drive tissue specificity (Farley et al. 2016).

We have found a direct link between *nhr-23* and *elt-1* and the regulation of *scm::gfp*. The uncoupling of *scm::gfp* or *arf-3::mCherry* expression with seam cell fate upon knockdown of these two transcription factors may suggest that simple expression of these constructs is less indicative of seam-ness than previously thought. However, while not clear-cut, there is nevertheless a link between the *scm::gfp* marker and the seam fate.

6.4 *arf-3* as a regulator of cuticle secretion and moulting - a link to sterol uptake?

Throughout this work the common link for *arf-3* appears to be in moulting. How *arf-3* fits in remains to be determined but the evidence described here may place it in the regulation of sterol uptake. Several nuclear hormone receptors, including *nhr-23* and *nhr-25* are required for molting in *C. elegans* suggesting steroid hormone signalling is important for moulting. Indeed, solutions containing specific ecdysteroids were found to stimulate moulting in *Ascaris suum* (Fleming 1985). Cholesterol is a precursor for steroid hormone biosynthesis, however *C. elegans* and other nematodes cannot synthesize cholesterol *de novo* therefore sterol uptake from the environment is crucial for the synthesis of steroid hormones and the regulation of moulting.

Sterol uptake in the epidermis is thought to depend on sterol-binding receptor: a conserved low-density lipoprotein receptor related to human megalin, *lrp-1*. Cholesterol-rich lipoproteins bind to *lrp-1* at the plasma membrane, this is then internalised by endocytosis. *lrp-1* is then trafficked back to the plasma membrane from the endosome while the lipoprotein is degraded and cholersterol is then used in the formation of intracellular steroid hormones which act on nuclear hormone receptors such as *nhr-23* and *nhr-25* (Antebi 2015).

Mutations in *lrp-1* cause moulting defects (Yochem et al. 1999) and LRP-1::GFP localises to apical puncta in the main hypodermal syncitium hyp7 and knockdown of several endocytosis-related genes leads to the accumulation of LRP-1::GFP at the plasma membrane including *dab-1, chc-1, epn-1, nekl-2, aps-2, dpy-23, abp-1* and *dyn-1* (Kamikura and Cooper 2003; Holmes et al. 2007; Yochem et al. 2015; Kang et al. 2013) suggesting a role for the endocytic pathway in LRP-1 internalisation. It is noteworthy that *dyn-1* and *dab-1* were both identified in my screen for interactors of ARF-3::mCherry. While I explored the role of *dyn-1* further the interaction with *dab-1* and any link to LRP-1 internalisation needs investigating further. The fact that expression of ARF-3::mCherry rescued the moulting defects observed in knockdown of *dyn-1* supports the role of *arf-3* as a positive regulator of endocytosis. Indeed Kang *et al* list *arf-3* in their list of genes that alter LRP-1::GFP distribution when knocked down by RNAi (Kang et al. 2013). Kang *et al* did not include the ARFGEF *agef-1* in their screen but my data suggest *agef-1* acts to activate *arf-3* as shown by the moulting defects observed upon knockdown of *arf-3* in the mutant *agef-1(vh4)* background. This being said, *lrp-1* is not expressed in the seam cells so *arf-3* may only play a role in this process in the hyp7 syncytium. Given the role of *nhr-23* and *nhr-25* in the seam however, some way of internalising cholesterol is needed and *arf-3* may play a role.

NHR-23 expression peaks at the intermoult (Kostrouchova et al. 2001) and promotes entry into the moult. Unfortunately *arf-3* was not studied in a search for genes acting downstream of NHR-23 using genome wide expression microarrays (Kouns et

al. 2011) but our data suggests NHR-23 binds at the *arf-3* locus. Upon knockdown of *nhr-23* I observed a decrease in seam cell number and the aberrant expression of *arf-3::mCherry* in cells that should have fused with the hypodermis. If *arf-3* does play a role in the internalisaion of cholesterol in the seam cells to produce steroid hormones then the obseravtion that *arf-3* is regulated by *nhr-23* at the level of transcription may indicate a feedback mechanism.

6.5 Seam cell development and the integration of cellular context and signalling pathways

Despite major differences in seam cell lineage along the anterior-posterior axis, they are often treated as equal. H0 is probably the best notable exception; H0 is present at hatching and expresses *scm* through the life of the worm and yet H0 never divides and has a distinct morphology from the other seam cells. In this study I have also found that the expression of *scm::gfp* in H0 is extremely robust and is almost never switched off.

A seam cell's location within the *C. elegans* body plan influences their lineage, for example patterning of the head seam cells is specified by the PAX-6 homologue vab-3/mab-18 and null mutants for PAX-6 transform the cell fates of H0 and H1 into a H2-like lineage (Chisholm and Horvitz 1995). Perturbing *ceh-20* and *unc-62* also leads to seam cell hyperplasia primarily in the anterior (Hughes et al. 2013) Cinar and Chisholm 2004) whereas *mab-5* and *pal-1* control posterior seam cell development (Hunter et al. 1999, Kenyon 1986). In this study I have observed that knockdown of ELT-1 appears to affect the V1-4 cells more than at the head or tail. The division pattern of seam cells also has sex-specific and stage-specific differences regulated by several different signalling pathways including nuclear hormone receptors, Wnts and the heterochronic pathway.

In Chapter 4 I examined the role intracellular trafficking plays in regulating seam cell fate. Overexpression of several reporter markers of organelles caused seam cell

defects including aberrant processes and gaps in the seam and alae. Defects in seam cell fusion cause dramatic defects in alae formation, even though the cells would still be considered seam cells as determined by expression of *scm::gfp* (Brooks et al. 2003). Similar defects are observed in *eff-1* mutants where the anterior daughters of seam divisions leave the line of the seam, accumulating alongside the lineage in a state of "developmental limbo", failing to fuse with the hypodermal syncytium (Brabin, Appleford, and Woollard 2011). I was unable to rescue the defects I observed in these reporter lines by knocking down EFF-1 or DYN-1, its negative regulator. It is possible post embryonic knockdown of EFF-1 or DYN-1 may not have been sufficient to counteract the effects of an hyperactive endocytic pathway. On the other hand these defects may represent a change in seam cell fate driven by the incorrect transduction of other extracellular signals such as Wnts.

A seam cell needs to process all these different signals in order to adopt the correct lineage. Given this it makes some sense that *arf-3*, and intracellular trafficking in general, is so tightly linked to seam cell fate. It is important to consider the genetic context of a cell, its history and crosstalk between these signalling pathways when investigating the fate of a seam cell.

Appendix A

Appendix Title

TABLE I: *Strains used in this study*

Strain	Genotype	Plasmids in extrachromosomal arrays
AW60	*him-5 (e1490); wIs51[scm::gfp + pAW135]V*	pAW135 = unc-119 rescue plasmid
AW715	*arf-3(tm1877)IV / dpy-20(e1282)IV; unc-24(e138)IV*	
AW716	*arf-3(tm1877)IV / dpy-20(e1282)IV; unc-24(e138)IV; wIs51[scm::gfp + pAW135]V*	pAW135 = unc-119 rescue plasmid
AW718	*rrf-3(pk1426)II; wIs51[scm::gfp + pAW135]V*	pAW135 = unc-119 rescue plasmid
AW740	*dpy-20(e1282)IV; unc-24(e138)IV; wIs51[scm::gfp + pAW135]V*	pAW135 = unc-119 rescue plasmid
AW860	*unc-119(ed3)III; ouEx721[pAW740 + pAW135]*	pAW135 = unc-119 rescue plasmid; pAW740 = arf-3::mCherry
AW1421	*blmp-1(tm548)I*	
AW1422	*blmp-1(tm548)I; wIs51[scm::gfp + pAW135]V*	pAW135 = unc-119 rescue plasmid

AW1791	*dpy-20(e1282)IV; unc-24(e138)IV; wIs51[scm::gfp + pAW135]V; ouEx1197[pAW558 + pAW378 + pCFJ90]*	pAW135 = unc-119 rescue plasmid; pAW558 = arf-3 locus including F57H12.10 pAW378 = unc-122p::rfp pCFJ90 = myo-2::mCherry
AW1792	*arf-3(tm1877)IV / dpy-20(e1282)IV; unc-24(e138)IV; wIs51[scm::gfp + pAW135]V; ouEx1197[pAW558 + pAW378 + pCFJ90]*	pAW135 = unc-119 rescue plasmid; pAW558 = arf-3 locus including F57H12.10 pAW378 = unc-122p::rfp pCFJ90 = myo-2::mCherry
AW1793	*arf-3(tm1877)IV; wIs51[scm::gfp + pAW135]V; ouEx1197[pAW558 + pAW378 + pCFJ90]*	pAW558 = arf-3 locus including F57H12.10 pAW378 = unc-122p::rfp pCFJ90 = myo-2::mCherry
AW1801	*pAW627 + pAW135*	pAW135 = unc-119 rescue plasmid; pAW627= scm::gfp fragment
AW1794	*unc-119(ed3)III; ouEx1198[pAW740 + pAW913 + pAW135]*	pAW135 = unc-119 rescue plasmid; pAW740 = arf-3::mCherry pAW913 = rab-5::gfp
AW1795	*unc-119(ed3)III; ouEx1199[pAW740 + pAW914 + pAW135]*	pAW135 = unc-119 rescue plasmid; pAW740 = arf-3::mCherry pAW914 = rab-6::gfp
AW1796	*unc-119(ed3)III; ouEx1200[pAW740 + pAW915 + pAW135]*	pAW135 = unc-119 rescue plasmid; pAW740 = arf-3::mCherry pAW915 = rab-7::gfp
AW1797	*unc-119(ed3)III; ouEx1201[pAW740 + pAW916 + pAW135]*	pAW135 = unc-119 rescue plasmid; pAW740 = arf-3::mCherry pAW916 = rab-11::gfp
AW1798	*unc-119(ed3)III; ouEx1202[pAW740 + pAW917 + pAW135]*	pAW135 = unc-119 rescue plasmid; pAW740 = arf-3::mCherry pAW917 = SP12::gfp

AW1799	*heIs63[wrt-2p::GFP::PH + wrt-2p::GFP::H2B + lin-48p::mCherry]V; ouEx721[pAW740 + pAW135]*	pAW135 = unc-119 rescue plasmid; pAW740 = arf-3::mCherry
AW1800	*elt-1(ku491)IV; wIs51[scm::gfp + pAW135]V*	
MH4799	*elt-1(ku491)IV*	
AW1802	*pAW918 + pAW135*	pAW135 = unc-119 rescue plasmid; pAW918 = arf-3 5' promoter::gfp
AW1803	*blmp-1(tm548)I; unc-119(ed3)III; ouEx721[pAW740 + pAW135]*	pAW135 = unc-119 rescue plasmid; pAW740 = arf-3mCherry
AW1804	*dpy-10(?)II; ouEx1203[pCFJ90 + pAW919 + pAW920 + pAW925 + pAW926 + dpy10(cn64)+]*	pAW919 = arf-3 5' gRNA pAW920 = arf-3 3' gRNA pAW925 = Cas9 expression vector pAW926 = dpy-10 gRNA expression vector
HZ194	*apr-1(bp298)I; wIs51[scm::gfp + pAW135]V*	pAW135 = unc-119 rescue plasmid
QR180	*agef-1(vh4)I*	
SV1009	*heIs63 [wrt-2p::GFP::PH + wrt-2p::GFP::H2B + lin-48p::mCherry]V*	

TABLE IV: *List of targets in RNAi screen*

Component	Family/Pathway	Cosmid	Gene name	Mislocalisation
Adaptor protein	Molting	*M110.5*	*dab-1*	+
Adaptor protein	Endocytosis	*Y71H2B.10*	*apb-1*	+
Adaptor protein	Vesicular trafficking	*R11A5.1*	*apb-3*	-

Adaptor protein	Vesicular trafficking	*K11D2.3*	*unc-101*	+
APC	Wnt signaling	*K04G2.8*	*apr-1*	+
ARF	Small GTPase	*ZK1320.6*	*arc-1*	-
ARF	Small GTPase	*F45E4.1*	*arf-1.1*	-
ARF	Small GTPase	*B0336.2*	*arf-1.2*	-
ARF	Small GTPase	*F57H12.1*	*arf-3*	-
ARF	Small GTPase	*Y116A8C.12*	*arf-6*	-
ARF	Small GTPase	*F54C9.10*	*arl-1*	-
ARF	Small GTPase	*F19H8.3*	*arl-3*	-
ARF	Small GTPase	*ZK632.8*	*arl-5*	-
ARF	Small GTPase	*C38D4.8*	*arl-6*	-
ARF	Small GTPase	*Y57G11C.13*	*arl-8*	+
ARF	Small GTPase	*Y37E3.5*	*arl-13*	-
ARF	Small GTPase	*F22B5.1*	*evl-20*	-
ARF	Small GTPase	*T28F3.6*	*ifta-2*	-
ARF	Small GTPase	*ZK180.4*	*sar-1*	-
Arf GEF	Golgi Transport	*Y6B3A.1*	*agef-1*	+
Arf GEF	Protein sorting	*Y55D9A.1*	*efa-6*	-
Arf GEF	Golgi Transport	*C24H11.7*	*gbf-1*	-
Arf GEF	Golgi Transport	*Y106G6G.6*	*Y106G6G.6*	-
Arf GEF	Endocytosis	*M02B7.5*	*bris-1*	-
Arf GEF	Protein sorting	*K06H7.4*	*grp-1*	-
Arf GEF	Golgi Transport	*F11A10.4*	*mon-2*	-
Arf-GEF	Endocytosis	*F23H11.4*	*F23H11.4*	-
Arf-GAP	Golgi Transport	*Y17G7B.15*	*cnt-1*	+
Arf-GAP	Golgi Transport	*Y39A1A.15*	*cnt-2*	+

Arf-GAP	RhoGAP GTPase	*F23H11.4*	*F23H11.4*	-
Arf-GAP	Golgi Transport	*W09D10.1*	*W09D10.1*	-
β-catenin	Wnt signaling	*C54D1.6*	*bar-1*	-
Coat protein	COPI complex	*Y71F9AL.17*	*copa-1*	-
Coat protein	COPI complex	*F45G2.4*	*cope-1*	-
Coat protein	COPI complex	*T14G10.5*	*copg-1*	-
Hedgehog receptor	Hedgehog	*F07C3.1*	*ptd-2*	-
Intracellular phospholipase	Lipid metabolism	*M03A1.6*	*ipla-1*	+
Kinase	Wnt signaling	*C03C10.1*	*kin-19*	-
Lipocalin	Intracellular signaling	*W04G3.2*	*lpr-5*	-
Lipocalin	Intracellular signaling	*Y65B4BR.2*	*lpr-1*	-
Lipocalin	Intracellular signaling	*W04G3.8*	*lpr-3*	-
N/A	EGF signaling	*C09H6.2*	*lin-10*	-
Non-muscle myosin	Elongation	*F52B10.1*	*nmy-1*	-
Non-muscle myosin	Elongation	*F20G4.3*	*nmy-2*	-
Other SNAREs	Vesicle fusion	*T10H9.4*	*snb-1/sup-8*	-
Other SNAREs	Vesicle fusion	*F23H12.1*	*snb-2*	-
Other SNAREs	Vesicle fusion	*ZK795.4*	*snb-7*	-
Other SNAREs	Vesicle fusion	*C30A5.5*	*snb-5*	-
Other SNAREs	Vesicle fusion	*T14D7.3*	*snb-6*	-

Other SNAREs	Vesicle fusion	*B0513.9*	*B0513.9*	-
Other SNAREs	Vesicle fusion	*Y69A2AR.6*	*Y69A2AR.6*	-
Other SNAREs	Vesicle fusion	*Y57G11C.4*	*vti-1*	+
Other SNAREs	Vesicle fusion	*Y59E9AL.7*	*nbet-1*	-
Other SNAREs	Vesicle fusion	*B0272.2*	*memb-1/gosr-2.1*	-
Other SNAREs	Vesicle fusion	*M03E7.5*	*memb-2*	-
Other SNAREs	Vesicle fusion	*F08F8.8*	*gos-28/gosr-1*	-
Other SNAREs	Vesicle fusion	*B0361.10*	*ykt-6*	-
Other SNAREs	Vesicle fusion	*F55A4.1*	*sec-22*	-
Other SNAREs	Vesicle fusion	*F40G9.1*	*sec-20*	-
Other SNAREs	Vesicle fusion	*Y110A7A.11*	*use-1*	-
Phophatase	Elongation	*C06C3.1*	*mel-11*	-
RAB	Small GTPase	*C39F7.4*	*rab-1*	-
RAB	Small GTPase	*F53F10.4*	*rab-2/unc-108*	-
RAB	Small GTPase	*C18A3.6*	*rab-3*	-
RAB	Small GTPase	*F26H9.6*	*rab-5*	-
RAB	Small GTPase	*F59B2.7*	*rab-6.1*	-
RAB	Small GTPase	*T25G12.4*	*rab-6.2*	+
RAB	Small GTPase	*D1037.4*	*rab-8*	-
RAB	Small GTPase	*T23H2.5*	*rab-10*	-
RAB	Small GTPase	*F53G12.1*	*rab-11.1*	-
RAB	Small GTPase	*W04G5.2*	*rab-11.2*	-
RAB	Small GTPase	*K09A9.2*	*rab-14*	-
RAB	Small GTPase	*Y92C3B.3*	*rab-18*	-
RAB	Small GTPase	*Y62E10A.9*	*rab-19*	-
RAB	Small GTPase	*T01B7.3*	*rab-21*	-
RAB	Small GTPase	*Y87G2A.4*	*rab-27*	-

RAB	Small GTPase	*Y11D7A.4*	*rab-28*	-
RAB	Small GTPase	*Y45F3A.2*	*rab-30*	-
RAB	Small GTPase	*F43D9.2*	*rab-33*	-
RAB	Small GTPase	*Y47D3A.25*	*rab-35*	-
RAB	Small GTPase	*W01H2.3*	*rab-37*	-
RAB	Small GTPase	*C56E6.2*	*C56E6.2*	-
RAB	Small GTPase	*F11A5.3*	*F11A5.3*	-
Rab GAP	Golgi Transport	*F32B6.8*	*tbc-3*	-
RAN	Small GTPase	*K01G5.4*	*ran-1*	-
Ras inhibition	Ras inhibition	*B0303.7*	*B0303.7*	-
RAS/RAP/RAL	Small GTPase	*ZK792.6*	*let-60*	-
RAS/RAP/RAL	Small GTPase	*F17C8.4*	*ras-2*	-
RAS/RAP/RAL	Small GTPase	*C44C11.1*	*ras-1*	-
RAS/RAP/RAL	Small GTPase	*C54A12.4*	*C54A12.4*	-
RAS/RAP/RAL	Small GTPase	*C27B7.8*	*rap-1*	-
RAS/RAP/RAL	Small GTPase	*C25D7.7*	*rap-2*	-
RAS/RAP/RAL	Small GTPase	*C08F8.7*	*rap-3*	-
RAS/RAP/RAL	Small GTPase	*T26C12.3*	*T26C12.3*	-
RAS/RAP/RAL	Small GTPase	*F54C8.5*	*F54C8.5*	-
RAS/RAP/RAL	Small GTPase	*Y53G8AR.3*	*Y53G8AR.3*	-
RAS/RAP/RAL	Small GTPase	*C14A11.7*	*ssr-1*	-
Receptor	Hh signaling	*ZK675.1*	*ptc-1*	-
Receptor	Hh signaling	*Y110A2AL.8*	*ptc-3*	-
Retromer	Retromer	*T20D3.7*	*vps-26*	-
Retromer	Retromer	*ZK1128.8*	*vps-29*	-
Retromer	Retromer	*F59G1.3*	*vps-35*	-
Rho GEF dynamin binding	Dynamin Binding protein	*T09B4.2*	*T09B4.2*	-

Rho GTPase	Small GTPase	*Y51H4A.3*	*rho-1*	-
Rho GTPase	Small GTPase	*R07G3.1*	*cdc-42*	+
Rho GTPase	Small GTPase	*C09G12.8*	*ced-10*	-
Rho GTPase	Small GTPase	*C35C5.4*	*mig-2*	-
Rho GTPase	Small GTPase	*F22E12.2*	*chw-1*	-
Rho GTPase	Small GTPase	*Y32F6B.3*	*crp-1*	+
Rho Kinase	Rho Kinase	*C10H11.9*	*let-502*	+
Secreted protein	TGFβ	*Y59A8B.20*	*lon-8*	-
SNAP-25	Vesicle fusion	*Y22F5A.3*	*ric-4/snap-25*	-
SNAP-25	Vesicle fusion	*T14G12.2*	*aex-4*	-
SNAP-25	Vesicle fusion	*K02D10.5*	*snap-29*	-
Sodium transport	Vesicle fusion	*T25B6.7*	*snf-12*	-
Swi/Snf	Wnt signaling	*C28H8.1*	*bcl-7*	-
SYNTAXIN	Vesicle fusion	*F56A8.7a,b*	*unc-64/syx-1*	-
SYNTAXIN	Vesicle fusion	*F48F7.2*	*syn-2/syx-2*	-
SYNTAXIN	Vesicle fusion	*F35C8.4*	*syn-1/syx-3*	-
SYNTAXIN	Vesicle fusion	*T01B11.3*	*syn-4/syx-4*	-
SYNTAXIN	Vesicle fusion	*F55A11.2*	*syn-3/syx-5*	-
SYNTAXIN	Vesicle fusion	*C15C7.1*	*syx-6*	-
SYNTAXIN	Vesicle fusion	*F36F2.4*	*syn-13/syx-7*	-
SYNTAXIN	Vesicle fusion	*ZC155.7*	*syn-16*	-
SYNTAXIN	Vesicle fusion	*VF39H2L.1*	*syx-17*	-
SYNTAXIN	Vesicle fusion	*T10H9.3*	*syx-18*	-
	Lipid tube assembly	*F58G6.1*	*amph-1*	-

TABLE II: *Plasmids used in this study*

Plasmid	Description
pAW135	unc-119 rescue plasmid
pAW378	unc-122p::rfp
pAW522	L4440 RNAi feeding vector
pAW558	arf-3 locus including F57H12.10
pAW566	bro-1 CNE in pCR-XL-TOPO
pAW627	scm::gfp fragment
pAW740	arf-3::mCherry
pAW913	seamp::rab-6::gfp
pAW914	seamp::rab-6::gfp
pAW915	seamp::rab-7::gfp
pAW916	seamp::rab-11::gfp
pAW917	seamp::SP12::gfp
pAW918	arf-3 5' promoter::gfp
pAW919	arf-3 5' gRNA with optimal PAM GGNGG
pAW920	arf-3 3' gRNA with optimal PAM GGNGG
pAW921	*dyn-1* fragment in pCR-XL-TOPO
pAW922	*dyn-1* in L4440 RNAi feeding vector
pAW923	*F57H12.10* fragment in pCR-XL-TOPO
pAW924	*F57H12.10* in L4440 RNAi feeding vector
pAW925	Cas9 expression vector
pAW926	dpy-10 gRNA expression vector
pCFJ90	myo-2::mCherry

A.1 Genetic Crosses

A.1.1 Generation of AW1792

AW1791 hermaphrodites carrying the *arf-3* rescue array ouEx1197 were crossed with AW716 males carrying the *arf-3(tm1877)* allele as shown:

$$\frac{dpy-20(e1282)unc-24(e138)}{dpy-20(e1282)unc-24(e138)}\ \frac{wIs51}{wIs51}(ouEx1197)\times\frac{arf-3(tm1877)}{dpy-20(e1282)unc-24(e138)}\ \frac{wIs51}{wIs51} \tag{A.1}$$

Hermaphrodites which displayed wildtype movement and carried the ouEx1197 (as determined by expression of mCherry in the pharynx) were isolatedfrom the progeny.

A.1.2 Generation of AW1793

AW1792 hermaphrodites were isolated and reproduced by selfing as shown:

$$\frac{arf-3(tm1877)}{dpy-20(e1282)unc-24(e138)}(ouEx1197)\ \frac{wIs51}{wIs51}\times\frac{arf-3(tm1877)}{dpy-20(e1282)unc-24(e138)}\ \frac{wIs51}{wIs51}(ouEx11 \tag{A.2}$$

Hermaphrodites which displayed wildtype movement and carried the ouEx1197 (as determined by expression of mCherry in the pharynx) were isolated selected from the progeny and genotyped for *arf-3(tm1877)* homozygosity.

A.1.3 Generation of AW1422

AW1422 was made by Olivia Bracken during her Masters project in the Woollard lab. AW1421 hermaphrodites were crossed with AW60 males carrying the seam cell marker *scm::gfp*.

$$\frac{blmp-1(tm5498)}{blmp-1(tm5498)}\ \frac{+}{+}\times\frac{+}{+}\ \frac{wIs51}{wIs51} \tag{A.3}$$

Heterozygotes from this cross were isolated and left to reproduce via selfing. Their progeny were then isolated and genotyped for *blmp-1(tm548)* homozygosity.

A.1.4 Generation of AW1799

AW1799 was made by crossing SV1009 (*heIs63*) males with AW860 hermaphrodites carrying the extrachromosomal array ouEx721 (*arf-3::mCherry*).

$$\frac{+}{+}\ \frac{heIs63}{heIs63} \times \frac{unc-119}{unc-119}\ \frac{+}{+}(ouEx721) \tag{A.4}$$

Heterozygotes from this cross were isolated and left to reproduce via selfing. Their progeny were then selected if they were homozygote for *heIs63* and also carried ouEx721.

A.1.5 Generation of AW1800

AW1800 was made by crossing MH4799 (*elt-1(ku491)*) hermaphrodites with AW60 males carrying the seam cell marker *scm::gfp*.

$$\frac{elt-1(ku491)}{elt-1(ku491)}\ \frac{+}{+} \times \frac{+}{+}\ \frac{wIs51}{wIs51} \tag{A.5}$$

Heterozygotes from this cross were isolated and left to reproduce via selfing. Their progeny were then isolated and genotyped for *elt-1(ku491)* homozygosity.

A.1.6 Generation of AW1803

AW1803 was made by crossing AW1421 (*blmp-1(tm548)*) hermaphrodites with AW860 males carrying ouEx721 (*arf-3::mCherry*).

$$\frac{blmp-1(tm5498)}{blmp-1(tm5498)}\ \frac{+}{+} \times \frac{+}{+}\ \frac{unc-119}{unc-119}(ouEx721) \tag{A.6}$$

Heterozygotes from this cross carrying ouEx721 were isolated and left to reproduce via selfing. Their progeny were then isolated if the expressed ouEx721 and

genotyped for *blmp-1(tm548)* homozygosity.

TABLE III: *Primers used in this study*

Primer	Sequence
ATW01	tcggcaatagcaacgtcgatttgc
ATW02	gacgaataagcggccaaatcgag
ATW04	CTGCAGGTCGACTCTAGAgcctatttcaacaca ttcccgttacg-tagagttatcag
ATW05	TGTACAGCGGCCGCGAATCGggatccaatcaatgc CT-GAAAGTTAAAAATTACAGTATAAAGATAAGGG
ATW06	TTCAGgcattgattggatccCGATTCGCGGCCG
ATW07	acgggaatgtgttgaaataggcTCTAGAGTCGACCTGCAGG
ATW49	gtgattcggatgtggacattg
ATW50	gagcgaatgtcagattggc
ATW51	GACCACTACGCACACAGAGAC
ATW53	GGACCGGAATCGAGTGTGTC
ATW57	CCGGGTGGAAGTGGAATCTACTC
ATW60	CACAAGTGAACGAGGCACTC
ATW65	CCAAAGCAAACCGATCATCAG
ATW66	GGCTTCACCAATGGACGAG
OB5	CTTGTATGTCCTGCTGAAGCATC
OB6	CTACGCTCCATTGCGTGCATC
ATW69	GTGCGAACGGCTGGTTTC
ATW70	AGATCTCGTGTCTGGGCAC
ATW85	ATGTGCAGCTGAAGAGAAAGC
ATW86	ACTTCTCATGTCAACGCCAAG
ATW87	ACTTCTCATGTCAACGCCAAG
ATW91	aatctgatccaccgcatcct
ATW92	gttaggccgaagcatccaag
ATW93	acgccgagttcctacacaag
ATW94	ccttcgcaagtttcaacgca
ATW95	aaatgatccaggccgcaaga
ATW96	gagccacgcacaaacgatac
ATW97	GTCGACGAGCGAATGTCAGATTGGC
ATW98	TCTAGAAATGGAGCTGATTCAACACC
ATW99	aattgctgcagtacatgcac
ATW100	AACAAGCGCAAGTTGACG

Bibliography

Abbott, Allison L., et al. 2005. "The let-7 MicroRNA family members mir-48, mir-84, and mir-241 function together to regulate developmental timing in Caenorhabditis elegans". *Developmental Cell* 9, no. 3 (): 403–414. ISSN: 15345807. arXiv: NIHMS150003.

Abete-Luzi, Patricia, and David M. Eisenmann. 2018. "Regulation of C. elegans L4 cuticle collagen genes by the heterochronic protein LIN-29". *Genesis* 56 (5). ISSN: 1526968X.

Ackema, Karin B, et al. 2014. "The small GTPase Arf1 modulates mitochondrial morphology and function." *The EMBO journal* 33, no. 22 (): 2659–75. ISSN: 1460-2075.

Akhatova, Farida, et al. 2018. "Atomic force microscopy for imaging and nanomechanical characterisation of live nematode epicuticle: A comparative Caenorhabditis elegans and Turbatrix aceti study". *Ultramicroscopy* 194 (): 40–47. ISSN: 18792723.

Ambros, V., and H. R. Horvitz. 1987. "The lin-14 locus of Caenorhabditis elegans controls the time of expression of specific postembryonic developmental events." *Genes & development* 1, no. 4 (): 398–414. ISSN: 08909369.

Ambros, V, and H R Horvitz. 1984. "Heterochronic mutants of the nematode Caenorhabditis elegans." *Science (New York, N.Y.)* 226, no. 4673 (): 409–16. ISSN: 0036-8075.

Amor, J Carlos, et al. 2005. “The structure of RalF, an ADP-ribosylation factor guanine nucleotide exchange factor from Legionella pneumophila, reveals the presence of a cap over the active site.” *The Journal of biological chemistry* 280, no. 2 (): 1392–400. ISSN: 0021-9258.

Angers, Stephane, and Randall T. Moon. 2009. “Proximal events in Wnt signal transduction”. *Nature Reviews Molecular Cell Biology* 10, no. 7 (): 468–477. ISSN: 14710072.

Antebi, Adam. 2015. “Nuclear receptor signal transduction in C. elegans”. *WormBook* (): 1–49. ISSN: 15518507.

Antonny, Bruno, et al. 1997. “N-Terminal Hydrophobic Residues of the G-Protein ADP-Ribosylation Factor-1 Insert into Membrane Phospholipids upon GDP to GTP Exchange ¡sup¿†¡/sup¿”. *Biochemistry* 36, no. 15 (): 4675–4684. ISSN: 0006-2960.

Balana, M. E., et al. 2005. “ARF6 GTPase controls bacterial invasion by actin remodelling”. *Journal of Cell Science* 118, no. 10 (): 2201–2210. ISSN: 0021-9533.

Baldwin, Austin T., Amy M. Clemons, and Bryan T. Phillips. 2016. “Unique and redundant β-catenin regulatory roles of two Dishevelled paralogs during ¡i¿C. elegans¡/i¿ asymmetric cell division”. *Journal of Cell Science* 129, no. 5 (): 983–993. ISSN: 0021-9533.

Baldwin, Austin T, and Bryan T Phillips. 2014. “The tumor suppressor APC differentially regulates multiple β-catenins through the function of axin and CKIα during C. elegans asymmetric stem cell divisions.” *Journal of cell science* 127, no. Pt 12 (): 2771–81. ISSN: 1477-9137.

Barrière, Antoine, Kacy L Gordon, and Ilya Ruvinsky. 2011. “Distinct functional constraints partition sequence conservation in a cis-regulatory element.” Ed. by Michael B. Eisen. *PLoS genetics* 7, no. 6 (): e1002095. ISSN: 1553-7404.

Beck, R., et al. 2008. “Membrane curvature induced by Arf1-GTP is essential for vesicle formation”. *Proceedings of the National Academy of Sciences* 105, no. 33 (): 11731–11736. ISSN: 0027-8424.

Behrens, Jürgen, et al. 1996. “Functional interaction of β-catenin with the transcription factor LEF- 1”. *Nature* 382, no. 6592 (): 638–642. ISSN: 00280836.

Bhanot, Purnima, et al. 1996. “A new member of the frizzled family from Drosophila functions as a wingless receptor”. *Nature* 382, no. 6588 (): 225–231. ISSN: 00280836.

Bilic, Josipa, et al. 2007. “Wnt induces LRP6 signalosomes and promotes dishevelled-dependent LRP6 phosphorylation.” *Science (New York, N.Y.)* 316, no. 5831 (): 1619–22. ISSN: 1095-9203.

Bird, A F, Ingrid Bonig, and A Bacic. 1988. “A Role for the Excretory[sub9] System in Secernentean Nematodes”. *Journal of Nematology* 20, no. 3 (): 493–496. ISSN: 0022-300X.

Blumenthal, Thomas, et al. 2002. “A global analysis of Caenorhabditis elegans operons”. *Nature* 417, no. 6891 (): 851–854. ISSN: 0028-0836.

Bobak, D A, et al. 1989. “Molecular cloning, characterization, and expression of human ADP-ribosylation factors: two guanine nucleotide-dependent activators of cholera toxin.” *Proceedings of the National Academy of Sciences of the United States of America* 86, no. 16 (): 6101–5. ISSN: 0027-8424.

Bobinnec, Yves, et al. 2003. “Dynamics of the endoplasmic reticulum during early development of ¡i¿Drosophila melanogaster¡/i¿”. *Cell Motility and the Cytoskeleton* 54, no. 3 (): 217–225. ISSN: 08861544.

Bottjer, K P, P P Weinstein, and M J Thompson. 1985. “Effects of an azasteroid on growth, development and reproduction of the free-living nematodes Caenorhabditis briggsae and Panagrellus redivivus.” *Comparative biochemistry and physiology. B, Comparative biochemistry* 82 (1): 99–106. ISSN: 0305-0491.

Brabin, Charles, Peter J. Appleford, and Alison Woollard. 2011. "The Caenorhabditis elegans GATA Factor ELT-1 Works through the Cell Proliferation Regulator BRO-1 and the Fusogen EFF-1 to Maintain the Seam Stem-Like Fate". Ed. by Jeffrey D. Hardin. *PLoS Genetics* 7, no. 8 (): e1002200. ISSN: 1553-7404.

Brenner, S. 1974. "The genetics of Caenorhabditis elegans." *Genetics* 77, no. 1 (): 71–94. ISSN: 0016-6731.

Brooks, Darren R., et al. 2003. "An Essential Role in Molting and Morphogenesis of Caenorhabditis elegans for ACN-1, a Novel Member of the Angiotensin-converting Enzyme Family That Lacks a Metallopeptidase Active Site". *Journal of Biological Chemistry* 278, no. 52 (): 52340–52346. ISSN: 00219258.

Byerly, L., R. C. Cassada, and R. L. Russell. 1976. "The life cycle of the nematode Caenorhabditis elegans. I. Wild-type growth and reproduction". *Developmental Biology* 51, no. 1 (): 23–33. ISSN: 00121606.

C. elegans Deletion Mutant Consortium, The C. elegans Deletion Mutant. 2012. "large-scale screening for targeted knockouts in the Caenorhabditis elegans genome." *G3 (Bethesda, Md.)* 2, no. 11 (): 1415–25. ISSN: 2160-1836.

C. elegans Sequencing Consortium. 1998. "Genome sequence of the nematode C. elegans: a platform for investigating biology." *Science (New York, N.Y.)* 282, no. 5396 (): 2012–8. ISSN: 0036-8075.

Cassada, Randall C., and Richard L. Russell. 1975. "The dauerlarva, a post-embryonic developmental variant of the nematode Caenorhabditis elegans". *Developmental Biology* 46, no. 2 (): 326–342. ISSN: 00121606.

Cassata, G., et al. 2005. "ceh-16/engrailed patterns the embryonic epidermis of Caenorhabditis elegans". *Development* 132, no. 4 (): 739–749. ISSN: 0950-1991.

Çelen, Irem, Jung H. Doh, and Chandran R. Sabanayagam. 2018. "Effects of liquid cultivation on gene expression and phenotype of C. elegans". *BMC Genomics* 19, no. 1 (): 562. ISSN: 14712164.

Chalfie, M, and M Au. 1989. "Genetic control of differentiation of the Caenorhabditis elegans touch receptor neurons." *Science (New York, N.Y.)* 243, no. 4894 Pt 1 (): 1027–33. ISSN: 0036-8075.

Chalfie, M, et al. 1994. "Green fluorescent protein as a marker for gene expression." *Science (New York, N.Y.)* 263, no. 5148 (): 802–5. ISSN: 0036-8075.

Chalfie, M, et al. 1985. "The neural circuit for touch sensitivity in Caenorhabditis elegans." *The Journal of neuroscience : the official journal of the Society for Neuroscience* 5, no. 4 (): 956–64. ISSN: 0270-6474.

Chen, Xiangyang, et al. 2014. "Dual sgRNA-directed gene knockout using CRISPR/Cas9 technology in Caenorhabditis elegans." *Scientific reports* 4:7581. ISSN: 2045-2322.

Chen, Zhe, Dennis J Eastburn, and Min Han. 2004. "The Caenorhabditis elegans nuclear receptor gene nhr-25 regulates epidermal cell development." *Molecular and cellular biology* 24, no. 17 (): 7345–58. ISSN: 0270-7306.

Choi, Seungwon, et al. 2006. "ARF6 and EFA6A regulate the development and maintenance of dendritic spines." *The Journal of neuroscience : the official journal of the Society for Neuroscience* 26, no. 18 (): 4811–9. ISSN: 1529-2401.

Cinar, H. N., and Andrew D Chisholm. 2004. "Genetic Analysis of the Caenorhabditis elegans pax-6 Locus: Roles of Paired Domain-Containing and Nonpaired Domain-Containing Isoforms". *Genetics* 168, no. 3 (): 1307–1322. ISSN: 0016-6731.

Coggins, J R, F W Schaefer, and P P Weinstein. 1985. "Ultrastructural analysis of pathologic lesions in sterol-deficient Nippostrongylus brasiliensis larvae." *Journal of invertebrate pathology* 45, no. 3 (): 288–97. ISSN: 0022-2011.

Cohen, Max L., et al. 2015. "The GATA Factor elt-1 Regulates C. elegans Developmental Timing by Promoting Expression of the let-7 Family MicroRNAs". Ed. by Susan E. Mango. *PLOS Genetics* 11, no. 3 (): e1005099. ISSN: 1553-7404.

Cour, T.F. la, et al. 1985. "Structural details of the binding of guanosine diphosphate to elongation factor Tu from E. coli as studied by X-ray crystallography." *The EMBO Journal* 4, no. 9 (): 2385–2388. ISSN: 1460-2075.

Cox, G N, and D Hirsh. 1985. "Stage-specific patterns of collagen gene expression during development of Caenorhabditis elegans." *Molecular and cellular biology* 5, no. 2 (): 363–72. ISSN: 0270-7306.

Cox, George N., et al. 1981. "Temporal regulation of cuticle synthesis during development of Caenorhabditis elegans". *Developmental Biology* 84, no. 2 (): 277–285. ISSN: 00121606.

Das, G. 2004. "Diego interacts with Prickle and Strabismus/Van Gogh to localize planar cell polarity complexes". *Development* 131, no. 18 (): 4467–4476. ISSN: 0950-1991.

Davis, M. W. 2004. "A conserved metalloprotease mediates ecdysis in Caenorhabditis elegans". *Development* 131, no. 23 (): 6001–6008. ISSN: 0950-1991.

Der, C J, T G Krontiris, and G M Cooper. 1982. "Transforming genes of human bladder and lung carcinoma cell lines are homologous to the ras genes of Harvey and Kirsten sarcoma viruses." *Proceedings of the National Academy of Sciences of the United States of America* 79, no. 11 (): 3637–40. ISSN: 0027-8424.

Dever, Thomas E, Manuel J Glyniast, and William C Merrick. 1987. "GTP-binding domain: Three consensus sequence elements with distinct spacing". *Biochemistry* 84:1814–1818.

Dieterich, Christoph, et al. 2008. "The Pristionchus pacificus genome provides a unique perspective on nematode lifestyle and parasitism." *Nature genetics* 40, no. 10 (): 1193–8. ISSN: 1546-1718.

Doench, John G., Christian P. Petersen, and Phillip A. Sharp. 2003. "siRNAs can function as miRNAs". *Genes and Development* 17, no. 4 (): 438–442. ISSN: 08909369.

Donaldson, J G, et al. 1992. “ADP-ribosylation factor, a small GTP-binding protein, is required for binding of the coatomer protein beta-COP to Golgi membranes.” *Proceedings of the National Academy of Sciences of the United States of America* 89, no. 14 (): 6408–12. ISSN: 0027-8424.

Edens, William A., et al. 2001. “Tyrosine cross-linking of extracellular matrix is catalyzed by Duox, a multidomain oxidase/peroxidase with homology to the phagocyte oxidase subunit gp91phox”. *Journal of Cell Biology* 154, no. 4 (): 879–891. ISSN: 00219525.

Eisenmann, D M, and S K Kim. 2000. “Protruding vulva mutants identify novel loci and Wnt signaling factors that function during Caenorhabditis elegans vulva development.” *Genetics* 156, no. 3 (): 1097–116. ISSN: 0016-6731.

Eisenmann, D M, et al. 1998. “The beta-catenin homolog BAR-1 and LET-60 Ras coordinately regulate the Hox gene lin-39 during Caenorhabditis elegans vulval development.” *Development (Cambridge, England)* 125, no. 18 (): 3667–80. ISSN: 0950-1991.

Eisenmann, David M. 2005. “Wnt signaling”. *WormBook* (): 1–17. ISSN: 15518507.

Farboud, Behnom, and Barbara J. Meyer. 2015. “Dramatic Enhancement of Genome Editing by CRISPR/Cas9 Through Improved Guide RNA Design”. *Genetics* 199, no. 4 (): 959–971. ISSN: 0016-6731.

Farley, Emma K, et al. 2016. “Syntax compensates for poor binding sites to encode tissue specificity of developmental enhancers.” *Proceedings of the National Academy of Sciences of the United States of America* 113, no. 23 (): 6508–13. ISSN: 1091-6490.

Fierst, Janna L., et al. 2015. “Reproductive Mode and the Evolution of Genome Size and Structure in Caenorhabditis Nematodes”. Ed. by Mark Blaxter. *PLOS Genetics* 11, no. 6 (): e1005323. ISSN: 1553-7404.

Fire, Andrew, et al. 1998. “Potent and specific genetic interference by double-stranded RNA in Caenorhabditis elegans”. *Nature* 391, no. 6669 (): 806–811. ISSN: 0028-0836.

Fleming, M W. 1985. “Ascaris suum: role of ecdysteroids in molting.” *Experimental parasitology* 60, no. 2 (): 207–10. ISSN: 0014-4894.

Frand, Alison R., Sascha Russel, and Gary Ruvkun. 2005. “Functional genomic analysis of c. elegans molting”. Ed. by Ronald Plasterk. *PLoS Biology* 3, no. 10 (): e312. ISSN: 15449173.

Fraser, Andrew G., et al. 2000. “Functional genomic analysis of C. elegans chromosome I by systematic RNA interference”. *Nature* 408, no. 6810 (): 325–330. ISSN: 0028-0836.

Friedland, A E, et al. 2013. “Heritable genome editing in C. elegans via a CRISPR-Cas9 system”. *Nat Methods* 10 (8): 741–743. ISSN: 1548-7105. arXiv: NIHMS150003.

Frøkjær-Jensen, Christian, et al. 2014. “Random and targeted transgene insertion in Caenorhabditis elegans using a modified Mos1 transposon”. *Nature Methods* 11, no. 5 (): 529–534. ISSN: 1548-7091.

Frøkjær-Jensen, Christian, et al. 2008. “Single-copy insertion of transgenes in Caenorhabditis elegans”. *Nature Genetics* 40, no. 11 (): 1375–1383. ISSN: 1061-4036.

Gavin, Brian J., Jill A. McMahon, and Andrew P. McMahon. 1990. “Expression of multiple novel Wnt-1/int-1-related genes during fetal and adult mouse development”. *Genes and Development* 4, no. 12 B (): 2319–2332. ISSN: 08909369.

George, Sean E., et al. 1998. “The VAB-1 Eph receptor tyrosine kinase functions in neural and epithelial morphogenesis in C. elegans”. *Cell* 92, no. 5 (): 633–643. ISSN: 00928674.

Gerstein, Mark B., et al. 2010. “Integrative analysis of the Caenorhabditis elegans genome by the modENCODE project”. *Science* 330, no. 6012 (): 1775–1787. ISSN: 00368075. arXiv: arXiv:1011.1669v3.

Gilleard, J S, and J D Mcghee. 2001. "Activation of Hypodermal Differentiation in the Caenorhabditis elegans Embryo by GATA Transcription Factors ELT-1 and Activation of Hypodermal Differentiation in the Caenorhabditis elegans Embryo by GATA Transcription Factors". *Molecular and Cellular Biology* Vol. 21, no. 7 (): 2533–2544. ISSN: 0270-7306.

Gissendanner, Chris R., et al. 2004. "Expression and function of conserved nuclear receptor genes in Caenorhabditis elegans". *Developmental Biology* 266, no. 2 (): 399–416. ISSN: 00121606.

Gissendanner, Christopher R, and Ann E Sluder. 2000. "nhr-25, the Caenorhabditis elegans Ortholog of ftz-f1, Is Required for Epidermal and Somatic Gonad Development". *Developmental Biology* 221, no. 1 (): 259–272. ISSN: 00121606.

Gleason, Julie E., and David M. Eisenmann. 2010. "Wnt signaling controls the stem cell-like asymmetric division of the epithelial seam cells during C. elegans larval development". *Developmental Biology* 348 (1): 58–66. ISSN: 00121606. arXiv: NIHMS150003.

Golden, J W, and D L Riddle. 1984. "The Caenorhabditis elegans dauer larva: developmental effects of pheromone, food, and temperature." *Developmental biology* 102, no. 2 (): 368–78. ISSN: 0012-1606.

Goldstein, Bob, et al. 2006. "Wnt signals can function as positional cues in establishing cell polarity". *Developmental Cell* 10, no. 3 (): 391–396. ISSN: 15345807.

Grant, Barth, and David Hirsh. 1999. "Receptor-mediated Endocytosis in the ¡i¿Caenorhabditis elegans¡/i¿ Oocyte". Ed. by Judith Kimble. *Molecular Biology of the Cell* 10, no. 12 (): 4311–4326. ISSN: 1059-1524.

Gravato-Nobre, M. J., et al. 2005. "Multiple Genes Affect Sensitivity of Caenorhabditis elegans to the Bacterial Pathogen Microbacterium nematophilum". *Genetics* 171, no. 3 (): 1033–1045. ISSN: 0016-6731.

Gravato-Nobre, Maria J., et al. 2011. "Glycosylation genes expressed in seam cells determine complex surface properties and bacterial adhesion to the cuticle of Caenorhabditis elegans". *Genetics* 187, no. 1 (): 141–155. ISSN: 00166731.

Green, Jennifer L, Takao Inoue, and Paul W Sternberg. 2008. "Opposing Wnt pathways orient cell polarity during organogenesis." *Cell* 134, no. 4 (): 646–56. ISSN: 1097-4172.

Haag, Andrea, et al. 2014. "An In Vivo EGF Receptor Localization Screen in C. elegans Identifies the Ezrin Homolog ERM-1 as a Temporal Regulator of Signaling". Ed. by Andrew D. Chisholm. *PLoS Genetics* 10, no. 5 (): e1004341. ISSN: 1553-7404.

Harandi, Omid F, and Victor R Ambros. 2015. "Control of stem cell self-renewal and differentiation by the heterochronic genes and the cellular asymmetry machinery in Caenorhabditis elegans." *Proceedings of the National Academy of Sciences of the United States of America* 112, no. 3 (): E287–96. ISSN: 1091-6490.

Harrison, P M, N Echols, and M B Gerstein. 2001. "Digging for dead genes: an analysis of the characteristics of the pseudogene population in the Caenorhabditis elegans genome." *Nucleic acids research* 29, no. 3 (): 818–30. ISSN: 1362-4962.

Hashmi, Sarwar, et al. 2004. "The Caenorhabditis elegans Cathepsin Z-like Cysteine Protease, Ce-CPZ-1, Has a Multifunctional Role during the Worms' Development". *Journal of Biological Chemistry* 279, no. 7 (): 6035–6045. ISSN: 00219258.

Hemalatha, Anupama, Chaitra Prabhakara, and Satyajit Mayor. 2016. "Endocytosis of Wingless via a dynamin-independent pathway is necessary for signaling in ¡i¿Drosophila¡/i¿ wing discs". *Proceedings of the National Academy of Sciences* 113, no. 45 (): E6993–E7002. ISSN: 0027-8424.

Hieb, W F, and M Rothstein. 1968. "Sterol requirement for reproduction of a free-living nematode." *Science (New York, N.Y.)* 160, no. 3829 (): 778–80. ISSN: 0036-8075.

Himmelhoch, Stanley, and Bert M. Zuckerman. 1978. *Caenorhabditis briggsae: Aging and the structural turnover of the outer cuticle surface and the intestine.* Tech. rep. 2.

Hodgkin, J, H R Horvitz, and S Brenner. 1979. "Nondisjunction Mutants of the Nematode CAENORHABDITIS ELEGANS." *Genetics* 91, no. 1 (): 67–94. ISSN: 0016-6731.

Hodgkin, Jonathan, and Tabitha Doniach. 1997. "Natural variation and copulatory plug formation in Caenorhabditis elegans". *Genetics* 146, no. 1 (): 149–164. ISSN: 00166731.

Holmes, Alex, et al. 2007. "C. elegans Disabled is required for cell-type specific endocytosis and is essential in animals lacking the AP-3 adaptor complex". *Journal of Cell Science* 120 (15).

Hope, I A. 1991. "'Promoter trapping' in Caenorhabditis elegans." *Development (Cambridge, England)* 113, no. 2 (): 399–408. ISSN: 0950-1991.

Horn, Moritz, et al. 2014. "DRE-1/FBXO11-dependent degradation of BLMP-1/BLIMP-1 governs C. elegans developmental timing and maturation." *Developmental cell* 28, no. 6 (): 697–710. ISSN: 1878-1551.

Hsu, Nai-Yun, et al. 2010. "Viral reorganization of the secretory pathway generates distinct organelles for RNA replication." *Cell* 141, no. 5 (): 799–811. ISSN: 1097-4172.

Huang, S., et al. 2007. "Binary cell fate specification during C. elegans embryogenesis driven by reiterated reciprocal asymmetry of TCF POP-1 and its coactivator - catenin SYS-1". *Development* 134, no. 14 (): 2685–2695. ISSN: 0950-1991.

Huang, Xinxin, et al. 2009. "The C. elegans engrailed homolog ceh-16 regulates the self-renewal expansion division of stem cell-like seam cells". *Developmental Biology* 333, no. 2 (): 337–347. ISSN: 00121606.

Hughes, S., et al. 2013. “CEH-20/Pbx and UNC-62/Meis function upstream of rnt-1/Runx to regulate asymmetric divisions of the C. elegans stem-like seam cells”. *Biology Open* 2, no. 7 (): 718–727. ISSN: 2046-6390.

Humphreys, Daniel, et al. 2013. “Arf6 coordinates actin assembly through the WAVE complex, a mechanism usurped by Salmonella to invade host cells.” *Proceedings of the National Academy of Sciences of the United States of America* 110, no. 42 (): 16880–5. ISSN: 1091-6490.

Hunter, C P, et al. 1999. “Hox gene expression in a single Caenorhabditis elegans cell is regulated by a caudal homolog and intercellular signals that inhibit wnt signaling.” *Development (Cambridge, England)* 126, no. 4 (): 805–14. ISSN: 0950-1991.

Hutvágner, György, and Phillip D. Zamore. 2002. “A microRNA in a multiple-turnover RNAi enzyme complex”. *Science* 297, no. 5589 (): 2056–2060. ISSN: 00368075.

Jackson, Belinda M., et al. 2014. “Use of an Activated Beta-Catenin to Identify Wnt Pathway Target Genes in ¡i¿Caenorhabditis elegans¡/i¿ , Including a Subset of Collagen Genes Expressed in Late Larval Development”. *G3: Genes—Genomes—Genetics* 4, no. 4 (): 733–747. ISSN: 2160-1836.

Jian, Xiaoying, et al. 2010. “Modifications to the C-terminus of Arf1 alter cell functions and protein interactions.” *Traffic (Copenhagen, Denmark)* 11, no. 6 (): 732–42. ISSN: 1600-0854.

Johnson, Thomas E., et al. 1984. “Arresting development arrests aging in the nematode Caenorhabditis elegans”. *Mechanisms of Ageing and Development* 28, no. 1 (): 23–40. ISSN: 00476374.

Johnstone, I L, and J D Barry. 1996. “Temporal reiteration of a precise gene expression pattern during nematode development.” *The EMBO journal* 15, no. 14 (): 3633–9. ISSN: 0261-4189.

Kage-Nakadai, Eriko, et al. 2018. "The small GTPase ARF-1.2 is a regulator of unicellular tube formation in Caenorhabditis elegans". *Journal of Physiological Sciences* (): 1–10. ISSN: 18806546.

Kagoshima, H., et al. 2007. "The C. elegans CBF homologue BRO-1 interacts with the Runx factor, RNT-1, to promote stem cell proliferation and self-renewal". *Development* 134, no. 21 (): 3905–3915. ISSN: 0950-1991.

Kahn, R A, and A G Gilman. 1984. "Purification of a protein cofactor required for ADP-ribosylation of the stimulatory regulatory component of adenylate cyclase by cholera toxin." *The Journal of biological chemistry* 259, no. 10 (): 6228–34. ISSN: 0021-9258.

— . 1986. "The protein cofactor necessary for ADP-ribosylation of Gs by cholera toxin is itself a GTP binding protein." *The Journal of biological chemistry* 261, no. 17 (): 7906–11. ISSN: 0021-9258.

Kahn, R A, C Goddard, and M Newkirk. 1988. "Chemical and immunological characterization of the 21-kDa ADP-ribosylation factor of adenylate cyclase." *The Journal of biological chemistry* 263, no. 17 (): 8282–7. ISSN: 0021-9258.

Kahn, R A, et al. 1991. "Human ADP-ribosylation factors. A functionally conserved family of GTP-binding proteins." *The Journal of biological chemistry* 266, no. 4 (): 2606–14. ISSN: 0021-9258.

Kamikura, D. M., and Jonathan A Cooper. 2003. "Lipoprotein receptors and a Disabled family cytoplasmic adaptor protein regulate EGL-17/FGF export in C. elegans". *Genes & Development* 17, no. 22 (): 2798–2811. ISSN: 0890-9369.

Kang, Yuan-Lin, et al. 2013. "Caenorhabditis elegans reveals a FxNPxY-independent low-density lipoprotein receptor internalization mechanism mediated by epsin1." *Molecular biology of the cell* 24, no. 3 (): 308–18. ISSN: 1939-4586.

Kelly, W G, and A Fire. 1998. "Chromatin silencing and the maintenance of a functional germline in Caenorhabditis elegans." *Development (Cambridge, England)* 125, no. 13 (): 2451–6. ISSN: 0950-1991.

Kenyon, C. 1986. "A gene involved in the development of the posterior body region of C. elegans." *Cell* 46, no. 3 (): 477–87. ISSN: 0092-8674.

Khan, Aziz, et al. 2018. "JASPAR 2018: update of the open-access database of transcription factor binding profiles and its web framework". *Nucleic Acids Research* 46, no. D1 (): D260–D266. ISSN: 0305-1048.

Kimble, Judith, and David Hirsh. 1979. "The postembryonic cell lineages of the hermaphrodite and male gonads in Caenorhabditis elegans". *Developmental Biology* 70, no. 2 (): 396–417. ISSN: 00121606.

Klass, M, and D Hirsh. 1976. "Non-ageing developmental variant of Caenorhabditis elegans." *Nature* 260, no. 5551 (): 523–5. ISSN: 0028-0836.

Klingensmith, John, Roel Nusse, and Norbert Perrimon. 1994. "The Drosophila segment polarity gene dishevelled encodes a novel protein required for response to the wingless signal". *Genes and Development* 8, no. 1 (): 118–130. ISSN: 08909369.

Koh, K, and J H Rothman. 2001. "ELT-5 and ELT-6 are required continuously to regulate epidermal seam cell differentiation and cell fusion in C. elegans." *Development (Cambridge, England)* 128, no. 15 (): 2867–2880. ISSN: 0950-1991.

Korswagen, Hendrik C., Michael A. Herman, and Hans C. Clevers. 2000. "Distinct β-catenins mediate adhesion and signalling functions in C. elegans". *Nature* 406, no. 6795 (): 527–532. ISSN: 00280836.

Kostrouchova, M., et al. 2001. "Nuclear hormone receptor CHR3 is a critical regulator of all four larval molts of the nematode Caenorhabditis elegans". *Proceedings of the National Academy of Sciences* 98, no. 13 (): 7360–7365. ISSN: 0027-8424.

Kouns, Nathaniel A, et al. 2011. "NHR-23 dependent collagen and hedgehog-related genes required for molting." *Biochemical and biophysical research communications* 413, no. 4 (): 515–20. ISSN: 1090-2104.

Kramer, J. M., G. N. Cox, and D. Hirsh. 1985. "Expression of the Caenorhabditis elegans collagen genes col-1 and col-2 is developmentally regulated". *Journal of Biological Chemistry* 260, no. 3 (): 1945–1951. ISSN: 00219258.

Kudron, Michelle M., et al. 2018. "The modern resource: genome-wide binding profiles for hundreds of Drosophila and Caenorhabditis elegans transcription factors". *Genetics* 208, no. 3 (): 937–949. ISSN: 19432631.

Lagos-Quintana, M., et al. 2001. "Identification of Novel Genes Coding for Small Expressed RNAs". *Science* 294, no. 5543 (): 853–858. ISSN: 00368075.

Lagos-Quintana, Mariana, et al. 2002. "Identification of tissue-specific MicroRNAs from mouse". *Current Biology* 12, no. 9 (): 735–739. ISSN: 09609822.

Lee, Rosalind C., Rhonda L. Feinbaum, and Victor Ambros. 1993. "The C. elegans heterochronic gene lin-4 encodes small RNAs with antisense complementarity to lin-14". *Cell* 75, no. 5 (): 843–854. ISSN: 00928674. arXiv: NIHMS150003.

Levy, Adam D., and James M. Kramer. 1993. "Identification, sequence and expression patterns of the Caenorhabditis elegans col-36 and col-40 collagen-encoding genes". *Gene* 137, no. 2 (): 281–285. ISSN: 03781119.

Li, Yawei, et al. 2004. "Functional genomic analysis of the ADP-ribosylation factor family of GTPases: phylogeny among diverse eukaryotes and function in C. elegans." *FASEB journal : official publication of the Federation of American Societies for Experimental Biology* 18, no. 15 (): 1834–50. ISSN: 1530-6860.

Liu, Jing, et al. 2008. "The C. elegans SYS-1 Protein Is a Bona Fide β-Catenin". *Developmental Cell* 14, no. 5 (): 751–761. ISSN: 15345807. arXiv: NIHMS150003.

Liu, Yizhou, Richard A Kahn, and James H Prestegard. 2010. "Dynamic structure of membrane-anchored Arf•GTP". *Nature Structural & Molecular Biology* 17, no. 7 (): 876–881. ISSN: 1545-9993.

Liu, Zhongchi, Susan Kirch, and Victor Ambros. 1995. "The Caenorhabditis elegans heterochronic gene pathway controls stage-specific transcription of collagen genes." *Development (Cambridge, England)* 121, no. 8 (): 2471–2478. ISSN: 0950-1991.

Livak, Kenneth J., and Thomas D. Schmittgen. 2001. "Analysis of Relative Gene Expression Data Using Real-Time Quantitative PCR and the 2ΔΔCT Method". *Methods* 25, no. 4 (): 402–408. ISSN: 10462023.

Lo, Miao-Chia, et al. 2004. "Phosphorylation by the beta-catenin/MAPK complex promotes 14-3-3-mediated nuclear export of TCF/POP-1 in signal-responsive cells in C. elegans." *Cell* 117, no. 1 (): 95–106. ISSN: 0092-8674.

Lu, Wange, et al. 2004. "Mammalian Ryk is a Wnt coreceptor required for stimulation of neurite outgrowth". *Cell* 119, no. 1 (): 97–108. ISSN: 00928674.

Maduro, M, and D Pilgrim. 1995. "Identification and cloning of unc-119, a gene expressed in the Caenorhabditis elegans nervous system." *Genetics* 141, no. 3 (): 977–88. ISSN: 0016-6731.

Maloof, J N, and C Kenyon. 1998. "The Hox gene lin-39 is required during C. elegans vulval induction to select the outcome of Ras signaling." *Development (Cambridge, England)* 125, no. 2 (): 181–90. ISSN: 0950-1991.

Margalit, Ayelet, et al. 2007. "Barrier to autointegration factor blocks premature cell fusion and maintains adult muscle integrity in C. elegans." *The Journal of cell biology* 178, no. 4 (): 661–73. ISSN: 0021-9525.

Matto, Meirav, et al. 2011. "Role for ADP ribosylation factor 1 in the regulation of hepatitis C virus replication." *Journal of virology* 85, no. 2 (): 946–56. ISSN: 1098-5514.

McCormick, F, et al. 1985. "A model for the tertiary structure of p21, the product of the ras oncogene." *Science (New York, N.Y.)* 230, no. 4721 (): 78–82. ISSN: 0036-8075.

McMahon, Andrew P., and Randall T. Moon. 1989. "Ectopic expression of the proto-oncogene int-1 in Xenopus embryos leads to duplication of the embryonic axis". *Cell* 58, no. 6 (): 1075–1084. ISSN: 00928674.

McMahon, Laura, et al. 2003. "Two sets of interacting collagens form functionally distinct substructures within a Caenorhabditis elegans extracellular matrix." Ed. by John Pringle. *Molecular biology of the cell* 14, no. 4 (): 1366–78. ISSN: 1059-1524.

Mello, C C, et al. 1991. "Efficient gene transfer in C.elegans: extrachromosomal maintenance and integration of transforming sequences." *The EMBO journal* 10, no. 12 (): 3959–70. ISSN: 0261-4189.

Mello, C, and A Fire. 1995. "DNA transformation." *Methods in cell biology* 48:451–82. ISSN: 0091-679X.

Meneely, Philip M, Anna F Farago, and Tate M Kauffman. 2002. "Crossover distribution and high interference for both the X chromosome and an autosome during oogenesis and spermatogenesis in Caenorhabditis elegans." *Genetics* 162, no. 3 (): 1169–77. ISSN: 0016-6731.

Miyabayashi, Tomoyuki, et al. 1999. "Expression and Function of Members of a Divergent Nuclear Receptor Family in Caenorhabditis elegans". *Developmental Biology* 215, no. 2 (): 314–331. ISSN: 00121606.

Mizumoto, Kota, and Hitoshi Sawa. 2007. "Cortical β-Catenin and APC Regulate Asymmetric Nuclear β-Catenin Localization during Asymmetric Cell Division in C. elegans". *Developmental Cell* 12, no. 2 (): 287–299. ISSN: 15345807.

Mohler, William A, et al. 2002. "The type I membrane protein EFF-1 is essential for developmental cell fusion." *Developmental cell* 2, no. 3 (): 355–62. ISSN: 1534-5807.

Molenaar, Miranda, et al. 1996. "XTcf-3 transcription factor mediates β-catenin-induced axis formation in xenopus embryos". *Cell* 86, no. 3 (): 391–399. ISSN: 00928674.

Muriel, Joaquin M., et al. 2003. "M142.2 (cut-6), a novel Caenorhabditis elegans matrix gene important for dauer body shape". *Developmental Biology* 260, no. 2 (): 339–351. ISSN: 00121606.

Murtagh, James J, et al. 1993. “Molecular Characterization of a Conserved, Guanine Nucleotide-Dependent ADP-Ribosylation Factor in Drosophila melanogasterf”. *Biochemistry* 32:6011–6018.

Nagai, H., et al. 2002. “A Bacterial Guanine Nucleotide Exchange Factor Activates ARF on Legionella Phagosomes”. *Science* 295, no. 5555 (): 679–682. ISSN: 00368075.

Naslavsky, Naava, and Steve Caplan. 2018. “The enigmatic endosome – sorting the ins and outs of endocytic trafficking”. *Journal of Cell Science* 131, no. 13 (): jcs216499. ISSN: 0021-9533.

Natarajan, Lakshmi, Nina E. Witwer, and David M. Eisenmann. 2001. “The divergent Caenorhabditis elegans ??-catenin proteins BAR-1, WRM-1 and HMP-2 make distinct protein interactions but retain functional redundancy in vivo”. *Genetics* 159, no. 1 (): 159–172. ISSN: 00166731.

Nelson, F. Kenneth, and Donald L. Riddle. 1984. “Functional study of the Caenorhabditis elegans secretory-excretory system using laser microsurgery”. *Journal of Experimental Zoology* 231, no. 1 (): 45–56. ISSN: 1097010X.

Nie, Zhongzhen, et al. 2003. “Specific regulation of the adaptor protein complex AP-3 by the Arf GAP AGAP1.” *Developmental cell* 5, no. 3 (): 513–21. ISSN: 1534-5807.

Nigon, Victor Marc, and Marie-Anne Félix. 2017. “History of research on C. elegans and other free-living nematodes as model organisms”. *WormBook* 2017 (): 1–84. ISSN: 15518507.

Niu, Wei, et al. 2011. “Diverse transcription factor binding features revealed by genome-wide ChIP-seq in C. elegans”. *Genome Research* 21, no. 2 (): 245–254. ISSN: 10889051.

Noordermeer, Jasprien, et al. 1994. “Dishevelled and armadillo act in the Wingless signalling pathway in Drosophila”. *Nature* 367, no. 6458 (): 80–83. ISSN: 00280836.

Nüsslein-Volhard, C, H G Frohnhöfer, and R Lehmann. 1987. "Determination of anteroposterior polarity in Drosophila." *Science (New York, N.Y.)* 238, no. 4834 (): 1675–81. ISSN: 0036-8075.

Olsen, Philip H., and Victor Ambros. 1999. "The lin-4 regulatory RNA controls developmental timing in Caenorhabditis elegans by blocking LIN-14 protein synthesis after the initiation of translation". *Developmental Biology* 216, no. 2 (): 671–680. ISSN: 00121606.

Page, Antony P., Gillian McCormack, and Andrew J. Birnie. 2006. "Biosynthesis and enzymology of the Caenorhabditis elegans cuticle: Identification and characterization of a novel serine protease inhibitor". *International Journal for Parasitology* 36, no. 6 (): 681–689. ISSN: 00207519.

Park, Seung Gu, Sridhar Hannenhalli, and Sun Shim Choi. 2014. "Conservation in first introns is positively associated with the number of exons within genes and the presence of regulatory epigenetic signals." *BMC genomics* 15, no. 1 (): 526. ISSN: 1471-2164.

Parks, W P, and E M Scolnick. 1977. "In vitro translation of Harvey murine sarcoma virus RNA." *Journal of virology* 22, no. 3 (): 711–9. ISSN: 0022-538X.

Pasquinelli, Amy E., et al. 2000. "Conservation of the sequence and temporal expression of let-7 heterochronic regulatory RNA". *Nature* 408, no. 6808 (): 86–89. ISSN: 0028-0836.

Peifer, M, et al. 1993. "A role for the Drosophila segment polarity gene armadillo in cell adhesion and cytoskeletal integrity during oogenesis." *Development (Cambridge, England)* 118, no. 4 (): 1191–207. ISSN: 0950-1991.

Peixoto, C A, J M Kramer, and W de Souza. 1997. "Caenorhabditis elegans cuticle: a description of new elements of the fibrous layer". *J Parasitol* 83, no. 3 (): 368–372. ISSN: 0022-3395.

Peng, Z G, et al. 1989. “Molecular cloning, sequence analysis and mRNA expression of human ADP-ribosylation factor.” *BioFactors (Oxford, England)* 2, no. 1 (): 45–9. ISSN: 0951-6433.

Perrimon, Norbert, and Anthony P. Mahowald. 1987. “Multiple functions of segment polarity genes in Drosophila”. *Developmental Biology* 119, no. 2 (): 587–600. ISSN: 00121606.

Pettitt, Jonathan, et al. 2014. “Operons are a conserved feature of nematode genomes.” *Genetics* 197, no. 4 (): 1201–11. ISSN: 1943-2631.

Podbilewicz, Benjamin, and John G. White. 1994. “Cell fusions in the developing epithelia of C. elegans”. *Developmental Biology* 161, no. 2 (): 408–424. ISSN: 00121606.

Poteryaev, Dmitry, et al. 2005. “Involvement of the Actin Cytoskeleton and Homotypic Membrane Fusion in ER Dynamics in ¡i¿Caenorhabditis elegans¡/i¿”. *Molecular Biology of the Cell* 16, no. 5 (): 2139–2153. ISSN: 1059-1524.

Puhka, Maija, et al. 2007. “Endoplasmic reticulum remains continuous and undergoes sheet-to-tubule transformation during cell division in mammalian cells.” *The Journal of cell biology* 179, no. 5 (): 895–909. ISSN: 1540-8140.

Randazzo, P. A., et al. 1993. “Activation of ADP-ribosylation factor by Golgi membranes. Evidence for a brefeldin A- and protease-sensitive activating factor on Golgi membranes”. *Journal of Biological Chemistry* 268, no. 13 (): 9555–9563. ISSN: 00219258.

Reinhart, B. J., et al. 2002. “MicroRNAs in plants”. *Genes & Development* 16, no. 13 (): 1616–1626. ISSN: 08909369.

Reinhart, Brenda J., et al. 2000. “The 21-nucleotide let-7 RNA regulates developmental timing in Caenorhabditis elegans”. *Nature* 403, no. 6772 (): 901–906. ISSN: 0028-0836.

Rennoll-Bankert, Kristen E., et al. 2015. “Which Way In? The RalF Arf-GEF Orchestrates Rickettsia Host Cell Invasion”. Ed. by Isabelle Coppens. *PLOS Pathogens* 11, no. 8 (): e1005115. ISSN: 1553-7374.

Resnick, Tamar D, Katherine A McCulloch, and Ann E Rougvie. 2010. “miRNAs give worms the time of their lives: small RNAs and temporal control in Caenorhabditis elegans.” *Developmental dynamics : an official publication of the American Association of Anatomists* 239, no. 5 (): 1477–89. ISSN: 1097-0177.

Rijsewijk, Frans, et al. 1987. “The Drosophila homology of the mouse mammary oncogene int-1 is identical to the segment polarity gene wingless”. *Cell* 50, no. 4 (): 649–657. ISSN: 00928674.

Roberts, Brett, Caroline Clucas, and Iain L. Johnstone. 2003. “Loss of SEC-23 in ¡i¿Caenorhabditis elegans¡/i¿ Causes Defects in Oogenesis, Morphogenesis, and Extracellular Matrix Secretion”. *Molecular Biology of the Cell* 14, no. 11 (): 4414–4426. ISSN: 1059-1524.

Rocheleau, C. E., et al. 1999. “WRM-1 activates the LIT-1 protein kinase to transduce anterior/posterior polarity signals in C. elegans”. *Cell* 97, no. 6 (): 717–726. ISSN: 00928674.

Rual, Jean-François, et al. 2004. “Toward improving Caenorhabditis elegans phenome mapping with an ORFeome-based RNAi library.” *Genome research* 14, no. 10B (): 2162–8. ISSN: 1088-9051.

Rubin, G M, et al. 2000. “Comparative genomics of the eukaryotes.” *Science (New York, N.Y.)* 287, no. 5461 (): 2204–15. ISSN: 0036-8075.

Ruvkun, Gary, and John Giusto. 1989. “The Caenorhabditis elegans heterochronic gene lin-14 encodes a nuclear protein that forms a temporal developmental switch”. *Nature* 338, no. 6213 (): 313–319. ISSN: 00280836.

Sammut, Michele, et al. 2015. “Glia-derived neurons are required for sex-specific learning in C. Elegans”. *Nature* 526, no. 7573 (): 385–390. ISSN: 14764687.

Sapio, Maria Rosaria, et al. 2005. "The Zona Pellucida domain containing proteins, CUT-1, CUT-3 and CUT-5, play essential roles in the development of the larval alae in Caenorhabditis elegans". *Developmental Biology* 282, no. 1 (): 231–245. ISSN: 00121606.

Sawa, Hitoshi, and Hendrik C. Korswagen. 2013. "Wnt signaling in C. elegans". *WormBook* (): 1–30. ISSN: 15518507. arXiv: NIHMS150003.

Schleifer, L S, et al. 1982. "Requirements for cholera toxin-dependent ADP-ribosylation of the purified regulatory component of adenylate cyclase." *The Journal of biological chemistry* 257, no. 1 (): 20–3. ISSN: 0021-9258.

Scolnick, E M, A G Papageorge, and T Y Shih. 1979. "Guanine nucleotide-binding activity as an assay for src protein of rat-derived murine sarcoma viruses." *Proceedings of the National Academy of Sciences of the United States of America* 76, no. 10 (): 5355–9. ISSN: 0027-8424.

Sebastiano, Marisa, Franco Lassandro, and Paolo Bazzicalupo. 1991. "cut-1 a Caenorhabditis elegans gene coding for a dauer-specific noncollagenous component of the cuticle". *Developmental Biology* 146, no. 2 (): 519–530. ISSN: 00121606.

Sefton, B M, et al. 1982. "The transforming proteins of Rous sarcoma virus, Harvey sarcoma virus and Abelson virus contain tightly bound lipid." *Cell* 31, no. 2 Pt 1 (): 465–74. ISSN: 0092-8674.

Sewell, J L, and R A Kahn. 1988. "Sequences of the bovine and yeast ADP-ribosylation factor and comparison to other GTP-binding proteins". *Proceedings of the National Academy of Sciences of the United States of America* 85, no. 13 (): 4620–4624. ISSN: 0027-8424.

Sharma, R. P., and V. L. Chopra. 1976. "Effect of the wingless (wg1) mutation on wing and haltere development in Drosophila melanogaster". *Developmental Biology* 48, no. 2 (): 461–465. ISSN: 00121606.

Shatilovich, A. V., et al. 2018. “Viable Nematodes from Late Pleistocene Permafrost of the Kolyma River Lowland”. *Doklady Biological Sciences* 480, no. 1 (): 100–102. ISSN: 0012-4966.

Sheen, Volney L, et al. 2004. “Mutations in ARFGEF2 implicate vesicle trafficking in neural progenitor proliferation and migration in the human cerebral cortex”. *Nature Genetics* 36, no. 1 (): 69–76. ISSN: 1061-4036.

Shemer, Gidi, et al. 2004. “EFF-1 Is Sufficient to Initiate and Execute Tissue-Specific Cell Fusion in C. elegans”. *Current Biology* 14, no. 17 (): 1587–1591. ISSN: 09609822.

Shih, T Y, et al. 1979. “p21 of Kirsten murine sarcoma virus is thermolabile in a viral mutant temperature sensitive for the maintenance of transformation.” *Journal of virology* 31, no. 2 (): 546–6. ISSN: 0022-538X.

Shih, Thomas Y., et al. 1980. “Guanine nucleotide-binding and autophosphorylating activities associated with the p21src protein of Harvey murine sarcoma virus”. *Nature* 287, no. 5784 (): 686–691. ISSN: 0028-0836.

Shimomura, O, F H Johnson, and Y Saiga. 1962. “Extraction, purification and properties of aequorin, a bioluminescent protein from the luminous hydromedusan, Aequorea.” *Journal of cellular and comparative physiology* 59 (): 223–39. ISSN: 0095-9898.

Shoubridge, Cheryl, et al. 2010. “Mutations in the guanine nucleotide exchange factor gene IQSEC2 cause nonsyndromic intellectual disability”. *Nature Genetics* 42, no. 6 (): 486–488. ISSN: 1061-4036.

Silhánková, Marie, Marek Jindra, and Masako Asahina. 2005. “Nuclear receptor NHR-25 is required for cell-shape dynamics during epidermal differentiation in Caenorhabditis elegans.” *Journal of cell science* 118, no. Pt 1 (): 223–32. ISSN: 0021-9533.

Singh, Komudi, et al. 2011. “C. elegans Notch Signaling Regulates Adult Chemosensory Response and Larval Molting Quiescence”. *Current Biology* 21, no. 10 (): 825–834. ISSN: 09609822.

Singh, R. N., and J. E. Sulston. 1978. “Some Observations on Moulting in Caenorhabditis Elegans”. *Nematologica* 24, no. 1 (): 63–71. ISSN: 00282596.

Singhvi, Aakanksha, et al. 2011. “The Arf GAP CNT-2 regulates the apoptotic fate in C. elegans asymmetric neuroblast divisions.” *Current biology : CB* 21, no. 11 (): 948–54. ISSN: 1879-0445.

Skorobogata, Olga, et al. 2014. “An AGEF-1/Arf GTPase/AP-1 Ensemble Antagonizes LET-23 EGFR Basolateral Localization and Signaling during C. elegans Vulva Induction”. Ed. by Andrew D. Chisholm. *PLoS Genetics* 10, no. 10 (): e1004728. ISSN: 1553-7404.

Slack, Frank J., et al. 2000. “The lin-41 RBCC gene acts in the C. elegans heterochronic pathway between the let-7 regulatory RNA and the LIN-29 transcription factor”. *Molecular Cell* 5, no. 4 (): 659–669. ISSN: 10972765.

Smulan, Lorissa J, et al. 2016. “Cholesterol-Independent SREBP-1 Maturation Is Linked to ARF1 Inactivation.” *Cell reports* 16 (1): 9–18. ISSN: 2211-1247.

Smurova, Ksenia, and Benjamin Podbilewicz. 2016. “RAB-5- and DYNAMIN-1-Mediated Endocytosis of EFF-1 Fusogen Controls Cell-Cell Fusion”. *Cell Reports* 14, no. 6 (): 1517–1527. ISSN: 22111247.

Stein, Lincoln D, et al. 2003. “The Genome Sequence of Caenorhabditis briggsae: A Platform for Comparative Genomics”. Ed. by Jonathan A. Eisen. *PLoS Biology* 1, no. 2 (): e45. ISSN: 1545-7885.

Stenvall, Jörgen, et al. 2011. “Selenoprotein TRXR-1 and GSR-1 are essential for removal of old cuticle during molting in Caenorhabditis elegans.” *Proceedings of the National Academy of Sciences of the United States of America* 108, no. 3 (): 1064–1069. ISSN: 0027-8424.

Sugioka, Kenji, and Hitoshi Sawa. 2012. "Formation and functions of asymmetric microtubule organization in polarized cells". *Current Opinion in Cell Biology* 24, no. 4 (): 517–525. ISSN: 09550674.

Sulston, J E, and H R Horvitz. 1977. "Post-embryonic cell lineages of the nematode, Caenorhabditis elegans." *Developmental biology* 56, no. 1 (): 110–56. ISSN: 0012-1606.

Sulston, J E, et al. 1983. "The embryonic cell lineage of the nematode Caenorhabditis elegans." *Developmental biology* 100, no. 1 (): 64–119. ISSN: 0012-1606.

Sulston, J. E., D. G. Albertson, and J. N. Thomson. 1980. "The Caenorhabditis elegans male: Postembryonic development of nongonadal structures". *Developmental Biology* 78, no. 2 (): 542–576. ISSN: 00121606.

Sulston, J., M. Dew, and S. Brenner. 1975. "Dopaminergic neurons in the nematode Caenorhabditis elegans". *Journal of Comparative Neurology* 163, no. 2 (): 215–226. ISSN: 10969861.

Tabara, H, A Grishok, and C C Mello. 1998. "RNAi in C. elegans: soaking in the genome sequence." *Science (New York, N.Y.)* 282, no. 5388 (): 430–1. ISSN: 0036-8075.

Takeshita, Hisako, and Hitoshi Sawa. 2005. "Asymmetric cortical and nuclear localizations of WRM-1/beta-catenin during asymmetric cell division in C. elegans." *Genes & development* 19, no. 15 (): 1743–8. ISSN: 0890-9369.

Tamai, Keiko, et al. 2004. "A Mechanism for Wnt Coreceptor Activation". *Molecular Cell* 13, no. 1 (): 149–156. ISSN: 10972765.

Tamkun, J W, et al. 1991. "The arflike gene encodes an essential GTP-binding protein in Drosophila." *Proceedings of the National Academy of Sciences of the United States of America* 88, no. 8 (): 3120–4. ISSN: 0027-8424.

Tanigawa, G, et al. 1993. "Hydrolysis of bound GTP by ARF protein triggers uncoating of Golgi-derived COP-coated vesicles." *The Journal of cell biology* 123, no. 6 Pt 1 (): 1365–71. ISSN: 0021-9525.

Teuliere, Jerome, et al. 2014. “Asymmetric neuroblast divisions producing apoptotic cells require the cytohesin GRP-1 in Caenorhabditis elegans.” *Genetics* 198, no. 1 (): 229–47. ISSN: 1943-2631.

Thein, Melanie C., et al. 2003. “Caenorhabditis elegans exoskeleton collagen COL-19: An adult-specific marker for collagen modification and assembly, and the analysis of organismal morphology”. *Developmental Dynamics* 226, no. 3 (): 523–539. ISSN: 10588388.

Thein, Melanie C., et al. 2009. “Combined extracellular matrix cross-linking activity of the peroxidase MLT-7 and the dual oxidase BLI-3 is critical for post-embryonic viability in Caenorhabditis elegans”. *Journal of Biological Chemistry* 284, no. 26 (): 17549–17563. ISSN: 00219258.

Thompson, Kenneth W, et al. 2016. “The Paired-box protein PAX-3 regulates the choice between lateral and ventral epidermal cell fates in C. elegans.” *Developmental biology* 412, no. 2 (): 191–207. ISSN: 1095-564X.

Tian, Huiyu, et al. 2008. “Wnt Signaling Induces Vulva Development in the Nematode Pristionchus pacificus”. *Current Biology* 18, no. 2 (): 142–146. ISSN: 09609822.

Timmons, Lisa, and Andrew Fire. 1998. “Specific interference by ingested dsRNA”. *Nature* 395, no. 6705 (): 854–854. ISSN: 0028-0836.

Tinevez, Jean-Yves, et al. 2017. “TrackMate: An open and extensible platform for single-particle tracking”. *Methods* 115 (): 80–90. ISSN: 10462023.

Van Buskirk, Cheryl, and Paul W. Sternberg. 2007. “Epidermal growth factor signaling induces behavioral quiescence in Caenorhabditis elegans”. *Nature Neuroscience* 10, no. 10 (): 1300–1307. ISSN: 10976256.

Volpicelli-Daley, Laura A., et al. 2005. “Isoform-selective Effects of the Depletion of ADP-Ribosylation Factors 1–5 on Membrane Traffic”. *Molecular Biology of the Cell* 16, no. 10 (): 4495–4508. ISSN: 1059-1524.

Wagner, Michael, et al. 1990. “Polarizing activity and retinoid synthesis in the floor plate of the neural tube”. *Nature* 345, no. 6278 (): 819–822. ISSN: 0028-0836.

Ward, Samuel, et al. 1975. “Electron microscopical reconstruction of the anterior sensory anatomy of the nematode caenorhabditis elegans”. *Journal of Comparative Neurology* 160, no. 3 (): 313–337. ISSN: 10969861.

Waterston, Robert H., et al. 2002. “Initial sequencing and comparative analysis of the mouse genome”. *Nature* 420, no. 6915 (): 520–562. ISSN: 00280836. arXiv: NIHMS150003.

Wehrli, Marcel, et al. 2000. “Arrow encodes an LDL-receptor-related protein essential for Wingless signalling”. *Nature* 407, no. 6803 (): 527–530. ISSN: 00280836.

White, J. G., et al. 1983. “Factors that determine connectivity in the nervous system of Caenorhabditis elegans.” *Cold Spring Harbor Symposia on Quantitative Biology* 48 Pt 2:633–640. ISSN: 00917451.

— . 1986. “The Structure of the Nervous System of the Nematode Caenorhabditis elegans”. *Philosophical Transactions of the Royal Society B: Biological Sciences* 314, no. 1165 (): 1–340. ISSN: 0962-8436.

— . 1976. “The structure of the ventral nerve cord of Caenorhabditis elegans.” *Philosophical transactions of the Royal Society of London. Series B, Biological sciences* 275, no. 938 (): 327–348. ISSN: 09628436.

Wightman, Bruce, Ilho Ha, and Gary Ruvkun. 1993. “Posttranscriptional regulation of the heterochronic gene lin-14 by lin-4 mediates temporal pattern formation in C. elegans”. *Cell* 75, no. 5 (): 855–862. ISSN: 00928674.

Willert, Karl, et al. 2003. “Wnt proteins are lipid-modified and can act as stem cell growth factors”. *Nature* 423, no. 6938 (): 448–452. ISSN: 00280836. arXiv: NIHMS150003.

Williams, B D, et al. 1992. “A genetic mapping system in Caenorhabditis elegans based on polymorphic sequence-tagged sites.” *Genetics* 131, no. 3 (): 609–24. ISSN: 0016-6731.

Willingham, M C, et al. 1980. “Localization of the src gene product of the Harvey strain of MSV to plasma membrane of transformed cells by electron microscopic immunocytochemistry.” *Cell* 19, no. 4 (): 1005–14. ISSN: 0092-8674.

Wood, William Barry. 1988. *The Nematode Caenorhabditis elegans*. 667. Cold Spring Harbor Laboratory. ISBN: 9780879694333.

Yadav, Smita, Manojkumar A Puthenveedu, and Adam D Linstedt. 2012. “Golgin160 recruits the dynein motor to position the Golgi apparatus.” *Developmental cell* 23, no. 1 (): 153–65. ISSN: 1878-1551.

Yamamoto, Yuko, Hisako Takeshita, and Hitoshi Sawa. 2011. “Multiple Wnts redundantly control polarity orientation in Caenorhabditis elegans epithelial stem cells”. Ed. by Andrew D. Chisholm. *PLoS Genetics* 7, no. 10 (): e1002308. ISSN: 15537390.

Yang-Snyder, J, et al. 1996. “A frizzled homolog functions in a vertebrate Wnt signaling pathway.” *Current biology : CB* 6, no. 10 (): 1302–6. ISSN: 0960-9822.

Yang, X.-D., et al. 2011. “Distinct and mutually inhibitory binding by two divergent -catenins coordinates TCF levels and activity in C. elegans”. *Development* 138, no. 19 (): 4255–4265. ISSN: 0950-1991.

Yochem, John, et al. 2015. “C. elegans NIMA-related kinases NEKL-2 and NEKL-3 are required for the completion of molting”. *Developmental Biology* 398, no. 2 (): 255–266. ISSN: 00121606.

Yochem, J, et al. 1999. “A gp330/megalin-related protein is required in the major epidermis of Caenorhabditis elegans for completion of molting.” *Development (Cambridge, England)* 126, no. 3 (): 597–606. ISSN: 0950-1991.

Yoshikawa, Shingo, et al. 2003. “Wnt-mediated axon guidance via the Drosophila derailed receptor”. *Nature* 422, no. 6932 (): 583–588. ISSN: 00280836.

Zeng, Y., R. Yi, and B. R. Cullen. 2003. “MicroRNAs and small interfering RNAs can inhibit mRNA expression by similar mechanisms”. *Proceedings of the National Academy of Sciences* 100, no. 17 (): 9779–9784. ISSN: 0027-8424.

Zeng, Yan, Eric J. Wagner, and Bryan R. Cullen. 2002. "Both natural and designed micro RNAs can inhibit the expression of cognate mRNAs when expressed in human cells". *Molecular Cell* 9, no. 6 (): 1327–1333. ISSN: 10972765.

Zhang, Donglei, et al. 2016. "RAB-6.1 and RAB-6.2 Promote Retrograde Transport in C. elegans". Ed. by Ludger Johannes. *PLOS ONE* 11, no. 2 (): e0149314. ISSN: 1932-6203.

Zhang, Donglei, et al. 2012. "RAB-6.2 and the retromer regulate glutamate receptor recycling through a retrograde pathway". *The Journal of Cell Biology* 196, no. 1 (): 85–101. ISSN: 0021-9525.

Zhang, Yong, et al. 2008. "Model-based analysis of ChIP-Seq (MACS)." *Genome biology* 9 (9): R137. ISSN: 1474-760X.

Zhang, Yun, et al. 2002. "Identification of genes expressed in C. elegans touch receptor neurons". *Nature* 418, no. 6895 (): 331–335. ISSN: 0028-0836.

Zhao, L, et al. 1997. "Direct and GTP-dependent interaction of ADP ribosylation factor 1 with coatomer subunit beta." *Proceedings of the National Academy of Sciences of the United States of America* 94, no. 9 (): 4418–23. ISSN: 0027-8424.

Zuckerman, Bert M., Itzhak Kahane, and Stanley Himmelhoch. 1979. "Caenorhabditis briggsae and C. elegans: Partial characterization of cuticle surface carbohydrates". *Experimental Parasitology* 47, no. 3 (): 419–424. ISSN: 10902449.